BEYOND BOUNDARIES

AUXDEFENSE

2024

4TH WORLD CONFERENCE ON ADVANCED MATERIALS FOR DEFENSE

BOOK OF ABSTRACTS

Edited by Raul Fangueiro

BOOK OF ABSTRACTS

Edited by
RAUL FANGUEIRO

Design
PRAGMATIC BY PIXARTIDEA

Publisher
SCIENCENTRIS

Representation in whole or in part by any means is not permitted without consent of the editors

Authors
Multiple

Title
Proceedings of the 4th World Conference on Advanced Materials for Defense

ISBN
978-989-54808-9-0

Organizers

REPÚBLICA PORTUGUESA
DEFESA NACIONAL

Universidade do Minho

Fibrenamics

SCIENCENTRIS
From Knowledge to Market

Gold Sponsors

Silver Sponsor

Bronze Sponsor

econcore
economic core technologies

piep
innovation in polymer engineering

Riopele
SINCE 1927

MDPI

FOREWORD

It is with great pleasure that we present the Book of Abstracts for AUXDEFENSE2024 – the 4th World Conference on Advanced Materials for Defense. This compilation is a testament to the remarkable progress and innovation in the field of advanced materials, underscoring their critical role in enhancing defense capabilities and ensuring security.

In today's rapidly evolving technological landscape, the development and application of advanced materials have become pivotal to addressing the multifaceted challenges faced by modern defense systems. From lightweight composites and high-strength alloys to smart materials and nanotechnology, the advancements in this domain are transforming the defense sector, offering unprecedented performance, durability, and functionality.

This conference, now in its fourth edition, brings together leading researchers, scientists, engineers, and industry experts from around the world to share their latest findings, discuss cutting-edge technologies, and explore new directions for future research and development. The diverse range of topics covered in these abstracts reflects the breadth and depth of ongoing research and its potential impact on defense applications.

As you delve into these abstracts, you will encounter groundbreaking studies on materials that promise to revolutionize protective gear, enhance the survivability and efficiency of military vehicles, improve the resilience of critical infrastructure, and provide novel solutions for sensing and communication technologies. The innovative approaches and methodologies presented here not only highlight the current state of the art but also pave the way for future breakthroughs that will further strengthen our defense capabilities.

We extend our deepest gratitude to all the contributors for their dedication and hard work in advancing the field of advanced materials. Their collective efforts are instrumental in driving progress and fostering collaboration within the defense community. We also thank the organizing committee, reviewers, and sponsors for their invaluable support in making this conference a success.

It is our hope that this Book of Abstracts will serve as a valuable resource and inspiration for researchers, practitioners, and policymakers alike. By fostering a deeper understanding of advanced materials and their applications, we can collectively contribute to a safer and more secure future.

Braga/Portugal, 20th June 2024

Raul Fangueiro
Conference Chairman

CONFERENCE CHAIR

Raul Fangueiro, President of Fibrenamics / Vice-Dean School of Engineering – University of Minho

SECRETARIAT

Claúdia Silva, Fibrenamics, University of Minho
Pedro Pacheco, Fibrenamics, University of Minho
Rui Azevedo, Fibrenamics, University of Minho

ORGANIZING COMMITTEE

Ana Fangueiro, Sciencentris
Adriana Alves, Sciencentris
Carlos Mota, Fibrenamics, University of Minho
Carina Leitão, Pragmatic by Pixartidea
Daniela Pinto, Pragmatic by Pixartidea
Diana Ferreira, Fibrenamics, University of Minho
Fernando Cunha, Fibrenamics, University of Minho
João Bessa, Fibrenamics, University of Minho
João Sampaio, Pragmatic by Pixartidea
Joana Antunes, Fibrenamics, University of Minho
Sara Silva, Fibrenamics, University of Minho
Tiago Sousa, Pragmatic by Pixartidea

SCIENTIFIC COMMITTEE

António Torres Marques, University of Porto, Portugal

Andreas Heine, Fraunhofer Institute, Germany

Ayse Bedeloglu, Bursa Technical University, Turkey

Chee Lip Gan, Nanyang Technological University, Singapore

Conceição Paiva, University of Minho, Portugal

Daniel Ambrosini, National University of Cuyo, Argentina

Daniel Rittel, Faculty of Mechanical Engineering, Technion, Israel

Denis Josse, Alpes-Maritimes Fire & Rescue Services, France

Diana Ferreira, University of Minho, Portugal

Evaldo Corat, INPE – National Institute for Space Research, Brazil

Fabiana Arduini, University of Rome "Tor Vergata", Italy

Fabrizio Scarpa, University of Bristol, UK

Fernando Cunha, University of Minho, Portugal

Ferrie van Hattum, Saxion University of Applied Sciences, The Netherlands

Filipe Teixeira-Dias, The University of Edinburgh, UK

Francois Boussu, ENSAIT – GEMTEX Laboratory, France

Genevieve Langdon, The University of Sheffield, UK

Gustavo Dias, University of Minho, Portugal

Haim Abramovich, Technion - Israel Institute of Technology, Israel

Harri Lipsanen, Aalto University, Finland

Hong Hu, The Hong Kong Polytechnic University, Hong Kong

Igor L. Medintz, U.S. Naval Research Laboratory, USA

Joaquim Vieira, University of Aveiro, Portugal

José Borges, CINAMIL, Portugal

Jun Lou, Rice University, USA

Lars Montelius, International Iberian Nanotechnology Laboratory, Portugal

Michael May, Ernst-Mach-Institut, Germany

Michele Meo, University of Bath, UK

Nunzio Cennamo, University of Campania Luigi Vanvitelli, Italy

Patricia Verleysen, Ghent University, Belgium

Pedro Rosa, University of Lisbon, Portugal

Per - Erik Johansson, Umea University, Sweden

Raffaele Solimene, University of Campania Luigi Vanvitelli, Italy

R. Alagirusamy, Indian Institute of Technology Dehli, India

René Rossi, Laboratory for Biomimetic Membranes and Textiles, Empa, Switzerland

Robert Young, University of Manchester, UK

Sandra Carvalho, SPM – Sociedade Portuguesa dos Materiais, Portugal

Seeram Ramakrishna, National University of Singapore, Singapore

Seshadri Ramkumar, Texas Tech University, USA

Sohel Rana, University of Huddersfield, UK

Steven Savage, Swedish Defence Research Agency, Sweden

Xiaogang Chen, University of Manchester, UK

Xin-Lin Gao, Southern Methodist University, USA

TABLE OF CONTENTS

INVITED LECTURE
STATIC AND DYNAMIC FRACTURE MECHANICS OF PRINTED ALUMINUM LATTICES
Daniel Rittel, Yahav Boim and Amnon Shirizly

INVITED LECTURE
COMPOSITE MANUFACTURING PROCESS SIMULATION: THEORETICAL AND PRACTICAL PERSPECTIVE
Raúl Guichón

INVITED LECTURE
GRAPHENE AEROGELS DEVELOPMENT FOR AEROSPACE APPLICATIONS
Evaldo Corat

INVITED LECTURE
A NEW PROCESSING ROUTE FOR IMPROVING FIBRE-MATRIX INTERFACE AND MECHANICAL PROPERTIES OF PLANT-FIBRE REINFORCED THERMOPLASTIC COMPOSITES
Sohel Rana

ORAL PRESENTATIONS
ID 1
INTEGRATION OF STRATEGIC DESIGN AND 3D SIMULATION TECHNOLOGIES TO ENHANCE ECG SIGNAL QUALITY AND CUSTOMIZED FIT FOR IMPROVED HEALTH MONITORING

Seonyoung Youn, Kavita Mathur, Amanda C. Mills

ID 4
FUZZY TOPSIS FOR GROUP DECISION MAKING: A CASE STUDY FOR NIGHT VISION GOGGLES
İsmail Gevrek, Metin Gürü, Fatih Emre Boran

ID 5
HIGH-VELOCITY IMPACTS AGAINST PLAIN CONCRETE
Conceição, J. F. M., Corneliu, C., Rebelo, H., Chambino, M., Pereira, L.

ID 6
THE DIGITAL PILOT – FIBER-BASED SENSORS FOR EARLY DIAGNOSTICS OF COGNITIVE IMPAIRMENTS OF AIR FORCE PILOTS
René Michel Rossi ,Denis Bron , Bauer Frederik , Simon Annaheim

ID 7
HETEROSTRUCTURES OF PT-AG/LAYERED DOUBLE HYDROXIDES WITH PHOTOCATALYTIC ABILITIES TO DEGRADE BACTERIA AND TOXIC CHEMICALS
Gabriela Carja, Denis Cutcovschi, Sofronia Bouariu

ID 8

A NEW PETAL-LIKE STRUCTURE WITH LIGHTWEIGHT, HIGH STRENGTH, HIGH ENERGY ABSORPTION, AND AUXETIC CHARACTERISTICS

Zhenyu Li, Jian Xiong, Hong Hu

ID 9

OUT OF PLANE STRATEGY FOR MANUFACTURE LARGE SCALE DRONE COMPOSITE MOLDS WITH ADDITIVE MANUFACTURING

César García-Gascón, Pablo Castelló-Pedrero, and Juan A. García-Manrique

ID 12

AN EXPERIMENTAL STUDY ON THE INFLUENCE OF BACKING MATERIAL ON THE BALLISTIC IMPACT RESPONSE OF MULTI-LAYERED COMPOSITE STRUCTURES

Oscar Lafuente Arjona, Lucas Amaral, Nick Eleftheroglou

ID 13

DETECTION OF VIRUSES AND BACTERIA FOR DEFENSE VIA INTERNET OF THINGS AND OPTICAL CHEMICAL SENSORS

Francesco Arcadio, Ines Tavoletta, Chiara Marzano, Fiore Capasso, Luca Pasquale Renzullo, Luigi Zeni,Nunzio Cennamo

ID 14

A NOVEL 3D HYBRID AUXETIC LATTICE STRUCTURE WITH ENHANCED LOAD BEARING CAPACITY.

Keda Li, Binggang Xu, Jian Xiong, Hong Hu

ID 16

ADVANCED 3D MODELLING AND SIMULATION METHODOLOGY TO IMPROVE DESIGN PROCESS FOR HYBRID COMBAT-READY CBRN SUITS

Afonso Gonçalves, Tânia Ferreira, A. Catarina Vale, Carlos Silva, Paula Lopes, Inês Cruz, Amin Taoufiq, Raquel Pinheiro, Humberto Guimarães, Pedro Magalhães, Luisa M. Arruda, Joana C. Antunes, Pedro Neto, Wilson Antunes, Clementina Freitas, Fernando Cunha, Inês P. Moreira and Raul Fangueiro

ID 17

NATURAL FIBERS AND NANOMATERIALS FOR ADVANCED MULTIFUNCTIONAL PROTECTIVE FIBROUS STRUCTURES

Joana C. Araújo, Raul Fangueiro, Diana P. Ferreira

ID 18

OPTIMIZING BLAST RESPONSE: MATERIAL IMPROVEMENT FOR SANDWICH STRUCTURES WITH LATTICE CORE MANUFACTURED VIA L-PBF

Elisa Guimaraens1, Konstantin Kappe1, Aron Pfaff1, Jürgen Herrmann1, Klaus Hoschke1

ID 20

ENERGY RELEASE CHARACTERISTICS OF REACTIVE SHAPED CHARGE LINERS PENETRATION INTO UNDERWATER

Tianchu Wang, Pengwan Chen, Chuan Zhao, Shouren Wang

ID 22
THERMAL MANAGEMENT OF ELECTRONIC COMPONENTS IN UNMANNED AERIAL VEHICLES USING PDMS HEAT SINKS
Ana S. Moita, João Paulo N. Torres, Énio Chambel, Luís Quinto, Pedro Pontes, António L. N. Moreira

ID 24
EXPERIMENTAL INVESTIGATION OF THE DYNAMIC RESPONSE OF LOW-DENSITY FOAM-WRAPPED ALUMINUM TUBES UNDER LOCALIZED BLAST LOADING
Ben Rhouma Mohamed, Aminou Aldjabar, Maazoun Azer, Belkassem Bachir, Tine Tysmans, and Lecompte David

ID 25
PARAMETRIC STUDIES OF A 2D EXTRUDED MODIFIED DOUBLE ARROWHEAD STRUCTURE FOR ENERGY ABSORPTION PERFORMANCE
Vivianne Marie Bruère, Andrei Constantinescu

ID 26
FRAGMENT IMPACT ON CONCRETE SLABS – AN EXPERIMENTAL AND NUMERICAL STUDY
Øystein E.K. Jacbosen, Martin Kristoffersen, Sumita Dey, Tore Børvik

ID 28
DYNAMIC RESPONSE AND ENERGY ABSORPTION OF MENGER FRACTAL-INSPIRED POROUS STRUCTURES
Madhusha Bogahawaththa, Damith Mohotti, Paul J. Hazell, Hongxu Wang

ID 29
ADDITIVE MANUFACTURING OF RADAR ABSORBING MATERIALS
Matthias Bleckmann, Stefan Ehard, Maximilian Krönert, Sebastian Peters, Joshua L. Obermeyer

ID 31
STUDY OF IMPACT BEHAVIOUR OF SHEAR THICKENING FLUID (STF)REINFORCEMENTS IN CORK COMPOSITE STRUCTURES
Telmo R.M. Fernandes, Gabriel F. Serra, R.J. Alves de Sousa, Fábio A.O. Fernandes

ID 32
ADDITIVE MANUFACTURED MARAGING STEEL UNDER BALLISTIC IMPACT: EXPERIMENTS AND NUMERICAL MODELLING
Maisie Edwards-Mowforth, Miguel Costas, Martin Kristoffersen, Filipe Teixeira-Dias, Tore Børvik

ID 33
NANOPARTICLE-MEDIATED BACTERICIDAL ACTION AGAINST THE MOST COMMON GRAM-POSITIVE PATHOGEN CAPABLE OF COLONIZING DIABETIC FOOT ULCERS
Joana M. Domingues , Rosana Monteiro, Carla Silva, Helena P. Felgueiras, Maria Olívia Pereira,

Joana C. Antunes

ID 34

INTEGRATION OF FLEXIBLE INTERCONNECT FOR MULTILAYER TEXTILE-BASED WEARABLE DEVICE
Prateeti Ugale

ID 35

AN INNOVATIVE SOLUTION FOR FEMALE BODY ARMOUR
Mulat Alubel Abtew, Francois Boussu, P. Bruniaux

ID 36

EXPERIMENTAL INVESTIGATION OF COMPRESSIVE BEHAVIOR IN CALCIUM-SILICATE MINERAL FOAM
Aldjabar Aminou, Mohamed Ben Rhouma, Bachir Belkassem, Lincy Pyl, David Lecompte

ID 37

COMPARATIVE ANALYSIS OF THERMAL RESISTANCE PROPERTIES IN ACTIVITY WEAR FABRICS: CASE STUDY
Inga DABOLINA, Liene SILINA, Eva LAPKOVSKA

ID 38

DIAMOND TEMPERATURE SENSORS FOR HARSH ENVIRONMENTS
Miguel A. Neto, Bernardo L. Tavares, Sérgio Pratas, Eduardo L. Silva, Filipe J. Oliveira, Rui F. Silva

ID 39

DEVELOPMENT OF CUSTOM LARGE SCALE 3D PRINTING TECHNOLOGIES FOR IN SITU THERMOPLASTIC MATERIAL REUSE AND VALORISATION IN AREA OF OPERATIONS
Luis Ignacio Suárez, Juan Carlos Piquero, Blas Puerto Valcarce, Raúl Marqués Bada.

ID 40

PIEZORESISTIVE PRINTED SENSORS FOR MEASURING ELONGATION OF PARACHUTE CANOPY FABRIC AND RIBBONS
DORMOIS THIBAULT, COCHRANE CÉDRIC, KONCAR VLADAN
ID 41

COMPUTATIONAL MODELING AND EXPERIMENTAL TESTING OF A NEW FOAM-FILLED GRADED AUXETIC PANEL
Hasan AL-RIFAIE,Nejc NOVAK, Alessandro AIROLDI, Tomasz ŁODYGOWSKI

ID 42

CHALLENGES IN THE VIRTUAL PRODUCT DEVELOPMENT OF PROTECTION VESTS
Sophie Herz, Felix Kunzelmann, Yordan Kyosev

ID 43

A USER-CENTRIC EVALUATION OF THERMOPHYSIOLOGICAL COMFORT OF DEFENSE CLOTHING SYSTEMS USED IN HOT CLIMATE OPERATIONS

Magdalena Georgievska, Sheilla Odhiambo, Cosmin Copot, Hilda Wullens, Benny Malengier, Lieva Van Langenhove

ID 44

ON THE MULTISCALE MODELLING OF THE IMPACT BEHAVIOUR OF WOVEN MATERIALS USING EQUIVALENT MICROSCOPIC FIBERS WITH 3D SHELL ELEMENTS

Tuan-Long Chu, Cuong Ha-Minh, Abdellatif Imad, Quoc-Hoan Pham

ID 45

ELECTROCHEMICAL IMPEDANCE SPECTROSCOPY OF DEBYE DIELECTRIC SPECTRA: A NUMERICAL COMPARISON

Roberto Dima, Maria Antonia Maisto, Luigi Rubino, Raffaele Solimene

ID 46

POLY(LACTIC ACID) AS A PROMISING MATERIAL FOR SELF-HEALING FIBRE-REINFORCED COMPOSITES

Luísa Durão, Carlos Mota, Luís Nobre, João Bessa, Fernando Cunha, Raúl Fangueiro

ID 47

ANALYTICAL DESIGN OF AUXETIC COMPOSITE LAMINATES

Cristiano Veloso, Carlos Mota, Luís Nobre, João Bessa, Fernando Cunha, Raúl Fangueiro

ID 48

EXPERIMENTAL AND NUMERICAL ANALYSIS OF STAINLESS-STEEL AND UHMWPE FML PLATES UNDER BALLISTIC IMPACT

Valverde Marcos, Borja, Rubio Díaz, Ignacio, Wang, Liu-Jiao, Santiuste Romero, Carlos, Miguélez Garrido, M.Henar, Loya Lorenzo, José Antonio

ID 51

HIGH TEMPERATURE REGULATION OF IMPROVED FLEXIBLE COMPOSITES FOR SATALLITE IMPACT SHIELDS

Daniel Barros(*), Carlos Mota, Luís Nobre João Bessa, Fernando Cunhaand Raul Fangueiro

ID 52

COMPARISON OF MECHANICAL BEHAVIOR AGAINST LOW AND HIGH VELOCITY IMPACT ON ARAMID AND UHMWPE PLATES

Valverde Marcos, Borja, Rubio Díaz, Ignacio, Wang, Liu-Jiao, Santiuste Romero, Carlos , Miguélez Garrido, M.Henar, Loya Lorenzo, José Antonio

ID 54

RECENT DEVELOPMENTS OF AUXETIC KNITTED FABRICS AND THEIR POTENTIAL APPLICATIONS

Hoa Nguyễn, Raul Fangueiro, Fernando Ferreira, and Quyền Nguyễn

ID 55

NUMERICAL STUDY OF VERTICAL BARRIERS AGAINST ACCIDENTAL BLASTS CAUSED BY FAILURE OF SAFETY MEASURES

Abraham Fernández del Rey, Josué Aranda Ruiz, José A. Loya Lorenzo

ID 56

STUDY OF THE MECHANICAL PERFORMANCE OF ALUMINUM 5083-H111 FOR A WIDE RANGE OF TEMPERATURES AND LOADING RATES

Afonso Gregório, Leigh Sutherland, Tiago Silva, Abílio de Jesus, Pedro Rosa

ID 58

LOAD CARRYING SYSTEM DESIGN OPTIMIZING

Nataliya Sadretdinova, Chi Tiet Nung, Yordan Kyosev

ID 59

CORRELATION BETWEEN EXPERIMENTAL THERMAL RESISTANCES AND VARIOUS MODELS

Solène Champigny, Cyprien Bourrilhon, Fabien Salaün, Cédric Cochrane

ID 61

ASSESSMENT OF THE INFLUENCE OF GRAPHENE SHEET SIZE ON THE DEVELOPMENT OF ADVANCED TEXTILE SUBSTRATES WITH CONDUCTIVE PROPERTIES FOR DEFENSE FIELD

Maria J. Martins, Leonor Cunha, Adriana Pereira, Ana Barros, André Barbosa, Nuno Araujo, Maria António, Gilda Santos

ID 62

FERRITE-GRAFT-CNT AND PBSA COMPOSITES FOR EM SHIELDING AND HEAT DISSIPATION IN DEFENCE APPLICATIONS

Miks Bleija, Artis Krikovs, Sergejs Gaidukovs

ID 66

UNIFYING COMFORT AND PROTECTION IN A CBRN SUIT

Tânia Ferreira, A. Catarina Vale, Alexandra Pinto, Diana Sousa, Inês P. Moreira,Carlos Silva, Fernanda Gomes, Paula Lopes, Inês Cruz, Amin Taoufiq, Raquel Pinheiro, Pedro Magalhães, Joana C. Antunes, Mariana Henriques Pedro Neto, Wilson Antunes, Fernando Cunha, and Raul Fangueiro

ID 67

EXPERIMENTAL INVESTIGATION OF THE DYNAMIC RESPONSE OF LOW-DENSITY FOAM-WRAPPED ALUMINUM TUBES UNDER LOCALIZED BLAST LOADING

Ben Rhouma Mohamed, Aminou Aldjabar, Maazoun Azer, Belkassem Bachir, Tysmans Tine, and Lecompte David

ID 68

EVALUATION OF TENSILE PROPERTIES OF INPLANE AUXETIC COMPOSITE LAMINATES

Cristiano Veloso, Carlos Mota, Luís Nobre, João Bessa, Fernando Cunha, Raúl Fangueiro

ID 69

DAMAGE MONITORIZATION CAPACITY OF BALLISTIC COMPOSITES AFTER A HIGH-VELOCITY IMPACT: SMART SHIELDS

Daniel Barros(*), Luís Nobre, Carlos Mota, João Bessa, Fernando Cunhaand Raul Fangueiro

ID 70

ELECTROSPUN MEMBRANES BASED ON PAN/AC FOR AIR FILTRATION AND ACTIVE DEGRADATION OF MICROORGANISMS

Joana M. Rocha, Rui P. C. L. Sousa, Joana C. Araújo, Sofia M. Costa, Vasco Pontes, Wilson Antunes, Raul Fangueiro, Diana P. Ferreira

ID 71

THE IMPACT OF ZINC OXIDE AND GRAPHENE-BASED NANOPARTICLES ON THE CHEMICAL AND BIOLOGICAL PROTECTION OF 3D KNITTED STRUCTURES

Liliana Leite , Vânia Pais, João Bessa, Fernando Cunha, Cátia Relvas, Noel Ferreira, Raul Fangueiro

ID 72

EVALUATING THE CHARACTERISTICS OF SANDWICH COMPOSITE STRUCTURES UNDER QUASI-STATIC LOADING

Opukuro David-West, Anish Girish Advani

ID 73

BALLISTIC RESISTANCE OF MODULAR PROTECTIVE SANDWICH PANELS

Petr Hála, Jiří Mašek, Alexandre Perrot, Přemysl Kheml, Radoslav Sovják

ID 74

MECHANICAL BEHAVIOR SIMULATION OF POLYMER BONDED EXPLOSIVE AT MESO SCALE BY NUMERICAL MANIFOLD METHOD

Ge Kang, Peng-wan Chen

ID 75

SIMPLE MECHANOCHEMICAL SYNTHESIS OF TRANSITION METAL HYDRIDES FOR ENERGY STORAGE APPLICATIONS

Marek Polański, Iwona Wyrębska,

ID 76

TUNING THE MECHANICAL PROPERTIES OF CRCOFEMNNI HIGH ENTROPY ALLOY VIA COLD SPRAY ADDITIVE MANUFACTURING ASSOCIATED WITH HEAT TREATMENT

Bemechal Tsegaye Mengiste, Ali Arab, Yansong Guo, Yinze Lei, Xiaoshuai Li, Pengwan Chen, Jing Xie

ID 77

POLYMER COMPOSITE AND STRUCTURES FOR ENHANCED ELECTROMAGNETIC PROTECTION AND CYBERSECURITY

Sergejs Gaidukovs, Miks Bleija, Oskars Platnieks

ID 112

EFFECT OF GRAPHENE NANOPLATELET CONTENT AND TEXTILE SUBSTRATE ON THE THERMOELECTRIC PROPERTIES OF CONDUCTIVE TEXTILES

Luisa M. Arruda, Beate Krause, Antonio J. Paleo, Petra Pötschke, Raul Fangueiro

ID 115

ACCELERATED AGING OF DYNEEMA® SB21 UD OBTAINED FROM 20 YEARS OLD BALLISTIC RESISTANT VEST

Harm van der Werff, Hans Meulman, Raul Perez-Graterol

ID 116

IMPACT BEHAVIOUR ON COMPOSITE MATERIAL WITH EMBEDDED NON-NEWTONIAN FLUIDS

Konstantinos Myronidis, Abdelrahman Hegazy, Fulvio Pinto, Michele Meo*

ID 117

SHAPE INFLUENCE ON THE CRASHWORTHINESS PERFORMANCE OF FLAX AND HYBRID/EPOXY COMPOSITES

Valentina Giammaria, Giulia Del Bianco, Monica Capretti, Simonetta Boria

ID 120

SURFACE FUNCTIONALIZATION STRATEGIES FOR THE CREATION OF MULTIFUNCTIONAL FABRICS

Sourabh Kulkarni , Shiran Yu , Zhiyu Xia , Alexander B. Morgan , Jayant Kumar , Ravi Mosurkal *, Ramaswamy Nagarajan *

POSTER PRESENTATIONS

ID 2

DEVELOPMENT OF TECHNICAL TEXTILE FABRICS FOR ELECTROMAGNETIC SHIELDING PURPOSES

Kadriye Kutlay, Nejla Degirmenci, Özlem Buluş

ID 3

HAND ANTHROPOMETRY OF BANGLADESHI UNIVERSITY STUDENTS

Engr. Md. Eanamul Haque Nizam, Emeritus Prof. Darko Ujevic, Prof. Dr. Engr. Ayub Nabi Khan, Bristy Rani Roy, Badhan Chandra Roy

ID 11

MG-BASED ALLOYS THIN FILMS DERIVED FROM MGAL LAYERED DOUBLE HYDROXIDES RECONSTRUCTED IN OXYGEN-RICH ENVIRONMENTS

Loredana Andreea Gavrila, Elena Mihaela Seftel, Gabriela Carja*

ID 49

BEHAVIOR OF HANDGUN PROJECTILES FIRED TO BLOCKS OF BALLISTIC GELATIN

Ruano Rando, Manuel Jesús , Jiménez Jiménez, José Ángel, Loya Lorenzo, José Antonio

ID 50

LOW TEMPERATURE REGULATION OF IMPROVED FLEXIBLE COMPOSITES FOR SATALLITE IMPACT SHIELDS

Daniel Barros(*), Carlos Mota, Luís Nobre João Bessa, Fernando Cunhaand Raul Fangueiro

KEYNOTE LECTURE
IS MATERIALS RESEARCH A FOUNDATIONAL PILLAR OF THE EU DEFENSE INNOVATION?

Giuseppe G. Daquino[1][(*)]
[1] European Defence Agency, Brussels, Belgium
[(*)] Email: giuseppe.daquino@eda.europa.eu

ABSTRACT

The European Defence Agency (EDA) launched in 2022 the Hub for EU Defence Innovation (HEDI) with the aim to serve as platform to stimulate and facilitate cooperation on defence innovation among Member States while ensuring synergies with related European Commission activities and coherence with NATO innovation initiatives. The innovation in EU defence spans at different stages of the Technology Readiness Level (TRL). For this purpose, HEDI is meant to focus on activities from proof of concept to uptake of innovation.

EU defence innovation is strongly linked to the EU strategic autonomy, which is deployed into the capability to cover many sectors of the supply chain, especially in critical technologies. In addition, the (almost) full EU dependency from specific Third Countries for some critical raw materials (CRM) implies the need of advanced process to re-use, recycle and replace (if necessary) the most strategic CRMs.

Materials research is one of the R&T activity pillars at the European Defence Agency as well as within the European Defence Fund (EDF) of the European Commission. In order to support the HEDI framework a multi-year programme (ICARO) was launched at the end of 2023, structured on 4 Strategic Research Clusters, embedding development areas in the land, maritime, air and cross-cutting domains.

In EDF a full category is dedicated to Materials & Components research since 2021, with the goal to enabling defence capabilities, yet not mature at EU level. In addition, the European Defence Innovation Scheme (EUDIS) initiative is more and more fostering materials R&T in order to enhance the dual-use technology transfer mechanism (DU2TM).

INTRODUCTION

The EU defence is still too fragmented and needs a strong collaboration effort to enhance its capabilities. In addition, EU is strongly dependent on Third Countries for certain critical raw materials (CRM), used in civilian and military industry. Therefore, urgent actions are required to facilitate EU-shared interventions in the concerned supply chains, along the full spectrum.

In this context, the European Commission (EC) and the European Defence Agency (EDA) are fully involved to prepare the grounds for investments helping the Member States and their defence industry/research centres to collaborate and provide solutions to enhance the EU strategic autonomy. These actions require investment plans tackling the circularity of CRMs (re-use, recycling, replacement with innovative advanced materials), the shared enhancement of defence capabilities and unleashing the potentiality of dual use technology transfer mechanism, as powerful economic driver in the EU internal market.

RESULTS AND CONCLUSIONS

The EU geopolitical scenario is dramatically changed in the recent years. The war in Ukraine is the evident effect. However, the need of a coordinated effort in EU defence was under the lens of the subject matter experts much before the advent of the war.

The mantra is "spending more and better to protect the EU people". There are too many weapons platforms in the

EU Member States (MS). An evident example is the number of tanks: there are 17 different tanks in EU, while only 1 in the USA (see Fig.1 [1]). In turn, this implies duplications, dysfunctional budget use, serious issues of interoperability and military mobility.
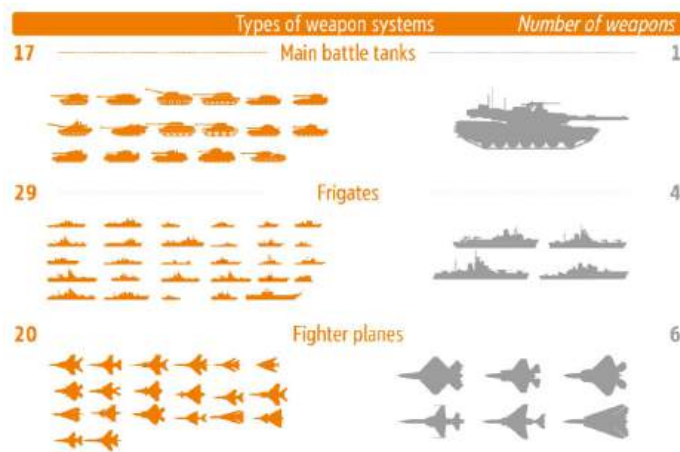
Fig. 1 Types of weapon systems in EU

To respond to this general issue, the EU MS should enhance their cooperation, not only in the acquisition phase, but starting from the beginning of the supply chain, where the technology readiness level (TRL) is still low.

In other words, EU MS should invest in enabling EU innovation, through sharing their capabilities to the maximum extent possible.

In turn, this can only happen if the EU defence is developed from the beginning of the supply chain. And in this context, the materials research plays an outstanding role.

Making the EU defence stronger, it also means making strategic autonomy a reality. The European Union is strongly dependent from Third Countries for the extraction of critical raw materials. For some of them, the dependence is also in the manufacturing and assembly lines (see Fig.2 [2] and Fig.3 [3])
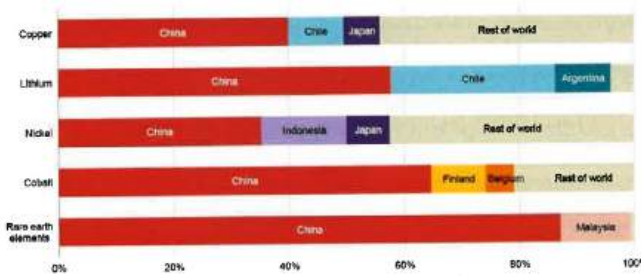
Fig. 2 EU dependence on Third Countries for CRM
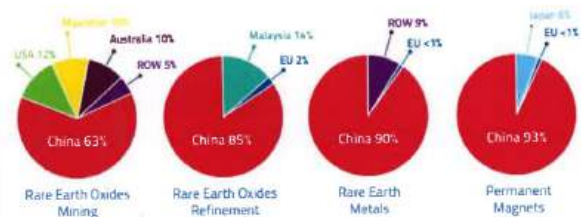
Fig. 3 Permanent magnets, EU dependence breakdown along the supply chain

This situation needs important investments in the extraction sector in a sustainable approach, but also enhanced recycling processes or, whenever necessary, replacement of the materials. In this context, materials research and innovative manufacturing processes play a fundamental role, in finding alternatives that offer similar or even better performances. For example, additive manufacturing can help in reducing the water need in the production, but also in optimising the material source, as well as in enhancing the logistics performance (very relevant in the defence sector, that operates often in remote world places).

In this context, the European Commission identified 16 strategic critical materials (within the 34 CRMs), whose supply chain deserve additional focus in the coming years.

EU Ministries of Defence at the EDA Steering Board on 17 May 2022 established in EDA the Hub for EU Defence Innovation (HEDI) [4]. It is composed by different actions, with communication/awareness focus (e.g. innovation prizes, innovation papers, innovation days) and with implementation actions (e.g. innovation challenges, proof of concept generation, uptake of innovation).

Enhancement of inter-institutional collaboration through HEDI and the EU Defence Innovation Scheme (EUDIS) [5] is desirable, unleashing the potentiality of dual-use technologies in order to enhance the strategic autonomy in critical technologies and materials.

Materials research is a cornerstone in this challenge, because it can offer solutions for all the HEDI innovation actions. In addition, the European Defence Fund (EDF) category of action Materials and Components contains specific mention to the EUDIS scheme, to which the EDF funding is expected to provide a strong contribution. At

the same time, the EDA ICARO CatB programme, under implementation within the EDA Materials CapTech, focus to the same role, which will be more and more relevant due to the exponential market demand of new technologies, dramatically in need of ***advanced circular materials and manufacturing processes***.

REFERENCES

[1] European Parliamentary Research Service, "Ten ways that Europe could do more for you", Feb 2024, ISBN 9789284815364

[2] International Energy Agency, "The role of critical minerals in clean energy transitions", 2022 (Data for 2019)

[3] European Commission, "EU strategic dependencies and capacities: second stage of in-depth reviews", SWD(2022) 41 final

[4] EDA Factsheet, Hub for EU Defence Innovation (HEDI), https://eda.europa.eu/docs/default-source/brochures/hedi-factsheet-(final).pdf

[5] EU Defence Innovation Scheme Factsheet, https://eudis.europa.eu/document/download/3d382c48-1dec-4de0-97bf-15bbabea7024_en?filename=20240312%20-%20EUDIS%20factsheet%20v11.pdf

KEYNOTE LECTURE
MATERIAL RELATED CHALLENGES FOR MAINTAINING AND DEVELOPING AIRFRAMES FOR SUSTAINABLE AIRPOWER

Thomas Koerwien

Airbus Defence and Space GmbH, Rechliner Str., 85077 Manching, Germany

(*) Email: thomas.koerwien@airbus.com

ABSTRACT

Materials, in particular material systems, are the very foundation of each aircraft. In military applications performance and durability are key drivers. E.g. the C160 Transall transport aircraft has been in service since 1967 while being replaced by A400M now. This translates to roughly 50+ years of service life. For fighter aircrafts the service life is similar. The material systems are subjected to multiple stresses during its lifetime ranging from environmental stresses to actual damages, e.g. ground operations or in flight incidents like bird strike or other ballistic threats. Maintenance and repair technology is a must to keep the fleet airborne. At the same time the running production of aircrafts is heavily impacted by legislation. The eradication of hazardous substances imposed by REACH such as CrIV poses a major challenge since multiple materials, in particular surface protection systems are affected. Other substances are emerging, ranging from BPA, affecting composites, to PFAS, affecting e.g. sealants and lubricants. The substance replacements are also impacting new emerging programs and airpower capabilities such as Eurodrone and Future Combat Air System (FCAS) with its 6th generation fighter (New generation weapon system – NGWS) and drone systems. In particular for NGWS durable low observability material systems of the airframe are key along with composite materials sustaining higher temperatures. Potential introduction into service is foreseen in the 204x, while prototypes are foreseen within this decade. With the war theatres raging in Ukraine and the middle east conflicts are inching closer to Europe. This is driving scalability and affordability in building aircrafts at the same time.

The challenges, in particular for military air systems are common for maintenance, operation, and development of new platforms. Even though the defence market is perceived as a relatively big industrial player the material demand is very specific in requirements, low in volume, long duration of programs and commitments, and long time to market. This makes the defence business for suppliers a potential niche rather than a mass market. While the supplier landscape poses challenges, so do the national defence budgets which put certain strain also on the R&T as well as R&T efforts. Smart spending is key to wisely develop technologies while building up a strategic network with established and evolving / non-traditional suppliers. A vital key to this approach are funding schemes on national as well as European level like European Defense Fund (EDF).

An overview will be given for development of repair solutions for metallic as well as composite parts using additive and bonding technology. Examples will be presented to ensure continuous production of platforms such as e.g. Eurofighter and C295 in the wake of Reach imposed substance replacements. Furthermore, challenges in the development of materials for low observability applications will be presented together with structural concepts and technology aiming for scalability.

KEYNOTE LECTURE
SUSTAINABLE SHIELDING: BALLISTIC PERFORMANCE OF LOW-CARBON CONCRETE

Øystein E.K. Jacbosen[1], Martin Kristoffersen[1], Sumita Dey[2], Tore Børvik[1,2(*)]

[1] Structural Impact Laboratory (SIMLab), Department of Structural Engineering, NTNU – Norwegian University of Science and Technology, NO-7491, Trondheim, Norway.

[2] Research and Development Department, Norwegian Defence Estates Agency, NO-0151, Oslo, Norway.

[(*)] Email: tore.borvik@ntnu.no

ABSTRACT

The increasing global demand for sustainable materials and material usage in both civilian applications and the military sector raises the question whether low-carbon concrete can withstand extreme loads equally well as standard concrete. Few studies have investigated the protective performance of low-carbon concrete where low-emissions supplementary cementitious materials replace all or part of the cement.

To address this question, we conducted ballistic experiments firing ogival steel projectiles at 100 mm thick concrete targets. We used standardised material tests to compare the quasi-static material behaviour of three concretes with different levels of CO_2 emissions. The ballistic experiments revealed no significant difference in protectional ability when reducing CO_2 emissions, demonstrating promising potential in protecting against extreme loads. For additional details of this study the reader is referred to Jacobsen et al. [1].

INTRODUCTION

Concrete is the second most consumed material in the world after water, owing to its durability, availability, high compressive strength, and cost efficiency. Estimates in the literature show that the emission from concrete production is between 5-7% of the annual anthropogenic carbon emission, with the main part of the emissions stemming from the production of cement clinker [2]. A common way to reduce emissions is to reduce part of the cement with supplementary cementitious materials, so-called SCMs. The main industrial SCMs are fly ash, silica fume and ground granulated blast furnace slag. When replacing the cement with either of these materials, it is important that the mechanical properties of the lower-emission concretes are not inferior to standard concretes. The use of low-carbon concrete should not compromise its durability nor its resistance to conventional loads [3]. Critical infrastructure, civilian buildings and military equipment are at constant risk of both intentional and unintentional extreme dynamic loads. We thus need detailed knowledge of how such an important building material behaves under these loads. One of the most severe forms of extreme dynamic loads is ballistic impact. In this study, we investigate the ballistic perforation resistance of 100 mm thick concrete slabs, cast from three commercially available C75 concretes with different amounts of CO_2 emissions. The LC20 concrete had 22% reduction in CO_2 emissions compared to the standard concrete (NC), while the LC50 concrete had 58% reduction in CO_2 emissions. Please leave this line blank

RESULTS AND CONCLUSIONS

Fig. 1 shows the ballistic limit curves for all three concretes tested 28 days post casting tested in a gas-gun facility. The data points for the initial and residual velocities are fitted to the Recht-Ipson model, commonly used to compare ballistic perforation resistance across material characteristics, target configurations and projectile characteristics. The results from 28 days post casting show that all three materials have approximately the same ballistic limit velocity, vbl. However, for velocities well above vbl, we see that LC50 slightly underperforms compared to

NC and LC20. This is probably related to the compressive strength of the LC50 being slightly lower than NC and LC20 on day 28. When we look at the long-term ballistic results (Fig. 2), we see that there is almost no difference between LC20 and LC50.

The results from the ballistic impact tests showed no significant differences in ballistic perforation resistance when reducing CO_2 emissions. Table 1 summarises the properties of the three materials. It is evident that by reducing the standard cement by SCMs, we can keep the equivalent binder content similar. The CO_2 intensity is essentially the global warming potential (GWP) from cradle-to-gate divided by the unconfined compressive strength, f_c. The lower values for LC20 and LC50 show that they give more compressive strength for each CO_2 equivalent related to their production.

Table 1 Key parameters of the three concretes.

Concrete	NC	LC20	LC50
Equivalent binder content [kg/m³]	484	453	487
GWP [kg CO_2e/m³]	287	223	120
28-day compressive strength, f_c [MPa]	82.7	80.5	73.1
CO_2 intensity [kg CO_2e/(m³ MPa)]	3.5	2.8	1.6
Long-term compressive strength, f_c [MPa]	91.6 (91 days)	97.7 (245 days)	88.6 (92 days)
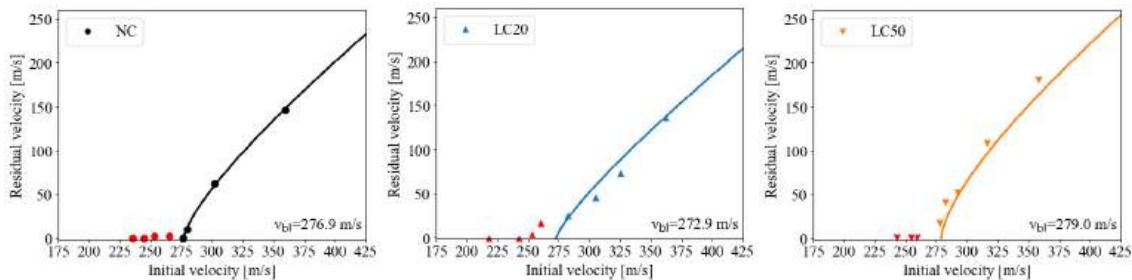
Fig. 1 Ballistic limit curves for plain normal concrete (a), plain LC20 (b) and plain LC50 (c), 28 days post casting.
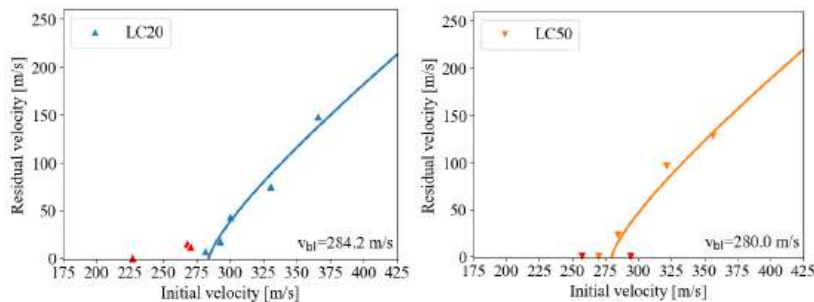
Fig. 2 Ballistic limit curves for plain LC20 (a) and plain LC50 (b), 245 and 92 days post casting, respectively.

In this study, the results from 72 ballistic experiments show that there is no significant difference in ballistic perforation resistance when replacing standard cement with supplementary cementitious materials and thus reducing CO_2 emissions. The authors believe this to be an excellent result, both from an environmental and protective point of view.

REFERENCES

[1] Ø.E.K. Jacobsen, M. Kristoffersen, S. Dey, T. Børvik, "Sustainable shielding: Ballistic performance of low-carbon concrete", Construction and Building Materials 415, (2024), https://doi.org/10.1016/j.conbuildmat.2024.135103.

[2] L.K. Turner, F.G. Collins, "Carbon dioxide equivalent (CO2-e) emissions: A comparison between geopolymer and OPC cement concrete", Construction and Building Materials 43, (2013), http://doi.org/10.1016/j.conbuildmat.2013.01.023.

[3] The European Committee for Standardization (CEN), Eurocode 2: Design of Concrete Structures Part 1.1: General Rules and Rules for Buildings, The European Committee for Standardization, 2018.

INVITED LECTURE
PAPER AS THE REDISCOVERED MATERIAL TO DEVELOP SMART AND SUSTAINABLE ELECTROCHEMICAL DEVICES FOR THE DEFENSE FIELD

Fabiana Arduini

University of Rome, Italy

ABSTRACT

In the field of biosensors, the use of paper has established a new route considering its several features, including its i) capillary-driven flowing pathways avoiding the use of external pumps, ii) capability to work as a reservoir for storing the reagents, delivering a reagent-free analytical tool, iii) capacity to work without sample treatment, i.e. filtration and dilution, iv) flexibility and foldability, boosting the origami configuration easily without any additional device, vi) feature to work as a reactor to synthesized inside nanomaterials by follow a sustainable approach, vii) ability to detect the target analyte not only in solution but also in aerosol and solid samples without any sampling system, and viii) characteristics to design combined hybrid systems to boost easy analysis, overcoming the on-going limitation using polyester-based printed electrochemical biosensors. The advantages of using paper-based electrochemical biosensors have also been demonstrated in the defense field. In this presentation, I report the research activity carried out in my group for the measurement of chemical warfare agents namely nerve agents and mustard agents as well as the biological warfare agents namely botulinum toxins by using paper-based printed electrochemical biosensors. In addition, the results focused on paper-based point-of-care devices, including wearable ones, to support the evaluation of people exposed to cholinesterase inhibitors e.g. nerve agents, or to evaluate the stress level of the soldier will be presented.

INVITED LECTURE
FROM FIBER TO POWER: WEARABLE TEXTILES REVOLUTIONIZE ENERGY GENERATION AND STORAGE

Ayse Bedeloglu

Bursa Technical University, Turkey

ABSTRACT

The ever-increasing demand for portable and autonomous technologies in the defense field necessitates innovative solutions for energy production and storage. Textiles, with their inherent flexibility, large surface area, and compatibility with various structures, present themselves as a promising platform to meet this critical need. This work explores the cutting-edge potential of textile-based technologies to power military equipment and ensures uninterrupted operation, covering a range of materials from nanofibers to conventional fibers, yarns, and fabrics. Recent advancements in nanotechnology and materials science have unveiled a plethora of possibilities for textile-based energy devices (piezoelectric nanogenerators, solar cells, batteries, supercapacitors, triboelectric nanogenerators, etc.), offering significant advantages over conventional rigid systems.

The unique properties of textile-based technologies, particularly their compatibility, adaptability to various surfaces, and lightweight construction make them ideal for military applications. Their unobtrusive integration into clothing and equipment minimizes logistical burdens and increases operational efficiency. Additionally, the scalability and affordability of textile production methods hold significant promise for large-scale production and cost-effective application, further strengthening their practicality in military and defense environments.

This study discusses the latest research and developments in textile-based energy production and storage and highlights their important role in shaping the future of military operations. By exploring the diverse applications of these technologies, from self-powered camouflage and communications systems to energy-harvesting textiles and wearable sensors, the discussion will highlight the transformative impact of textiles in enabling energy autonomy and adaptability in the ever-evolving military environment.

KEYWORDS:

 wearables, piezoelectric nanogenerators, solar cells, batteries, supercapacitors, triboelectric nanogenerators, nanofiber-based energy generation, defense applications

INVITED LECTURE
ADVANCED MATERIALS IN FUTURE DEFENSE SCENARIOS. A MILITARY AND ENGINEERING APPROACH

Jose L. Mingote

Former National Armaments Director Representative in the NATO HQ, Spain

ABSTRACT

The serious threats and risks faced throughout the 21st century associated with climate changes, massive urbanization, overpopulation, and competition from all types of natural resources (water, energy, minerals, agricultural products,..) probably will raise the number of conventional, irregular, asymmetric and hybrid conflicts with different level of intensity in different environments around the world. Checking future military capabilities and trends discussed in NATO, the European Union, US DoD, and other countries one can appreciate the extreme complexity of scenarios of future conflicts and theatres of operations in the short, medium, and long term.

In this sense and if we think about defense issues, can we ask ourselves, what could be the future defense and security requirements? And how will disruptive science, technology, and engineering meet those requirements? what materials could be used in the field of security and defense, for instance, in the year 2050? This is all a science fiction exercise? Some ideas arise taking into account these approaches.

Cutting-edge innovations in materials science, such as metamaterials with unprecedented properties, self-healing composites, and nanotechnology-infused armor, are poised to redefine the boundaries of military technology and associated capabilities. These materials offer enhanced protection and provide lightweight modular and scalable solutions, crucial for agility and maneuverability in future military scenarios. Smart textiles, embedded with sensors and communication devices, further amplify the capabilities of soldiers, enabling real-time data acquisition and improved situational awareness on the battlefield. Biomaterials and artificial intelligence will allow "humanoid soldiers" to carry out complex operations under the neural control of commanders. Advanced materials should be able to be 3D printed on board big naval platforms and in the logistic support chain on military theatre using advanced engineering techniques as digital twins. The convergence of artificial intelligence with advanced materials opens the door to autonomous systems, from unmanned vehicles to intelligent wearables, revolutionizing military operations in a future robotic environment. Integration of conventional and swarms of unmanned platforms well connected will strengthen military capabilities and performances. An intensely robotic era in the defense field is certainly on the short horizon. Hypersonics and powerful lasers will increase defense capabilities by increasing the range of action and reducing the effective time together with very high precision munitions and missiles and reducing storage and consumption of munitions. Stealth technology featuring adaptive camouflage, radar-absorbing, and invisibility materials, ensures a stealthy presence in ground, naval, and air domains, confounding adversaries in an era where electronic and cybersecurity warfare plays an increasingly pivotal role in any cross-domain. As we navigate the intricacies of future military landscapes, the research, development, design, and integration of these advanced defense materials with advanced industrial and engineering processes stands as a testament to the relentless pursuit of cutting-edge research, and innovation, ultimately shaping the defense strategies of tomorrow. New advanced materials and disruptive technologies will provide advantages and superiority in the field of defense and security of the future.

INVITED LECTURE
SUSTAINABLE DETOXIFYING AND SENSING MATERIALS FOR IMPROVED PERSONAL PROTECTIONS

Gang Sun
University of California, USA

ABSTRACT

Current textile materials employed in personal protective equipment (PPE) are mostly serving as barriers to targeted hazards with compromised environmental and health concerns. The development of sustainable functional materials with improved personal protective performance has become an urgent demand. This research group at the University of California, Davis has been studying reusable, rechargeable, and biodegradation biocidal textiles, chemically detoxifying, highly sensitive, and highly selective personal use biosensors for occupational and public protective applications for decades. In recent years, we have shifted the focus to the preparation of fibers and fabric materials with integrated reactive and sensing functions against vaporous pesticides and pathogens as well as with reuse and rechargeability. Among them, fibers possessing hierarchical porous structures were fabricated through simple chemical modifications and have demonstrated ultrahigh capacity and efficacy in detoxifying target chemicals. This presentation will provide a summary of the progress in the preparation of cellulose fiber-based detoxifying and sensing materials for applications in biological and chemical protective clothing. We hope the results could contribute to the development of next-generation personal protective materials with demonstrated sustainable and multifunctional performances.

ACKNOWLEDGMENT

INVITED LECTURE
MILITARY TEXTILE WASTE RECYCLING AND VALORIZATION: ADVANCED TEXTILES FOR DEFENCE

Diana P. Ferreira
University of Minho, Portugal

ABSTRACT

The textile industry is one of the most important economic sectors, but also one of those responsible for the largest generation of waste. Global textile consumption has increased substantially in the last decades and, consequently, millions of tons of textile waste have been discarded every year. Europe generates 7 – 7.5 million tons of textile waste per year, of which only 30 – 35% is collected for possible recycling. The generation of textile waste is problematic, as incineration and landfills – both inside and outside Europe – are its primary end destinations. This has several negative consequences for people and the environment. Therefore, due to its significant contribution to environmental pollution, along with the already recognized scarcity of petroleum resources, the use and recovery of this type of waste has been appointed as an urgent need.

In the military sector, the problem reaches even greater proportions since military uniforms cannot be reused by civilians, preventing the possibility of being used second-hand as common clothes. In fact, the only available solution for military textiles' disposal is the complete destruction by incineration. Considering that military clothing is a very technical product composed of high-added-value components, the embedded value of the waste is very high, which opens the opportunity not only from the environmental point of view but also from the economic point of view. There is an increasing concern about what to do with the huge amounts of military textile waste, therefore, it is imperative to develop new strategies to overcome this problem using the most sustainable technologies and processes to respect a circular economy concept and valorize the final products of recycling.

INVITED LECTURE

HISTRATE: A ROUTE TO CERTIFICATION-BY-ANALYSIS FOR IMPACT-LOADED AERONAUTICAL COMPOSITE STRUCTURES

Patricia Verleysen
Ghent University, Belgium

ABSTRACT

The HISTRATE project, initiated in 2022 as part of the EU Cost Action program, addresses certification challenges in the aeronautical industry by advancing certification-by-analysis for composite load-bearing structures under high-rate loading. Seeking a paradigm shift, HISTRATE aims to replace conventional validation approaches with simulation-based methodologies, minimizing the need for complex testing. Leveraging a diverse network of academic and industrial experts, the project emphasizes collaborative knowledge exchange. By integrating insights across length scales from material constituents to composite components, HISTRATE aspires to revolutionize the development of ultra-high-performance, safe, and innovative advanced composites for real-world applications facing high strain rate loading.

INVITED LECTURE
STATIC AND DYNAMIC FRACTURE MECHANICS OF PRINTED ALUMINUM LATTICES

Daniel Rittel, Yahav Boim and Amnon Shirizly

Faculty of Mechanical Engineering, Technion, 32000 Haifa, Israel

https://www.rittel.group

ABSTRACT

With the advent of metal printing technologies, the creation of lattices that was extremely arduous until now, has become much easier, allowing for a variety of parameters such as lattice unit cell, struts thickness among others. While the mechanical response of lattices, under both static and dynamic conditions, has and still is extensively studied mostly for energy absorption purposes, the fracture mechanics of the said lattices has been widely overlooked.

Experiments were carried out for two notched lattice geometries (diamond and diagonal) that were tested under quasi-static and dynamic (impact) loading using one point impact experiments. This type of loading allows not only mode I but also mode II testing of the notched specimens.

The salient characteristics of the fracture process will be reported, together with a systematic comparison between static and dynamic failure modes. In addition, the combined use of our ultra-high speed and the thermal cameras will be shown to complement the visual information by thermal measurements that are characteristic of the failure process.

INVITED LECTURE
COMPOSITE MANUFACTURING PROCESS SIMULATION: THEORETICAL AND PRACTICAL PERSPECTIVE

Raúl Guichón
Embraer, Portugal

ABSTRACT

One of the main setbacks of the composite structures manufacturing is the geometrical distortion after curing, commonly known as process-induced distortions (PID). A great number of studies about PID and its simulation have been performed in the last 20 years, most of them focused on tool compensation. Computational capacity has increased exponentially in recent years, allowing high accuracy predicting PID through simulation and, therefore, extending its applicability.

The presentation focuses on the state-of-the-art in curing process simulation of composite structures from a theoretical and practical perspective, addressing how PID can be predicted through finite element analysis and the mitigation strategies.

INVITED LECTURE
GRAPHENE AEROGELS DEVELOPMENT FOR AEROSPACE APPLICATIONS

Evaldo Corat

INPE - National Institute for Space Research, Brazil

ABSTRACT

Graphene science and applications have emerged and developed a lot in recent years, with a considerable increase in its availability and commercialization, mainly for graphene produced by a non-oxidative exfoliation. Graphene aerogels (GA) are a new class of solid, extremely lightweight made from graphene. The GA has a porous structure with a specific mass of only a few g/L, that may be used for thermal insulation, acoustic insulation, and many other applications from clothing and footwear to military and aerospace vehicles. Most GA is made from graphene oxide (GO). GO has a natural tendency to form a gel in water, and its reduction may form a graphene hydrogel. Freeze--drying the hydrogel yields the simplest GA. In this presentation, we show the GA developments at the National Institute for Space Research in Brazil. Besides the traditional GO route, the development includes alternative chemical reduction and the use of emulsion to control the internal porosity. Including chitosan as a gelling alternative produced two new materials, one using never-oxidized graphene, and the other in mixtures with GO. The thermal characterization of the different materials will be discussed.

INVITED LECTURE

A NEW PROCESSING ROUTE FOR IMPROVING FIBRE-MATRIX INTERFACE AND MECHANICAL PROPERTIES OF PLANT-FIBRE REINFORCED THERMOPLASTIC COMPOSITES

Sohel Rana
Indian Institute of Technology, India

ABSTRACT

Plant fibre-reinforced polymer composites are attractive in various industrial applications due to their low cost and high specific strength. However, one of the key challenges with these composites is the poor fibre-matrix interface which strongly affects their mechanical properties. In thermoplastic matrices, the high melt viscosity of the polymers leads to improper impregnation of fibres with the polymer, leading to the generation of voids and inferior mechanical performance. Therefore, the fabrication of high-quality and high-strength plant fibre-based thermoplastic composites is always a challenge. Homogeneous mixing of plant fibres with thermoplastic fibres (such as polypropylene) and their subsequent melting and consolidation results in better fibre impregnation, significantly lower void content and improved fibre-matrix interface. In this talk, the use of the carding process in the homogeneous mixing of plant and thermoplastic fibres will be discussed. The effect of this mixing process on the void content and various properties of plant fibre-reinforced thermoplastic composites such as pull-out strength, interlaminar shear strength and mechanical properties (tensile, flexural, impact, etc.) will be discussed in detail.

ORAL PRESENTATIONS
ID 1
INTEGRATION OF STRATEGIC DESIGN AND 3D SIMULATION TECHNOLOGIES TO ENHANCE ECG SIGNAL QUALITY AND CUSTOMIZED FIT FOR IMPROVED HEALTH MONITORING

Seonyoung Youn[1](*), Kavita Mathur[2], Amanda C. Mills[3]
Fiber and Polymer Science, Ph.D. Candidate, NC State University, Raleigh, United States
Department of Textile and Apparel, Technology and Management, NC State University, Raleigh, United States
Department of Textile Engineering, Chemistry and Science, NC State University, Raleigh, United States
(*) Email: syoun@ncsu.edu

ABSTRACT

Wearable biosignal monitoring systems are emerging as a crucial tool for autonomous health monitoring. However, these systems' design often neglects anthropometric considerations for the female form, resulting in ineffective, ill-fitting devices. This oversight is particularly evident in the suboptimal placement of 3-lead electrodes, inappropriate material selection, and poor fit for women. This study introduces a customized electrocardiogram (ECG) sports bra design, balancing enhanced biosignal quality with wearing comfort. This study focuses on determining the optimal electrode placements under the chest, selecting strategic knit fabrics, and simulating targeted garment pressure using digital twins. The efficacy of the devised ECG sports bras is evaluated against the standard wet-electrode, assessing ECG data quality, signal-to-noise ratio (SNR), and skin-to-electrode impedance. We also explore the aspects of fit comfort and garment washability.

INTRODUCTION

Advancement in wearable health monitoring systems continue to confront challenges in obtaining high-quality biosignals. Key issues include motion artifacts (MAs) and high skin-toelectrode impedance. Several studies (Takeshita et al., 2022) have shown that the proper contact pressure significantly reduce MAs and skin impedance, thereby improving biosignal quality. Nonetheless, design considerations specific to the female anatomy, such as body curvature and breast tissue, often remain unaddressed. This oversight leads to difficulties in obtaining high-fidelity signal (Macfarlane et al. 2003). Recently Schauss et al. (2022)'s study on health monitoring sports bras emphasized the significance of fit in such wearable devices. However, the study only focuses on specific sizes and did not explore optimal electrode placement or trade-off between biosignal quality and wearing comfort. This study introduces a novel ECG sports bra with a detachable chest band incorporating textile-based electrodes. The approach used in this study utilizes 3D garment simulation (3DGS) and digital twin technology, focusing on garment pressure and female anthropometric factors. The study is divided into three phases: 1) Electrode placement: The optimal horizontal placement for 3lead electrodes beneath the chest area is identified, targeting a compatible configuration to the conventional system. Five variables' configurations include two from commercial ECG sports bras and three based on previous studies. 2) Sensor fabrication: Textile-based sensors are fabricated via screen printing using Ag/AgCl on strategically selected knit fabrics.
The material selection and sizing are guided by contact pressure prediction model (CP model) (Youn et al., 2023).

3) Garment assembly and test: The sensors are integrated into the sports bra band, featuring a detachable, Velcro-adjustable fit allowing size alterations up to 20% (Youn et al., 2023). ECG signal quality is evaluated via SNR measurement, Rmagnitude, Peak detection, and the electrical impedance, compared against the standard wet electrode. Comfort is evaluated using a 7-point Likert scale and Kikuhime pressure sensor measurements. The study will include at least three female participants in sizes S, M, and L, in compliance with IRB protocols.

RESULTS AND CONCLUSIONS

The preliminary phase of this study focused on optimizing ECG electrode placement and involved a healthy female participant wearing a medium-sized 32B bra. Figure 1 shows the tested configurations, while Figure 2 displays results for ECG signal quality, SNR, and skinto-electrode impedance.
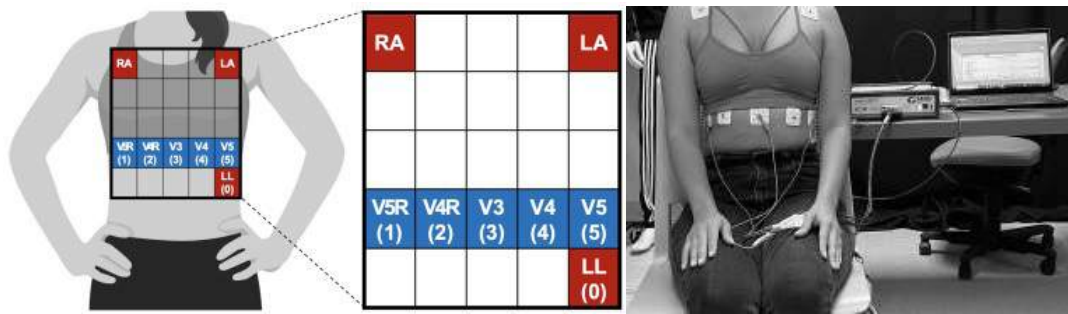
Fig. 1 The 3-lead electrode placement for conventional (red) and the experimental (blue) configurations with a zoomed-in view (left) and the participant's resting position for recoring electrical impedance and ECG signals (right).
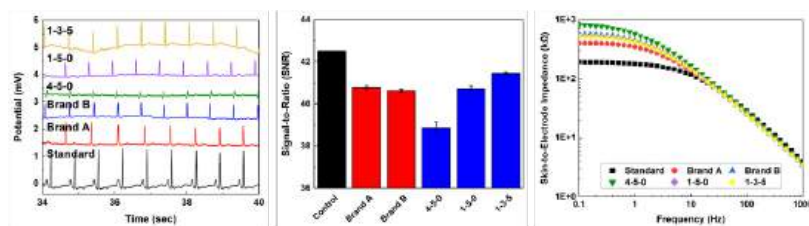
Fig. 2 The ECG signal biopotential (Left), SNR (Middle), and Skin-to-electrod Impedance (Right)

In our study, the standard placement of LA (Left arm), RA (Right arm), and LL (Left leg) electrodes in the traditional 3-lead Mason-Likar precordial location showed superior performance, with the highest biopotential amplitude (SNR: 42.52) and the lowest electrical impedance, indicating excellent signal quality. Remarkably, the 1-3-5 electrode configuration outperformed those from commercial brands A and B, achieving an SNR of 41.45 and a lower electrical impedance, suggesting its potential compatibility with the standard. Additionally, our results revealed that any horizontal arrangement of the RA-LA-LL electrodes outperformed configurations with LA and LL electrodes on differing horizontal planes, such as the 4-5-0 and 1-5-0 setups. This finding suggests that optimal signal transmission may be achieved by positioning the RA and LA electrodes in closer proximity, while increasing the separation between the LA and LL electrodes along the same horizontal line. Future research will involve diverse-sized female participants to examine how body size and BMI affect signal quality. The presentation will cover the desired signal placement, the enhanced garment assembly, and tests for signal quality, comfort, and washability.

REFERENCES

[1] T. Takeshita, et al. "Relationship between contact pressure and motion artifacts in ECG measurement with electrostatic flocked electrodes fabricated on textile." *Scientific reports* 9.1 (2019): 5897.

[2] P. Macfarlane, et al. "Precordial electrode placement in women." *Netherlands Heart Journal* 11.3 (2003): 118.

[3] G. Schauss, et al. "ARGONAUT: An inclusive design process for wearable health monitoring systems." Proceedings of the 2022 CHI Conference on Human Factors in Computing Systems. 2022.

[4] S. Youn, et al. "Simulation-Based Contact Pressure Prediction Model to Optimize Health Monitoring Using Etextile Integrated Garment." *IEEE Sensors Journal* (2023).

ID 4
FUZZY TOPSIS FOR GROUP DECISION MAKING: A CASE STUDY FOR NIGHT VISION GOGGLES

İsmail Gevrek[1](*), Metin Gürü[2] , Fatih Emre Boran[3]

[1,] Gazi University, Department of Environmental and Technical Investigation of Accidents Maltepe Ankara, Turkey.

[2,] Gazi University, Faculty of Engineering, Department of Chemical Engineering, Maltepe Ankara, Turkey.

[3,] Gazi University, Department of Energy Systems Engineering,Yenimahalle, Ankara, Turkey.

(*) Email: ismail.gevrek@gazi.edu.tr

ABSTRACT

This paper aims to present a fuzzy decision-making approach to dealing with the Night Vision Goggle (NVG) selection problem in rotary-wing aircraft. Focusing on the selection of certain criteria—key performance metrics that can help one make a rational choice of enabling technology—is essential for a successful study. In NVG designs, where phosphor screens offer some quality choices, and different weights exist, fuzzy multi-criteria decision-making (F-MCDM) approaches can be used as a system decision mechanism. Especially, some decision-making data like depth perception, contrast, and clarity are undefined, vague, and fuzzy. Fuzzy Analytic Hierarchy Process (F-AHP) is used to determine the importance and weight of evaluation criteria. For the final selection, fuzzy Technique for Order of Preference by Similarity to Ideal Solution (F-TOPSIS) is used to evaluate the alternatives. Findings indicated the main criteria for the consideration of NVG selection as depth perception, clarity, halo effect adjustment, contrast, and weight. The results showed that NVG C was the optimal choice of the seven candidates. Due to the high cost of flight experiments and the rarity of pilot subjects, we consider this study valuable and rare.

INTRODUCTION

NVG's are an optoelectronic device that allows visualization of images in low light levels, improving the user's night vision. These systems support a wide range of military operations that would not otherwise have been possible. However, the additional capabilities provided by NVGs also create new risks. Night operations result in significantly more accidents and incidents than their daytime counterparts (Ruffner et al., 2004). Flight crew members have identified inaccurate distance estimation with NVGs as a severe problem (Harding et al., 2010). Accident rates for night sorties by helicopters traveling to offshore oil and gas platforms are at least five times higher than during the daytime (Nascimento et al., 2012).

This study aimed to investigate the most suitable NVG criteria for night flights, which have increased in importance in recent years, both in military terms and in natural disasters (floods, fire, earthquakes, etc.), and to investigate the most appropriate NVGs according to these criteria. In this regard, experts (**Table 1**) assessed different phosphor screens (white and green) that enable the identification of objects, support cognitive activities, and provide spatial orientation in helicopter flights (Penkelink and Besuijen, 1996) as well as having the potential to reduce workload and improve visual performance (Capó-Aponte et al., 2009) and compared them with each other.

In the solution methodology, first of all, experts were determined, a decision hierarchy was created, weights were calculated with the F-AHP method (Chang, 1996), and lastly, F-TOPSIS methods (Chen, 2000) were applied.

RESULTS AND CONCLUSIONS

As a result, NVG C (white phosphorus and the lightest) was found to be the best alternative (Table 2). At this point, it should be noted that NVG A (green phosphorus) is the last alternative. In Multi-Domain Operations, U.S. Army

aviation emphasizes the critical significance of enhanced night vision, utilizing white phosphorus image intensifier tubes integrated into ANVIS systems for aircrew engaged in night missions (Flightfax, 2020). The paper provides a holistic perspective of the NVGs and can be useful for researchers and practitioners involved in managing NVG product quality and new product development.

Finally, it should be emphasized that this work is a preliminary study considering significant technical criteria and the experience of an advisory group composed of examiner and instructor pilots.

Table 1. Profile of experts

Expert	Year of experince	Areas of expertise	Academic Degree
1	26	Project Branch, R&D Branch. And Fleet Cmdr.	MSc
2	25	Examiner, Project and Fleet Cmdr.	MSc
3	25	Examiner, Project and Fleet Cmdr.	MSc
4	11	Instructor Pilot, Project Branch.	MSc

Table 2. Alternatives, Weights(g.) and ranking

Alternatives	Weigt(g.)	Phosphor screen	Depth perception =0.141			Clarity =0.113			Halo effect =0.17			Adjustment =0.04			Contrast =0.203			Weight =0.332			Ranking
NVG A	592	Green	2	4	6	2	4	6	1	3	5	7	9	10	1	3	5	1	3	5	7
NVG B	506	Green	4	6	8	4	6	8	4	6	8	7	9	10	4	6	8	3	5	7	6
NVG C	424	White	9	10	10	6	8	9	9	9	10	7	9	10	7	9	10	9	10	10	1
NVG D	525	Green	7	9	10	4	6	8	7	9	10	6	8	9	6	8	9	7	9	10	2
NVG E	650	White	5	7	9	6	8	9	6	8	9	4	6	8	6	8	9	5	7	9	4
NVG F	560	Green	4	6	8	6	8	9	6	8	9	6	8	9	4	6	8	5	7	9	5
NVG G	600	White	4	6	8	6	8	9	6	8	9	4	6	8	4	6	8	7	9	10	3

The results showed that the most critical criterion in NVG is weight, followed by the halo effect, and white phosphorus with the lightest NVG took the first alternative in the fuzzy-TOPSIS method.

REFERENCES

[1] CAPÓ-APONTE, J. E., TEMME, L. A., TASK, H. L., PINKUS, A. R., KALICH, M. E., PANTLE, A. J. & RASH, C. E. 2009. Visual perception and cognitive performance. *Helmet-mounted displays: sensation, Perception and Cognitive Issues*, 335-390.

[2] CHANG, D.-Y. 1996. Applications of the extent analysis method on fuzzy AHP. *European journal of operational research,* 95, 649-655.

[3] CHEN, C.-T. 2000. Extensions of the TOPSIS for group decision-making under fuzzy environment. *Fuzzy sets and systems,* 114, 1-9.

[4] HARDING, T. H., RASH, C. E. & LANG, G. T. Perceptual and cognitive effects on the use of helmet-mounted displays due to external operational factors. Head-and Helmet-Mounted Displays XV: Design and Applications, 2010. SPIE, 77-87.

[5] NASCIMENTO, F. A., MAJUMDAR, A. & JARVIS, S. 2012. Nighttime approaches to offshore installations in Brazil: Safety shortcomings experienced by helicopter pilots. *Accident Analysis & Prevention,* 47, 64-74.

[6] PENKELINK, G. & BESUIJEN, J. 1996. Chromaticity contrast, luminance contrast, and legibility of text. *Journal of the Society for Information Display,* 4, 135-144.

[7] RUFFNER, J. W., ANTONIO, J., JORALMON, D. & MARTIN, E. Night vision goggle training technologies and situational awareness. Proceedings of the Advanced Technology Electronic Defense System (ATEDS) Conference/Tactical Situational Awareness (SA) Symposium, 2004. Citeseer.

[8] U.S.ARMY-FLIGHTFAX, 2020. White Phosphor NVG's: How the Army is "Making Owning the Night" safer.

ID 5
HIGH-VELOCITY IMPACTS AGAINST PLAIN CONCRETE

Conceição, J. F. M.[1(*)], **Corneliu, C.**[2], **Rebelo, H.**[1], **Chambino, M.**[3], **Pereira, L.**[4]

[1] Centro de Investigação da Academia Militar (CINAMIL), Instituto Universitário Militar / NOVA School of Science and Technology – Universidade Nova de Lisboa, Lisboa, Portugal [2] Civil Engineering Research and Innovation for
[2] Sustainability (CERIS NOVA), NOVA School of Science and Technology – Universidade Nova de Lisboa, Lisboa, Portugal

[3] Centro de Investigação da Academia Militar (CINAMIL), Academia Militar, Lisboa, Portugal

[4] Centro Investigação Academia Força Aérea (CIAFA), Academia da Força Aérea, Instituto Universitário Militar, Lisboa, Portugal

[(*)] Email: joaofilipemelro@gmail.com / conceicao.jfm@academiamilitar.pt

ABSTRACT

This research analyses the response of two distinct types of concrete blocks, each possessing an approximate unconfined compressive strength of 30MPa, when exposed to high-velocity impacts produced by an Explosively Formed Penetrator (EFP) traveling at an initial velocity of 1200 m/s. Given the scarcity of studies exploring high-velocity impacts on concrete, the primary aim of this study is to scrutinize how concrete behaves under high-speed impacts, ultimately contributing valuable insights to the development of protective structures. To achieve this objective, a comprehensive numerical analysis was carried out in LS-DYNA to delve into the fracture mechanisms inherent in concrete under such extreme conditions. Subsequently, the obtained numerical outcomes were compared and validated through eight experimental field tests. The methodology employed involved a robust combination of numerical simulations and real-world experiments, ensuring a comprehensive understanding of concrete behavior in scenarios involving rapid, high-energy impacts.

INTRODUCTION

With the increased penetration capability of weapons and the heightened occurrence of fragment projection resulting from explosions, as well as the frequent instances of local wars or terrorist attacks, research on the resistance of novel building materials to projectile impacts has garnered significant attention among engineers and researchers. Hence, it becomes imperative to investigate how materials respond when subjected to such impacts. Concrete, widely employed in construction for its structural capacity and cost-effectiveness, holds a crucial place in these inquiries. Its extensive use encompasses the construction of protective structural elements and vital infrastructure [1]. Despite numerous studies on concrete's dynamic behavior, understanding its response to high-velocity impacts remains an ongoing challenge due to difficulties in characterization [2], [3].

To comprehend how concrete behaves under high-velocity impacts (v > 1000m/s), a 2D axisymmetric numerical model of an Explosively Formed Penetrator (EFP) was developed, capturing its formation process and essential traits. Upon validating the EFP's attainable speed, an experimental study involving two types of concrete blocks was conducted: 4 blocks containing basalt aggregates and 4 blocks containing limestone aggregates. Subsequently, a three-dimensional model was developed, enhancing the realism of simulating the EFP's impact on the concrete block and facilitating a more accurate assessment of the impact dynamics. Analysis encompassed penetration depth, fragmentation, and overall impact dynamics, juxtaposing these findings with experimental results for comparison.

RESULTS AND CONCLUSIONS

The results indicated no significant difference between the experimental projectile's velocity and the numerical model (with an error of 7.24%) (Fig. 1). Additionally, a greater energy dissipation capacity was observed when using harder aggregates such as basalt compared to limestone. Furthermore, the study confirmed failure mechanisms in alignment with the existing literature (Fig. 2). Concrete blocks incorporating limestone aggregates exhibited higher fragmentation and greater projectile penetration. This suggests that employing harder aggregates enhances resistance to penetration by high-velocity projectiles within this regime.
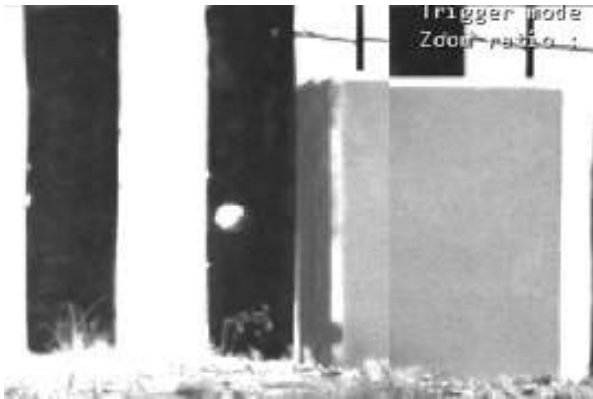
Fig.1 Projectile approaching concrete block
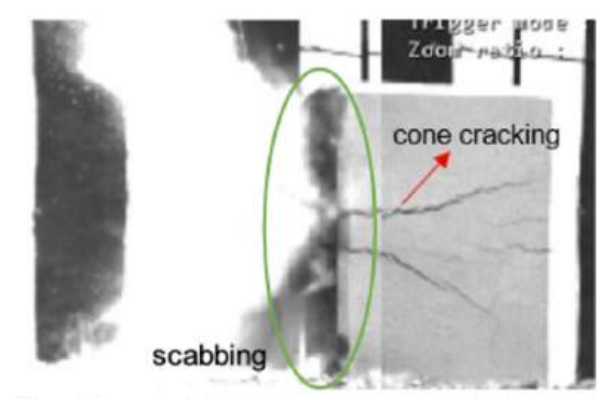
Fig. 2 Impact failure mechanisms: scabbing and cone cracking
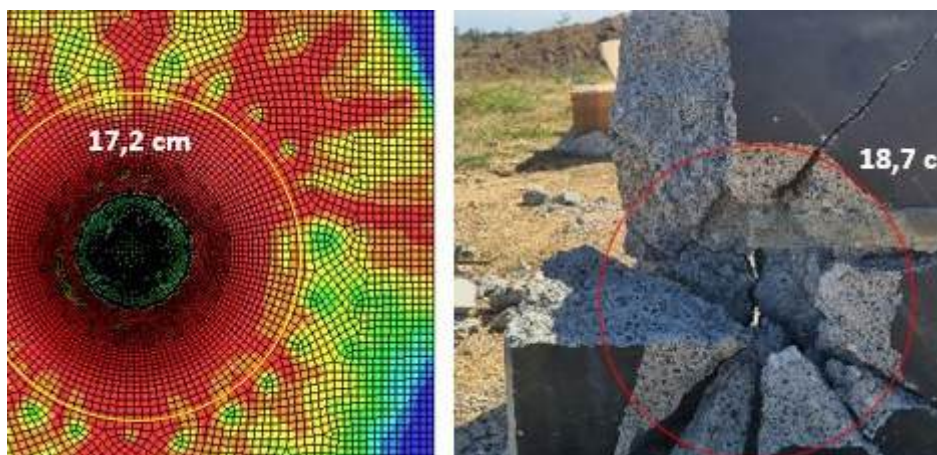
Fig. 3 Comparison of the craters from the numerical model and the experimental campaign

Additionally, Fig. 3 presents a side-by-side comparison of the craters generated by the numerical model and those observed in the experimental campaign. The significance of numerical modelling in this research cannot be overstated. These models were pivotal in validating our experiments and offering insights that were not directly measurable in the field. The correlation between the values derived from our experiments and those predicted by the numerical models underscores the significance of this approach in conserving resources and offering more efficient methodologies for studying high-velocity impacts.

REFERENCES

[1] B. Esteban, L. M. Lenhart, L. Rüdiger, and N. Gebbeken, "An evaluation of shaped charge experiments using concrete components," Int. J. Prot. Struct., vol. 6, no. 3, pp. 439–455, 2015, doi: 10.1260/2041-4196.6.3.439.

[2] A. N. Dancygier, "High-performance concrete engineered for protective barriers," Philos. Trans. R. Soc. A Math. Phys. Eng. Sci., vol. 375, no. 2085, 2017, doi: 10.1098/rsta.2016.0180.

[3] B. Erzar, C. Pontiroli, and E. Buzaud, "Ultra-high performance fibre-reinforced concrete under impact: Experimental analysis of the mechanical response in extreme conditions and modelling using the Pontiroli, Rouquand and Mazars model," Philos. Trans. R. Soc. A Math. Phys. Eng. Sci., vol. 375, no. 2085, 2017, doi: 10.1098/rsta.2016.0173.

ID 6

THE DIGITAL PILOT – FIBER-BASED SENSORS FOR EARLY DIAGNOSTICS OF COGNITIVE IMPAIRMENTS OF AIR FORCE PILOTS

René Michel Rossi [1(*)], **Denis Bron** [2], **Bauer Frederik** [1], **Simon Annaheim** [1]

[1,] Empa, Laboratory for Biomimetic Membranes and Textiles, St. Gallen, Switzerland

[2, 3] Swiss Air Force, Aeromedical Center, Dübendorf, Switzerland

[(*)] Email: rene.rossi@empa.ch

ABSTRACT

Pilots flying at high altitude may face situations with insufficient oxygen supply. We developed a textile-based sensor system to continuously monitor different vital signs (heart rate, breathing pattern and body temperature) of pilots for an early detection of possible cognitive impairments. We could show that low-oxygen exposures immediately affect physiological responses after removing the oxygen mask at a simulated altitude of 7500m, with a potential influence on psychophysiological conditions and working performance.

INTRODUCTION

Pilots on duty are exposed to very diverse stressors and need a high cognitive performance to perform their tasks. We developed a fiber- and textile-based physiological multi-parameter monitoring tool able to continuously record vital signs, including heart rate (HR) and heart rate variability (HRV), breathing frequency (BF) and breathing variability (BFV) as well as body temperature and heat flux for an early diagnostics of possible cognitive impairments under stressful conditions like hypoxia.

The monitoring tool consisted of two clinically-validated knitted ECG electrodes [1] integrated into the textile system, a conductive stretch-sensitive textile sensor to measure respiration by monitoring chest expansion, and a foil heat-flux and temperature sensor. Ten male military pilots in training were monitored during a low-pressure exposition training session in a pressure cabin including breathing without oxygen mask at a simulated altitude of 7500m and 9000m. In a second trial, the pilots were exposed to various g-forces. Measurements were conducted according to the Declaration of Helsinki and written informed consent was obtained from each participant.

RESULTS AND CONCLUSIONS

The results show that the textile-based diagnostics system reached a high reliability with 95% of ECG data usable for further analysis in the simulated altitude conditions and 90% in the high performance centrifuge with g-force exposure. Removing the mask in the simulated high altitude conditions resulted in clear physiological reactions with an immediate drop of 22% in heart rate variability and an increase in heart rate by 26%. Breathing was also clearly affected with an increase of breathing frequency of 21% and a reduction of breathing amplitude of 20%. At the end of the hypoxia exposure, the reduction in heart rate variability reached 64%. In the centrifuge at a 3g exposure, the breathing frequency increased by 25% while the breathing depth decreased by 44%.
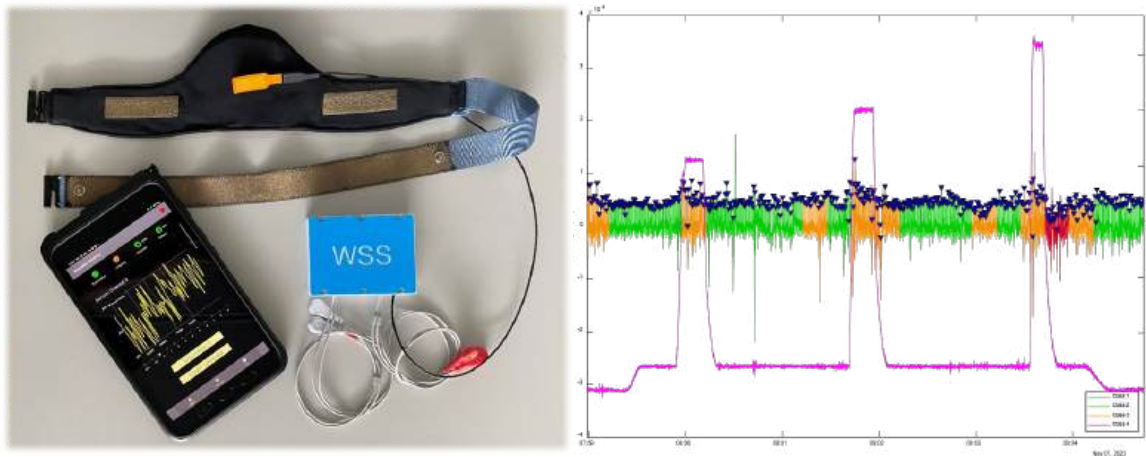
Fig. 1 left: Textile-based sensor system, right: ECG measurements during different g-exposures (purple line: acceleration)

We confirmed the feasibility of conducting continuous measurements of vital signs during the training programs of military pilots. Furthermore, we were able to detect changes in physiological variables related to hazardous conditions. In a next step, this multisensing textile system shall be directly integrated into the pilot suits.

REFERENCES

[1] P. Fontana, N. R. A. Martins, M. Camenzind, R.M. Rossi, F. Baty, M. Boesch, M. Brutsche and S. Annaheim, "Clinical applicability of a textile 1-lead ECG device for overnight monitoring" *Sensors*, 19(11), 2436, 2019.

ID 7

HETEROSTRUCTURES OF PT-AG/ LAYERED DOUBLE HYDROXIDES WITH PHOTOCATALYTIC ABILITIES TO DEGRADE BACTERIA AND TOXIC CHEMICALS

Gabriela Carja[1(*)], **Denis Cutcovschi**[2], **Sofronia Bouariu**[3]

[1,2,3] Technical University "Gheorghe Asachi" of Iasi, Faculty of Chemical Engineering and environmental Protection "Cristofor Simionescu", Department of Physical Chemistry, Bd. D. Mangeron no 71, Iasi, 700050, Romania

[(*)] Email: gcarja@tuiasi.ro

ABSTRACT

In light of the growing concerns regarding drug-resistant bacteria in wounds, as well as the presence of hazardous toxic compounds in air and water, novel phototherapy strategies hold great promise. These strategies are based on photoresponsive catalysts that can be easily integrated into cutting-edge military technologies, with applications ranging from water purification to wound dressings and antimicrobial coatings. In this context, this work presents ZnAl layered double hydroxides (LDH) heterostructured with nanoparticles of Pt and Ag as novel light-responsive photocatalysts for degrading hazardous compounds and bacteria. The specific formulation of the Pt-Ag/ZnAlLDH catalyst appears to be particularly effective. Such that, at the low dose (0.25 mg/mL), under irradiation with solar light, Pt-Ag/ZnAlLDH showed an inactivation ability as high as 94.7 % against Staphylococcus Aureus, whereas the degradation of p-dichlorobenzene, as pollutant in water, was 97%.

INTRODUCTION

Pathogens and harmful toxic chemicals rise great challenges to human health (Zhou et al; 2021) and their rapid destruction is particularly important to safeguard the well-being of humans involved in military operations. In recent years, the development of photoresponsive antibacterial catalysts are becoming one of the most hopeful substitutions to antibiotics for dealing with the bacterial diseases and further with pollution of water sources. Layered double hydroxides (LDH) and their derivatives are a family of anionic clays with interesting properties, such as: the ease of synthesis, tailored chemical composition and photocatalytic properties (Carja et al. 2013). Herein we present Pt/ZnAlLDH, Ag/ZnAlLDH and Pt-Ag/ZnAlLDH as novel heterostructures with photoresponsive catalytic activity to degrade specific hazardous compounds (e.g.: p-dichlorobenzene) and bacteria (e.g.: Staphylococcus aureus).

RESULTS AND CONCLUSIONS

The fabrication of the tested photocatalysts was based on a facile procedure to obtain heterostructures of nanoparticles of metals/layered double hydroxides, by exploiting the manifestation of the „structural memory effect", of the LDH in aqueous solutions of metal salts (Darie et al. 2018). More precisely, the heterostructured catalysts were obtained by the reconstruction process of the mixed oxides derived by calcination of ZnAlLDH Zn^{2+}/Al^{3+} = (2/1molar ratio) in the aqueous solutions of H_2PtCl_6 or Ag_2NO_3 and H_2PtCl_6/Ag_2NO_3, respectively. The structure, composition and optical responses of the catalysts were verified by XRD, EDX (Fig. 1a), XPS (Fig.1b-c) and UV-Vis analyses. The results reveal heterostructering between Pt, Ag or Pt-Ag and the reconstructed ZnAlLDH. The photocatalytic tests to study the degradation of p-dichlorobenzene were carried out in a glass-reactor with a cooling system and under a full illumination by a solar light simulator (UNNASOL US800, 250 W) used as an irradiation

source.
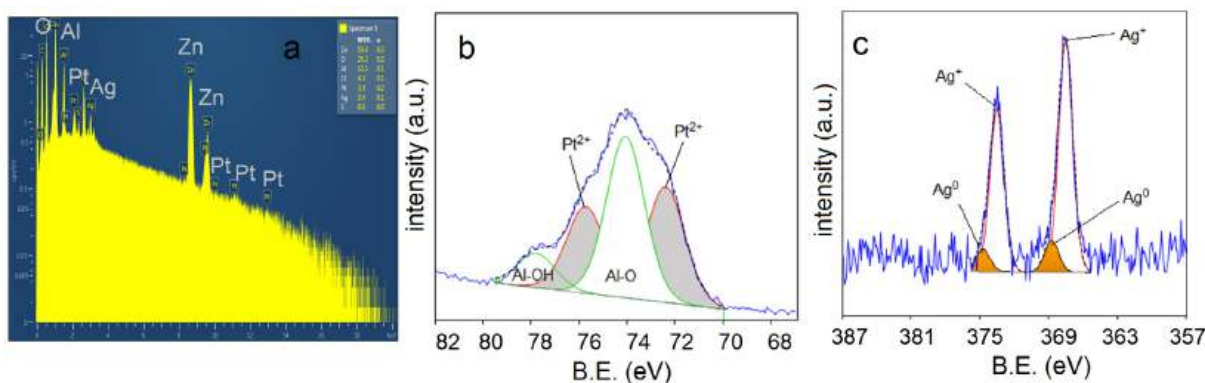
Fig. 1 (a) EDX and (b-c) XPS analyses results of Pt-Ag/ZnAlLDH photocatalyst.
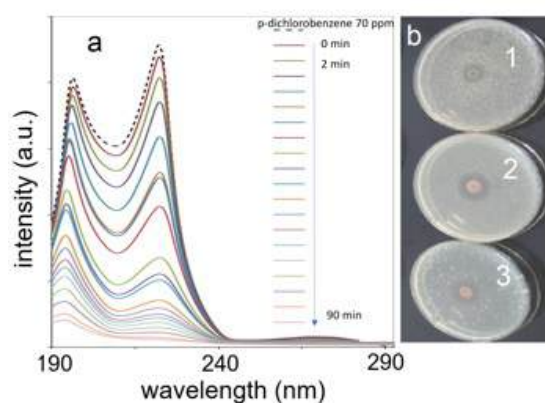
Fig. 2 (a) UVVIS profiles for p-dichlorobezene degradation and zones of inhibition of S. Aureus on Pt-Ag/ZnAlLDH under solar light irradiation.

The antibacterial activities against Staphylococcus aureus (S. aureus) were studied under solar light irradiation and qualitatively and quantitatively assessed by agar diffusion tests and MIC (minimal inhibitory concentration), respectively. When tested against S. aureus, the Pt-Ag/ZnAlLDH heterostructure showed the best performance, killing 94.7% of the bacteria, within 18 hours (Fig. 2b). Further, the photocatalytic degradation of p-dichlorobenzene reached an efficiency of 97%, after 90 min of reaction (Fig. 2a). These results highlight the potential of the novel heterostructures as effective photocatalysts to decompose dangerous bacteria and water pollutants, showcasing their catalytic ability to harness solar energy for impactful applications in military technologies.

REFERENCES

[1] Z. Zhou, B. Li, X. Liu, Z. Li, S. Zhu, Y. Liang, Z. Cui, "Recent progress in photocatalytic antibacterial", ACS Applied Bio Materials vol. 4, no.5, January, pp. 3909–3936, 2021.

[2] G. Carja, L. Dartu, K. Okada, E. Fortunato, "Nanoparticles of copper oxide on layered double hydroxides and the derived solid solutions as wide spectrum active nano-photocatalysts", Chemical Engineering Journal, vol. 222, April, pp. 60–66, 2013.

[3] M. Darie, E.M. Seftel, M. Mertens, R.G. Ciocarlan, P. Cool, G. Carja, "Harvesting solar light on a tandem of Pt or Pt-Ag nanoparticles on layered double hydroxides photocatalysts for p-nitrophenol degradation in water", Applied Clay Science, vol. 182, December, pp. 105250, 2019.

ID 8

A NEW PETAL-LIKE STRUCTURE WITH LIGHTWEIGHT, HIGH STRENGTH, HIGH ENERGY ABSORPTION, AND AUXETIC CHARACTERISTICS

Zhenyu Li[1], Jian Xiong[2], Hong Hu[1(*)]

[1] School of Fashion and Textiles, The Hong Kong Polytechnic University, Hung Hom, Kowloon, Hong Kong, China

[2] Center for Composite Materials, Harbin Institute of Technology, Harbin 150001, China

[(*)] Email: hu.hong@polyu.edu.hk

ABSTRACT

In this study, a novel petal-like structure with commendable mechanical properties was designed and fabricated by integrating the multi-stage deformation process of the structure with the inherent characteristic of fiber-reinforced composites. The intended application of this new structure is in the construction and automobile industry. A novel petal-like structure, incorporating different Angle parameters, was produced employing the traditional hot moulding method, utilizing continuous fiber-reinforced composite as the base material. Subsequently, compression tests and finite element analysis were conducted to evaluate the structure's performance. Comparative analysis of other 3D auxetic structures revealed that the proposed novel structure possesses superior attributes such as lightweight, high strength, and favorable auxetic characteristics. Furthermore, through reasonable structural design, the multi-cell structure prepared by fiber-reinforced composite material can also have a good stress platform stage.

INTRODUCTION

Various types of mechanical metamaterials with auxetic characteristics can be categorized based on different design parameters, including re-entrant honeycomb, double arrow, chiral/anti-chiral structures, among others (Wang, 2018). Although these structures demonstrate impressive deformations and energy absorption capabilities, their increased functionality is often accompanied by a decrease in structural strength and stiffness, posing limitations on their applicability in engineering. Utilizing continuous fiber reinforced composites presents a promising strategy for developing novel auxetic structures with improved properties (Li, 2023).

The incorporation of multi-stage deformation capabilities into the structure enhances its energy absorption properties (Zhu, 2024), resulting in significant potential for application in vehicle engineering, aerospace, and construction industries. This study investigates the development of a novel petal-like structure by combining multi-stage deformation with continuous fiber reinforced composite material. The structural attributes including strength, stiffness, auxetic characteristics, and energy absorption capacity under quasi-static and low-speed impact loads are comprehensively examined.

RESULTS AND CONCLUSIONS

The results show that petal-like structures with multi-stage deformation capacity prepared by continuous fibers have good strength, stiffness and energy absorption properties. A comparative analysis of stress-strain and energy absorption curves for the newly developed structures illustrates their performance under both quasi-static compression and surface impact loads, as depicted in Fig. 1. The petal-like structures composed of fiber-reinforced composites demonstrate a distinct stress plateau phase when subjected to compression analysis. Alterations in the Angle parameters have a significant impact on the mechanical properties, including strength, stiffness, and

the height of the stress plateau, of such structures. Furthermore, these structures demonstrate efficient energy absorption properties when subjected to surface impact loads. Specifically, when subjected to a 20J impact energy, the energy absorption capacity of the novel petal-like structure surpasses that of traditional structures by a factor of 8-40, indicating promising practical applications.
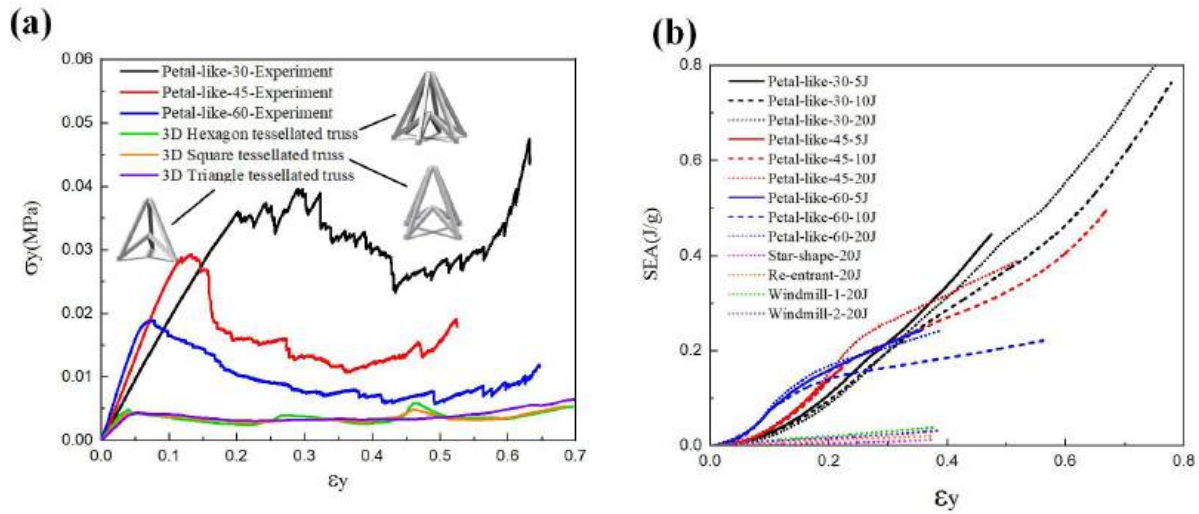
Fig. 1 Performance comparison of the structure under different loads a) Quasi-static compression load b) Energy absorption characteristics under surface impact load

This study shows that the incorporation of a petal-like configuration using fiber reinforced composite material yields notable enhancements in the specific strength and specific stiffness of the structure. Upon thoughtful design consideration, the structure exhibits favorable energy absorption traits. Subsequent research endeavors will delve into the utility of these structures as crushing boxes in automotive applications, with particular focus on exploring the influence of layer quantity on their mechanical performance.

REFERENCES

[1] Wang XT, Wang B, Wen ZH, et al. "Fabrication and mechanical properties of CFRP composite three-dimensional double-arrow-head auxetic structures," *Composites Science and Technology*. vol. 164, pp. 92-102, 2018.

[2] Li ZY, Wang XT, Ma L, et al. "Auxetic and failure characteristics of composite stacked origami cellular materials under compression," *Thin-Walled Structures*. vol. 184, 2023.

[3] Zhu YL, Gao DF, Shao YB, et al. "A novel prefabricated auxetic honeycomb meta-structure based on mortise and tenon principle," *Composite Structures*. vol. 329, 2024.

ID 9
OUT OF PLANE STRATEGY FOR MANUFACTURE LARGE SCALE DRONE COMPOSITE MOLDS WITH ADDITIVE MANUFACTURING

César García-Gascón[1], Pablo Castelló-Pedrero[2], and Juan A. García-Manrique[3](*)

[1, 2, 3] Universitat Politècnica de Valencia, Valencia, Spain, Design for Manufacturing Research Institute (IDF)

(*) Email: jugarcia@upv.edu.es

ABSTRACT

This work proposes the development of a deposition strategy that operates out of the traditional plane for Large Scale Additive Manufacture (LSAM) processes. In a preliminary approach, short fiber thermoplastic matrix composites will be used, as there is a significant lack of under-standing regarding the physical phenomena that occurs during fused material deposition and subsequent cooling. Unconventional methods will be used for layer deposition, such as 45-degree nozzle or Out of Plane trajectories. The layer deposition time must be optimized in order to improve the product mechanical behaviour, as longer layer times lead to an over-cooled surface, resulting in weak bonding, cracking, or deformation between layers. On the other hand, shorter layer times lead to high substrate temperatures, thus the part could collapse during manufacturing. Deposition at 45 or Out of Plane trajectories affect the internal stresses generated during the part cooling, specially with short fiber reinforcement parts (Figure 1). These stresses cause deformations in the parts. Typically, these components are molds used in the manufacturing of composite material parts, hence require high dimensional accuracy. Therefore, optimizing the layer time in additive manufacturing (AM) is critical to obtain a high-quality product.

The recommendation for quality printing is to print a new layer when the temperature of the upper layer is slightly higher than the glass transition temperature of the material. By approximating cooling as an exponential function of time, an optimized layer time can be obtained based on a target temperature while maintaining a minimum printing time. In this article, a minimum time per layer of 50 seconds has been set for every experimental sample. For the experimental validation of this work, a LSAM equipment will be used, and Acrylonitrile Butadiene Styrene (ABS) with a 20% carbon fiber reinforcement (CF/ABS) will be printed. Numerical simulations of the AM process, using a finite element approach, have been performed to predict internal stresses and warpage in the printed parts. This work compares the porosity, puncture, tensile and stiffness properties of two novel hybrid woven fabrics with two basic woven fabrics (matt and 6 ends Satin). The fabrics were developed using a natural fibre Jute yarn on rapier dobby machine present in a in-house lab. The tests were performed on a universal testing machine and circular bend procedure stiffness tester. The satin weave showed maximum deformation during a puncture test. Moreover, the hybrid weave demonstrated improvement in tensile property during a tensile test. The stiffness of hybrid weave is better as compared to other fabrics.

KEYWORDS

Additive Manufacturing; Material Extrusion (Mex), Formula Student, Composite, Carbon Fiber
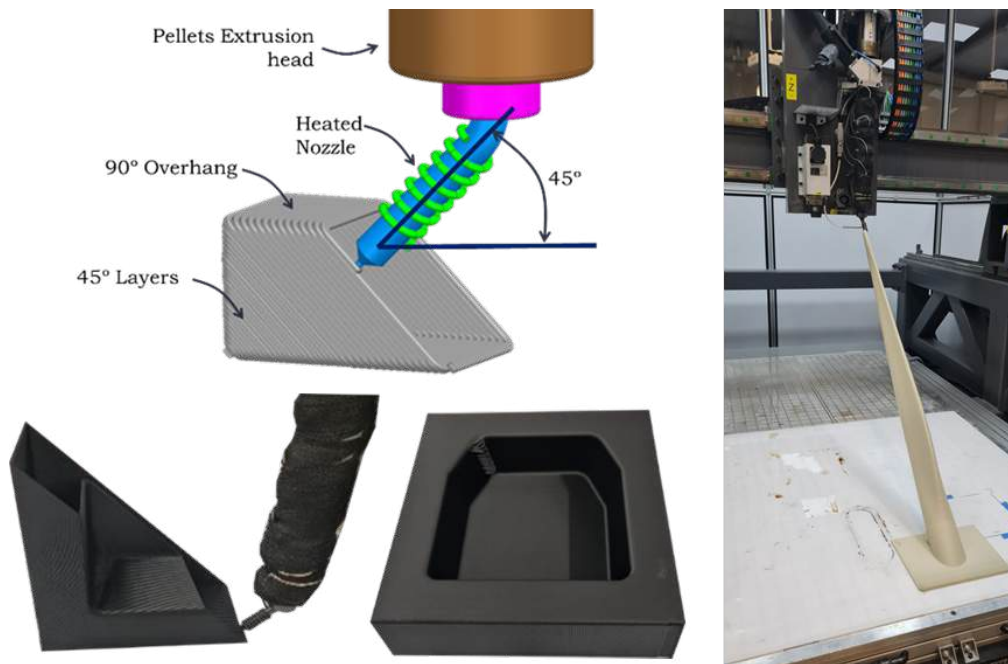
Figure 1: FGF extrusion with a 45º nozzle. Manufacture of an impact attenuator and wind turbine blade.

REFERENCES

[1] C.M.S. Vicente, M. Sardinha, L. Reis et al., "Large-format additive manufacturing of polymer extrusion-based deposition systems: review and applications", 2023, *Progress in Additive Manufacturing*. https://doi.org/10.1007/s40964-023-00397-9.

[2] G. Barera, S. Dul and A. Pegoretti, "Screw Extrusion Additive Manufacturing of Carbon Fiber Reinforced PA6 Tools", *Journal of Materials Engineering and Performance*, 2023. doi.org/10.1007/s11665-023-08342-1

[3] E. Eyercioglu, E. Tek, M. Aladag, G. Tas. "Effect of different amounts of carbon fiber additive ABS on thermal distortion and cooling time", *The International Journal of Materials and Engineering Technology (TIJMET)*, 5(1), 2022.

[4] J. Bryła, A. Martowicz, "Study on the Importance of a Slicer Selection for the 3D Printing Process Parameters via the Investigation of G-Code Readings", *Machines*, 9, 163, 2021. https://doi.org/10.3390/machines9080163.

ID 12

AN EXPERIMENTAL STUDY ON THE INFLUENCE OF BACKING MATERIAL ON THE BALLISTIC IMPACT RESPONSE OF MULTI-LAYERED COMPOSITE STRUCTURES

Oscar Lafuente Arjona[1](*), Lucas Amaral[2], Nick Eleftheroglou[3]

[1, 2] TNO Group Platform Protection and Advanced Materials, The Hague, The Netherlands

[3] Faculty of Aerospace Engineering, TU Delft, Delft, The Netherlands

(*) Email: oscar.lafuentearjona@tno.nl

ABSTRACT

This paper investigates the ballistic impact response of multi-layered composite structures against armour-piercing projectiles. The results show that fibre-reinforced polymer composite plates bonded to a ceramic strike face can dissipate more projectile kinetic energy at a lower mass penalty than armour steel. Furthermore, the addition of a metal interlayer to the ceramic-faced composite-backed armour is shown to be a promising alternative for providing greater protection against 7.62x51mm AP8 (tungsten carbide core) projectiles impacting at 930m/s. Finally, the current study compares the performance of both E-glass fibre/epoxy and carbon fibre/epoxy as composite backing materials for ballistic protection.

INTRODUCTION

The development of new material and protection concepts that are integrally designed in the vehicle hull aims to increase the mobility and payload carrying capability of military ground vehicles by reducing weight. Lightweight armour systems that function as the main load-bearing structure can be achieved by using multi-layered composite armour concepts (Quéfélec and Dartois, 2016). A multi-layered composite armour consists of a fibre-reinforced polymer composite plate bonded to a ceramic strike face, a metal interlayer, or a combination thereof. For their application in military vehicles, composite backing materials must meet both structural and ballistic performance requirements. While carbon fibre is suitable for vehicle structural elements, its ballistic performance is considered to be poor as opposed to glass fibre, a more ballistic-resistant material (Chocron et al., 2019).

This work aims to gain insight into the performance of these two lightweight composite backing materials and how they compare to each other. The ballistic impact response of different target configurations containing an aluminium oxide strike face, a composite backing and/or an aluminium plate is studied by testing against 7.62x51mm AP8 (Armour Piercing - tungsten carbide core) projectiles. The plates are adhesively bonded to one another with Permacol 5134, vacuum-bagged and cured. The projectiles are fired at 930m/s and the remaining portion of the projectile after penetration is captured using a water tank. An infrared device measures the impact velocity and the residual velocity of the projectile is measured from the high-speed video recording. Comparisons are made in terms of energy absorption and damage mechanisms, as well as with regards to Armox 500T (armour steel) as a reference material.

RESULTS AND CONCLUSIONS

The projectile residual velocity follows a decreasing trend with respect to the target areal density, which becomes steeper as soon as a ceramic strike face is added to the composite plate, as depicted in Fig. 1a. A similar correlation is found between the energy absorbed by the target and its areal density (see Fig. 1b), highlighting the

influence of damage mechanisms specific to a material on the target resistance, beyond the effect of mass addition. The presence of a interlayer triggers a new trend, which is the ability of the multi-layered composite target to neutralise the projectile. Comparable values of projectile residual velocity and energy absorbed by the target are observed between the two composite backing materials when adding a metal interlayer. Using a carbon fibre/epoxy composite backing may therefore seem a better choice given its lower areal density. However, target configurations with E-glass fibre/epoxy composite backings and aluminium interlayers achieved a greater number of stops (see Table 1) at a similar areal density than 9mm Armox 500T. The protective capability of the multi-layered composite target is also increased when the aluminium interlayer is placed between the ceramic strike face and the composite backing.

Table 1 Number of shots, number of stops and percentage of projectile defeat per target configuration.

Sample type	Description	Areal density [kg/m²]	No. of shots	No. of stops	Percentage of projectile defeat
0A	9mm Armox 500T	70.65	10	0	0%
0B	12mm Armox 500T	94.20	10	0	0%
1A	11.60mm CFRP	18.72	8	0	0%
1B	8.12mm CFRP	12.92	8	0	0%
2A	11.52mm GFRP	22.34	10	0	0%
2B	17.28mm GFRP	34.31	10	0	0%
3A	8mm Al_2O_3/11.60mm CFRP	49.49	8	0	0%
3B	8mm Al_2O_3/8.12mm CFRP	43.69	8	0	0%
4A	8mm Al_2O_3/11.52mm GFRP	53.11	13	0	0%
4B	8mm Al_2O_3/17.28mm GFRP	65.08	13	0	0%
5A	8mm Al_2O_3/6.35mm Al/11.60mm CFRP	67.33	7	3	43%
6A	8mm Al_2O_3/6.35mm Al/11.52mm GFRP	70.95	10	6	60%
7A	8mm Al_2O_3/11.60mm CFRP/6.35mm Al	67.33	7	0	0%
8A	8mm Al_2O_3/11.52mm GFRP/6.35mm Al	70.95	10	5	50%
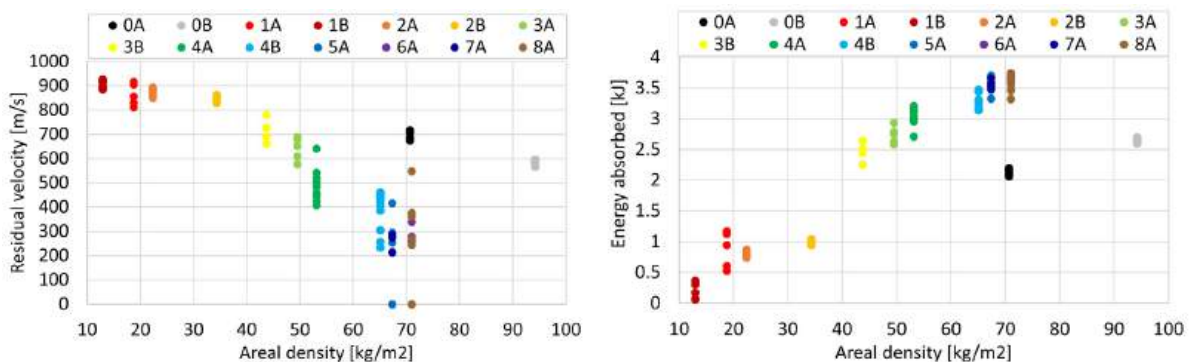
Fig. 1 Target performance comparison in terms of a) residual velocity and b) energy absorbed.

This study shows the potential of integrating multi-layered composite structures in the vehicle design for enhanced protection capability and mobility, and the suitability of E-glass fibre/epoxy laminates as composite backing material given its superior mechanical properties, which rule the damage mechanisms observed in impacted samples.

REFERENCES

[1] B. Quéfélec and M. Dartois, "Ceramic-faced molded armor," in *Lightweight Ballistic Composites: Military and Law-Enforcement Applications: Second Edition*. Elsevier Inc., 2016, pp. 369–391.

[2] S. Chocron et al., "Impact on carbon fiber composite: Ballistic tests, material tests, and computer simulations," *International Journal of Impact Engineering*, vol. 131, no. Septembre, pp. 39–56, 2019.

ID 13
DETECTION OF VIRUSES AND BACTERIA FOR DEFENSE VIA INTERNET OF THINGS AND OPTICAL CHEMICAL SENSORS

Francesco Arcadio[1], Ines Tavoletta[1], Chiara Marzano[1], Fiore Capasso[1], Luca Pasquale Renzullo[1], Luigi Zeni[1], Nunzio Cennamo[1(*)]

[1] Department of Engineering, University of Campania Luigi Vanvitelli, Aversa, Italy

[(*)] Email: nunzio.cennamo@unicampania.it

ABSTRACT

The rapid and effective detection of viruses and bacteria in several matrices can be obtained via low-cost and small-size sensors to thwart possible acts of bioterrorism. Surface Plasmon Resonance (SPR) sensors can be efficiently combined with specific receptors, either biological (e.g., antibodies and aptamers) or biomimetic, such as molecularly imprinted polymers (MIPs), for the detection of dangerous microorganisms involved in biological warfare. This work describes a multidisciplinary model exploiting the Internet of Things (IoT) and innovative sensing approaches based on SPR optical fibre probes combined with MIPs. The SARS-CoV-2 detection is described as an example of the proposed sensing approach. By only changing the imprinting of the MIP, the same model can be extended to detecting other viruses and bacteria.

INTRODUCTION

The global fight against the COVID-19 pandemic has exposed the vulnerability of societies to natural and man--made biological threats, leading experts to warn of a possible increase in the use of biological weapons such as viruses or bacteria. Bioterrorism is the deliberate release and dissemination of pathogens with the intent to cause illness or death in humans, animals, or plants. In particular, the fight against bioterrorism generally focuses on mitigating human casualties, but technological innovation makes it possible to detect and identify pathogens promptly (Jansen et al., 2014). In this context, SPR bio/chemical sensors are widely used for rapid, low-cost, and specific detection. In fact, several SPR bio/chemical sensors for the detection of viruses and bacteria have been reported in the literature (Cennamo et al., 2021; Pasquardini et al., 2023). Specifically, Cennamo et al. developed an SPR sensor to determine SARS-CoV-2 virions in aqueous solutions via MIP and aptamer receptors (Cennamo et al., 2021). Instead, Pasquardini et al. have developed an SPR biosensor for the specific recognition of the *Brucella* that causes Brucellosis. This infectious disease can be transferred to humans from animals (Pasquardini et al., 2023). This work presents the BETTER project results as an example, which involves using the Internet of Things and a selective sensor system based on plastic optical fiber (POF) platforms combined with MIPs to detect SARS-CoV-2.

RESULTS AND CONCLUSIONS

In order to show the capabilities of the proposed method, some results obtained in the BETTER project are reported as a paradigm. The project, funded by the Campania Region (Italy), has produced and tested, with the support of the company Moresense srl (Milan, Italy), about 1,000 specific optical chemical sensors to measure SARS--CoV-2 in the Universal Transport Medium (UTM). Approximately 100 positive and 800 negative nasopharyngeal samples were tested by the SPR-POF-MIP sensor system and checked via standard Real-time PCR (Polymerase Chain Reaction) method. Thanks to the method's high sensitivity, the virus's presence can be successfully detected even in diluted samples. In particular, the sensor approach is based on a very sensitive SPR-POF platform combined with a specific MIP receptor layer (see Fig. 1a). The BETTER project demonstrated that the developed

sensor system could detect the presence of the virus in a few minutes (about 10 minutes) in UTM and transmit the result to a platform via the Internet of Things, providing real-time automatic statistics useful for the monitoring and management of pandemics, as shown in the results reported in Fig. 1b (more details are reported on the website: https://www.progettobetter.eu/).
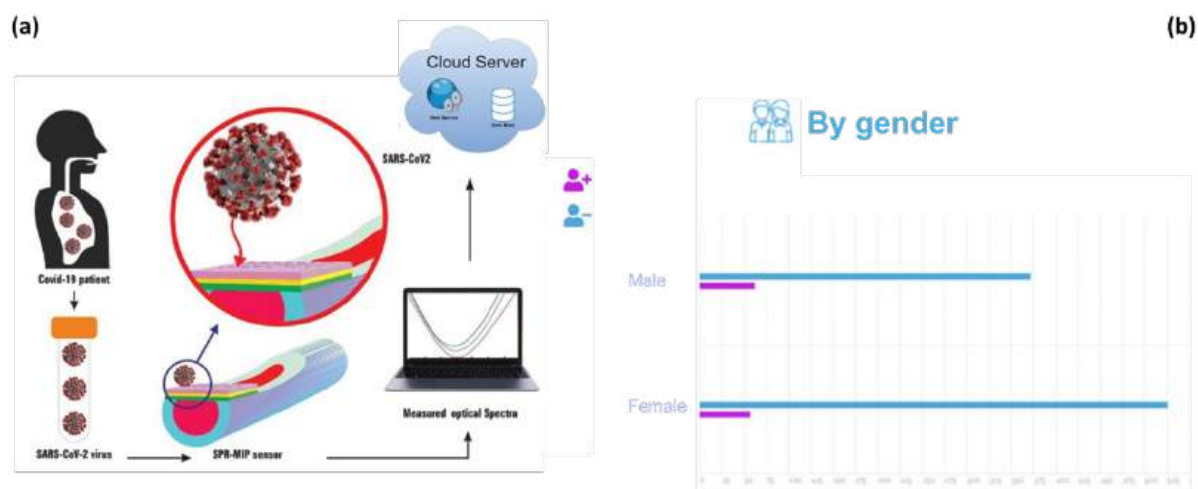
Fig. 1 a) Outline of the sensing approach used for the detection of SARS-CoV-2 via SPR-POF-MIP sensors and IoT b) An example of automatic statistics, divided by gender, of data acquired by the SPR-POF-MIP sensors and automatically transmitted to the Internet during the BETTER project (https://www.progettobetter.eu/).

Moreover, the proposed technology, already used in the BETTER project, is highly versatile; in fact, it is possible to produce other types of sensors involved in biodefense, specific for different microorganisms of interest, simply by coding the MIP receptor layer. Specifically, the proposed approach would allow extremely fast, highly sensitive, low-cost, and reusable diagnosis and tracking dangerous viruses and bacteria.

REFERENCES

[1] H.J. Jansen, F.J. Breeveld, C. Stijnis, and M.P. Grobusch, "Biological warfare, bioterrorism, and biocrime," in *Clinical microbiology and infection: the official publication of the European Society of Clinical Microbiology and Infectious Diseases*, vol. 20(6), pp. 488– 496, 2014.

[2] N. Cennamo, G. D'Agostino, C. Perri, F. Arcadio, G. Chiaretti, E.M Parisio, G. Camarlinghi, C. Vettori, F. Di Marzo, R. Cennamo, G. Porto, and L. Zeni, "Proof of Concept for a Quick and Highly Sensitive On-Site Detection of SARS--CoV-2 by Plasmonic Optical Fibers and Molecularly Imprinted Polymers," *Sensors (Basel, Switzerland)*, vol. 21(5), pp.1681, 2021.

[3] N. Cennamo, L. Pasquardini, F. Arcadio, L. Lunelli, L. Vanzetti, V. Carafa, L. Altucci, L. Zeni, "SARS-CoV-2 spike protein detection through a plasmonic D-shaped plastic optical fiber aptasensor," *Talanta*, vol. 233, pp. 122532, 2021.

[4] L. Pasquardini, N. Cennamo, F. Arcadio, C. Perri, A. Chiodi, G. D'Agostino, and L. Zeni, "Immuno-SPR biosensor for the detection of Brucella abortus," *Scientific Reports*, vol. 13, pp. 22832, 2023.

ID 14
A NOVEL 3D HYBRID AUXETIC LATTICE STRUCTURE WITH ENHANCED LOAD BEARING CAPACITY.

Keda Li[1], Binggang Xu[1], Jian Xiong[2], Hong Hu[1]*

[1] School of Fashion & Textiles, The Hong Kong Polytechnic University, Hong Kong, China

[2] Center for Composite Materials & Structures, Harbin Institute of Technology, Harbin, China [(*)] Email: hu.hong@polyu.edu.hk

ABSTRACT

This study presents novel 3D hybrid auxetic lattice structure based on stretching-dominated deformation mechanisms that exhibit excellent load-bearing capacity. The unit cell of the proposed 2D hybrid structure was designed through the hybridization of a double arrowhead part with a re-entrant quadrilateral part. The 2D auxetic parts were first alternatively assembled into a 3D configuration via the interlocking assembly method. The mechanical properties of four structures with different cell-wall angles were systematically characterized through the finite element (FE) method. Furthermore, the structures fabricated with highmodulus Carbon fiber-reinforced polymer (CFRP) laminate composites were subjected to quasi-static compression tests to experimentally study their compressive properties. Both experimental and numerical analysis evaluated Yong's modulus, shear modulus and NPR value of structures along the compression direction, and good agreement was found between them. The results indicated the novel CFRP composite 3D auxetic structures realized a significant improvement in structural stiffness compared to either conventional reentrant structure or double arrowhead structure. The proposed structure can be used for practical applications requiring load-bearing capacity.

INTRODUCTION

Auxetic lattices with a negative Poisson's ratio effect are specially designed mechanical metamaterial with unique mechanical characteristics, including exceptional energy absorption, higher resistance to indentation and enhanced fracture toughness [1-2]. Several research studies have focused on improving auxetic lattice structures to enhance their loadbearing capability [3-5]. The hybrid auxetic structure that are deformed through a stretchdominated process has been extensively researched due to its superior structural stiffness compared to structures with bending-dominated processes [6].

Meanwhile, many studies revealed the manufacturing of auxetic lattice structures using fiber reinforced composites exhibits high stiffness [7-10]. One major advantage of fabricating lattice structures using composites is that their mechanical performance can be improved along the principal axial direction by controlling material anisotropy [11]. The combination of material properties and lattice structure can make composite lattice structures to have superior load-bearing capabilities, in which the principal loading direction can be arranged in line with the primary fibre direction of the composites during the structural design [12].

However, the efficient manufacturing of auxetic composites with enhanced load-bearing capacities and cost-effective methods remains to be uncovered and improved. This study introduces a novel concept for a 3D hybrid auxetic structure combining CFRP composite and an interlocking assembly method. The quasi-static compressive properties and auxetic behavior of the proposed structures with different geometric parameters are studied through FE simulation and experimental tests.

RESULTS AND CONCLUSIONS

The results show that the CFRP 3D auxetic lattice structures exhibit excellent load bearing stiffness and negative Poisson's ratio effect. A parametric analysis (Fig. 1) was performed to investigate the effect of design parameters (L/t_0, t_1/t_0, t_2/t_0 and θ_2) and their interactions on the mechanical properties of the auxetic composite. The statistical model was developed by using Box–Behnken response surface technique to drive elastic constant equations. L/t_0 has the most significant effect on the normalized Young's modulus (E_y) and shear modulus (G_{xy}), followed by t_1/t_0 and t_2/t_0, while the angle (θ_2) of the oblique struts in the quadrilateral part has the negligible effect on stiffness. The load-bearing capacity of the 3D auxetic lattice structures can be enhanced by increasing the width of vertical struts (t_0) and oblique struts (t_1 and t_2). The NPR effect can be enhanced by simultaneously reducing t_0, t_1, t_2, and θ_2. It is interesting to note the effect of L/t_0 on v_{yx} depends on either t_1/t_0 or t_2/t_0, while the effect of t_2/t_0 on v_{yx} depends on t_1/t_0.
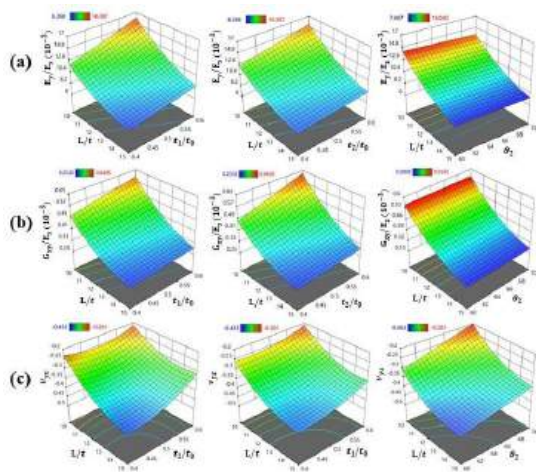
Fig. 1 Effect of design parameters on mechanical properties (a) E_y / E_s; (b) G_{xy} / E_s; (c) v_{yx}
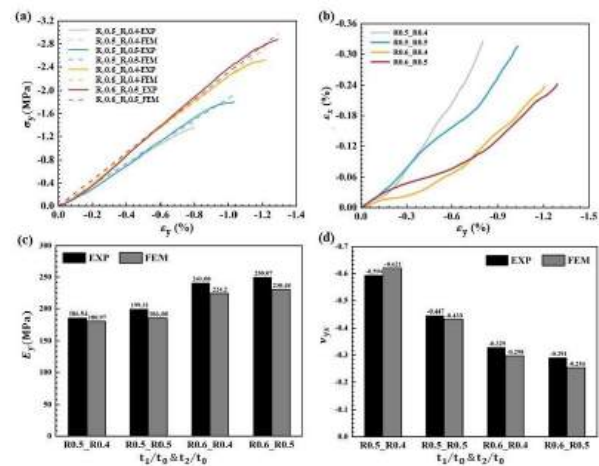
Fig. 2 a) stress- strain curves between the experimental and FE results b) lateral strain-strains curves

c) Young's modulus (Ey) d) maximum negative Poisson's ratio (vyx)

Fig. 2(b) shows the experimental deformation behaviors of the four specimens under the compression loading along the y-axis. As the compression increased, the samples experienced transverse contraction, resulting in an increase in lateral strains. the lower t_1/t_0 samples exhibits larger lateral contraction, and the higher t_2/t_0 samples have higher compressive failure strain while the t_1/t_0 remains constant. Fig. 2(a), (c) and (d) compare the experimental and FE stress-strain curves, Young's modulus, and maximum negative Poisson's ratio values for four specimens. Good agreements are found between the FE simulations and experimental tests.

Both experimental and numerical analysis shows the novel 3D auxetic structures are very suitable for uniaxial loading. Moreover, the fast fabrication method presented in this study provides a promising solution to the challenge of manufacturing composite 3D auxetic lattice structures. This study provides a better understanding of compressive elastic properties and deformation behavior of the 3D auxetic lattice structure, which made them highly appealing for use in various load-bearing applications.

REFERENCES

[1] Ren, X., Das, R., Tran, P., Ngo, T. D., & Xie, Y. M. (2018). Auxetic metamaterials and structures: a review. Smart materials and structures, 27(2), 023001.

[2] Saxena, K. K., Das, R., & Calius, E. P. (2016). Three decades of auxetics research– materials with negative Poisson's ratio: a review. Advanced Engineering Materials, 18(11), 1847-1870.

[3] Ingrole, A., Hao, A., & Liang, R. (2017). Design and modeling of auxetic and hybrid honeycomb structures for in-plane property enhancement. Materials & Design, 117, 72-83.

[4] Osman, M. M., Shazly, M., El-Danaf, E. A., Jamshidi, P., & Attallah, M. M. (2020). Compressive behavior of stretched and composite microlattice metamaterial for energy absorption applications. Composites Part B: Engineering, 184, 107715.

[5] Xue, Y., Wang, W., & Han, F. (2019). Enhanced compressive mechanical properties of aluminum based auxetic lattice structures filled with polymers. Composites Part B: Engineering, 171, 183-191.

[6] Gao, Y., Wu, Q., Wei, X., Zhou, Z., & Xiong, J. (2020). Composite tree-like re-entrant structure with high stiffness and controllable elastic anisotropy. International Journal of Solids and Structures, 206, 170-182.

[7] Evans, K. E., & Alderson, A. (2000). Auxetic materials: functional materials and structures from lateral thinking!. Advanced materials, 12(9), 617-628.

[8] Scarpa, F., Ciffo, L. G., & Yates, J. R. (2003). Dynamic properties of high structural integrity auxetic open cell foam. Smart materials and structures, 13(1), 49.

[9] Madke, R. R., & Chowdhury, R. (2020). Anti-impact behavior of auxetic sandwich structure with braided face sheets and 3D re-entrant cores. Composite Structures, 236, 111838.

[10] Lakes, R. S., & Elms, K. (1993). Indentability of conventional and negative Poisson's ratio foams. Journal of Composite Materials, 27(12), 1193-1202.

[11] Hunt, C. J., Morabito, F., Grace, C., Zhao, Y., & Woods, B. K. (2022). A review of composite lattice structures. Composite Structures, 284, 115120.

[12] Wang, H. W., Zhou, H. W., Gui, L. L., Ji, H. W., & Zhang, X. C. (2014). Analysis of effect of fiber orientation on Young's modulus for unidirectional fiber reinforced composites. Composites part B: engineering, 56, 733-739.

ID 16

ADVANCED 3D MODELLING AND SIMULATION METHODOLOGY TO IMPROVE DESIGN PROCESS FOR HYBRID COMBAT-READY CBRN SUITS

Afonso Gonçalves[1], Tânia Ferreira[1], A. Catarina Vale[1], Carlos Silva[2], Paula Lopes[5], Inês Cruz[5], Amin Taoufiq[5], Raquel Pinheiro[5], Humberto Guimarães[3], Pedro Magalhães[2], Luisa M. Arruda[1], Joana C. Antunes[1], Pedro Neto[5], Wilson Antunes[5], Clementina Freitas[3], Fernando Cunha[1], Inês P. Moreira[1] and Raul Fangueiro[1]

[1] Fibrenamics, Institute of Innovation of Fiber-based Materials and Composites, University of Minho 4710-057 Guimarães, Portugal.

[2] TINTEX Textiles SA, Zona Industrial, Polo 1, Camps, 4924-909 Vila Nova de Cerveira, Portugal.

[3] Latino Group, Parque Industrial de Adaúfe D4, 4710-571 Braga, Portugal

[5] Centro de Investigação da Academia Militar (CINAMIL), Unidade Militar Laboratorial de Defesa Biológica e Química (UMLDBQ, Instituto Universitário Militar) Av. Dr. Alfredo Bensaúde, 1849-012 Lisboa, Portugal.

(*) Email: afonsogoncalves@fibrenamics.com

ABSTRACT

This research explores the development of a combat-ready hybrid CBRN suit, aiming to meet strict defense requirements while blending with existing military uniform designs. It focuses on ease-of-use, thermophysiological comfort, and mobility. The study introduces a methodology to expedite the design-to-prototype process for textile wearables by digitizing material properties, utilizing CLO 3D software for advanced simulations. Textile tests measured thickness, density, stretch, bending, and friction. The initial prototype scored 4.7 out of 5 in AEP-38 based tests for thermophysiological properties, comfort, and safety. Innovations in protection technologies and digital simulations resulted in a final product 31% lighter than other lightweight CBRN suits.

INTRODUCTION

Amidst the current escalation of global conflicts, the imperative for rapid response in defense readiness is critical [1]. This project focuses on improving the wearability, comfort, and performance of CBRN suits and notably shortens the time from prototype to production using advanced 3D modeling and simulation. This faster production enables quicker deployment of protective gear to high-risk situations. The current market for CBRN suits focuses on protection, often at the expense of mobility and comfort due to the bulkiness and weight of materials [2] like activated carbon nanospheres [3]. This research introduces an innovative method that employs 3D modeling and simulation with CLO 3D software [4]. The aim is to maintain high protection standards while significantly enhancing wearability and user performance in CBRN and combat scenarios, addressing the defense sector's need for equipment that provides both safety and operational efficiency. In tangent to this work, an active CBRN defense multilayer solution was developed which greatly reduces bulkiness and weight compared to traditional activated carbon protection technologies (unpublished work).

RESULTS AND CONCLUSIONS

Through material digitization, simulations in various poses (Fig. 1) were conducted and the geometric improvement methodology was applied, allowing to quickly improve suit designs (Fig. 2). The final design, meeting all required characteristics, was developed, presented, and sent for prototype production in under 10 working days,

showcasing the rapid product development that is possible with this methodology.
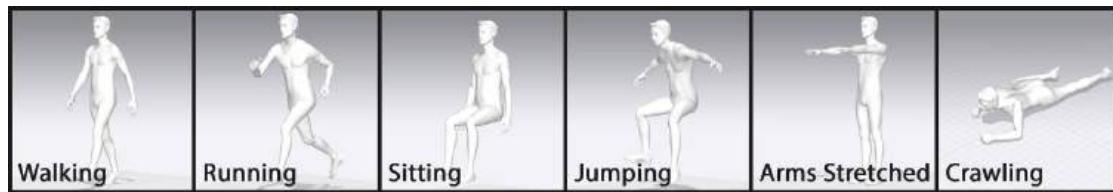
Fig. 1 Image set of the main avatar poses used for realistic movement simulations
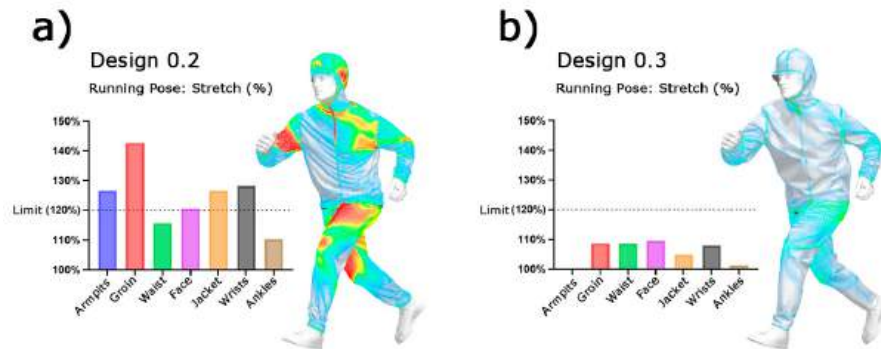
Fig. 2 Comparison of key results from two design iterations. a) Design 02 and b) Design 0.3

Usability tests with the Portuguese army based on AEP-38 showed positive results for user comfort, including ease of movement, temperature regulation, compatibility with other protective equipment and gear, and breathability. However, improvements were needed in certain areas: the chin's elastic bands were too tight, the pants' liner fabric was too loose making removal with boots difficult, and knee pad integration complicated wearing the pants. This experience revealed potential differences between simulated outcomes and actual implementation, showing that manufacturing and testing can introduce unexpected variables not predicted in digital models. In conclusion, the military's usability assessment was a 4.7 out of 5. The prototype was awarded the Army Tested Seal, signifying that it met the standards and requirements established by armed forces during testing, providing official validation of its performance and utility in military scenarios. The satisfactory performance of the prototype is closely linked to the strategic use of digital simulation software in its design, demonstrating how state-of-the-art digital tools can enhance prototyping and end products.

REFERENCES

[1] Sharma, N., Nair, A., Gupta, B., Kulshrestha, S., Goel, R., & Chawla, R. (2020). "Chemical, biological, radiological, and nuclear textiles: current scenario and way forward", in *Advances in Functional and Protective Textiles*, Elsevier, pp. 117–140, 2020.
[2] Antunes, J. C., Moreira, I. P., Gomes, F., Cunha, F., Henriques, M., & Fangueiro, R., "Recent Trends in Protective Textiles against Biological Threats: A Focus on Biological Warfare Agents", in *Polymers* (Vol. 14, Issue 8), 2022
[3] Khalilur, M., & Khan, R., "CBRN Personal Protective Clothing", in *Kohan Textile Journal*, 2021.
[4] Boldt, R. S., "Contribuições dos sistemas CAD 3D no processo de validação do produto de moda", 2018.

ID 17
NATURAL FIBERS AND NANOMATERIALS FOR ADVANCED MULTIFUNCTIONAL PROTECTIVE FIBROUS STRUCTURES

Joana C. Araújo[1(*)], **Raul Fangueiro**[1], **Diana P. Ferreira**[1]
[1]Centre for Textile Science and Technology (2C2T), University of Minho, 4710-057 Guimarães, Portugal
[(*)] Email: joanaaraujo@det.uminho.pt

ABSTRACT

This work aims to develop multifunctional fibrous structures for personal protection applications based on natural fibers and nanomaterials. Biopolymers and natural fibers, like flax and jute, were functionalized with carbon nanomaterials and metal oxide nanoparticles (NPs). Straightforward and environmentally conscious processes and materials were employed to achieve multifunctionality, including the degradation of chemical and biological harmful agents. Field Emission Scanning Electron Microscopy (FESEM), Attenuated Total Reflectance-Fourier-Transform Infrared Spectroscopy (ATR-FTIR) and Ground-State Diffuse Reflectance (GSDR) were used in order to characterize the developed samples. Functional roperties like harmful chemicals degradation, antibacterial activity, hydrophobicity, electrical conductivity and ultraviolet (UV) protection were also assessed.

INTRODUCTION

There has been an extraordinary surge in the creation of human protection products and technologies in recent years. More than ever, there are several risks to the health and well-being of the global population. Hazardous chemicals and biological agents are among the greatest risks to civilians as well as military personnel. As a result, it is critical to create personal protective equipment (PPE) that can both actively and passively shield its wearer by absorbing and eliminating noxious substances [1].

Functionalization of active fibrous structures using nanomaterials is one emerging method for creating structures with enhanced functionality and novel features. Notwithstanding their well-established efficacy in the degradation of hazardous substances, nanomaterials could possibly incorporate additional functions into the same structure without gaining undue weight. Since natural fibers are highly abundant in nature, inexpensive, and biodegradable, they have also become a great alternative to synthetic ones [2].

Therefore, in this work, several natural fibers and biopolymers were functionalized with carbon nanomaterials and metal oxide NPs (CaO, MgO, SiO2, TiO2 and CeO2) by very simple and sustainable methods. The developed samples were characterized, and their functional properties were evaluated.

RESULTS AND CONCLUSIONS

Natural fibers like jute and flax, and biopolymers like chitosan (CS) and polycaprolactone (PCL) were functionalized with CaO, MgO, SiO2, TiO2 and CeO2 NPs and graphene nanoplatelets (GNPs). Several functionalization methods like, in-situ synthesis, dip-pad-dry, electrospinning and electrospraying deposition were applied. The sustainability of the processes and materials was always taken into account. FESEM images of a) jute fabrics functionalized with CaO-SiO2 NPs, flax fabrics functionalized with MgO-SiO2 core-shell NPs and c) electrospun PCL microfibers functionalized with GNPs are shown in Fig. 1. As can be seen the functionalization of the fibrous substrates with the nanomaterial was successful, ensuring a homogenous distribution.
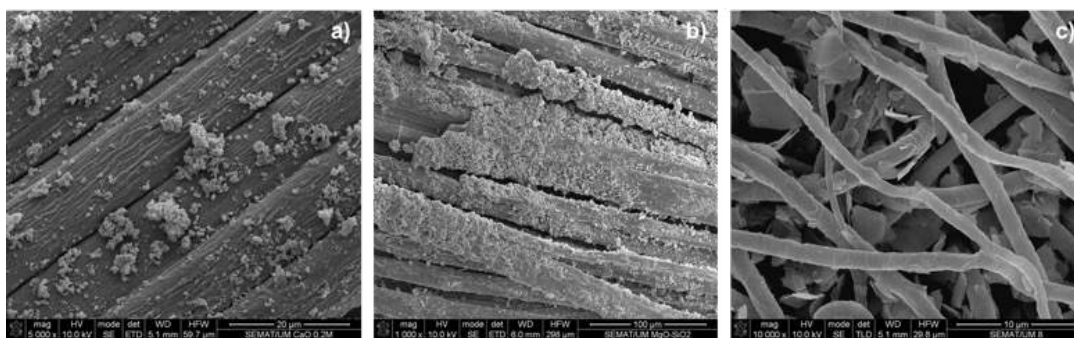
Fig. 1 FESEM images of **a)** jute fabrics functionalized with CaO-SiO$_2$ NPs, **b)** flax fabrics functionalized with MgO--SiO$_2$ core-shell NPs and **c)** PCL microfibers functionalized with GNPs

Several properties, especially the protection against chemical and biological hazardous agents were also evaluated. As an example, Table 1 shows the antibacterial activity of jute fabrics functionalized with CaO-SiO$_2$ NPs and flax fabrics functionalized with MgO-SiO$_2$ core-shell NPs against Gram-positive and Gram-negative bacteria. The introduction of the NPs undoubtedly allowed the obtention of antibacterial textiles.

Table 1 Antibacterial activity (%) values of jute fabrics functionalized with CaO-SiO$_2$ NPs and flax fabrics functionalized with MgO−SiO$_2$ core--shell NPs.

Sample	*Staphylococcus aureus*	*Escherichia coli*
Jute+CaO-SiO$_2$	99.96 ± 0.07	99.80 ± 0.29
Flax+MgO-SiO$_2$	99.99±0.01	99.42±0.20

This study introduces innovative solutions for the development of multifunctional fibrous systems using natural fibers and nanomaterials, with great potential for application in personal protection.

ACKNOWLEDGMENTS

REFERENCES

[1] J. C. Araújo, R. Fangueiro, and D. P. Ferreira, "Protective multifunctional fibrous systems based on natural fibers and metal oxide nanoparticles", *Polymers*, vol. 13, no. 6, pp. 2654, 2021.

[2] J. C. Araújo, P. Teixeira, R. Fangueiro, and D. P. Ferreira, "Multifunctional natural fibers: the potential of core shell MgO−SiO$_2$ nanoparticles", Cellulose, vol. 29, no. 10, pp. 5659-5676, 2022.

ID 18

OPTIMIZING BLAST RESPONSE: MATERIAL IMPROVEMENT FOR SANDWICH STRUCTURES WITH LATTICE CORE MANUFACTURED VIA L-PBF

Elisa Guimaraens1(*), Konstantin Kappe1, Aron Pfaff1, Jürgen Herrmann1, Klaus Hoschke1
1Fraunhofer Institute for High-Speed Dynamics, Ernst-Mach-Institut, EMI, Freiburg, Germany
 (*)Email: elisa.guimaraens@emi.fraunhofer.de

ABSTRACT

Additive Design and Manufacturing potentialities in Fraunhofer EMI will be presented. Amalia (Additive Manufacturing of Metallic Auxetic Structures and Materials for Lightweight Armour 2022 – 2025) is an EDA cat. B project that aims for lighter blast protection and ballistic armor using auxetic structures. A study from the Amalia project involving two main work fields of our working group, design optimization for additive manufacturing and material optimization during L-PBF process, will be shown.

Laser powder bed fusion (L-PBF) offers many possibilities not only in what refers to component design freedom but also in in situ modification of materials properties. L-PBF has the potential to create novel functionally graded microstructures (FGMi) with properties tailored to specific applications. As build material for the investigated sandwich structures with lattice core three steel alloys were investigated and their properties were empirical optimized for the use in the lattice structures.

A study of different modelling concepts of additive manufactured lattice structures under high-speed dynamic loading will be presented. To validate the different approaches, experimental investigations on the most promising lattice structures and steel were performed. The structures are additive manufactured and their structural behaviour under high-speed dynamic loading is investigated and analysed using digital image correlation. The simulation approaches show a good agreement with the experimental results.

INTRODUCTION

For the last years lightweight cellular structures, including honeycombs, foams, and lattices have gained notable attention [1]. These structures possess impressive mechanical properties, such as increased specific strength and stiffness, as well as excellent energy absorption capabilities [2]. They find applications in dynamic load scenarios, such as crash, impact, or blast mitigation. However, the fabrication of geometrically defined lattice structures is challenging. In this context, additive manufacturing (AM) advancements offer opportunities to create complex structures with new materials and tailored properties, enhancing the mechanical properties of cellular structures [3, 4].

However, due to the various possibilities for geometries, arrangements, and dimensions of unit cells, finding an optimal design for different requirements can be challenging and time-consuming [5]. Here is where the component, in this case a sandwich structure with a lattice core, behaviour can be simulated in function of its geometry. In this study, cellular lattice structures are used as the core of sandwich structures for the mitigation of blast loads. For this purpose, the sandwich structures are optimized regarding the maximum transmitted force for the loading scenario (see Figure 1 a)). Thereby, different cell topologies and gradients of relative density are investigated. Through many simulations, a neural network is trained as a surrogate model and utilized for optimization with a genetic algorithm.

Parallel to the development of the cellular lattice structure three steel alloys were investigated. For that L-PBF different process properties, such as laser power and pace, were tested. In this work a new double laser exposure approach was used to obtain an in-situ thermal treatment of the alloys during the L-PBF manufacturing was investigated to obtain a FGMi.

The most promising simulated structures were fabricated using 30CrMoNb5-2 low alloy steel as this material showed the most suitable properties for the fabrication of the studied structures via L-PBF. The additive manufactured sandwich core structures were then tested, and the result used to validate and improve the simulation models.

RESULTS AND CONCLUSIONS

An explosive-driven shock tube is utilized to generate a planar pressure front, which enables the investigation of the sandwich structures on a laboratory scale (see Figure 1 b)). The structures are subjected to a reflected impulse and pressure of 2600 kPa*ms and 25000 kPa, which corresponds to an equivalent of approx. 3.9 kg TNT in 1 m distance of a hemispherical free field air-blast.
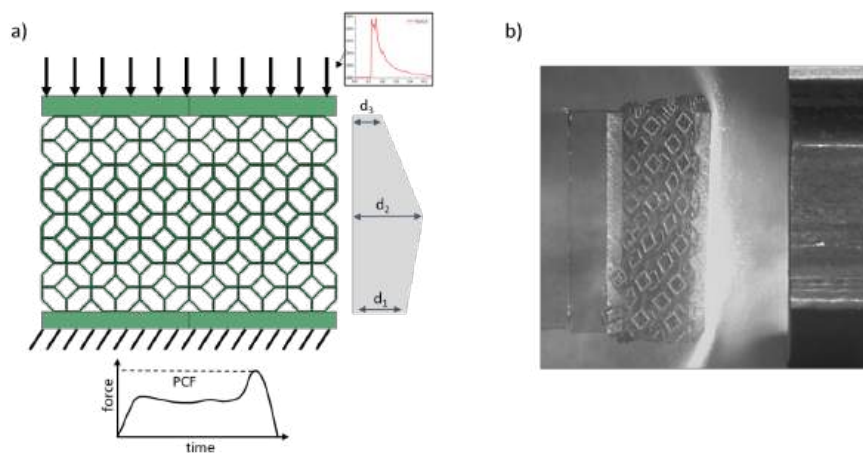
Figure 1 a) Optimization problem of a sandwich structure under blast loading with variables d1, d2 and d3 with regard to the maximum transmitted force (PCF) and b) optimized sandwich structure under blast loading in explosive-driven shock tube experiment.

The experimental results show good agreement with the predicted optimized structural response, depending on the cell topology. However, deviations can be observed, due to manufacturing inaccuracies of some geometries. This study shows that material properties of 30CrMoNb5-2 steel could be tailored during AM process. A functionally graded microstructure (FGMi) for this steel and application with hardness range from ca. 380 to 510 HV10 could be achieved. Analysis based on EBSD (electron back scattering diffraction) could be successfully used to reveal micro- and macro-graduation regarding tempering state through the sample.

REFERENCES

[1] Altenbach, H., Öchsner, A.: Cellular and porous materials in structures and processes. CISM courses and lectures, no. 521. Springer Verlag, Wien, New York (2010)

[2] Gibson, L.J., Ashby, M.F.: Cellular Solids. Structures and properties - Second edition. Cambridge University Press (2014)

[3] Pfaff, A., Jäcklein, M., Hoschke, K., Wickert, M.: Designed Materials by Additive Manufacturing—Impact of Exposure Strategies and Parameters on Material Characteristics of AlSi10Mg Processed by Laser Beam Melting. Metals (2018). https://doi.org/10.3390/met8070491

[4] Thompson, M.K., Moroni, G., Vaneker, T., Fadel, G., Campbell, R.I., Gibson, I., Bernard, A., Schulz, J., Graf, P., Ahuja, B., Martina, F.: Design for Additive Manufacturing: Trends, opportunities, considerations, and constraints. CIRP Annals (2016). https://doi.org/10.1016/j.cirp.2016.05.004

[5] Kappe, K., Hoschke, K., Riedel, W., Hiermaier, S.: Multi-objective optimization of additive manufactured functionally graded lattice structures under impact. International Journal of Impact Engineering (2023). https://doi.org/10.1016/j.ijimpeng.2023.104789

ID 20

ENERGY RELEASE CHARACTERISTICS OF REACTIVE SHAPED CHARGE LINERS PENETRATION INTO UNDERWATER

Tianchu Wang[1][(*)], Pengwan Chen[2], Chuan Zhao[3], Shouren Wang[4]

[1, 2, 3, 4] State Key Laboratory of Explosion Science and Technology, Beijing Institute of Technology, Beijing, China

[(*)] Email: 740454927@qq.com

ABSTRACT

In this paper, the reaction between the reactive liner shaped charge (RLSC) and underwater environment has been investigated. The reactive materials liner with a density of 5 g/cm^3 was prepared by cold spraying. The material of the reactive materials liner is Ni-Al energetic structural material. Compared with the Cu shaped charge, the RLSC has higher pressure into underwater. Moreover, the penetration depth of the RLSC is close to that of the Cu shaped charge. The damage characteristics into underwater of RLSC is better than Cu shaped charge.

Keyword: Reactive liner shaped charge, Ni-Al energetic structural material, Underwater

INTRODUCTION

Energetic materials are widely used in military and civilian fields due to their high energy density and rapid energy release characteristics. In recent years, the research on the underwater application of energetic materials has become a hot spot (Z. Shao et al. 2022). Previous studies on the underwater damage characteristics of the reactive liner shaped charge (RLSC) mostly used materials such as Al (J. Moore et al. 2013). These studies enhanced the underwater damage ability of the shaped charge by utilizing the aluminumwater reaction (Brown and Russell 1996). However, aluminum has a low density and lacks sufficient axial penetration capability into underwater.

The Ni-Al energetic structural material prepared by cold spraying has the advantages of high energy density, high compactness, low porosity and high bonding strength, which is suitable for the preparation of reactive liners (Won et al. 2014). However, there is currently a lack of research on the underwater damage performance of Ni-Al reactive liner shaped charge.

This work studies the damage characteristics of the Ni-Al RLSC by conducting underwater explosion experiments and comparing the pressure and penetration depth of the RLSC and the Cu shaped charge into underwater.

RESULTS AND CONCLUSIONS

In this research, the first observed flare photo was defined as the start time (t=0), coinciding with the shaped charge detonation. High-speed photographs of jet penetration into water are shown in Fig. 1. After 300 µs, strong light generated by the RLSC reaction in water was observed, providing experimental evidence for the occurrence of the RLSC reaction in water. The pressure sensors were located above the water surface with a distance of 30 cm and 20 cm away from the axis of shaped charge jet. Fig. 2. shows the pressure change of the two shaped charge jet into underwater as a function of time. The maximum pressure of the RLSC is 0.5 MPa, while that of the Cu shaped charge is 0.09 MPa. The maximum pressure of the RLSC and the Cu shaped charge are 0.5 MPa and 0.09 MPa, respectively. The maximum pressure of the RLSC is 455.6% higher than that of the Cu shaped charge. This is further evidence that the RLSC reacts underwater and releases energy, which has a stronger radial damage capacity than the Cu shaped charge. Fig. 3. shows the impact crater generated on the 45# steel target plate by shaped charge after penetrating 120 cm of water. After penetrating 120 cm of water, the Cu shaped charge exhibited a penetration

depth of 1 cm on the 45# steel target, while the RLSC didn't form a significant crater on the target. This suggests that the axial damage capability of the RLSC is slightly lower than that of the Cu shaped charge. Considering both radial and axial damage capabilities, the RLSC exhibits superior overall destructive performance compared to the Cu shaped charge.
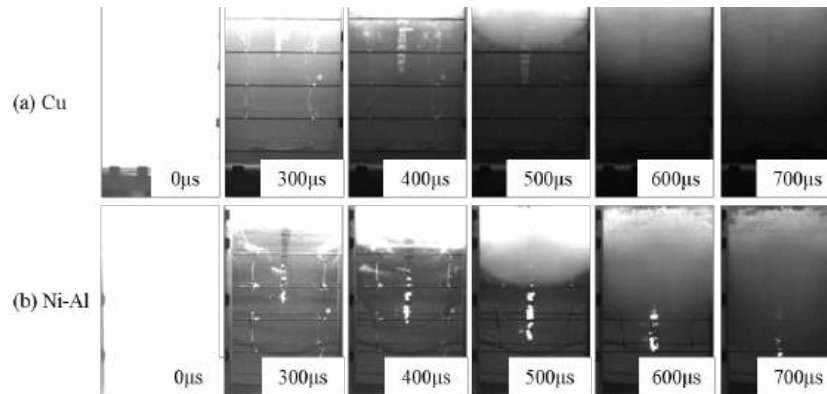
Fig. 1 High-speed photographs of jet penetration into water with different materials: (a) Cu; (b) NiAl
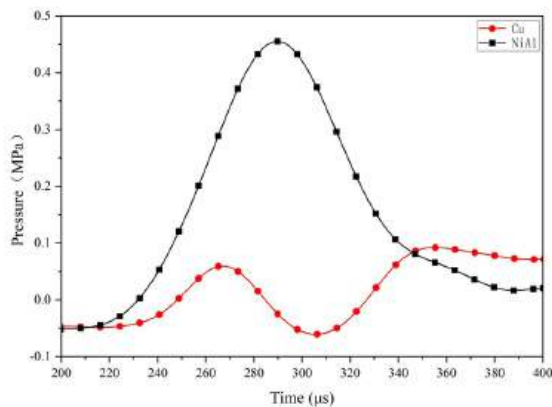
Fig. 2 Pressure curves of jets penetration into underwater with different materials.

Fig. 3 Target state after two penetration tests.

In this study, the underwater damage characteristics of the RLSC and the Cu shaped charge were compared through static explosion experiments. The results can provide data support for the underwater application of the Ni-Al RLSC.

REFERENCES

[1] C. A. Brown, and T. P. Russell. 1996. "Time Resolved Emission Studies of Aluminum and Water High Pressure Reactions," in *Proceedings of Materials Research Society Symposium,* 1996, pp. 391-395.

[2] J. Moore, C. Gloßner and W. Craig et al. "Quantitative Evidence of Reaction during Hypervelocity Penetration of Aluminum through Oxygenated Fluids," *Procedia Engineering,* 2013, pp. 157-166.

[3] J. Won, G. Bae and K. Kang et al. "Bonding, Reactivity, and Mechanical Properties of the Kinetic-Sprayed Deposition of Al for a Thermally Activated Reactive Cu Liner," *Journal of Thermal Spray Technology,* vol. 23, no. January, pp. 818–826, 2014.

[4] Z. Shao, C. Dong and S. Wu et al. "Energy Release Characteristics of Kinetic Energy Rod with Reactive Material Headduring Water Entry and Penetration into Underwater Target," *Acta Armamentarii*, vol. 43, no. 10, pp. 2517–2526, 2022.

ID 22

THERMAL MANAGEMENT OF ELECTRONIC COMPONENTS IN UNMANNED AERIAL VEHICLES USING PDMS HEAT SINKS

Ana S. Moita[1,2(*)], João Paulo N. Torres[2], Énio Chambel[2], Luís Quinto[2], Pedro Pontes[1], António L. N. Moreira[1]

[1] IN+, Centro de Estudos em Inovação, Tecnologia e Políticas de Desenvolvimento, Instituto Superior Técnico, Universidade de Lisboa. Av. Rovisco Pais, 1049-001 Lisboa, Portugal.

[2,3] CINAMIL - Centro de Investigação Desenvolvimento e Inovação da Academia Militar, Academia Militar, Instituto Universitário Militar, Rua Gomes Freire, 1169-203 Lisboa

(*) Email: anamoita@tecnico.ulisboa.pt

ABSTRACT

Unmanned vehicles play a paramount role in Defense and emergency operations. Its use in demanding environments requires very stable working conditions, including a stable and efficient thermal management of the electronic components. In this context, this work proposes the development and test of a cooling system for the electronic components of unmanned vehicles, modular and easy to adapt to different vehicles. The base element of this systema is a small heat sink based on microchannels, which can be easily assembled by addictive manufacturing. Despite being made from PDMS – Polydimethylsiloxane, a material with low values for many thermal properties such as thermal conductivity, it can be put in direct contact with the system to cool, significantly decreasing the thermal resistance of the heat exchanger and overall showing better cooling efficiencies when compared to traditional metallic heat exchangers, of the order of 17%. Furthermore, being based on a straight microchannels geometry allows for a more uniform cooling, offering a process with higher efficacy when compared to more traditional heat exchangers.

INTRODUCTION

Unmanned vehicles are becoming increasingly important in aerospace and defense applications, being used for a large range of situations, from intelligence to communication relays [1wnag]. As these systems become smaller and more complex, challenges arise in terms of heat dissipation [2] (e.g. Sienski et al., 1996). Microchannel based heat sinks are considered a cooling solution with high potential to dissipate high power loads. The device proposed here is a single microchannel based heat sink, produced in PDMS. The results shown and discussed here explore the use of unusual nanofluids with also unusual concentrations, together with a particular geometry, with and without phase change, which overall are quite effective in the thermal management of high power systems, and therefore, for the application proposed.

RESULTS AND CONCLUSIONS

Heat sinks were designed, and their shape and dimensions were optimized using an in-house genetic algorithm. Tests were performed on PDMS heat exchangers which were compared with traditional copper heat exchangers. Despite their worse thermal properties, the material is closely adapted to the cooling surfaces, resulting overall in higher thermal efficiencies, up to 17%. Details on the experiments can be found in [3] and the details on PDMS exchangers properties can be found in patent registration number 118128 (Ref. DMP/01/2022/2064537).

The results show advantages in using two-phase flows. However, flow instabilities caused by the presence of bubbles in the microchannels may lead to high instabilities in the temperature and increase the pumping power to values which turn this into a not feasible solution. In this context, the use of one-step method nanofluids is advan-

tageous. Comparing water based nanofluids using gold and silver nanoparticles (with concentrations of 1wt%), results show that these nanofluids result in improved cooling performances of the heat exchanger. This trend is depicted in Figure 1 a) b) which show much lower values of the non-dimensional temperature of the heated surface (the stainless-steel surface), $T^*=T-T_{amb}/T_{min}-T_{amb}$ (T_{amb} is the ambient temperature and T_{min} is the lowest temperature measured on the sheet) when using the gold nanoparticles. Concentrations were not increased up to 1%, as there is a maximum plateau after which the disadvantage of losing stability of the fluid surpasses any small improvement observed in the heat transfer. Smaller concentrations are also recommended for a sustainable commercial use of such fluid.
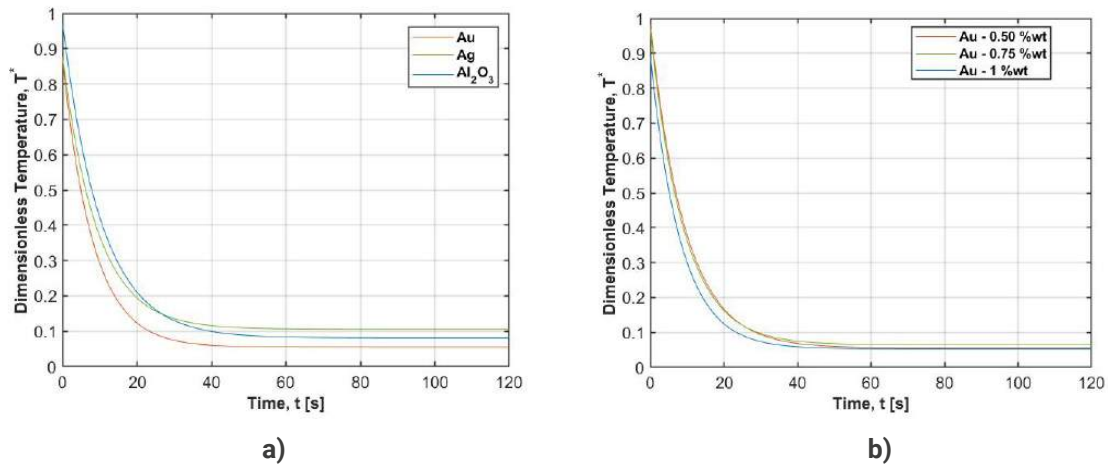
Fig. 1 Load extension curves of a) Puncture test b) Tensile test (warp wise) Cooling of the stainless-steel sheet overtime, based on the non--dimensional temperature ($T^*=T-T_{amb}/T_{min}-T_{amb}$), for: a) Different nanoparticle materials; b) Different nanoparticles concentration.

ACKNOWLEDGEMENTS

REFERENCES

[1] X. J. Wang, W.G. Kai, X. Sheng and S.N. Wang, "Review of aerospace-oriented spray cooling technology", *Progress in Airspace Sci*ence, vol. 116, 2020.

[2] K. Sienski, R. Eden and D. Schaefer, "3-D electronic interconnect packaging", In *Proceedings IEEE Aerospace Applications Conference*, Vol. 10, pp. 363–373, 1996.

[3] R.R. Souza, F.M. Sá Barbosa, G. Nobrega, E.M. Cardoso, J.C.F. Teixeira, A.S. Moita and R. Lima, "Experimental study of an innovative elastomer-based heat exchanger", Case Studies in Thermal Engineering, vol. 49, pp. 103365, 2023.

ID 24

EXPERIMENTAL INVESTIGATION OF THE DYNAMIC RESPONSE OF LOW-DENSITY FOAM-WRAPPED ALUMINUM TUBES UNDER LOCALIZED BLAST LOADING

Ben Rhouma Mohamed[1,2(*)], **Aminou Aldjabar**[1,2], **Maazoun Azer**[3], **Belkassem Bachir**[1], **Tine Tysmans**[2], and **Lecompte David**[1]

[1]Royal Military Academy, Propellant Explosives and Blast Engineering Department
Avenue de la Renaissance 30, 1000 Brussels, Belgium

[2]Vrije Universiteit Brussels, Mechanics of Materials and Constructions Department
Pleinlaan 2, 1050 Brussels, Belgium

[3] Military Academy of Fondouk Jedid, Civil Engineering Department, 8021 Nabeul, Tunisia

[(*)] Email: *e-mail: Mohamed.BenRhouma@mil.be

ABSTRACT

This study aims to assess the effectiveness of a sacrificial cladding system, consisting of a low-density foam and an outer lightweight skin, enveloping a specifically studied structure. The structure in question is a simply supported aluminum column exposed to a blast wave generated by an explosive-driven shock tube. The chosen sacrificial cladding includes closed-cell polyurethane foam (PU) with a density of 30 kg/m³ and a 1mm aluminum sheet. The raw specimens, with dimensions of 1200 mm x 100 mm x 2 mm (height x diameter x wall thickness), are obtained by cutting from 6m-long aluminum columns. The study involves a series of experiments using the Explosive shock-driven shock tube (EDST) as a laboratory loading tool. The local deformation, indicated by mid-span indentation, is quantified through 3D laser scanner measurements. Furthermore, the impact of the proposed cladding on local deformations of the retrofitted aluminum columns is examined. The results reveal that the maximum localized indentation is reduced by 5%, 28% and 46% when using 30 mm, 50 mm and 100 mm of PU foam, respectively.

INTRODUCTION.

In 2022, the Explosive Violence Monitoring Project documented 22,772 deaths and injuries resulting from the use of explosive weapons globally [1]. Over the past two decades, the frequency of incidents involving explosives has increased fivefold, impacting civilian populations, military personnel and infrastructure [2]. Consequently, there is a critical need to study the behavior of structures, structural components and materials under blast loading.

Sacrificial cladding emerges as a passive protective solution designed to absorb blast-induced energy, thereby reducing damage to the target [3]. The crushable core typically involves cellular structures or materials, such as metallic foam [4]–[6], polymeric foam [3][7], thin-walled tubular cores [8][9] and mineral foam [10][11]. Polyurethane (PU) foam, widely adopted for its lightweight nature, cost-effectiveness and low plateau stress characteristics, serves as a common choice for energy absorption [12]. It is often affixed to the façade of the protected structure to mitigate transmitted pressure to an acceptable threshold. While research on sacrificial cladding's anti-blast performance is extensive, studies focusing on circular structures are relatively limited. This paper aims to assess the blast absorption capacity of a sacrificial cladding composed of polymeric foam and a thin outer skin. The evaluation is conducted around a thin-walled circular member serving as a witness structure, represented by a pinned-pinned aluminum column. The investigation focuses on the reduction of damage to the aluminum column, providing insights into the protective capabilities of the proposed sacrificial cladding.

RESULTS AND CONCLUSIONS

To measure the deformation on the loaded side of different test configurations, indentation assessments are carried out using a handheld scanner combined with the Krypton K610 camera system. This methodology is distinguished by its non-invasive and non-destructive characteristics, ensuring the maintenance of the structural integrity of the scanned object.

In the analysis, the deformation parameters are identified and illustrated in Fig. 1, with detailed values provided in Table 1. Specifically, *d1* and *d2* denote the axial and radial width of the local deformation zone, corresponding to the loaded side of the area of interest, as depicted in Fig. 1.a. The parameter *b* represents the distance from the highest point of the concave deformation zone to the back surface of the column's cross-section, while *a* is the distance from the lowest point of the center of the concave deformation zone to the back surface of the column's cross-section. The variable *l* signifies the width of the radial center section of the concave deformation zone, and *r* denotes the diameter of the non-deformed column, as illustrated in Fig. 1.b. Global and local deflections are respectively represented by δ_g and δ_l, while $\varnothing$ denotes the central flexural angle of the aluminum column, as depicted in Fig. 1.c. These identified parameters offer a comprehensive understanding of the deformation characteristics on the loaded side of the tested configurations.

Fig. 1 Schematic representation of deformation parameters of the aluminum column showing: (a) blast-loaded area of interest, (b) cross-section deformation parameters (c) global and local deflection investigated parameters.

Table 1 Deformation parameters of the aluminum column

configuration	d_1(mm)	d_2(mm)	b(mm)	a(mm)	l(mm)	δ_g(mm)	δ_l(mm)	$\varnothing$(°)
Bare aluminum column	85.1	204.2	73.8	56.2	110.8	112.3	48.1	171
30mm- PU foam-1mm thin outer skin	96.3	161.7	74.2	61.0	116.7	107.6	44.9	173.0
50mm- PU foam-1mm thin outer skin	80.3	150.3	77.0	72.2	107.5	106.4	33.7	177.0
100mm- PU foam-1mm thin outer skin	59.4	121.9	94.7	83.9	101.1	104.1	18.8	178.5

It is shown based on the experimental results that the deformation parameters are greatly influenced by the application of the different layers of PU foam wrapped around the aluminum column. Notably, a reduction of 21%, 26% and 40% in radial width *d2* is observed for the aluminum columns enveloped with PU foam of thicknesses 30 mm, 50 mm, and 100 mm, respectively.

The levels of flattening and radial deformation experience a significant reduction in the wrapped columns compared to their bare counterparts. The inclusion of a 30mm PU foam layer yields a significant reduction in deflection at the central point δl, amounting to a reduction ratio of 6.7%. Furthermore, when the layer thickness is increased to 100 mm, the deflection value further diminishes to 18.8 mm, showcasing a substantial 58.1% reduction compared to the case with a 30mm PU layer thickness.

Based on the experimental findings, it is shown that the application of different layers of PU foam around the aluminum column has an impact on deformation parameters. Specifically, there is a reduction in radial width (d2) for the aluminum columns enveloped with PU foam of varying thicknesses. The reductions are 21%, 26%, and 40% for PU foam thicknesses of 30 mm, 50 mm and 100 mm, respectively.

The levels of flattening and radial deformation exhibit a significant decrease in the wrapped columns compared to their bare counterparts. Introducing a 30mm PU foam layer results in a 6.7% reduction in deflection at the central point (δl). Moreover, increasing the layer thickness to 100 mm leads to a further reduction in the deflection value to 18.8 mm, indicating a 58.1% reduction compared to the case with a 30mm PU layer thickness. These results underscore the efficacy of the PU foam layers in minimizing deformation and enhancing the structural performance of the aluminum columns under the applied loading conditions.

REFERENCES

[1] "Report on Improvised Explosive Device (IED) Incidents. Available online." https://reliefweb.int/report/world/report-improvised-explosive-device-ied-incidents-january-june-2023 (accessed Jul. 17, 2023).

[2] "START. National Consortium for the Study of Terrorism and Responses to Terrorism.," *Global Terrorism Database.*, 2017. https://www.start.umd.edu/gtd/ (accessed Jul. 20, 2023).

[3] H. Ousji, B. Belkassem, M. A. Louar, B. Reymen, L. Pyl, and J. Vantomme, "Experimental Study of the Effectiveness of Sacrificial Cladding Using Polymeric Foams as Crushable Core with a Simply Supported Steel Beam," *Adv. Civ. Eng.*, vol. 2016, 2016, doi: 10.1155/2016/8301517.

[4] J. Lu, Y. Wang, X. Zhai, X. Zhi, and H. Zhou, "Impact behavior of a cladding sandwich panel with aluminum foam-filled tubular cores," *Thin-Walled Struct.*, vol. 169, p. 108459, 2021, doi: https://doi.org/10.1016/j.tws.2021.108459.

[5] L. Jing, Z. Wang, V. P. W. Shim, and L. Zhao, "An experimental study of the dynamic response of cylindrical sandwich shells with metallic foam cores subjected to blast loading," *Int. J. Impact Eng.*, vol. 71, pp. 60–72, 2014, doi: https://doi.org/10.1016/j.ijimpeng.2014.03.009.

[6] L. Jing, Z. Wang, and L. Zhao, "Dynamic response of cylindrical sandwich shells with metallic foam cores under blast loading — Numerical simulations," *Compos. Struct.*, vol. 99, pp. 213–223, 2013, doi: 10.1016/j.compstruct.2012.12.013.

[7] S. Vavilala, P. Shirbhate, J. Mandal, and M. D. Goel, "Blast mitigation of RC column using polymeric foam," *Mater. Today Proc.*, vol. 26, no. xxxx, pp. 1347–1351, 2019, doi: 10.1016/j.matpr.2020.02.273.

[8] X. Li, P. Zhang, Z. Wang, G. Wu, and L. Zhao, "Dynamic behavior of aluminum honeycomb sandwich panels under air blast : Experiment and numerical analysis," *Compos. Struct.*, vol. 108, pp. 1001–1008, 2014, doi: 10.1016/j.compstruct.2013.10.034.

[9] S. Palanivelu *et al.*, "Performance of a sacrificial cladding structure made of empty recyclable metal beverage cans under large-scale air blast load," *Appl. Mech. Mater.*, vol. 82, pp. 416–421, 2011, doi: 10.4028/www.scientific.net/AMM.82.416.

[10] A. Aminou, B. Belkassem, O. Atoui, L. Pyl, and D. Lecompte, "Numerical modeling of brittle mineral foam in a sacrificial cladding under blast loading," *Mech. Ind.*, vol. 24, p. 27, 2023.

[11] A. Jonet, B. Belkassem, O. Atoui, L. Pyl, and D. Lecompt, "Blast Mitigation Using Brittle Foam Based Sacrificial Cladding: A Feasibility Study," 2019.

[12] H. Ousji *et al.*, "Air-blast response of sacrificial cladding using low density foams: Experimental and analytical approach," *Int. J. Mech. Sci.*, vol. 128–129, pp. 459–474, 2017, doi: 10.1016/j.ijmecsci.2017.05.024.

ID 25

PARAMETRIC STUDIES OF A 2D EXTRUDED MODIFIED DOUBLE ARROWHEAD STRUCTURE FOR ENERGY ABSORPTION PERFORMANCE

Vivianne Marie Bruère[(*1)]**, Andrei Constantinescu**[1]

[1] Laboratoire de Mécanique des Solides, CNRS, École Polytechnique, Institut Polytechnique de Paris, Palaiseau, France

[(*)] Email: vivianne.bruere@polytechnique.edu

ABSTRACT

This study evaluates the crushing behaviour of a periodic architectured material and the effect of geometric parameters on its energy absorption capacity. The unit cell based on the traditional double arrowhead auxetic configuration is composed of two spline curves of different peak heights. Parametric studies are carried out for various unit cell distributions and values of the ratio "alpha" (difference in the peak heights to the height of the bottom curve). Numerical analyses show that an increase in the number of rows in the lattice is more efficient than an increase in the number of columns for lower relative density, while a better energy performance is limited to alpha values up to 2.0 due to buckling of the structure.

INTRODUCTION

Architectured materials for lightweight structures have been in focus in recent years in search of improved mechanical properties and final performance. Higher energy absorption capacity for reduced weight is one of their greatest advantages. They can be particularly beneficial in protective equipment against ballistic and blast impacts, offering better user comfort for personal safety gear and fuel savings in armoured vehicles. Among these structures, one can find auxetic lattices. They are classified into re-entrant, chiral honeycomb and rotating unit structures, and common cellular configurations comprise re-entrant hexagon, double arrowhead, star-shaped, hexachiral and rotating quadrangle (Yin et al., 2023). There is a growing interest in research into topology optimization of auxetic structures (Clausen et al., 2015), experimental analysis aided by Additive Manufacturing for specimen production (Balit et al., 2021) and development of new designs (Gao et al., 2021). In this investigation, lattices based on the traditional double arrowhead auxetic configuration are numerically analysed under compressive quasi-static loading. The unit cell consists of an upper and a lower spline instead of the straight triangular shapes (Fig. 1), avoiding sharp corners. Parametric studies are carried out in an 80x80x20 mm3 cuboid, evaluating the specific energy absorption (SEA) regarding the amount of periodic unit cells distributed inside the lattice and the ratio of the height difference between the two unit cell curves (d) to the height of the lower curve (h).

RESULTS AND CONCLUSIONS

The lattice geometry and mesh variations were generated in open source 3D finite element (FE) software Gmsh and the computations were performed in commercial FE solver Abaqus/Explicit for a 50% compressive deformation at a 0.1 s-1 rate and material properties from Balit et al. (2021). The explicit solver was used due to the large deformations while avoiding convergence issues and saving computational cost. Mass scaling was applied and kinetic energy was negligible compared to internal energy, satisfying quasi-static conditions.

The ratio d/h is called alpha, and assumed values below and above 1.0 for a 10x10 cell distribution in the lattice. In addition, the number of rows and number of columns of the periodic cells were varied independently, reflecting

on the change in height and width of the cell, respectively, for a constant alpha of 1.0 and starting from the 10x10 lattice.
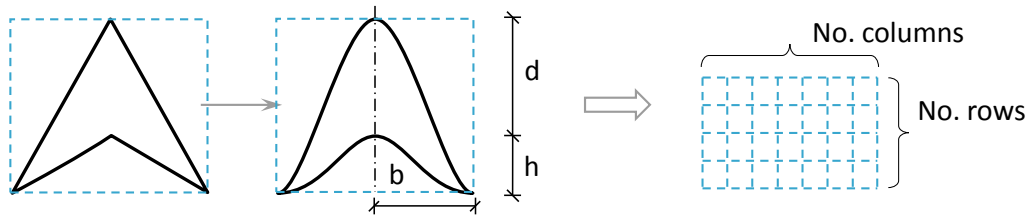
Fig. 1 Modified cell from traditional double arrowhead configuration and lattice distribution.

The results in Fig. 2 show that higher numbers of both rows and columns lead to higher SEA. The more cells inside the structure, the more plastic deformation it has, thus storing more energy. However, this also increases the relative density of the lattice. There is a rise in SEA with a smaller gain in weight for an increasing number of rows compared to an increase in columns. This indicates a more efficient improvement in energy absorption capacity for more cells distributed in rows of the lattice. By increasing parameter alpha, the weight decreases exponentially, while SEA values increase up to alpha=2.0 and then drop. For alpha>2.0, there is in fact considerable buckling of the whole structure, with a deformation mode of "V" rotated by 90° and less densification compared to the other alpha values. Hence, an alpha close to 2.0 is more appropriate for better energy absorption. Due to the low strain rate, densification starts later and the compressive forces acting on the structure are lower than in dynamic conditions, which gives comparatively lower SEA values.
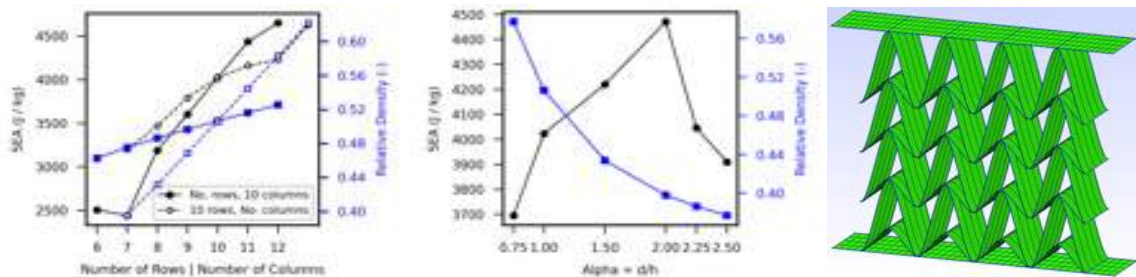
Fig. 2 Specific Energy Absorption (SEA) for varying the cell distribution in the lattice (left) and parameter alpha in the unit cell (middle), and example of generated FE mesh (right).

From these parametric studies, it can be seen that an increase in the number of cells is accompanied by a greater compromise in the weight of the structure, while the more limiting factor for better energy absorption when varying alpha is the control of lattice buckling. For the latter case, an alternative would be to increase the thickness of the cells or use different thicknesses for the top and bottom curves. This alternative is currently under study, along with experiments and numerical analysis with dynamic loads in prospective works.

REFERENCES

[1] H. Yin, W. Zhang, L. Zhu, F. Meng, J. Liu and G. Wen, "Review on lattice structures for energy absorption properties," Composite Structures, vol. 304, no. January, pp. 116397, 2023.

[2] A. Clausen, F. Wang, J. S. Jensen, O. Sigmund and J. A. Lewis, "Topology optimized architectures with programmable Poisson's ratio over large deformations," Advanced Materials, vol. 27, pp. 5523-5527, 2015.

[3] Y. Balit, P. Margerit, E. Charkaluk and A. Constantinescu, "Crushing of additively manufactured thin-walled metallic lattices: Two-scale strain localization analysis." Mechanics of Materials, vol. 160, no. September, pp. 103915, 2021.

[4] Y. Gao, Z. Zhou, H. Hu and J. Xiong, "New concept of carbon fiber reinforced composite 3D auxetic lattice structures based on stretching-dominated cells." Mechanics of Materials, vol. 152, no. January, pp. 103661, 2021.

ID 26
FRAGMENT IMPACT ON CONCRETE SLABS – AN EXPERIMENTAL AND NUMERICAL STUDY

Øystein E.K. Jacbosen[1](*), Martin Kristoffersen[1], Sumita Dey[2], Tore Børvik[1,2]

[1] Structural Impact Laboratory (SIMLab), Department of Structural Engineering, NTNU – Norwegian University of Science and Technology, NO-7491, Trondheim, Norway.

[2] Research and Development Department, Norwegian Defence Estates Agency, NO-0151, Oslo, Norway.

(*) Email: oystein.e.k.jacobsen@ntnu.no

ABSTRACT

In this study, we investigated the ballistic perforation resistance of thin concrete slabs against fragment impact. We cast concrete material specimens (cubes and cylinders) and 50 mm thick slabs of commercially available C35 concrete. We performed ballistic impact tests on a number of slabs with idealised fragments (i.e., 7.62 mm AP cores, 15 mm fragment simulating projectiles (FSPs), 15 mm ball bearings) to reveal their ballistic capacity. Alongside the ballistic tests, we performed quasi-static material tests instrumented with digital image correlation (DIC). Data from the material tests have been used to calibrate a constitutive relation for concrete to be used in numerical simulations in the non-linear finite element software LS-DYNA.

INTRODUCTION

Concrete is by far the most used building material in the world. Due to its vast availability, high strength, abundance, and relatively low cost, it serves as an excellent choice in fortification installations and for defence purposes. Due to the widespread usage of the material, numerous studies (see e.g., Rajput et al., 2017, Kristoffersen et al., 2018) have been performed on concrete to study the effects of extreme loads such as ballistic impacts and blasts. In real blast-load events, it is well known that the combined effect of fragment impact and blast loading will be more severe than that of the blast loading alone (Elveli et al., 2023). An explosion is likely to cause both a blast and fragment impact on a nearby structure. It is thus important to have detailed knowledge on how these fragments affect the structure. By investigating three small projectiles, we get a better understanding of the effect of fragment shape on damage potential. Of the three projectiles used, the 7.62 mm AP cores represent a fragment with the highest perforation capability in terms of residual projectile velocity. The standardised 15 mm FSPs and 15 mm ball bearings are presumed to have the second highest and lowest perforation capability, respectively.

RESULTS AND CONCLUSIONS

The commercially available C35 concrete was used to cast cylinders and cubes for material tests, as well as 50 mm thin concrete slabs with side lengths 400 mm. The concrete density was 2360 kg/m3. The unconfined compressive strength was found to be 40.3 MPa after 28 days, and 45.4 MPa after 57 days, while the tensile splitting strength was 3.4 MPa after both 28 and 57 days. Key projectile parameters are presented in Table 1. It is evident that the AP core mass is less than half of the other masses.

Table 1 Key parameters for the projectiles.

Projectile	Diameter [mm]	Initial velocities [m/s]	Mass [g]	Concrete age at testing date
Ball bearing	15.0	438-719	13.8	28-30 days
FSP	12.7	451-1116	13.4	47-48 days
AP core	7.62 (6.1)	481-957	5.0	28-30 days

Fig. 1 shows the ballistic limit curves for the three projectiles, where the Recht-Ipson model has been fitted using a least-squares fit to find the ballistic limit velocities, vbl. The three ballistic limit velocities are similar. However, the slopes of the curves differ substantially. The experimental results also showed that the spalling and scabbing areas were larger for the ball bearings and FSPs compared to the AP cores. The backsides of three representative slabs with approximately the same initial velocity are shown in Fig. 2. In general, the scabbing craters were larger than the spalling craters. The experimental results show that the ballistic perforation resistance of thin slabs varies greatly with projectile geometry and mass. These idealised fragment geometries serve as a good basis for validation of numerical models where fragments impact structures.
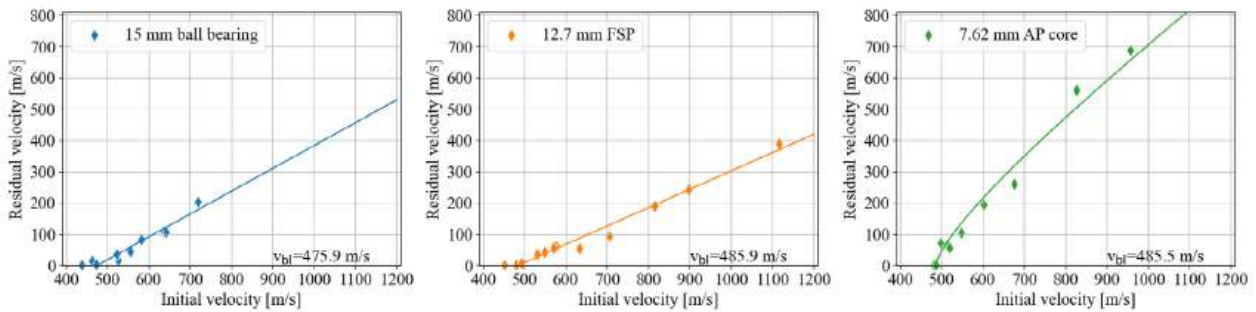
Fig. 1 Ballistic limit curves for three projectiles: (a) 15 mm ball bearing, (b) 12.7 mm FSP, and (c) 7.62 mm AP core.

Fig. 2 Scabbing craters on three concrete plates at approximately the same impact velocity, vi:
(a) ball bearing at 641 m/s: (b) FSP at 634 m/s, and (c) AP core at 676 m/s.

REFERENCES

[1] A. Rajput, M.A. Iqbal, "Impact behaviour of plain, reinforced and prestessed concrete targets", in *Materials & Design, 2017*, Volume 114.

[2] M. Kristoffersen, J.E. Pettersen, V. Aune, T. Børvik, "Experimental and numerical studies on the structural response of normal strength concrete slabs subjected to blast loading", in *Engineering Structures*, *2018*, Volume 174.

[3] B.E. Elveli, T. Berstad, T. Børvik, V. Aune, "Performance of thin blast-loaded steel plates after ballistic impact from small-arms projectiles", in *International Journal of Impact Engineering, 2023*, Volume 173.

ID 28

DYNAMIC RESPONSE AND ENERGY ABSORPTION OF MENGER FRACTAL-INSPIRED POROUS STRUCTURES

Madhusha Bogahawaththa, Damith Mohotti[(*)]**, Paul J. Hazell, Hongxu Wang**

School of Engineering and Technology, The University of New South Wales, Canberra, ACT 2600, Australia

[(*)] Email: d.mohotti@unsw.edu.au

ABSTRACT

The study explores the energy absorption properties of Menger Fractal Cubes (MFCs) fabricated through Selective Laser Melting (SLM) with AlSi7Mg material. Quasistatic and dynamic compression experiments and simulations were conducted investigating four orders of MFCs. Digital image correlation identified stress concentration areas within the elastic deformation range, and the Gibson-Ashby model was applied successfully in quasistatic tests. The fourth-order MFCs exhibited the highest specific energy absorption, densification displacement, and energy absorption efficiency. Additionally, the research highlighted higher-order MFCs as protective sacrificial structures, reducing force transmission to protected structures and making them promising for various structural applications requiring energy-damping characteristics.

INTRODUCTION

Extensive research in the field of energy-absorbing cellular structures has shown their efficacy in mitigating damage from impacts and explosions [1]. Often constructed from high-performance, lightweight materials such as aluminum alloys, these structures are notable for their strength, energy absorption efficiency, and thermal properties. The use of aluminum alloy porous structures is increasingly prevalent in sectors such as aerospace and automotive, attributed to these beneficial qualities. The emergence of additive manufacturing technologies, particularly selective laser melting (SLM), has transformed the production of these structures, enabling intricate designs and enhanced control over their physical features. This technological advancement has significantly contributed to a more profound understanding of how material design, manufacturing parameters, and energy absorption characteristics are interconnected.

The Menger fractal cube, a three-dimensional extension of the Cantor set and Sierpinski carpet, is a topology optimization concept originating from Karl Menger's 1926 work. This study focuses on the first to third-order Menger fractal designs (M1-M3), where the volume and surface area of these cubes vary with their fractal order, as shown in Fig. 1 (a) and (b). Higher-order Menger fractal cubes are particularly notable for their lightweight energy-absorbing characteristics, possessing significantly increased surface areas and decreased volumes, enhancing their capacity for energy absorption [2].

RESULTS AND CONCLUSIONS

MFCs were fabricated using Selective Laser Melting (SLM) with optimized printing parameters to achieve specific density levels and experimentally tested in quasistatic and low-velocity dynamic loading rates. Investigations were carried out for the densification and energy absorption of MFCs across three fractal orders experimentally and fourth order numerically and presented in Table 1. The study employed Digital Image Correlation (DIC) to analyze strain development and stress propagation on the MFC's face. Key findings include varying energy absorption and densification levels in different fractal orders of MFCs, unique force-displacement characteristics, and hierarchical deformation modes. The experimental outcome validates the Gibson-Ashby model's predictions for elastic stress

in SLM-printed MFCs. Additionally, LS-DYNA Finite Element Method (FEM) simulations corroborate the experimental data, confirming the accuracy and reliability of the constructed constitutive model. The dynamic compression tests further demonstrated the MFCs' ability to absorb energy efficiently through the deformation of internal columns at various levels.

Table 1 Qausistatic mechanical properties of MFCs

Fractal Order	1	2	3	4
Densification displacement (x_d)	9.2	11.0	13.0	14.0
Crush efficiency (CF)	46%	55%	65%	70%
Energy absorbed (J)	704.0	573.6	433.6	284.4
Specific energy absorption (J/g)	45.4	49.6	50.2	45.1
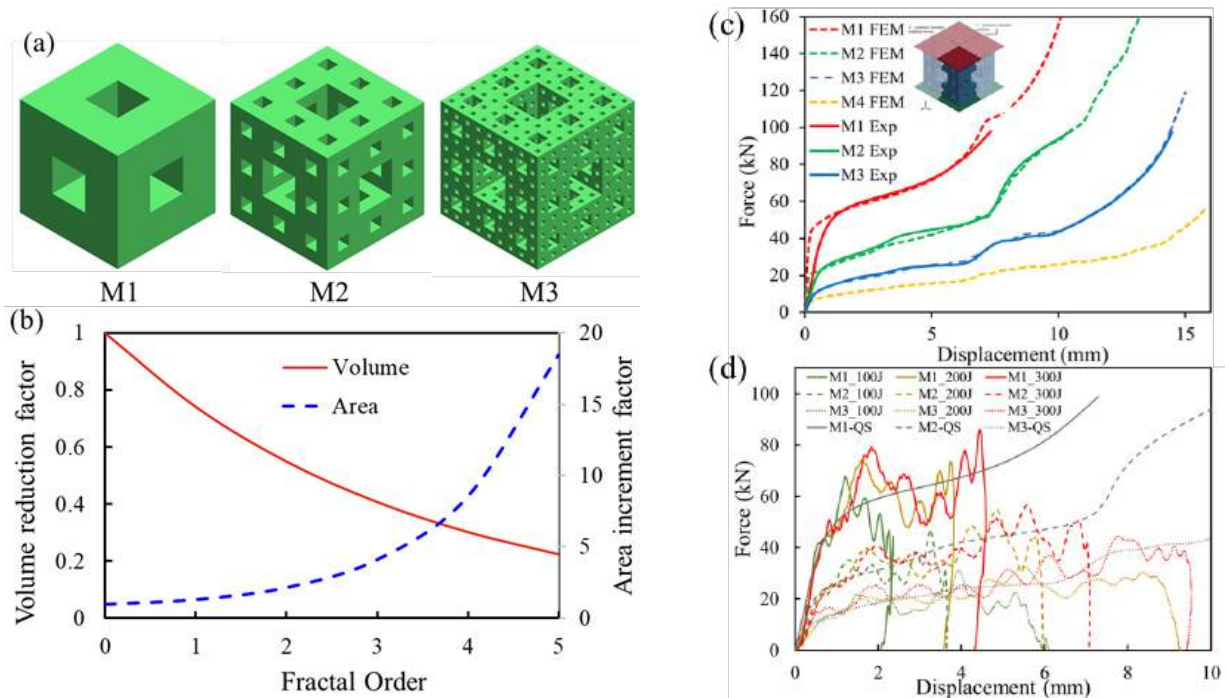
Fig. 1 (a) First to third order MFCs (b) Volume and surface area variation of MFCs against their order (c) force-displacement (F-D)curve for quasistatic response (d) F-D curve dynamic compression test

This study shows that higher-order MFCs demonstrated excellent energy absorption efficiency while crashworthiness improved compressibility. Compared to other energy-absorbing porous structures, MFCs exhibit SEA values in the 45−50 J/g range, which can be categorized as a top performer.

REFERENCES

[1] S. H. Siddique, P. J. Hazell, H. Wang, J. P. Escobedo, and A. A. H. Ameri, "Lessons from nature: 3D printed bio-inspired porous structures for impact energy absorption – A review," Additive Manufacturing, vol. 58, p. 103051, 2022/10/01/ 2022, doi: https://doi.org/10.1016/j.addma.2022.103051.

[2] D. Mohotti, D. Weerasinghe, M. Bogahawaththage, H. Wang, K. Wijesooriya, and P. J. Hazell, "Quasistatic and dynamic compressive behaviour of additively manufactured Menger fractal cube structures," Defence Technology, 2023/12/23/ 2023, doi: https://doi.org/10.1016/j.dt.2023.12.010.

ID 29
ADDITIVE MANUFACTURING OF RADAR ABSORBING MATERIALS

Matthias Bleckmann[1(*)], **Stefan Ehard**[2], **Maximilian Krönert**[1], **Sebastian Peters**[2], **Joshua L. Obermeyer**[2]

[1] The Bundeswehr Research Institute for Materials, Fuels and Lubricants (WIWeB), Erding, Germany

[2] Airbus Defence & Space, Manching, Germany

[(*)] Email: matthiasbleckmann@bundeswehr.org

ABSTRACT

This work investigates the possibilities of FDM to produce Radar Absorbing Materials. For this purpose modified filaments have been produced. The produced filaments were characterized by means of particle distribution, differential scanning calorimetry and tensile test. Printed samples with different additive volume content were compared by means of mechanical and electromagnetic characterisation.

INTRODUCTION

Radar-absorbing material on a camouflaged aircraft is intended to suppress those radar reflections that cannot be avoided through geometric measures [1,2,3]. This is the case where functional boundary conditions do not allow the geometrically optimal shape. Typical examples of this are front edges or air inlets. These geometries have a complex shape and are difficult to produce.

In additive manufacturing (AM), material is applied layer by layer until the computer-controlled print is a 3D image of a CAD file. Hence, AM has the ability to produce complex shapes with an internal material gradient. Optimized filaments for radarabsorbing materials were produced, printed and mechanically and electromagnetic characterized.

RESULTS AND CONCLUSIONS

Four different fillers, carbon black [2], carbonyl iron powder [1,2], magnetite [1,2] and micro balls has been investigated with two different concentrations, respectively. During filament production it has been shown that, especially with additives with low densities and particle sizes, floating occurs more frequently in the extruder inlet. In some configurations, increased agglomerate formation was also observed in the extruded filament and brittleness of the filaments increases with increasing additive content and brittleness of the filaments increases with increasing additive content.

Multiple extrusion, i.e. re-extrusion after shredding the previously produced filaments, has shown significant improvement in some cases. Altogether, eight types of filaments have been produced and investigated.

The DSC measurements on the filaments do not reveal any discernible trends with additive content. The deviations in the tensile strength range for printed samples in the negative direction can be explained by the occurrence of slicing errors in the printed tensile samples. The deviations in the positive direction, on the other hand, are due to the inhomogeneity of the filaments, which represent weak points in the filament cross section. This shows that the agglomerate density in the filament reduces the strength, but at the same time the printing process breaks up and smears the particle accumulations in such a way that they do not cause any loss of strength in the printed component.

The electromagnetic curves (Fig.2) of the carbonyl iron filament show a positive offset of the ε' curve and an inclination of the μ' curve. The changes in properties are too small to be used effectively in RAM. A significant increase in the proportion of additives must also take place here.

For magnetite, the curves of the EM measurement show that the present magnetite content significantly increases the permittivity and creates a slope of the curve in the permeability range.

The filaments with carbon black, show hardly any change in the μ' and ε' values compared to pure PLA in the investigated additive amount, which suggests that the additive proportion is too low for property changes. However, even with these small amounts of additive, electrical losses are evident through the ε'' curve (see Fig.2). Finally, the results for hollow glass microsphere filaments in the range 24-27 vol.% show a reduction in ε' as expected.
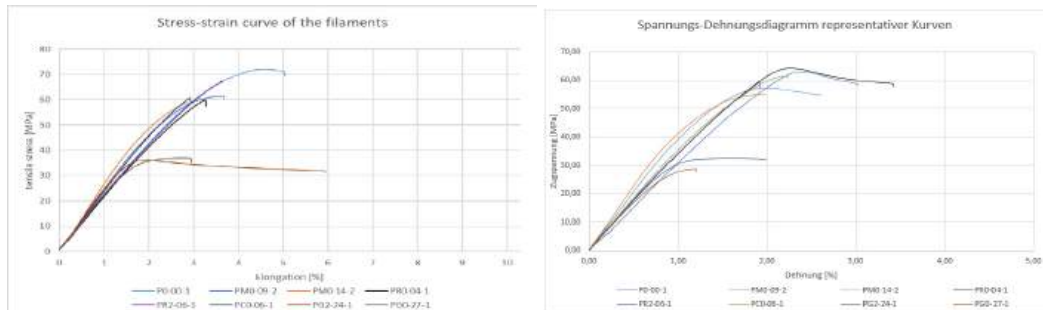
Figure 1: Tensile test of filament (left) and printed samples (right) for different fillers
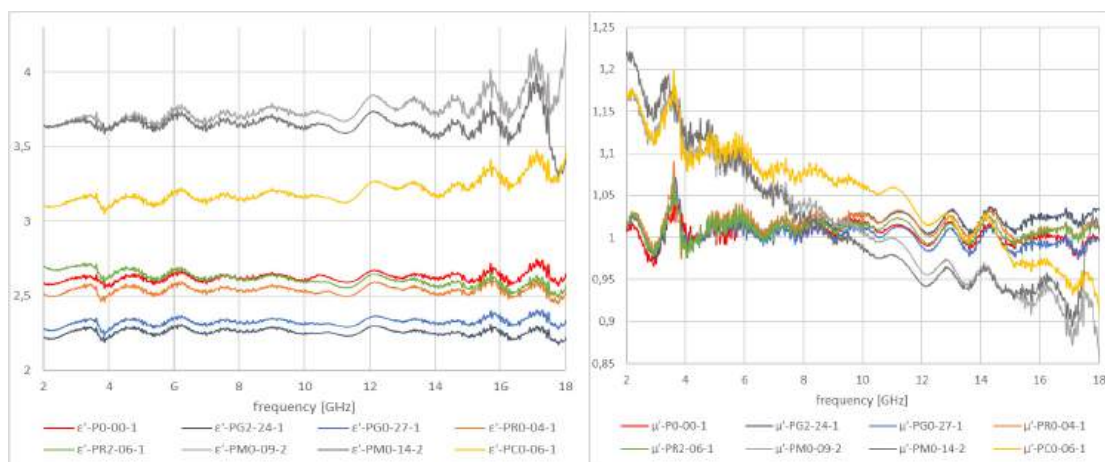
Figure 2: Permeability μ' and permittivity ε' at the test frequency

This study shows the potential of additive manufacturing for radarabsorbing materials. However, the amount of fillers is too low for an application as radar absorber. In prospective future work different filaments with different type and increasing amount of fillers will be investigated as well as the printing of complex absorber parts with an internal structure.

REFERENCES

[1] H. Ahmad et al., „Stealth technology: Methods and composite materials - A review", Polym. Compos., Jg. 40, Nr. 12, S. 4457–4472, 2019.

[2] P. Saville, „Review of Radar Absorbing Materials". [Online]. Available online at: https://apps.dtic.mil/sti/citations/ADA436262.

[3] A. Aytaç, H. İpek, K. Aztekin und B. Çanakçı, „A review of the radar absorber material and structures", SJMULF, Jg. 198, Nr. 4, S. 931–946, 2020

[4] T. Bernsteiner, „Untersuchung und Entwicklung von modifizierten Filamentwerkstoffen für das FDM Verfahren" Masterthesis 2022

ID 31

STUDY OF IMPACT BEHAVIOUR OF SHEAR THICKENING FLUID (STF) REINFORCEMENTS IN CORK COMPOSITE STRUCTURES

Telmo R.M. Fernandes[1], Gabriel F. Serra[2], R.J. Alves de Sousa[3], Fábio A.O. Fernandes[4(*)]

[1, 2, 3, 4] Centre for Mechanical Technology and Automation (TEMA), Department of Mechanical Engineering, University of Aveiro, Campus Universitário de Santiago, 3810-193 Aveiro, Portugal

[2, 3, 4] LASI—Intelligent Systems Associate, Portugal

[(*)] Email: fabiofernandes@ua.pt

ABSTRACT

This work presents the latest advancements in cork composite structures reinforced with shear thickening fluids (STF). It investigates a novel concept of 3D STF containers for impact force mitigation of penetrating objects. The low-energy impact tests were performed on a drop-weight impact machine with a hemispherical impactor. Cork structures with and without the STF reinforcement were compared, and the influence of its container depth was investigated. Results showed a significant reduction of the maximum impact force compared to a neat cork structure. Although the evolution is not properly linear, the STF 3D volume slows down the increasing rate of the impact force.

INTRODUCTION

Cork composite structures interfacially reinforced with STF have already been studied [1,2]. Although the STF interface positively influences the external force mitigation, this gain is usually marginal. These materials have gained significant attention for their distinctive properties and versatile applications, including defence [3,4]. Three-dimensional STF structures are a new concept proposed in the present work. The main goal is to investigate the influence of larger STF reinforcements on the impact behaviour of composite structures, focusing on the maximum impact force.

In this study, 50 x 50 x 20 mm samples were produced. The final structures consist of two 10 mm thick agglomerated cork layers on top of each other. A 25 mm diameter hole is machined on the impacted layer containing the STF. Its volume is one of the parameters that vary with the depth: 1 mm, 2 mm, 3 mm, 5 mm, and 8 mm. The suspension is based on polyethylene glycol with a molecular weight of 400 g/mol and 30% of fumed silica particles. After filling the hole with STF, the two layers are then glued. The final sample configuration is illustrated in Figure 1. The impact test parameters are presented in Table 1.

Table 1 Impact test conditions.

Impact Energy (J)	Fall Height (mm)	Velocity (mm/s)	Mass (kg)	Impactor Type	Impactor Diameter (mm)
10	323.7	2.52	3.15	Hemispherical	20
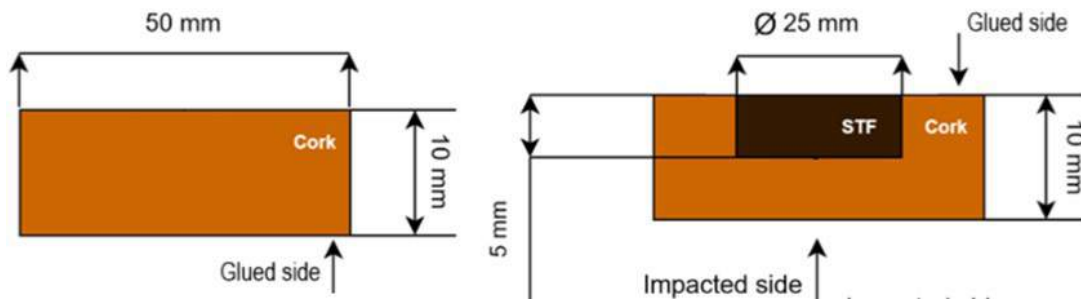
Fig. 1 Illustration of the samples configuration for a specific case of a 5mm thick STF container.

RESULTS AND CONCLUSIONS

The results showed a significant decrease in the maximum force, as shown in Fig.1(a). The presence of STF justifies these results, depicting a clear relation between the amount of STF and the impact force reduction. The force increase in the case of 8 mm depth is probably related with loss of stiffness due the low thickness of cork in the impacted layer. The results are also compared with samples made only of cork, and the effect of STF is clear in the impact behaviour of the cork composite layered structure, achieving an impact force reduction over than 50% for a 5 mm depth. Fig.1(b) shows a representative force-displacement curve, depicting a desired force plateau.
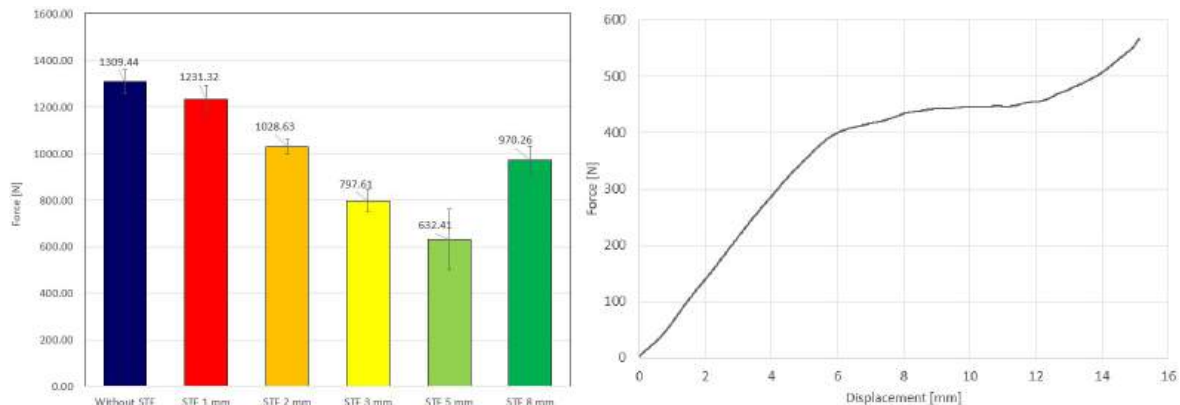
Fig. 1 Results from impact test **a)** Peak Force [N] **b)** force-displacement curve for 5 mm STF

This study shows that the presence of STF is critical and can be optimised to reduce the impact force. Although this work focuses on cork composite structures, there is potential for reinforcement of other materials and structures.

ACKNOWLEDGMENTS

REFERENCES

[1] Gürgen, S., Fernandes, F.A.O., de Sousa, R.J.A. et al. Development of Eco-friendly Shock-absorbing Cork Composites Enhanced by a Non-Newtonian Fluid. *Appl Compos Mater*, 28, 165–179, 2021.

[2] Serra, G.F.; Fernandes, F.A.O.; de Sousa, R.; Noronha, E.; Ptak M. New hybrid cork-STF (Shear thickening fluid) polymeric composites to enhance head safety in micro-mobility accidents, *Compos. Struct.*, 301, 116138, 2022.

[3] A. Majumdar, B.S. Butola, A. Srivastava. Optimal designing of soft body armour materials using shear thickening fluid. *Materials and Design*, 46, 191–198, 2013.

[4] Pernas-Sánchez, J.; Artero-Guerrero, J.A.; Varas, D.; Teixeira-Dias, F. Cork Core Sandwich Plates for Blast Protection. *Appl. Sci.*, 10, 5180, 2020.

ID 32

ADDITIVE MANUFACTURED MARAGING STEEL UNDER BALLISTIC IMPACT: EXPERIMENTS AND NUMERICAL MODELLING

Maisie Edwards-Mowforth[1](*), Miguel Costas[2], Martin Kristoffersen[3], Filipe Teixeira-Dias[4], Tore Børvik[5]

[1, 4] Institute of Infrastructure and Environment (IIE), School of Engineering, The University of Edinburgh, Edinburgh, UK

[2, 3, 5] Structural Impact Laboratory (SIMLab), Department of Structural Engineering, NTNU – Norwegian University of Science and Technology, Trondheim, Norway

(*) Email: Maisie.Edwards-Mowforth@ed.ac.uk

ABSTRACT

As additive manufacturing (AM) brings the advantages of on-demand production and customised or optimised parts to the defence industry, important questions arise regarding the structural integrity of AM components in armour systems. It is well established that high-strength is correlated with ballistic performance in metallic materials [1], yet the effect of AM fabrication on mechanical properties is debated in the literature [2]. The ballistic perforation resistance of high-strength AM materials may therefore prove difficult to predict. Several studies have examined the ballistic limit of AM metallic targets experimentally [3,4,5], where few attempts have been made to simulate the impact response. Those that have, however, found promise in the ability of well-established numerical models to capture the ballistic performance of AM targets equally as well as traditionally manufactured targets [5]. In this study, a high-strength, low carbon martensitic steel named maraging steel, known for its superior mechanical properties and suitability for AM, has been considered. The material characteristics and ballistic limit velocity in the as-printed state were disclosed from experimental tests. Numerical models of the impact are to be established in the IMPETUS Afea Solver and the results of bullet residual velocity obtained from the simulations compared with the ballistic impact tests. Conclusions are drawn concerning how well the numerical model performs despite that the AM processing of the target is not accounted for.

METHODOLOGY AND RESULTS

Maraging steel specimens were produced by the AM technique laser powder-bed fusion, a widely-used AM technique by which powder is spread onto a substrate and melted layer by layer to produce a part. Parameters utilised for the printing process are displayed in Table 1.

Quasi-static tensile tests and tensile tests at elevated strain rates in the as-printed state were performed to characterise the material. A yield strength of 1113 MPa averaged over six specimens was found. The ballistic limit velocity was obtained by use of a ballistic range where 7.62 mm armour piercing bullets were fired towards single layer, 5 mm thick targets at a range of impact velocities below 1000 m/s. A high-speed camera recorded the impact and the initial and residual velocity of the projectile was measured. A schematic of the armour piercing bullet and target set-up is shown in Figure 1a alongside preliminary experimental results of the ballistic impact tests in Figure 1b. Very little scatter is present in the ballistic limit curve which has a ballistic limit velocity of 395 m/s, and only a small amount of fragmentation in the as-printed AM target was observed in the high-speed camera images. SEM images of tensile test specimen fracture surfaces and ballistic penetration channels were examined to shed light on the material behaviour. The Modified Johnson-Cook elastic-thermo-viscoplastic constitutive relation and

the Cockcroft-Latham failure criterion have been calibrated according to the disclosed characteristics of the AM maraging steel. A finite element model of the ballistic impact will be constructed and the results compared to the experiments.

Table 1 Laser powder-bed fusion process parameters for the maraging steel.

Laser power	Layer thickness	Laser velocity	Focus diameter	Hatch distance	Powder size
180 W	30 μm	600 mm/s	150 μm	105 μm	10 - 45 μm
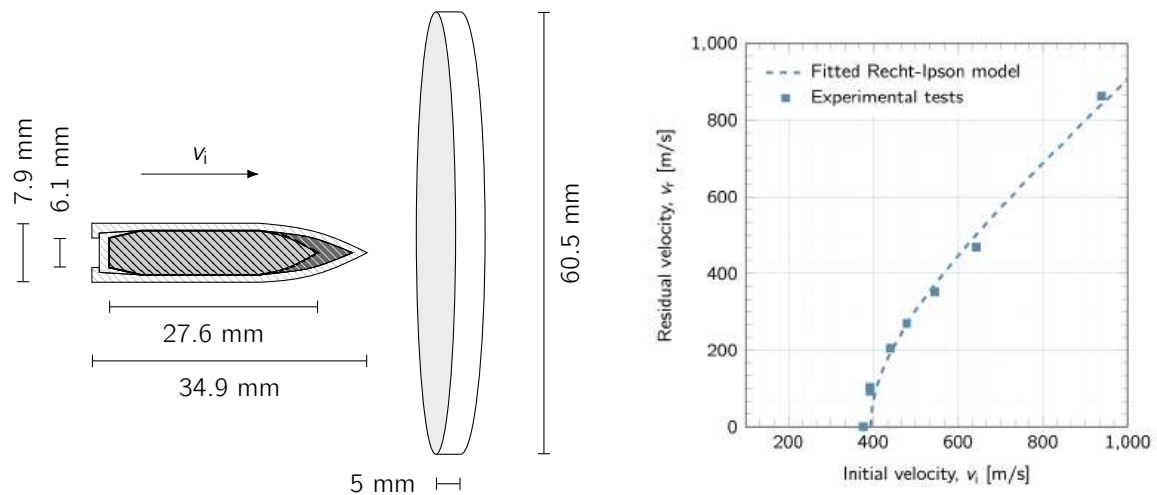
Fig. 1 a) Schematic of armour piercing bullet and AM maraging steel target with dimensions and b) Experimental results of ballistic impact tests on as-printed AM maraging steel showing a ballistic limit velocity of 394 m/s.

REFERENCES

[1] T. Børvik, S. Dey, and A. Clausen. Perforation resistance of five different high-strength steel plates subjected to small-arms projectiles. International Journal of Impact Engineering, 36(7):948–964, 2009.

[2] A.E. Medvedev, T. Maconachie, M. Leary, M. Qian, and M. Brandt. Perspectives on additive manufacturing for dynamic impact applications. Materials & Design, 221:110963, 2022.

[3] M. Costas, M. Edwards-Mowforth, M. Kristoffersen, F. Teixeira-Dias, V. Brøtan, C.O. Paulsen, and T. Børvik. Ballistic impact resistance of additive manufactured high-strength maraging steel: An experimental study. International Journal of Protective Structures, 12(4):577–603, 2021.

[4] A.E. Medvedev, E.W. Lui, D. Edwards, M. Leary, M. Qian, and M. Brandt. Improved ballistic performance of additively manufactured Ti6Al4v with α – β lamellar microstructures. Materials Science and Engineering: A, 825:141888, 2021.

[5] M. Kristoffersen, M. Costas, T. Koenis, V. Brøtan, C.O. Paulsen, and T. Børvik. On the ballistic perforation resistance of additive manufactured AlSi10mg aluminium plates. International Journal of Impact Engineering, 137:103476, 2020.

ID 33

NANOPARTICLE-MEDIATED BACTERICIDAL ACTION AGAINST THE MOST COMMON GRAM-POSITIVE PATHOGEN CAPABLE OF COLONIZING DIABETIC FOOT ULCERS

Joana M. Domingues [1, 2 *]**, Rosana Monteiro**[2]**, Carla Silva**[3,4]**, Helena P. Felgueiras**[1]**, Maria Olívia Pereira**[2,4]**, Joana C. Antunes**[5]

[1]Centre for Textile Science and Technology (2C2T), University of Minho, 4800-058, Guimarães, Portugal.

[2]Centre of Biological Engineering, LIBRO - Laboratório de Investigação em Biofilmes Rosário Oliveira, University of Minho, Campus de Gualtar, Braga, 4710-057, Portugal.

[3]Centre of Biological Engineering, University of Minho, Campus de Gualtar, Braga, 4710-057, Portugal.

LABBELS - Associate Laboratory, Braga/Guimarães, Portugal

Fibrenamics Association, Institute for Innovation in Fibre and Composite Materials, University of Minho, 4800-058, Guimarães, Portugal.

[*] Email: joana.domingues@2c2t.uminho.pt

ABSTRACT

This work presents simple, versatile, and easily industrialized polyelectrolyte complexed (PEC) nanoparticles (NPs) with bactericidal action against the gram-positive opportunistic pathogen *Staphylococcus aureus* that is one of the most prevalent bacteria present in diabetic foot ulcers (DFUs). *S. aureus* typically resides in DFUs in the form of mature biofilms, which enhances its adaptation to soft tissue infections and potentiates antibiotic resistance. Also, the expression of virulence factors avoids host immune response leading to a deep and bone infection that is very difficult to treat with antibiotic therapy. The NPs were developed using a lignocellulosicbased material, lignin, which was chemically modified in-house to obtain the polyelectrolytes quaternized lignin (QL) and carboxymethyl lignin (CML) as the building blocks of the NPs. Further, a crosslinking agent, tannic acid (TA), was added to the dispersion to obtain a more homogeneous, and stable, NP population. The size, PDI and zeta potential values were determined via dynamic and electrophoretic light scattering (ZetaSizer Nano ZS, Malvern) and the antimicrobial activity was determined by CFUs counting using a *S. aureus* reference strain.

INTRODUCTION

Diabetes Mellitus (DM) is a chronic disease that affects more than 422 million people worldwide (8.5% of the adult population) (WHO, 2020). This pathology is also highly prevalent in Portugal (13.6% of the people with 20-79 years of age), yet continuously rising and accompanied by a growing burden of healthcare-related expenses (Raposo, 2020). Patients with chronically infected wounds are typically colonized by polymicrobial environments with a mix of Grampositive and Gram-negative bacteria, such as *S. aureus* and *Pseudomonas aeruginosa* (Andrews et al., 2015 and Machado et al., 2020).

Renewable and cheap plant-derived products, with quick and effective antimicrobial properties, are increasingly studied as a replacement, or adjuvants of antibiotics. In plants, lignin protects against biochemical stress, and confers rigidity, bringing strength and avoiding structural collapse. After isolation, lignin is endowed with biocompatibility, biodegradability, antidiabetic, immunomodulating and antioxidant abilities, mostly connected to its aromatic groups (Lourençon et al., 2021 and Tao et al., 2020). PEC NPs present several attractive features for biomedical applications, such as mild assembly conditions, hydrophilicity, cytocompatibility, pH-responsiveness and small size. These characteristics, combined with a three-dimensional (3D) architecture, favor an enhanced ability to

penetrate thick bacterial biofilms due to their size and surface properties (Zhou et al., 2018). Hence, the proposed combinatory bactericidal action on the bacteria's cell wall, accompanied by reduced side effects, is expected to encourage commensal fitness and boost skin homeostasis.

RESULTS AND CONCLUSIONS

The results showed that the chemical modification performed in raw lignin was successful, as shown in Figure 1. In the FTIR spectra of lignin and CML, two absorption bands related to C=O stretching at 1710 cm^{-1} and C-H stretching at 1417 cm^{-1} bands can be observed, confirming the introduction of negatively charged carboxyl groups, while in the spectrum of QL, the incorporation of the quaternized moieties was confirmed by the presence of a methyl groups peak at 1487 cm^{-1}.

QL and CML were then combined in the form of NPs via polyelectrolyte complexation, through electrostatic interactions between oppositely charged polyelectrolytes, with QL serving as the polycation (positive charge) and the CML as the polyanion (negative charge). The obtained results are displayed in Figure 2. A NP dispersion was produced: QL/CML/TA, with the mass proportions of 1:1:30 of each compound, respectively. TA was introduced, given that it possesses unique antibacterial properties, being additionally useful as a capping agent and stabilizer of NP's dispersions. Also, it is important to highlight that both QL and CML, and the NPs, were dispersed in water at pH 8, mimicking the pH of a chronic infected wound. The developed NPs present a small size conferring them ability to internalize into biofilm channels and improve their penetration within (Al-Wrafy et al., 2022). Also, a monodispersed NP population was achieved, accompanied by a strong surface charge, which is very important for the stability of NPs is suspension (Rasmussen et al., 2020).

In the next step, antimicrobial activity assays were performed using a reference strain of *S. aureus* (ATCC 25923). The results showed that the NPs' constituents have antimicrobial activity against *S. aureus* as shown in Figure 3. However, it should be noted that the TA total inhibits the growth of the bacteria after 24 h of incubation. Thus, a time to effect and duration of action of TA was performed indicating that in the first 2 h of incubation with bacteria there is a similar growth compared to the positive control, but from 2 h to 24 h a significant reduction of bacteria growth can be observed, eventually killing the bacteria at 24 h of incubation.
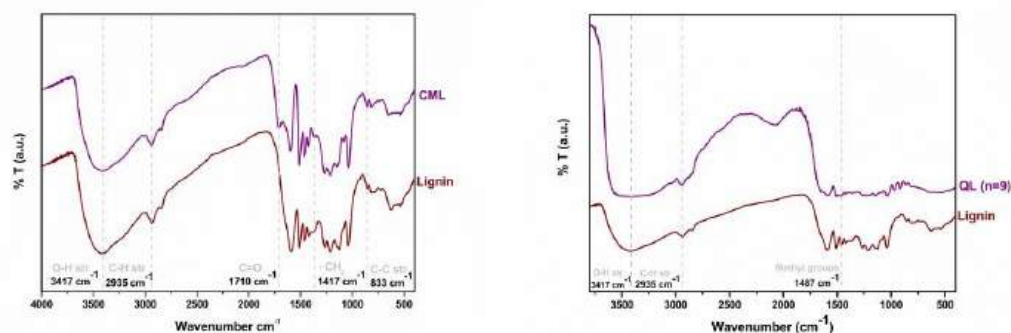
Fig. 1 FTIR spectra of a) lignin and CML b) lignin and QL.
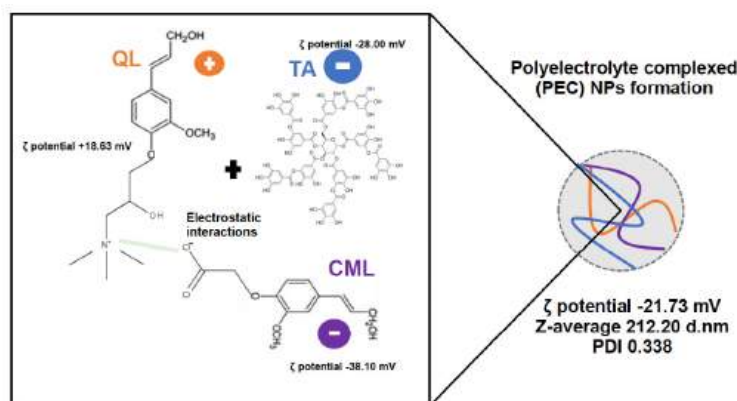
Fig. 2 PEC NPs production method and their properties.
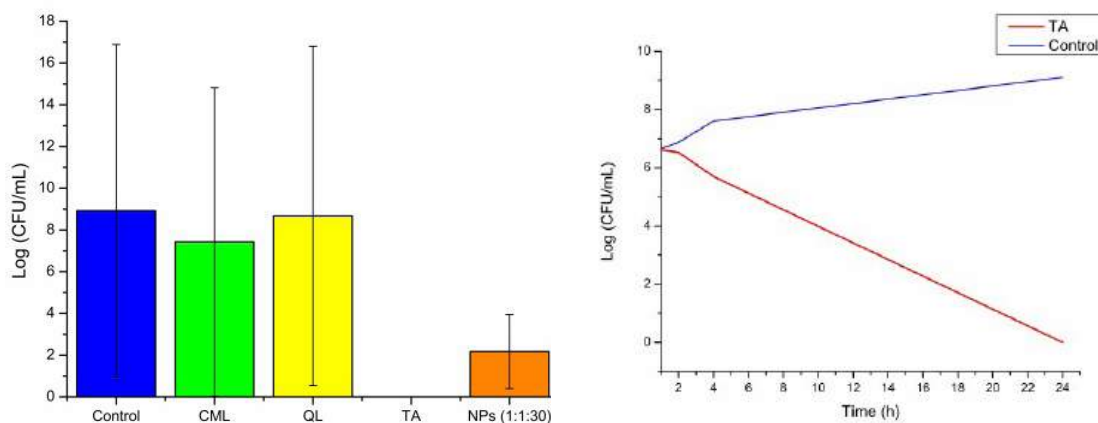
Fig. 3 Antimicrobial activity of CML, QL, TA and the developed NPs. Time to effect and duration of action of TA.

In short, this study shows that innovative lignin-derived PEC NPs were successfully produced and revealed high potential for use in chronic infected wounds. The PEC NPs produced exhibited potent antimicrobial activity against *S. aureus* which continues to be one of the most prevalent pathogens recovered from DFUs, expressing several virulence factors that hamper the treatment of these wounds leading to antibiotic resistance and prolonged wound duration. In the future, the developed NPs will be tested in a scenario of biofilm formation to ensure that the bacterial infection is eradicated, and homeostasis can be achieved.

REFERENCES

[1] WHO, "Diabetes", 2020, Available from: https://www.who.int/health-topics/diabetes/

[2] J. Raposo, "Diabetes:Factos e Números 2016, 2017 e 2018.," *Revista Portuguesa Diabetes*, pp. 15-19, 2020.

[3] K. L. Andrews et al., " Wound management of chronic diabetic foot ulcers: from the basics to regenerative medicine", *Prosthetics and Orthotics International*, vol. 39 (1), pp. 29-39, 2015

[4] C. Machado et al., "Evolutionary trends in bacteria isolated from moderate and severe diabetic foot infections in a Portuguese tertiary center", *Diabetes & Metabolic Syndrome*, vol. 14 (3), pp. 205-209, 2020.

[5] T. V. Lourençon et al., "Antioxidant, antibacterial and antitumoural activities of kraft lignin from hardwood fractionated by acid precipitation", *International Journal of Biological Macromolecules,* vol. 1:166, pp. 1535-1542, 2021.

[6] J. Tao et al., "Lignin - An underutilized, renewable and valuable material for food industry", *Critical Reviews in Food Science and Nutrition,* vol. 60 (12), pp. 2011-2033, 2020.

[7] K. Zhou et al., "A review on nanosystems as an effective approach against infections of *Staphylococcus aureus*", *International Journal of Nanomedicine*, vol. 9 (13), pp. 7333-7347, 2018.

[8] F. Al-Wrafy et al., "Nanoparticles approach to eradicate bacterial biofilm-related infections: A critical review", *Chemosphere*, vol. 288, 2022.

[9] M. Rasmussen et al., "Size and surface charge characterization of nanoparticles with a salt gradient", *Nature communications*, 2020.

ID 34
INTEGRATION OF FLEXIBLE INTERCONNECT FOR MULTILAYER TEXTILE-BASED WEARABLE DEVICE

Prateeti Ugale[1]

[1] North Carolina State University, USA

ABSTRACT

TBA

ID 35
AN INNOVATIVE SOLUTION FOR FEMALE BODY ARMOUR

Mulat Alubel Abtew[1,2], Francois Boussu[1(*)], P. Bruniaux[1]

[1] ENSAIT-Univ. Lille, GEMTEX Laboratory, F-59000 Lille, France

[2] University of Missouri, Dept. of Textile and Apparel Management, Columbia, USA

(*) Email: francois.boussu@ensait.fr

ABSTRACT

Textile materials has been used as a soft solution to protect the human torso from various threats. The current research investigates the ballistic performances of female seamless soft body armour panels made of 3D warp interlock and 2D plain woven fabric. The two fabrics are manufactured from p-aramid yarns with similar yarn densities. Two panels, one from each fabric, with forty layers with similar areal density were prepared. The ballistic performances of both targets were investigated based on NIJ standards considering energy absorption capability, BFS and post-mortem analysis. The result shows that armour panel made of 3D warp interlock revealed higher level of impact protection without compromising the adaptation of the armour panel to the body shape due to its excellent mouldability behaviours.

INTRODUCTION

Textiles have been widely used to protect the human body of a soldier from head to torso, arms to legs and their respective extremities, hands, and feet [1]. The wide variety of existing textile solutions based on different polymers are available to provide different protective performances [2][2]. In addition, some textile materials can be moulded into different shapes and provide interesting mechanical performance/weight ratio, which makes it possible to achieve lightweight solutions and fitness [3][4]. According to various research, the 3D warp interlock fabric became promising structure for the development of women's body armour due to its good formability [5]. However, the performance of the fabric under ballistic impact for various threats should be investigated and compared with its counterparts 2D plain woven fabric before application [6]. The objective of this study is to investigate and compare the ballistic performance in terms of energy absorption, Back face Signature (BFS) and Post-mortem analysis of the frontal female torso shaped soft body armour panel made of the above two fabrics with the same areal density.

RESULTS AND CONCLUSIONS

The two panel targets made of the two different fabrics were moulded on customized frontal female shaped bench to give the required women torso. Six different bullets were shot at different, formed, and flat, area of the panel targets based on the NIJ standard. As shown in Fig. 1 (a), the of panels made with 3D WIFs possess higher energy absorption in most of the shot areas. This shows that by deforming the intended 3D fabrics the material properties including the rigidity of panels which affect the ballistic impact were not significantly changed. Based on the BFS and post-mortem analysis, Fig. 1 (b) and (c), panels made with 3D warp interlock fabric reveal high number of BFS values and number of layers penetrated within the panels in majority shot location, as compared to 2D plain weave fabrics in most shot locations. However, the BFS values were much lower than the standard values and there was no full penetration of the panels observed in the different shots. However, 3D warp interlock fabrics show better shaping ability according to the female contour while designing the body armour.
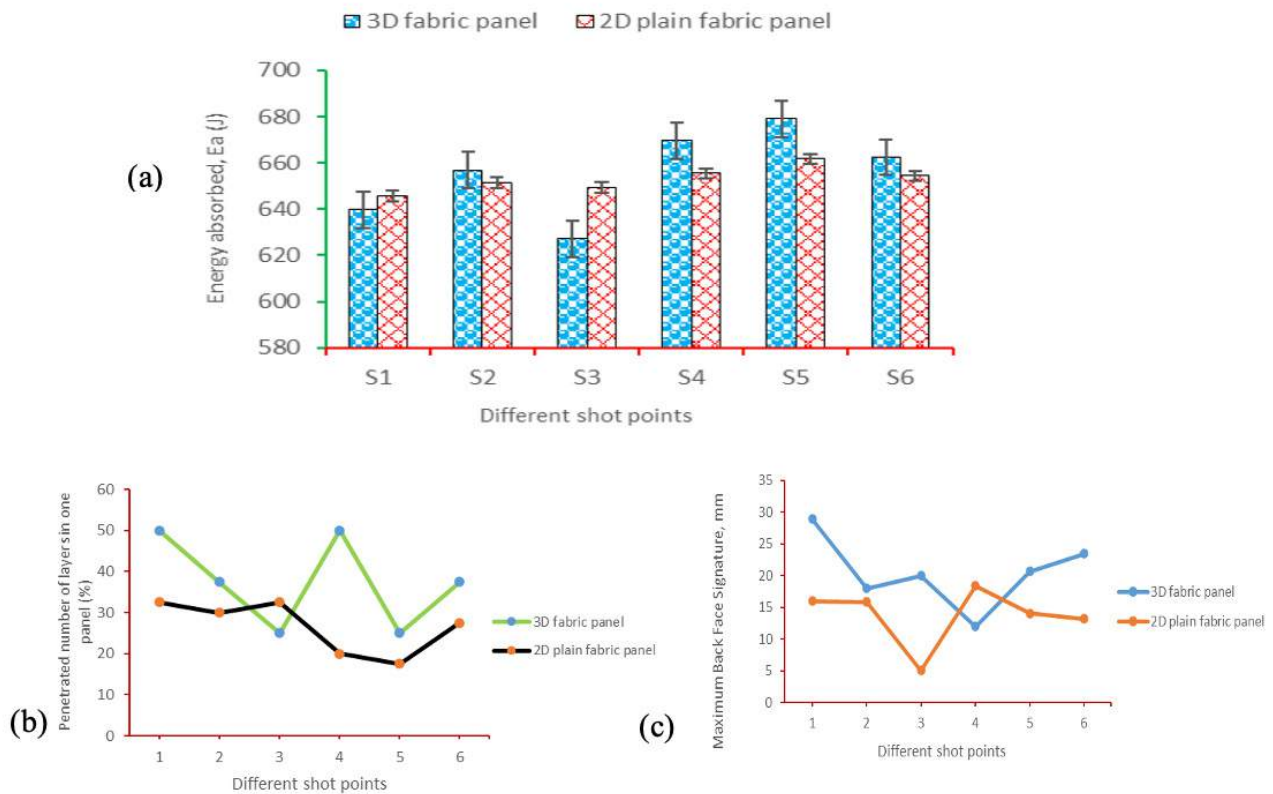
Fig. 1 (a) The percentage energy absorbed (%) (b) penetrated number of layers and (c) BFS of the formed women armor panels made of 2D plain and 3D warp interlock fabrics at different shot areas

Besides, the 3D warp interlock fabric, which incorporates optimised and balanced warp yarn within its structure, gives much better ballistic performance and lower BFS values.

REFERENCES

[1] Abtew MA, Boussu F, Bruniaux P, et al. Ballistic impact mechanisms – A review on textiles and fibre-reinforced composites impact responses. *Compos Struct* 2019; 223: 110966.

[2] Abtew MA, Boussu F, Bruniaux P. Dynamic impact protective body armour: A comprehensive appraisal on panel engineering design and its prospective materials. *Def Technol* 2021; 17: 2027–2049.

[3] Abtew MA, Boussu F, Bruniaux P, et al. Influences of fabric density on mechanical and moulding behaviours of 3D warp interlock para-aramid fabrics for soft body armour application. *Compos Struct* 2018; 204: 402–418.

[4] Boussu F, Cristian I, Nauman S. General definition of 3D warp interlock fabric architecture. *Compos Part B Eng* 2015; 81: 171–188.

[5] Yang D, Chen X, Sun D, et al. Ballistic performance of angle-interlock woven fabrics. *J Text Inst* 2017; 108: 586–596.

[6] Chen X, Sun D, Wang Y, et al. 2D / 3D Woven Fabrics for Ballistic Protection. In: *4th World Conference on 3D Fabrics and Their Applications ; 10 Sep 2012-11 Sep 2012; Aachen, Germany. Manchester: TexEng/RWTH Aachen*. 2012, pp. 1–12.

ID 36

EXPERIMENTAL INVESTIGATION OF COMPRESSIVE BEHAVIOR IN CALCIUM-SILICATE MINERAL FOAM

Aldjabar Aminou[1][(*)], Mohamed Ben Rhouma[2], Bachir Belkassem[3], Lincy Pyl[4], David Lecompte[5]

[1, 2, 3, 5] Structural and Blast Engineering Department, Royal Military Academy, Brussels, Belgium

[1, 2, 4] Mechanics of Materials and Constructions Department, Vrije Universiteit Brussel, Brussels, Belgium

[(*)] Email: aldjabar.aminou.malam.kailou@vub.be

ABSTRACT

This study investigates the compressive behavior of calcium-silicate mineral foam, with a density of 110 kg/m³, under quasi-static loading. Samples of varying sizes and shapes, including prismatic and cylindrical forms, were tested. Results indicate a convergence in plateau stress for prismatic samples at 8 cm width and cylindrical samples at 9 cm diameter. Cylindrical samples with radii below 9 cm exhibit higher plateau stress. Additionally, adding a wrapping enhances plateau stress by 10% and 15% for prismatic and cylindrical specimens, respectively. These findings provide valuable insights for optimizing mineral foam's performance in energy absorption and blast mitigation applications.

INTRODUCTION

Cellular materials, such as honeycombs or foams, have demonstrated exceptional capabilities as energy absorbents. They can undergo large deformation under quasi-constant stress conditions. Often used as crushable cores in sacrificial cladding for blast load mitigation, these materials play a crucial role in enhancing structural safety and resilience. In this study, we focus on investigating the compressive behaviors of calcium-silicate mineral foam under quasi-static loading conditions. With a density of 110 kg/m³, this mineral foam has intriguing properties that deserve further investigation. Understanding how various factors, such as sample sizes, shapes, and confinement, influence its compressive response is essential for optimizing its performance in practical applications.

RESULTS AND CONCLUSIONS

Experimental investigations were conducted on prismatic and cylindrical samples with thicknesses of 60 mm and 120 mm, subjected to a strain rate of 1.67×10^{-3} s^{-1}. Prismatic samples were varied in width from 40 mm to 160 mm (see Fig. 1), while cylindrical samples were selected to maintain consistent cross-sectional areas. To ensure the reliability of the findings, three samples per size and shape were tested.

Analysis of the results revealed significant insights into the compressive behavior of calcium-silicate mineral foam, as shown in Fig. 2. It was observed that the plateau stress converges notably for prismatic samples with a width of 8 cm or cylindrical samples with a diameter of 9 cm, indicating a critical threshold in specimen dimensions. Furthermore, cylindrical samples exhibited higher plateau stress when their radii were below 9 cm. This observation underscores the influence of sample geometry on the material's response to compression. Moreover, adding a wrapping around specimens with widths above 80 mm or diameters bigger than 90 mm resulted in a notable increase in plateau stress. Specifically, the addition of wrapping led to enhancements of 10% and 15% in plateau stress for prismatic and cylindrical specimens, respectively.
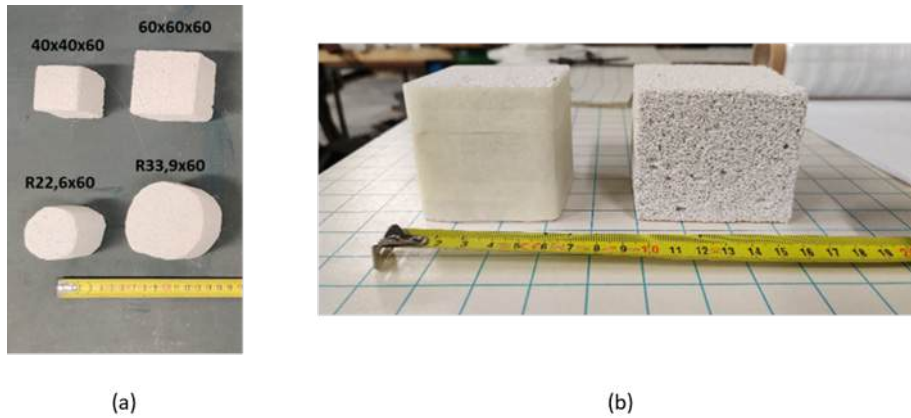
Fig. 1 Examples of (a) prismatic and cylindrical samples; (b) prismatic confined (left) and unconfined (right) samples

In conclusion, this study provides valuable insights into the compressive behavior of calcium-silicate mineral foam under quasi-static loading conditions. By elucidating the effects of sample sizes, shapes, and confinement, the findings contribute to the optimization of mineral foam-based structures for enhanced energy absorption and blast load mitigation applications. Further research in this direction holds promise for advancing the design and performance of cellular materials in various engineering contexts.
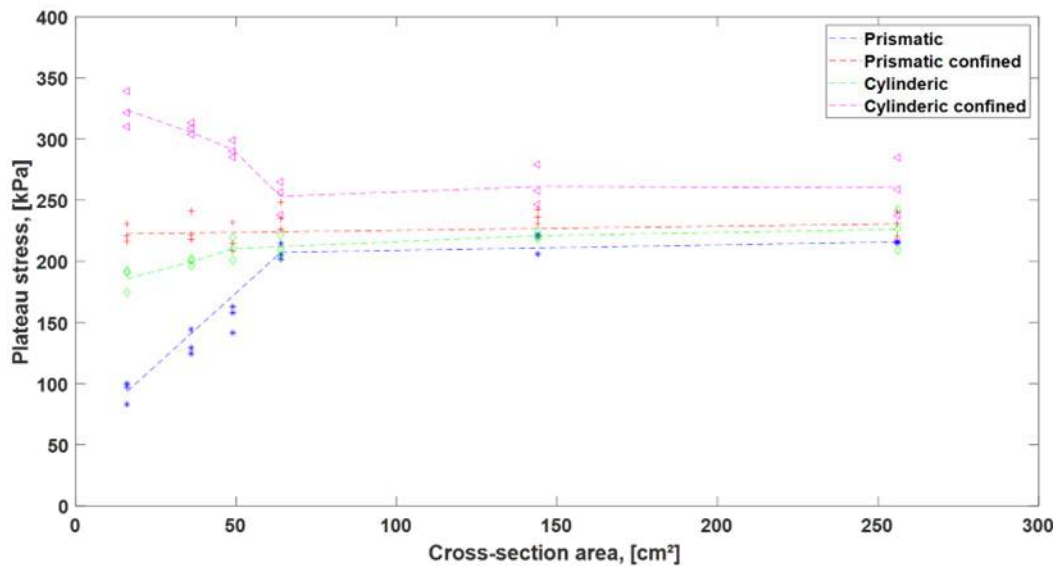
Fig. 2 Comparison of the plateau stress values for different configurations

REFERENCES

[1] H. B. Rebelo, D. Lecompte, C. Cismasiu, A. Jonet, B. Belkassem, and A. Maazoun, "Experimental and numerical investigation on 3D printed PLA sacrificial honeycomb cladding," *Int J Impact Eng*, vol. 131, pp. 162–173, Sep. 2019, doi: 10.1016/j.ijimpeng.2019.05.013.

[2] A. Aminou, B. Belkassem, O. Atoui, L. Pyl, and D. Lecompte, "Numerical modeling of brittle mineral foam in a sacrificial cladding under blast loading," *Mechanics and Industry*, vol. 24, no. 27, 2023, doi: 10.1051/meca/2023021.

ID 37
COMPARATIVE ANALYSIS OF THERMAL RESISTANCE PROPERTIES IN ACTIVITY WEAR FABRICS: CASE STUDY

Inga DABOLINA[1(*)], Liene SILINA[1], Eva LAPKOVSKA[1]

[1] Personal Protective Equipment Laboratory, Faculty of Civil and Mechanical Engineering, Riga Technical University, Riga, LATVIA

[(*)] Email: inga.dabolina@rtu.lv

ABSTRACT

This scientific research focuses on the thermal resistance properties of fabrics used in activewear, military under-garments, and a first layer of uniform; aiming to provide valuable insights for the optimization of specialized apparel in defense applications. The study compares the thermal resistance of three different knitted fabrics (100% WO; 94% CO / 6% El; 51% PES / 49% CO) using two distinct testing methods – a guarded hotplate and a thermal manikin [1]. The primary objective is to assess and analyze the trends in thermal resistance, evaluating the compatibility and interchangeability of results obtained from both testing methodologies.

INTRODUCTION

The physical properties of the fabrics, including wool, cotton, and polyester, are examined, highlighting their relevance in the context of textile material performance [2]. Key factors such as density, elasticity, thermal conductivity, and strength are discussed to underscore their influence on the thermal behavior of the materials. The literature review also emphasizes the significance of thermal resistance as a crucial parameter in evaluating the thermal insulation properties of textiles.

The methodology involves the preparation of fabric samples, conditioning, and testing on a guarded hotplate to simulate realistic conditions. Additionally, tests are conducted on the thermal manikin [3], allowing for a controlled environment to assess the behavior of textile materials. The obtained data are processed using statistical analysis methods to ensure accurate and reliable fabric comparison.

RESULTS AND CONCLUSIONS

Results reveal similar trends in the thermal resistance of the knitted fabrics under investigation, demonstrating variations just between different materials and not as much between testing methods [4-5]. Materials used for tests are shown in Table 1.

Table 1 Properties of fabrics

Fiber composition	100% Wool	94% Cotton/ 6% Elastane	51% Polyester/ 49% Cotton
Fabric structure	Single jersey	Single jersey	Doubleface
Thickness (mm)	0,61	0,71	0,79
Mass per unit area (g/cm2)	147,86	195,74	179,50

The primary research focus is to investigate the thermal resistance and weight change characteristics observed during testing with a hotplate. The study aims to analyze thermal resistance outcomes, taking into account variations in measurement methods and testing conditions. By exploring the thermal resistance behavior under different measurement methodologies and conditions, research shows the relationship between thermal properties and weight changes when utilizing a hotplate.
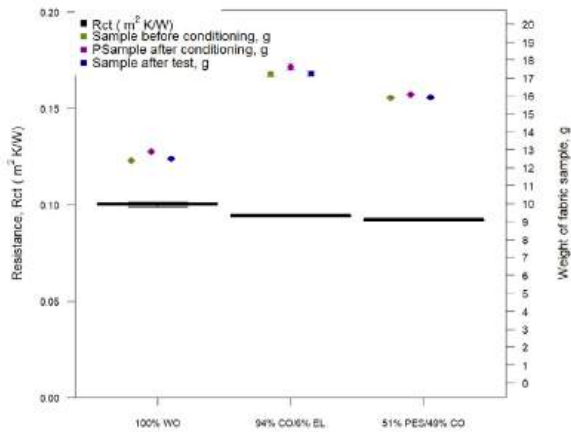
Fig. 1 Thermal resistance and weight change when testing with a shielded hotplate.

Fig. 2 Thermal resistance results depending on the used measurement method and conditions.

The moisture capacity of each material can also be deduced from the changes in the weight of the samples (Fig.1). It can be seen that the knitted fabric 100% WO and the knitted fabric 94% CO/6% EL absorb a lot of moisture, which is also released in almost all tests with a guarded hotplate. The knitted fabric 51% PES/49% CO is partially hydrophobic, because it absorbed relatively little moisture during conditioning, giving it back completely during testing. Summarizing the research results (Fig.2), it can be concluded that the results of thermal resistance measurements do not differ significantly depending on the used measurement method and conditions. When testing on a thermal manikin, the results of thermal resistance measurements are more variable. Looking at the results of the thermal resistance of knitted fabric 100%WO, when testing on a thermal manikin at 22°C, it can be seen that the deviation is relatively large in proportion to the measurement deviations of other knitted fabrics in tests on a thermal manikin, which is an additional phenomenon to be investigated.

This study aligns with the broader objective of enhancing the comfort and performance of military personnel by refining the thermal characteristics of their clothing systems. The comparative analysis of thermal resistance in fabrics presented in this research aims to inform the development of advanced materials for defense applications. The research findings contribute to the scientific understanding of textile material behavior in defense applications and offer practical insights for the selection and integration of suitable fabrics in military undergarments.

ACKNOWLEDGEMENT

REFERENCES

[1] R. Nayak and R. Padhye, Manikins for Textile Evaluation, Woodhead Publishing, 2017

[2] L. Wang, Performance Testing of Textiles: Methods, Technology and Applications, Woodhead Publishing, 2016

[3] ANDI Thermal Simulation Manikin; Online https://thermetrics.com/products/manikin/andi/, accessed 04.jan.2024

[4] ISO 11092:2014 Textiles Physiological effects Measurement of thermal and water-vapour resistance under steady-state conditions (sweating guarded-hotplate test).

[5] ISO 15831:2004 Clothing Physiological effects Measurement of thermal insulation by means of a thermal manikin.

ID 38
DIAMOND TEMPERATURE SENSORS FOR HARSH ENVIRONMENTS

Miguel A. Neto[(*)], **Bernardo L. Tavares, Sérgio Pratas, Eduardo L. Silva, Filipe J. Oliveira, Rui F. Silva**
Department of Materials and Ceramics Engineering, CICECO—Aveiro Institute of Materials, University of Aveiro, Portugal
[(*)] Email: mangelo@ua.pt

ABSTRACT
Diamond surfaces with thermal sensitive properties are presented as effective temperature sensors (thermistors) for application in harsh environments. The novelty of these sensors is their ability to withstand very high mechanical loads and strong aggressive chemicals. Since these sensors are made from well-known biomaterials, they are also suitable to be used in direct contact with biological media without the risk of inducing cytotoxicity effects. Furthermore, the temperature sensitive element of these sensors is a very thin layer of diamond, the material with the highest thermal conductivity, leading to very fast response times to very small temperature variations. Another particularity of these sensors is their capability to detect temperature by infra-red radiation. During synthesis, the optoelectronic properties of the diamond surface can be modified to give extraordinary sensitivity to light radiation, particularly in the infrared region. This property is very useful when contact measurements is not possible or unwanted.

INTRODUCTION

Temperature is a key parameter which requires constant monitoring in many technological applications in harsh environments. From deep ocean exploration to the manipulation and storage of nuclear fission products, combustion engines, cancer therapy and space exploration, all these applications require very specialized temperature sensors that can maintain their operability under very stressful situations. As such, these sensors must satisfy a complete set of outstanding physical, mechanical and chemical properties.

The technology for the synthesis of these unique sensors is based on thin polycrystalline diamond films, doped with boron, grown using the hot-filament chemical deposition technique (HFCVD) on flat sintered silicon nitride ceramic substrates [1, 2].

RESULTS AND CONCLUSIONS

Figure 1 shows the dimensions of a thin film nanocrystalline diamond (NCD) temperature sensor compared to those of a typical commercial sensor based of transition metal oxide technology. The plots of Figure 2 evidence the electrical resistance of the diamond thermistor as a function of temperature in the [25-400ºC] range and the calculated thermal sensitivity (β) values. These diamond sensors have a negative temperature coefficient (NTC), since its resistance decreases with increasing temperature. This data also shows that the thermoelectric performance of the diamond thermistors follows the Steinhart-Hart equation (which describes de behaviour of the most common thermistors). We also found that the thermal sensitivity for these sensors can be controlled and fine-tuned by changing the HFCVD growth parameters such as the methane to hydrogen ratio, the pressure, the argon and boron flow and the process temperature.

These new type of temperature sensors was tested in three real applications requiring devices with exceptional physical, mechanical and chemical properties. First, these sensors were incorporated in a high-speed milling machine with the objective of detect temperature variations, by infrared radiation, in the working tool during operation.

Secondly, a similar sensor was used to test its sensitivity to blood flow for dental viability assessment. Finally, diamond thermistors with both thermal and optical properties were incorporated in a firefighter helmet in conjunction with an alarm device to enhance safety during structural firefighting.
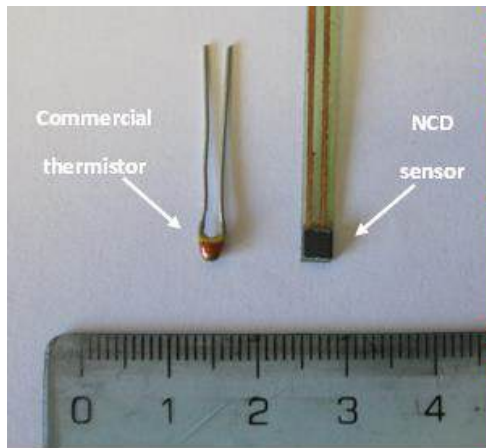
Figure 1 Size comparasion between a flat diamond thermistor and a commercial thermistor.
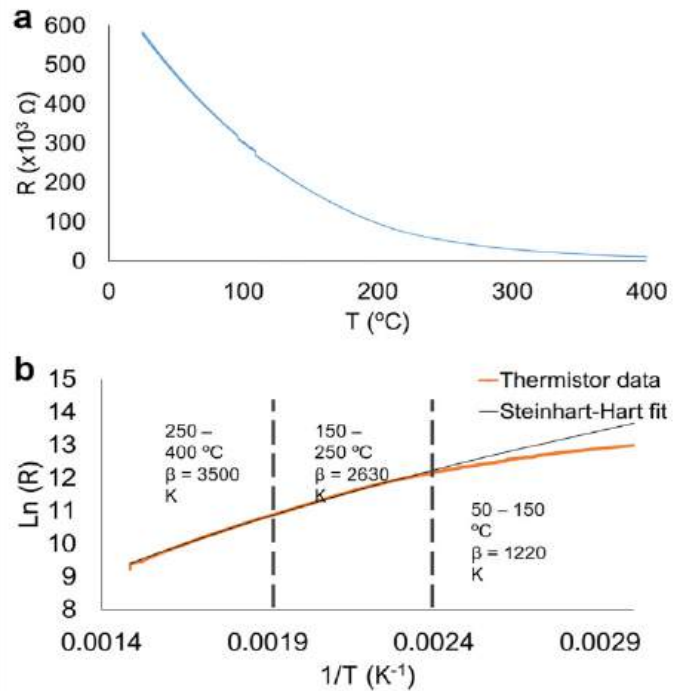
Figure 2 Resistance variation of the diamond NTC thermistor in the range 25–400 °C. (a) Measured curve. (b) Linear regression and fitting according to the "beta" and Steinhart-Hart models.

This study has shown that these sensors can detect temperature variations in a broad temperature interval with great sensitivity. Furthermore, such sensors can be used in very harsh environments in which the traditional sensors are prone to fail.

REFERENCES

[1] Neto, M.A.; Esteves, D.; Girão, A.V.; Oliveira, F.J.; Silva, R.F., "Tough negative temperature coefficient diamond thermistors comprising tungsten carbide ohmic contacts". Diam. & Relat. Mater. 109 (2020) 108036. DOI:10.1016/j.diamond.2020.108036

[2] Pratas, S.; Silva, E.L.; Neto, M.A.; Fernandes, C.M.; Fernandes, A.J.S.; Figueiredo, D.; Silva, R.F. "Boron Doped Diamond for Real-Time Wireless Cutting Temperature Monitoring of Diamond Coated Carbide Tools". Materials 2021, 14, 7334. https://doi.org/10.3390/ma14237334.

ID 39

DEVELOPMENT OF CUSTOM LARGE SCALE 3D PRINTING TECHNOLOGIES FOR IN SITU THERMOPLASTIC MATERIAL REUSE AND VALORISATION IN AREA OF OPERATIONS

Luis Ignacio Suárez[1](*), Juan Carlos Piquero[2], Blas Puerto Valcarce[3], Raúl Marqués Bada[4].

[1, 2, 3] IDONIAL technology center, Asturias, Spain.

(*) Email: luisignacio.suarez@idonial.com

ABSTRACT

IDONIAL has worked in the development and implementation of a technology for 3D printing using two reutilization pathways as raw materials: recycled plastic from packaging (PET) and high melting point technical plastics from withdrawn or discarded components (PC). This technology is capable of being incorporated into deployable mobile laboratories in operational zones, enabling on-site production of spare parts from the waste generated by settlement personnel. Additionally, IDONIAL has designed and manufactured a BAAM (Big Area Additive Manufacturing) head for 3D printing large components, with high deposition rates, and also capable of using recovered plastic in the aforementioned context.

INTRODUCTION

Currently, there is an increasingly widespread use of deployable laboratories or factories equipped with 3D printing systems for the on-site production of devices or spare parts with applications in the military sector[1]. Materials and technologies that offer the best compromise between the final properties of printed parts and versatility in terms of transport and deployment are those based on extrusion using filaments or pellets. This aspect is directly related to a critically important issue, namely sustainability and circularity based on recycling, as thermoplastic materials can be recovered and reprocessed with a relatively small loss.

A very specific application context within the defence sector (though applicable to other sectors) is operational deployments in remote areas, where certain circumstances favour the implementation of the developments outlined in this work. Ultimately, these converge on the possibility of establishing self-sufficient production models, independent of decentralized supply networks, that leverage waste material that can be collected on-site and even reuse plastics from components discarded due to breakage[2].

RESULTS AND CONCLUSIONS
Recycling Material Adaptation for Desktop 3D Printing

The equipment used in this initial phase of work is a TUMAKER BIGFOOT 500. Modifications are made to it regarding enclosure and temperature control of the working chamber. As for the preparation of the raw material, a desktop shredding system (SHRED IT) is used, allowing the obtainment of small flakes of material (2-3 mm^2). Printing tests are carried out with recovered plastic bottles (PET), which are crushed and properly sieved. A first operational drawback of this starting format is observed, namely the low density of the material flakes, causing irregularities in their feed. To address this, they are mixed with virgin material in granular pellet format. Through an iterative empirical process, it is concluded that the maximum load of recycled material vs. virgin material is 70%. A second approach used with this technology is the recovery of technical plastics from components in service that, after their initial use, become discarded pieces due to some type of deterioration. This case is illustrated with

a specific reference, LEXAN FST 3034, a type of polycarbonate designed to withstand high mechanical stresses and thermal properties in fire environments. The main technological challenge for processing this material lies in its high melting temperature (around 300ºC). Results with this material are more satisfactory than with PET, generating a more homogeneous plasticization that leads to a more orderly extrusion process. This has a very positive impact on the recyclability of the material, making it possible to achieve recycling rates of up to 100%.

Development of BAAM Head for High Deposition Ratio Work

The other line of work explored with recycled materials is the development of a BAAM (Big Area Additive Manufacturing) head. This technological development serves two fundamental purposes: 3D printing of large components in productive times with high deposition ratios and the possibility of revaluing large amounts of waste materials. The goal was to achieve material deposition rates as close as possible to 100 kg/h. Critical input parameters in the process include the torque and rotation of the spindle itself, as well as the temperature at each section, with the temperature at the nozzle tip being particularly important as it defines the melt process temperature during deposition. The head is integrated into a KUKA KR500 6-degree-of-freedom industrial robotic arm.

Numerous operational parameter adjustment tests were conducted with the head. Initially, PLA (polylactic acid) material in pellet form was used, encountering several problems associated with heat concentration in the deposited material mass. To reduce the impact of thermal effects, a formulation of PLA loaded with 20% cellulose was used. This helps mitigate the thermal load on the printed element, resulting in a more stable process. It is thus possible to print demonstrator components (aerodynamic profile) with respective height, length, and weight of 70 cm, 85 cm, and 5.8 kg of material in around 5 hours of processing. figure 3-.

Final results and conclusions

On one hand, technology has been implemented, and 3D printing tests have been conducted with recycled materials from two different sources, yielding good final results. The developed process chain is simple, requires minimal equipment, has low installation and maneuver complexity. A mobile 3D printing system could be integrated to benefit from the advantages of using recovered materials on-site in operational zones. Regarding the BAAM system, the head has been fully developed, making it susceptible to integration into a Cartesian system similar to 3D printers. The possibility of printing with pellet formats at reasonably high deposition rates is demonstrated, although there is a clear operational limitation in the heat concentration within the material itself
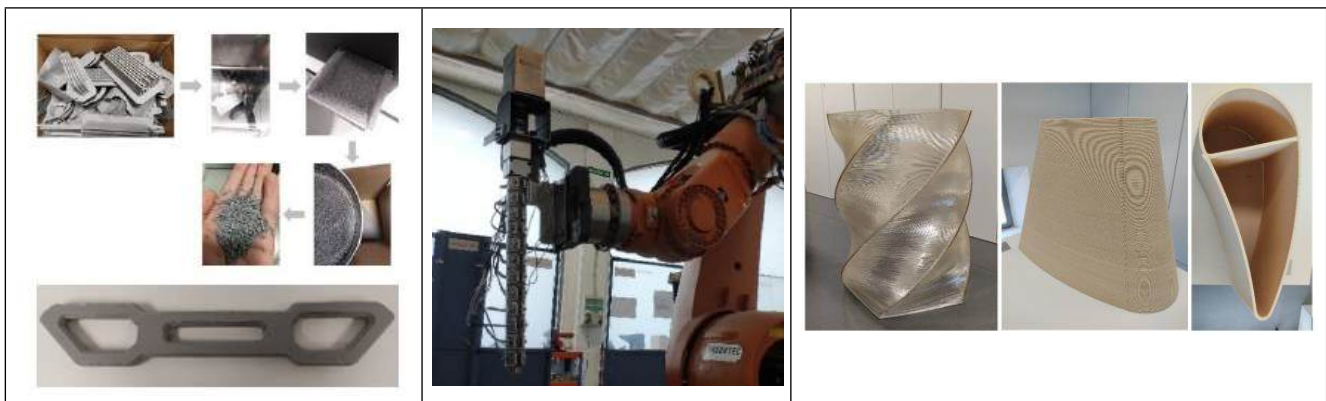
Figures: (1) recycling chain for PC technical parts, (2) BAAM system, (3) BAAM printed parts

REFERENCES

[1] den Boer, Jelmar & Lambrechts, Wim & Krikke, H.R.. (2020). Additive manufacturing in military and humanitarian missions: Advantages and challenges in the spare parts supply chain. Journal of Cleaner Production. 257. 10.1016/j.jclepro.2020.120301.

[2] Zander, Nicole. (2019). Recycled Polymer Feedstocks for Material Extrusion Additive Manufacturing. 10.1021/bk-2019-1315.ch003.

ID 40
PIEZORESISTIVE PRINTED SENSORS FOR MEASURING ELONGATION OF PARACHUTE CANOPY FABRIC AND RIBBONS

Dormois Thibault[1](*), Cochrane Cédric [1], Koncar Vladan [1]
[1]Univ.Lille, ENSAIT ULR 2461-GEMTEX–Génie et Matériaux Textiles, F-59000 Lille, France
(*) Email: thibault.dormois@ensait.fr

ABSTRACT
Canopies and parachute lines are subjected to high stresses during the opening phase of the canopy. The aim of this work is to measure the strain undergone by these components to obtain a better knowledge of these materials and their life span. In order to not modify the structure of the parachute and influence the obtained data, the measurements are carried out in a non-intrusive way. This constraint implies to design and realize a discrete and robust interface between the sensors and the textile. Another part of this work is to design and implement an electronic measurement device capable of recording the data from the embedded sensors.

INTRODUCTION
Parachutes and wing foils are complex systems with various textiles components (the canopy of parachutes is composed of panels of a thin fabric linked together by parallel and meridional ribbons) and their structure undergoes very important wind forces and stresses during the different stages of a flight (extraction, opening, stabilized descent and landing) [1]. The ability of monitoring a parachute canopy brings interesting prospects for the civil, military and defense sectors.

Different types of sensing technologies can be used to measure the strain or stress undergone by textiles. From optical fibers [2] and metallic yarns [3] to piezoresistive films or polymers [4], each technology has its pros and cons when combined with the structure complexity of textiles (highly deformable, stretchable…) and the application. The printing technology of inks with conductive fillers (carbon, metallic) opens a wide range of possibilities to obtain an optimum sensing system by quickly adapting the process to the ink's properties (viscosity, surface tension, composition), the substrate's properties (material, surface tension, porosity…) and the desired sensor's geometry.

The characterization of the sensors in static and dynamic strain is important to understand the sensing capabilities of the system and adapt the data processing and analysis depending on the sensor's gauge factor **(GF)** and the potential impact of exterior parameters (temperature and hygrometry) [4][5]. The GF is the ratio of the relative change in electrical resistance to the mechanical strain. It quantifies the sensitivity of a strain sensor (the higher the GF, the higher the change in resistance is to small elongation).

RESULTS AND CONCLUSIONS
To validate that the printed sensors will successfully measure the strain undergone by the parachute's components, it is necessary to determine its response in terms of linearity, repeatability, noise and the influence of exterior parameters. Table 1 shows the measured GF of carbon-based sensors printed onto the parachute's canopy fabric and ribbons (meridional and parallel). The GF was measured on an applied strain of 10%. The results show that the GF varies depending on the substrate (difference in rugosity and porosity).

	Meridional Ribbon	Parallel Ribbon	Canopy Fabric 1 (Ripstop)	Canopy Fabric 2
Gauge Factor	10 [+/- 4]	21 [+/- 2]	16 [+/- 2]	14.5 [+/- 0,2]

Table 1 Gauge Factor of carbon-based printed sensors on different textile components of parachute canopy

The results of the variation in relative resistance of a carbon-based printed sensor undergoing uni-axial stress at 100mm/min are shown in Fig 1.
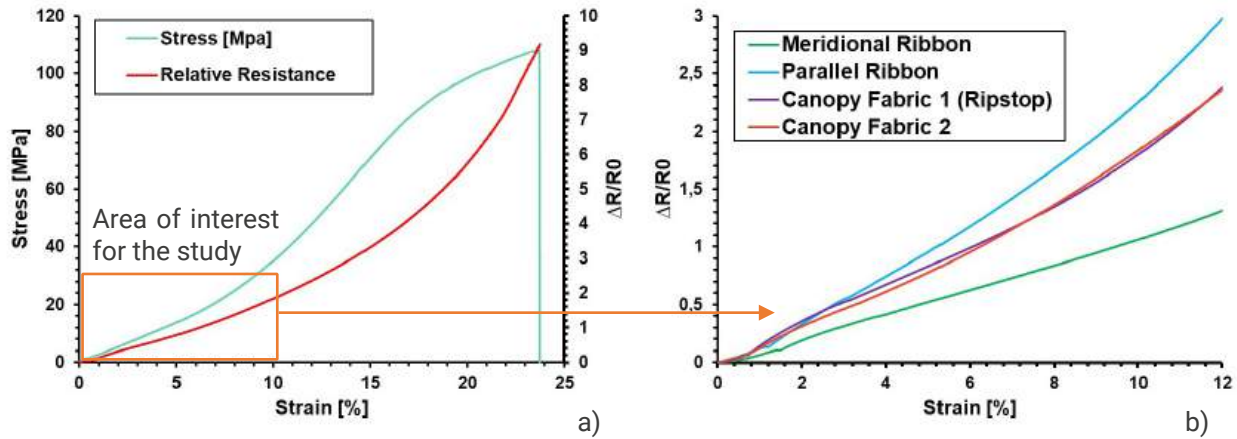
Fig. 1 a) Load strain curve of canopy fabric 2 and the measured relative resistance of the carbonbased printed sensor b) Relative resistance strain curve at 12% strain for 4 components of a parachute canopy

This study shows the performances in measuring strain in textiles of printed piezoresistive sensors. The response of the sensors to a controlled strain shows a behaviour close to linear at 10% strain but does depend on the ink's properties and printing conditions. The sensor's response also depends on the sensor - textile interface and the speed of the applied stress.

In the prospective future work, a new mean of measuring dynamically the elongation is being developed by applying a load through free-falling mass. This will more acutely represent the opening speeds of a parachute canopy during the opening phase of a flight. This work will also focus on proving the non-impact of the printed sensor on the mechanical properties of the parachute canopy fabric. The improvements of the robustness of the sensing systems connections and the development of the embedded recording device will also be worked on.

REFERENCES

[1] H. G. Heinrich et D. P. Saari, « Parachute Canopy Stress Measurements at Steady State and During Inflation », J. Aircr., vol. 15, no 8, p. 534-539, août 1978, doi: 10.2514/3.58402.

[2] M. El-Sherif et al., « A Novel Fiber Optic System for Measuring the Dynamic Structural Behavior of Parachutes », J. Intell. Mater. Syst. Struct., vol. 11, no 5, p. 351-359, mai 2000, doi: 10.1106/JF6U-2FQ9-FQGE-3VXK.

[3] B. Garnier, P. Mariage, F. Rault, C. Cochrane, and V. Koncar, "Electronic-components less fully textile multiple resonant combiners for body-centric near field communication," Sci. Rep., no. 0123456789, pp. 1–12, 2021, doi: 10.1038/s41598-021-81246-z.

[4] C. Cochrane, M. Lewandowski, and V. Koncar, "A Flexible Strain Sensor Based on a Conductive Polymer Composite for in situ Measurement of Parachute Canopy Deformation," Sensors, vol. 10, no. 9, pp. 8291–8303, 2010, doi: 10.3390/s100908291.

[5] D. Budolak, L. Hantsche, et E. Rossi De La Fuente, « Strain Sensor Survey for Parachute Canopy Load Measurements », in 26th AIAA Aerodynamic Decelerator Systems Technology Conference, Toulouse, FRANCE: American Institute of Aeronautics and Astronautics, mai 2022. doi: 10.2514/6.2022-2754.

ID 41

COMPUTATIONAL MODELING AND EXPERIMENTAL TESTING OF A NEW FOAM-FILLED GRADED AUXETIC PANEL

Hasan AL-RIFAIE[1](*), Nejc NOVAK[2], Alessandro AIROLDI[3], Tomasz ŁODYGOWSKI[4]

[1, 4] Faculty of Civil and Transport Engineering, Poznan University of Technology, Poland.

[2] Faculty of Mechanical Engineering, University of Maribor, Maribor, Slovenia.

[3] Department of Aerospace Science and Technology, Politecnico di Milano, Milano, Italy.

(*) Email: hasan.al-rifaie@put.poznan.pl

ABSTRACT

Auxetic topologies have superior energy-dissipation properties and can be employed as lightweight impact-energy absorbers. The objective of this work is to investigate the behaviour of new re-entrant auxetic graded aluminium panels filled with polyurethane foam in an auxetic pattern using both computational and experimental methods. The sandwich panel and its validated FE model showed high Specific Energy Absorption (SEA) providing auxetic response up to very large strains. The proposed panel could be a promising solution for modern crash absorption systems or blast protection elements.

INTRODUCTION

The lightweight nature and impact energy absorption of cellular structures have led to their widespread application in engineering [1]. Studies found that auxetic metamaterials (with negative Poisson's ratio) provide improved energy dissipation compared to conventional cellular topologies [2, 3]. Foam-filled sandwich panels are frequently used in building construction. Nevertheless, due to shear failure of the foam core or delamination between the face sheet and the core, this form of sandwich panel cannot withstand extreme impact [4]. As a result, the purpose of this work is to investigate the behaviour of a new re-entrant graded aluminium panel filled with polyurethane foam in an auxetic pattern. Performance is evaluated using quasi-static and dynamic drop tower experiments as well as advanced non-linear finite element modelling. This study looked at six distinct auxetic panels. Each panel has six re-entrant auxetic layers and is constructed by corrugating and gluing twelve aluminium sheets. The geometry of the fabricated auxetic panels was based on the numerical parametric study of Al-Rifaie and Sumelka [5] which was recently validated experimentally by Al-Rifaie, et al. [6]. The sheet thickness and PU foam content of the six auxetic panels vary. The first three non-graded auxetic panels feature uniform corrugated sheet thicknesses of 0.8 mm, 1.0 mm, and 1.2 mm throughout the whole panel. The fourth graded auxetic panel (Figure 1a) was made with varied sheet thicknesses (two layers of 0.8 mm, two layers of 1 mm, and two layers of 1.2 mm). The last two graded samples were filled with PU foam as a full-filled graded panel (Figure 1b) and an auxetic-filled graded panel (Figure 1c). The auxetic-filled arrangement was used to introduce multiscale auxetic behaviour to the panel, where filling may create additional auxetic effect.

Auxetic panels were tested quasi-statically using the universal testing equipment INSTRON 8801 at a position--controlled crosshead rate of 0.5 mm/s. The nominal stress-strain responses were estimated using the samples' original dimensions. In addition, drop tower testing was performed, which included a drop sledge with various masses guided by two 6 m tall columns. The overall weight of the impacting mass was 99.5 kg, and the loading velocity was 10 m/s, resulting in impact energy of 4975 J. Computational modelling was performed using LS-DYNA implementing 5 mm fully-integrated shell elements with 5 integration points throughout the thickness. The foam inserts were modelled with fully integrated 3D elements. The aluminium of the auxetic layers was modelled with

an elasto-plastic material model utilising strain hardening and rate dependence. Foam inserts were modelled with a crushable foam material model.

RESULTS AND CONCLUSIONS

The experimental and computational findings looked at stress-strain relationships, deformation patterns (Fig. 1), specific energy absorption, crash force efficiency, and Poisson's ratio. Foam-filled panels demonstrated better specific energy absorption and more stable deformation than non-filled panels. The numerical models successfully captured mechanical and deformation behaviour and may be utilized for future virtual testing of different combinations. The detailed results of this research are thoroughly presented in [7].

| a) non-filled graded | b) full-filled graded | c) auxetic-filled graded | d) numerical model |
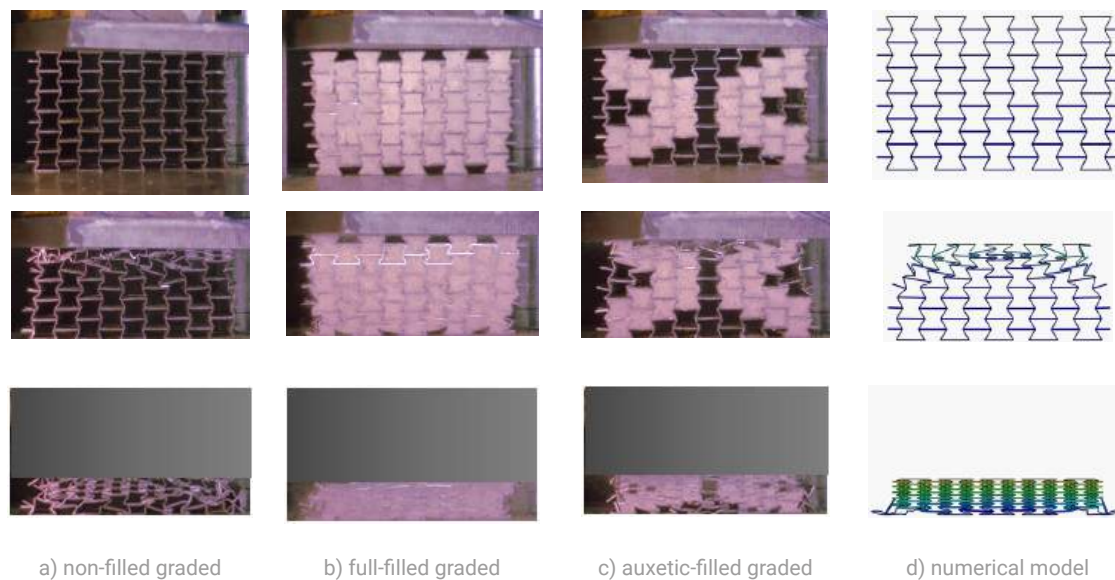
Fig. 1 Drop-Tower testing and numerical modelling of the auxetic panels considered in this study

REFERENCES

[1] H. Al-Rifaie, "Novel energy-absorbing auxetic sandwich panel with detached corrugated aluminium layers," Vibrations in Physical Systems, vol. 34, pp. p. 2023215-1-12, 2023.

[2] N. Novak, M. Vesenjak, and Z. Ren, "Auxetic cellular materials-a review," Strojniški vestnik-Journal of Mechanical Engineering, vol. 62, pp. 485-493, 2016.

[3] H. Al-Rifaie and W. Sumelka, "Improving the Blast Resistance of Large Steel Gates-Numerical Study," Materials, vol. 13, p. 2121, 2020.

[4] F. Usta, H. S. Türkmen, and F. Scarpa, "High-velocity impact resistance of doubly curved sandwich panels with re-entrant honeycomb and foam core," International Journal of Impact Engineering, vol. 165, p. 104230, 2022.

[5] H. Al-Rifaie and W. Sumelka, "The developement of a new shock absorbing Uniaxial Graded Auxetic Damper (UGAD)," Materials, vol. 12, p. 2573, 2019.

[6] H. Al-Rifaie, N. Novak, M. Vesenjak, Z. Ren, and W. Sumelka, "Fabrication and Mechanical Testing of the Uniaxial Graded Auxetic Damper," Materials, vol. 15, p. 387, 2022.

[7] N. Novak, H. Al-Rifaie, A. Airoldi, L. Krstulović-Opara, T. Łodygowski, Z. Ren, et al., "Quasi-static and impact behaviour of foam-filled graded auxetic panel," International Journal of Impact Engineering, vol. 178, p. 104606, 2023.

ID 42
CHALLENGES IN THE VIRTUAL PRODUCT DEVELOPMENT OF PROTECTION VESTS

Sophie Herz[1][(*)], **Felix Kunzelmann**[1], **Yordan Kyosev**[1]
[1] Chair for development and assembly of textile products, TU Dresden
[(*)] Email: sophie.herz@tu-dresden.de

ABSTRACT

The textile industry has made big steps towards digitizing product development [1]. Tools and software have been improved significantly. By further digitizing product development and extending virtual product databases, not only documentation is largely improved, but the created datasets can also be used for stress, fit and impact simulations [2]. Yet, there are still challenges to the virtual product development of complex and multi-layered products [1]. In this paper, the challenges and current limitations of virtual product development in the garment industry are identified and compared. A ballistic vest is reverse designed using VStitcher and Clo3D comparatively, and the differences, advantages, disadvantages and limitations explained.

INTRODUCTION

The recent increase in victims in armed conflicts to it's highest level since 1986 [3], and a strong increase in violent crime against law enforcement [4] show the rising importance of personal protective equipment (PPE). Improvements in modelling the fit, comfort [5] and the ballistic [6] and thermal capabilities [6] of protective vests are still ongoing. Size and fit are of protective gear are of utmost importance to maintain functionality [7]. Within the last decades, the tools for the virtual products development were improved to not only show the 2D cutting pattern, but also the 3D product [8]. However, differences persist between different 3D product design tools [8].

In this study, the 3D design software packages VStitcher by Browzwear and Clo3D by CLO are used to reverse design the same protective vests. Capabilities, limitations and particularities of the packages are shown. The results are compared regarding the extent of the model, the possibilities to export the virtual product to finite element modelling (FEM) software packages and the extent of information on the product included.

RESULTS AND CONCLUSIONS

The essential consideration is the transformation of 2D geometries into 3D simulations featuring avatars within both Clo3D and VSticher software. Both platforms successfully facilitate this process for soft ballistic vests, as shown in Figure 1. The evaluation of fit behavior is systematically conducted using diverse colormaps in both programs, enabling a nuanced analysis. Despite the shared objective, variations in assessment tools emerge, introducing differences that need careful consideration for result comparison. Among the more challenging aspects is the simulation of multilayer structures. Precisely representing the numerous aramid layers within the vest poses a noteworthy challenge due to potential intersection issues between layers, impacting the overall simulation outcome. This investigation sheds light on the intricate nature of modeling soft ballistic vests in the Clo3D and VSticher software applications.Regarding the development of PPE design software, efforts are veered toward including personalized and/or soft avatars, improving the simulation of multi-layered structures, including the simulation of external forces and enhancing the rendering capacities. Artificial intelligence is increasingly being used in clothing technology programs; AI-supported pattern optimization would be expected here. This would greatly simplify the development of customized products.
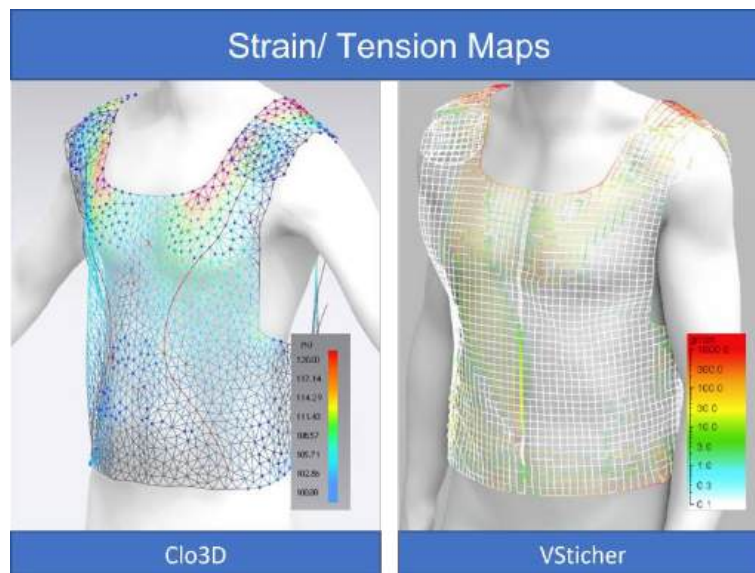
Figure 1 Strain/tension maps of vests on human avatars

REFERENCES

[1] E. Papahristou and N. Bilalis, "A New Sustainable Product Development Model in Apparel Based on 3D Technologies for Virtual Proper Fit," in *Sustainable Design and Manufacturing 2016*, R. Setchi, R. J. Howlett, Y. Liu, and P. Theobald, Eds., in Smart Innovation, Systems and Technologies. Cham: Springer International Publishing, 2016, pp. 85–95. doi: 10.1007/978-3-319-32098-4_8.

[2] Y. Kyosev, "Material description for textile draping simulation: data structure, open data exchange formats and system for automatic analysis of experimental series," *Text. Res. J.*, vol. 92, no. 9–10, pp. 1519–1536, May 2022, doi: 10.1177/00405175211061192.

[3] B. Herre, L. Rodés-Guirao, M. Roser, J. Hasell, and B. Macdonald, "War and Peace," *Our World Data*, Jan. 2024, Accessed: Jan. 29, 2024. [Online]. Available: https://ourworldindata.org/war-and-peace

[4] BKA, "Lagebilder Gewalt gegen Polizeivollzugsbeamtinnen/-beamte - Bundeslagebild Gewalt gegen Polizeivollzugsbeamtinnen und Polizeivollzugsbeamte 2022." Accessed: Jan. 29, 2024. [Online]. Available: https://www.bka.de/SharedDocs/Downloads/DE/Publikationen/JahresberichteUndLagebilder/GewaltGegenPVB/GewaltGegenPVBBundeslagebild2022.html?nn=60092

[5] R. Mahbub, R. Nayak, L. Wang, and L. Arnold, "Comfort properties of 3D-knitted seamless female body armour vests," *J. Text. Inst.*, vol. 108, no. 11, pp. 1997–2005, Nov. 2017, doi: 10.1080/00405000.2017.1306904.

[6] M. Boljen, M. Jenerowicz, S. Bauer, and E. Straßburger, "Combining protective clothes with human body models for finite element ballistic impact simulations," *Commun. Dev. Assem. Text. Prod.*, vol. 4, no. 2, Art. no. 2, May 2023, doi: 10.25367/cdatp.2023.4.p141-150.

[7] D. Muenks, J. Pilgrim, and K. Yordan, "Possibilities for qualitative evaluation of the protection area of protective clothing," *Commun. Dev. Assem. Text. Prod.*, vol. 3, no. 2, Art. no. 2, Sep. 2022, doi: 10.25367/cdatp.2022.3.p156-162.

[8] E. Papachristou, D. Kalaitzi, and V. Pissas, "A methodological framework for the integration of 3D virtual prototyping into the design development of laser-cut garments," *J. Eng. Fibers Fabr.*, vol. 18, p. 15589250231194621, Jan. 2023, doi: 10.1177/15589250231194621.

ID 43
A USER-CENTRIC EVALUATION OF THERMOPHYSIOLOGICAL COMFORT OF DEFENSE CLOTHING SYSTEMS USED IN HOT CLIMATE OPERATIONS

Magdalena Georgievska[1(*)], **Sheilla Odhiambo**[2], **Cosmin Copot**[2], **Hilda Wullens**[3], **Benny Malengier**[1], **Lieva Van Langenhove**[1]

[1] Department of Materials, Textiles and Chemical Engineering, Ghent University, Gent, Belgium

[2] Fashion and Textiles Innovation Lab (FTILab), HOGENT University of Applied Science and Arts, 9051 Ghent, Belgium

[3] Laboratoires de la Défense (DLD), 1800 Vilvoorde, Belgium

(*) Email: magdalena.georgievska@ugent.be

ABSTRACT

Subjective evaluation of the comfort of defense clothing systems is an important step in increasing the operational capability, health and overall well-being of military personnel. It can help in understanding individual perceptions of comfort, identifying issues and preferences that quantitative measures may overlook. This case study presents findings from a customized survey for evaluating thermal and ergonomic comfort of current Belgian defense clothing systems (CL) utilized in Hot Climate (T=22-41°C). Each participant was required to select one of four predefined clothing systems (CL1-CL4). The survey included sections on ergonomics, thermal comfort, smart functionalization, and future requirements. Upon filtering the responses based on gender (male), age (18-45) and weight (62-104kg; >110kg were excluded), 38 answers were selected for the analysis. The results from the survey highlighted clothing aspects that need to be improved and showed users attitude towards smart functionalities in garments. Results showed dissatisfaction with the dynamic fit of current clothing systems (fit during movement), flexibility in specific body areas like the crotch and knees, as well as backpack comfort particularly for CL1. Widespread dissatisfaction for all clothing systems was reported in terms of thermal comfort. Users indicated ventilation, sweating, and odor issues across clothing systems, highest for CL1 and CL2. The diversity of opinions provides insights into the multifaceted aspects of clothing comfort and user needs. Only by acknowledging them we can pave the way for targeted improvements and ultimately optimize the comfort of end-users operating in specific environments.

INTRODUCTION

Thermophysiological comfort is defined as a state of well-being, influenced by environmental conditions, body characteristics, activities, internal processes, and clothing factors.[8] Achieving a balance of heat and moisture among the body, environment, and clothing is complex but essential, particularly in personal protective equipment (PPE, under which defense clothing is classified), where comfort is to a certain extent sacrificed.[14] Enhancing comfort may be recognized as an additional protective requirement due to the potential life-threatening risks of heat stress, temperature loss or lack of focus. there has been a number of projects in the research and development of PPE for defence that emphasize clothing comfort and incorporation of smart textiles.[2-5,9-13] Comfort assessment encompasses anatomical, physiological, and psychological aspects, with individual perceptions varying based on factors like anthropometry and physical fitness.[2,6] Factors like body posture, movement, wind, fabric thermal properties and fabric-skin contact further affect overall comfort.[1,4,6] Thus, evaluating comfort includes a combination

of objective and subjective methods. For subjective evaluation of thermal comfort, guidelines on using methods like Likert scales are given in standard ISO 10551.[7,8]

In this study 4 clothing systems (CL) used for Hot Climate Conditions (T= 22-41°C) were defined by the Belgian defence, with specified ambient conditions (wet/dry) and human activity (static/active): CL1 (dry, active), CL2 (wet, active), CL3 (dry, static), and CL4 (wet, static). Figure 1a, defines the clothing system elements per CL; the differences lie in elements 5 and 13. Participants assessed these systems through a survey covering personal characteristics, ergonomics, thermal comfort, smart functionalization, and future requests. The survey, administered via LimeSurvey to soldiers, comprised 33 questions and responses structured as either yes/no or utilizing a 5-6 point Likert scale. Some of the questions included evaluation of the clothing systems per body areas defined in Fig.1b. The collected data was analyzed using Excel and SPSS, ensuring anonymity of all respondents. Statistical analysis involved Friedman's ANOVA and Wilcoxon Post-Hoc tests to examine significant differences in answers across different clothing systems and body areas.

(a)   (b)
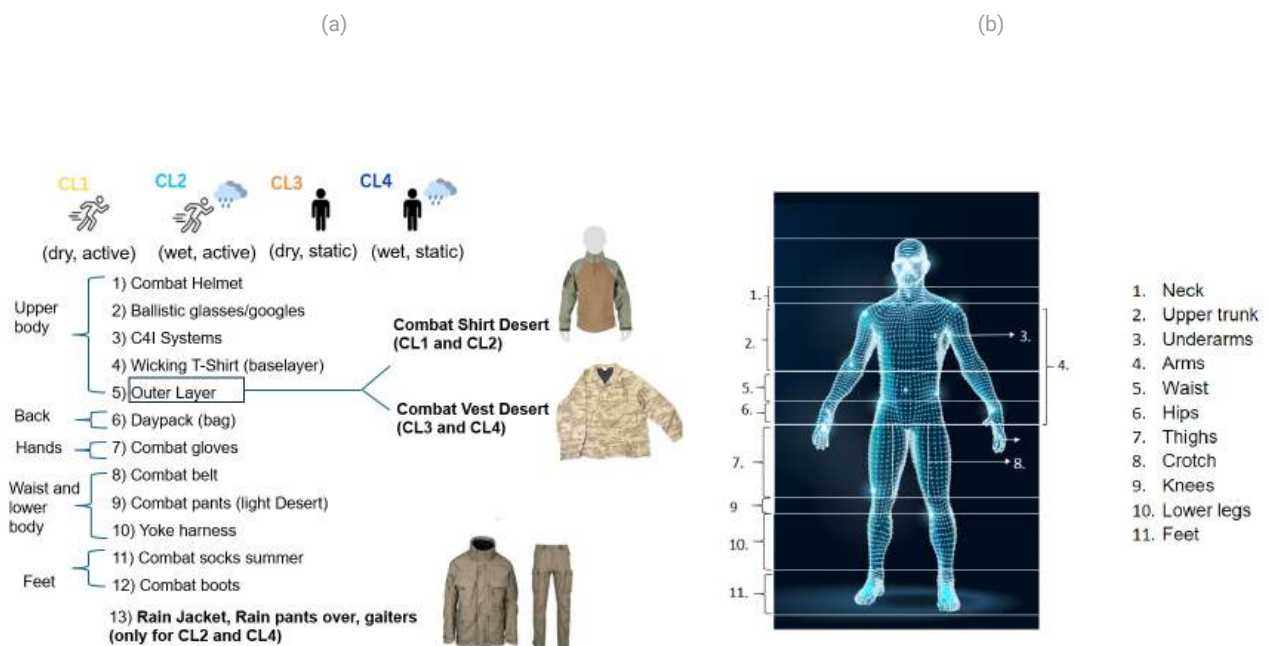
Fig.1. (a) Defined Clothing Systems for Hot Climate (T=22-41°C), (b) Defined body areas for local evaluation of comfort.

RESULTS AND CONCLUSIONS

Issues revealed from the survey results include dissatisfaction with the dynamic fit of all clothing systems, with 68.42% of participants expressing overall dissatisfaction. CL3 users found freedom of movement reasonable (77.38%) or bad (17.85%), especially in the arms and thighs. Backpack comfort was reasonable except for CL1 (70% 'a bit uncomfortable'). Certain body parts were perceived as more prone to tearing, notably the crotch area for CL1 and CL2 users. Thermal comfort dissatisfaction was prevalent across all systems with 91.47% being fairly satisfied or dissatisfied (Fig.2a). Users expressed dissatisfaction with ventilation (40%), suggesting the need for more ventilation strategies (Fig2b). CL1 users experienced significant sweating, especially in the feet and armpits. Feet and armpits were also the longest to dry for CL1 and CL2 (Fig.2c and 2d). CL2 users had a pronounced negative odor perception during active operation (90% found it "strongly unpleasant"). Respondents expressed strong interest in cooling materials and automatic cooling for hot climates (Fig.2e). Evaluating defense clothing comfort is complex; the survey provided valuable insights but had limitations. Enhancing thermal comfort in hot climates remains a significant challenge, necessitating novel cooling strategies.

a) Thermal comfort satisfaction

b) Current ventilation management

c) Drying perception per clothing system

d) Fastest/slowest drying areas
(Wilcoxon Signed Ranks Test - Post-Hoc)

CL1 (dry, active)		CL2 (wet, active)	
CL1 Body Parts	Rank	CL1 Body Parts	Rank
Feet	3.17	Feet	2.64
Upper trunk	3.23	Armpits	2.86
Armpits	3.3	Upper trunk	4
Crotch	4	Waist	4.5
Waist	4.67	Knees	4.5
Arms	4.77	Crotch	4.64
Knees	4.87	Arms	4.86
Friedman's ANOVA	p<0.01	Friedman's ANOVA	p<0.039

e) Interest in novel cooling strategies (N = 38)

*N= Number of participants; Total N=38.
CL1 (N*=14), CL2 (N=7), CL3 (N=12), CL4 (N=4)

Fig.2. a) Overall thermal comfort satisfaction per CL, b) Current ventilation strategies per CL, c) Drying perception per CL; d) Ranked groups of best/worst performing local areas in terms of drying. CL3 and CL4 are not included due to no statistical significance between ratings, e) Interest in cooling strategies

Fig.3. Interest in implementation of novel cooling strategies in the defense clothing systems.

REFERENCES

[1] Ciesielska-Wróbel IL, van Langenhove L. The hand of textiles – definitions, achievements, perspectives – a review. Textile Research Journal. 2012;82(14):1457-1468.

[2] Dāboliņa I, Lapkovska E. Sizing and fit for protective clothing. Anthropometry, Apparel Sizing and Design. 2019.

[3] Enescu D. Models and indicators to assess thermal sensation under steady-state and transient conditions. Energies. 2019;12(5).

[4] Ghaddar N, Ghali K. Modeling of heat and moisture transfer in porous textile medium subject to external wind: Improving clothing design. Handbook of Thermal Science and Engineering. 2018.

[5] Havenith G, Fiala D. Thermal indices and thermophysiological modeling for heat stress. Comprehensive Physiology. 2016;6(1). 5.

[6] International Organization for Standardization. (2007). ISO 9920:2007 Ergonomics of the thermal environment - Estimation of thermal insulation and water vapour resistance of a clothing ensemble. Geneva, Switzerland

[7] International Organization for Standardization. (2019). ISO 10551:2019 Ergonomics of the physical environment - Subjective judgement scales for assessing physical environments. Geneva, Switzerland.

[8] Islam MR, Golovin K, Dolez PI. Clothing Thermophysiological Comfort: A Textile Science Perspective. Textiles. 2023;3(4):353-407.

[9] Revaiah RG, Kotresh TM, Kandasubramanian B. Technical textiles for military applications. Journal of the Textile Institute. 2020; 111(2).

[10] Mlynarczyk M, Orysiak J. The air gaps in the protective clothing – methodology. In: Joint International Conference Clothing-Body Interaction; 2021.

[11] Psikuta A. Comprehensive model of human-clothing-environment system for application in apparel, built environment, and automotive fields. Joint International Conference Clothing-Body Interaction. 2021.

[12] Scadaglini S. Ergonomic of gesture. Effect of body posture and load on human performance. Published online 2017.

[13] Vestlife Project. Lightweight and modular bulletproof integral solution. Accessed July 1, 2021. http://vestlife-project.eu/

[14] Integration of CBRN Physical Protective Measures to Lessen the Burden on Personnel , STO Technical Report TR-HFM-199, June 2018

ID 44

ON THE MULTISCALE MODELLING OF THE IMPACT BEHAVIOUR OF WOVEN MATERIALS USING EQUIVALENT MICROSCOPIC FIBERS WITH 3D SHELL ELEMENTS

Tuan-Long Chu[1], Cuong Ha-Minh[2(*)], Abdellatif Imad[3], Quoc-Hoan Pham[4]

[1] Thuyloi University, Hanoi, Vietnam

[2] Université Paris-Saclay, CentraleSupélec, ENS Paris-Saclay, CNRS, LMPS - Laboratoire de Mécanique Paris-Saclay, 91190, Gif-sur-Yvette, France

[3] Université de Lille, ULR 7512-Unité de Mécanique de Lille-Joseph Boussinesq (UML), F-59000 Lille, France

[4] Faculty of Civil Engineering, Vietnam Maritime University, 484 Lach Tray Str., Haiphong city, Vietnam

[(*)] Email: cuong.ha-minh@ens-paris-saclay.fr

ABSTRACT

This work focuses on analyzing the ballistic impact behavior of woven fabric materials through the use of 3D shell elements instead of solid ones. This approach accurately captures micro-level impact mechanisms while significantly cutting computational time by reducing degrees of freedom. Microscopic yarns were represented with a simplified equivalent fiber concept to reduce their number of fibres from 400 to 42 for a computation gain. The proposed approach was validated quantitatively (force, projectile velocity) and qualitatively (fiber interactions, ruptures) in comparison with a verified mesoscopic model and experimental data. Results highlight the efficacy of 3D shell elements in describing micro mechanisms of the impact behaviour of woven materials.

INTRODUCTION

Numerical simulations are increasingly becoming important in the design and manufacturing industry of protective products in replacing expensive and time-consuming experiments and tests (Mourtzis et al., 2014). In this paper, to optimize the numerical prediction of the mechanical behavior of a 2D woven fabric submitted to ballistic impact, we present the approach using 3D shell elements for microscopic primary yarns in a micro-meso multiscale model instead of solid elements presented in the literature (Nilakantan, 2013; Yang et al., 2021). In particular, microscopic yarns were represented with a simplified equivalent fiber concept to reduce their number of fibres from 400 to 42 for a gain of computation time. Two impact configurations are chosen to show the performance of this approach in terms of predictions of important quantities as well as microscopic mechanisms:

- A crimped yarn submitted to a transversal impact
- A woven fabric submitted to a transversal impact

The material used is a 2D Kevlar KM2 fabric measuring 50.6x50.6 mm, with warp and weft densities of 13.4 yarns/cm, resulting in a distance of 1.49 mm between the yarns. The projectile is a steel sphere with a diameter of 5.35 mm and a mass of 6.25×10^{-4} kg. Based on tensile tests presented in our previous work (Ha-Minh et al., 2013), we assume that the fibres have a linearly transversely isotropic elastic behaviour until failure. In our case, the experimental value of the rupture strain for fibre is equal to ε_R = 4.58%, which is equivalent to a maximum rupture stress of σ_R = 3.88 GPa. The five elastic constants for a Kevlar KM2 fibre are measured: E_{11} of 84.62 GPa, $E_{11} = E_{33}$ of 1.34

GPa, G_{12} of 24.40 GPa, v_{13} of 0.60, v_{23} of 0.24 [8], where 1 is the longitudinal direction of the fibres, and 2, 3 are the transverse directions.

The validation of the approach is done by comparisons with the mesoscopic model presented in (23) and our experimental data.

RESULTS AND CONCLUSIONS

The results showed that the approach proposed with equivalent microscopic fibers using 3D shell elements effectively predicts the impact behaviour of a dry 2D fabric, considering essential microscopic fracture mechanisms in both impact configurations studied: on a crimped yarn and on an entire 2D fabric. Overall, the proposed approach exhibits similar behaviour to the mesoscopic model in terms of important quantities such as projectile velocity and force evolution (Fig. 1). However, the proposed approach is capable of capturing the microscopic phenomena at the fibre scale (Fig. 2b), which is not possible with the mesoscopic model (Fig. 2a).
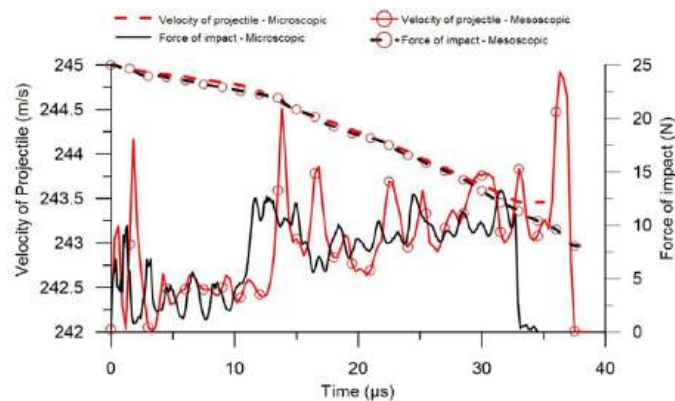
Fig. 1 Evolution of velocity and force in the impact case of a crimped yarn
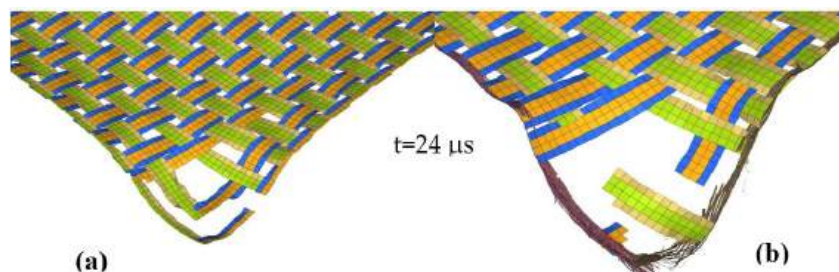
Fig. 2 Comparison of the damage state of the fabric at the impacted zone: Mesoscopic model (On the left); (b) Micro-meso multiscale model using 3D shell elements

In conclusion, 3D shell elements have also been demonstrated to be effective for the microscopic modelling of impact behaviour of 2D woven materials, compared to the solid elements often used in the literature. In the prospective future work, this approach will be studied for more complex cases such as 3D woven fabrics.

REFERENCES

[1] D. Mourtzis, M. Doukas, D. Bernidaki, "Simulation in Manufacturing: Review and Challenges", *Procedia CIRP*, 2014;25:213−29.

[2] G. Nilakantan, "Filament-level modeling of Kevlar KM2 yarns for ballistic impact studies", *Composite Structures*. 2013 Oct 1;104:1−13.

[3] Y. Yang, Y. Liu, S. Xue, X. Sun, "Multi-scale finite element modeling of ballistic impact onto woven fabric involving fiber bundles", *Composite Structures*, 2021 Jul;267:113856.

[4] C. Ha-Minh, A. Imad, T. Kanit, F. Boussu, "Numerical analysis of a ballistic impact on textile fabric", *International Journal of Mechanical Sciences*, 2013 Apr 1;69:32−9.

ID 45
ELECTROCHEMICAL IMPEDANCE SPECTROSCOPY OF DEBYE DIELECTRIC SPECTRA: A NUMERICAL COMPARISON

Roberto Dima[1(*)], Maria Antonia Maisto[1], Luigi Rubino[1], Raffaele Solimene[1]
[1] Department of Engineering, University of Campania, 81031 Aversa, Italy
(*) Email: roberto.dima@unicampania.it

ABSTRACT

Electrochemical Impedance Spectroscopy (EIS) is a powerful tool for investigating electrochemical phenomena. The deconvolution of the Distribution of Relaxation Times (DRT) is numerically solved by using the Method of Moments (MoM) and focusing on multiple-Debye processes. Different regularization methods will be shown and compared. In particular, we will show that, under specific conditions, the non-negative constraint regularizes the solution enough to make it stable and is comparable to $L1$ minimization.

INTRODUCTION

Electrochemical Impedance Spectroscopy (EIS) is a powerful tool to separate contributions of different electrochemical related to polarization losses, basic ion transport and kinetic parameters of electrochemical cells, electrolyzers and batteries [1], [2]. For example, EIS has been widely used to study Li-ion batteries and factors such as cell SoC, temperature and stateof-health have been shown to impact the spectra obtained [3].

There are two methods available for the analysis and interpretation of spectral data: complex nonlinear least squares fitting (CNLS) to an equivalent circuit (EqC) and the deconvolution of the Distribution of Relaxation Times (DRT).

The first method entails the resolution of a non-linear optimization and requires the *a priori* knowledge of the model, i.e. the EqC, whose choice is not straightforward.

An alternative way to describe a dielectric relaxation spectrum is in terms of an ensemble of Debye processes with a continuous relaxation time distribution: the DRT function. The impedance $Z(\omega)$ is related to its DRT $\gamma(\tau)$ by the equation

$$Z(\omega) = Z_\infty + \int_0^{+\infty} \frac{\gamma(\tau)}{1 + j\omega\tau} \, d\tau$$

This distribution in τ-domain can represent a wide variety of processes and emulate models of arbitrary complexity. Furthermore, it doesn't require a priori information about the system.

RESULTS AND CONCLUSION

Retrieving $\gamma(\tau)$ from data is an ill-posed problem since the above equation is a Fredholm integral equation of first kind. The inversion of the integral operator is in general not unique and does not depend continuously on data.

Numerous methods to analyze the spectrum via DRT have appeared in the literature [2], including ridge (or Tikhonov) regularization, preconditioned ridge regularization, lasso regularization, Fourier filtering and subsequent fitting, Monte Carlo methods, maximum entropy methods, and genetic programming.

In this paper the integral equation is numerically solved by using the Method of Moments (MoM) and focusing on multiple-Debye processes, our *prior* on the model.

Different regularization methods are presented and compared: $L2$ minimization, $L2$ minimization with smooth-

ness and non-negative constraints (such as in [4]), $L2$ minimization with non-negative constraint only, and $L1$ minimization. In our test case, a 3-Debye-pole spectrum is considered and only 10 log-spaced measurements are collected in the range [5mHz,**100**Hz]. Fig. 1 clearly shows that: the smoothness constraint is unnecessary because Debye processes are Dirac deltas in the transformed space; the $L2$ minimization with no constraints is unable to approximate the actual solution at all; at last, the $L2$ minimization with the non-negative constraint only is the best option because it is able to retrieve the correct sparse solution and requires less computational burden than the $L1$ minimization.
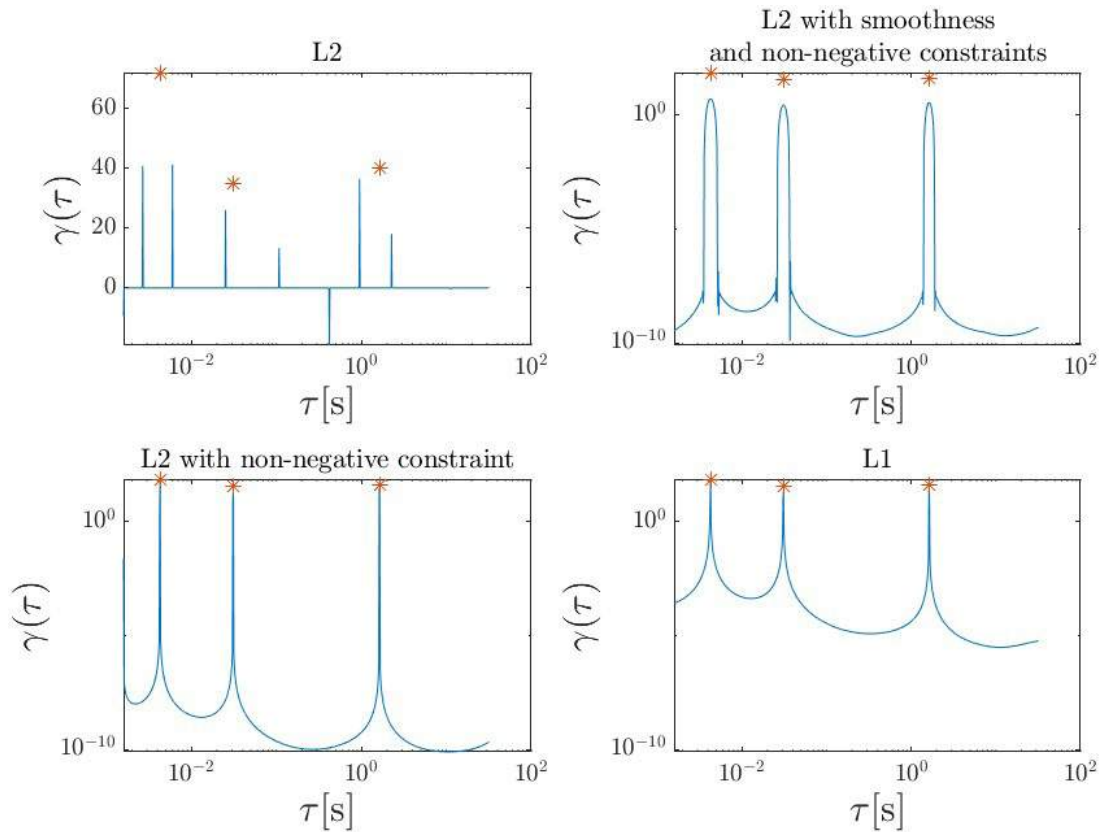
Fig. 1 Results of numerical simulations for comparison. Red asterisks show the position and magnitude of the actual Debye poles. Blue lines are the recontructed DRTs.

This study shows that the DRT distribution of Debye-only processes can be numerically retrieved with a few measurements solving a least square minimization with the non-negative constraint as a regularization term. The achieved results are comparable to those obtained through $L1$ minimization.

REFERENCES

[1] S. Wang, J. Zhang, O. Gharbi, V. Vivier, M. Gao, and M. E. Orazem, "Electrochemical impedance spectroscopy," *Nat Rev Methods Primers*, vol. 1, no. 1, p. 41, Jun. 2021, doi: 10.1038/s43586-021-00039-w.

[2] B. A. Boukamp, "Distribution (function) of relaxation times, successor to complex nonlinear least squares analysis of electrochemical impedance spectroscopy?," *J. Phys. Energy*, vol. 2, no. 4, p. 042001, Aug. 2020, doi: 10.1088/2515-7655/aba9e0.

[3] T. Paul, P. W. Chi, P. M. Wu, and M. K. Wu, "Computation of distribution of relaxation times by Tikhonov regularization for Li ion batteries: usage of L-curve method," *Sci Rep*, vol. 11, no. 1, Art. no. 1, Jun. 2021, doi: 10.1038/s41598-021-91871-3.

[4] A. Y. Zasetsky and R. Buchner, "Quasi-linear least squares and computer code for numerical evaluation of relaxation time distribution from broadband dielectric spectra," *J. Phys.: Condens. Matter*, vol. 23, no. 2, p. 025903, Dec. 2010, doi: 10.1088/09538984/23/2/025903

ID 46

POLY(LACTIC ACID) AS A PROMISING MATERIAL FOR SELF-HEALING FIBRE-REINFORCED COMPOSITES

Luísa Durão [1(*)], **Carlos Mota**[1], **Luís Nobre**[1], **João Bessa**[1], **Fernando Cunha**[1], **Raúl Fangueiro**[1,2]

[1] Fibrenamics, University of Minho, Guimarães, Portugal

[2] Center for Textile Science and Technology, University of Minho, Guimarães, Portugal

[(*)] Email: mariadurao@fibrenamics.com

ABSTRACT

The present work aims to develop a self-healing fibre-reinforced polymer composite, relevant for defense related applications, resorting to an approach grounded on the usage of thermoplastic particles incorporated into a thermosetting resin. To achieve such purpose, poly(lactic acid) (PLA) was chosen as the material responsible for the self-healing functionality and employed to a well-studied carbon fibre reinforced auxetic composite. Results record a healing efficiency of about 27 %, forecasting a future for PLA based selfhealing composites.

INTRODUCTION

In late years, the development of composite materials for defense applications has been of great interest, considering their outstanding mechanical and functional properties. Among those, auxetic materials stand out for their mechanical behavior that can translate into improved shear stiffness and fracture toughness and enhanced impact and indentation resistance (Veloso et al., 2023).

Nevertheless, during service life, these materials are prone to damage, such as fibre microdelamination or microcraking, as a result of exposure, not only to impact and/or mechanical and thermal loads, but also environmental factors, chemical abrasion, corrosion or photodegradation. If such microdamage grows and merges, ultimately catastrophic failure can occur, jeopardizing not only durability, but specially performance and security of the materials (Cioffi et al., 2022). It is on this context that self-healing composites emerge, as materials capable of autonomously and prematurely repair flaws, inspired by biomimetic. This can be achieved through multiple approaches, being one of them the incorporation of thermoplastic particles into thermosetting matrixes that can still be reinforced by other fibres (S. Islam et al., 2021). This simple principle is based on the melting of the thermoplastic, either induced directly by temperature or by alternative methods that promote localized melting, like incorporation of particles sensible to electricity or to infrared radiation. Subsequently, the melted polymer migrates into the flaw, where it establishes chemical bonds with the damaged surfaces. Hence, a good affinity between the filling thermoplastic and the thermosetting matrix is crucial, therefore poly(ethylene-co-methacrylic acid) has, until now, been preferably contemplated for this application (Nascimento et al., 2020), (Scheiner et al., 2016). However, alternatives should be considered, namely poly(lactic acid) (PLA) not only due to its widespread use, but specially because it is a biodegradable biopolymer, opening the door for the developed composites to meet environmental concerns. Its structure includes carboxyl and hydroxyl terminal groups that potentiate its chemical interaction with traditionally used epoxy-based thermosetting polymers (Revankar et al., 2022), namely through condensation between the cured resin hydroxyl groups and the PLA carboxyl ones or even by hydroxy/epoxy and carboxyl/epoxy interactions. These can contribute to a good affinity and consequently a promising interfacial adhesion between the 2 polymers, making PLA an interesting material to be investigated for self-healing composites.

When it comes to the operationalization of such self-healing composites' principle, up to date studies indicate that minor particle diameters, at least smaller than 500 μm, are preferable, so that the reinforcing fibre's arrangement

and consequently the material's mechanical properties are as less affected as possible. In contrast, in what regards the thermoplastic content, although some articles indicate that higher percentages, up to 20 wt%, provide more efficient healing processes, others put forward that smaller amounts, about 5 wt%, might lead to a better compromise between the self-healing and the mechanical properties of the composite (Nascimento et al., 2020), (Peñas-Caballero et al., 2023). For that reason, thermoplastic content stands outs as the critical variable when it comes to the composite's global performance.

RESULTS AND CONCLUSIONS

On this background, auxetic carbon fibre reinforced composites with the most promising fibre configuration, chosen based on previous work, were prepared, consisting of a SR8500 epoxy matrix reinforced with 16 layers of T300 carbon fibre alternately oriented in angles of 14 º and 64 º, in a symmetric configuration ($[14\,º, 64\,º)_n]_s$). PLA was then incorporated in contents between 5 wt% and 25 wt%, in intervals of 5 wt%, and a thermoplastic particle diameter smaller than 250 μm. Moreover, a control material, with no PLA integration was prepared, for comparison effects.

Mechanical testing was used to evaluate the healing performance of the developed composites. That way, materials were subjected to initial tests, until fracture occurred, and then heated to induce PLA melting and therefore the healing response. A study on the most adequate healing conditions was also performed by considering temperatures between 160 ºC and 200 ºC. After that, the composite was retested, under the same conditions. An average healing efficiency up to 27 % was calculated, based on the flexural strength. Within this scope, the present study indicates that PLA possesses potential as a self-healing material for carbon fibre reinforced composites employed to defense applications.

REFERENCES

[1] C. Veloso, C. Mota, F. Cunha, J. Sousa, R. Fangueiro, " A comprehensive review on inplane and through-the-thickness auxeticity in composite laminates for strutcural applications", *Journal of Composite Materials*, 2021, Vol. 57(26), 4215-4223;

[2] M. O. H. Cioffi, A. S. C. Bomfim, V. Ambrogi, S. G. Advani, "A review on self-healing polymers and polymer composites for structural applications", Polymer Composites, 2022, 43, 7643-7668;

[3] S. Islam, G. Bhat, "Progress and challenges in self-healing composite materials", *Materials Advances*, 2021, 2, 1896;

[4] A.A. Nascimento, F. Fernandez, F. S. Silva, E. P. C. Ferreira, J. D. D. Melo, A. P. C. Barbosa, *Composites Part A (*2020), 137, 106016;

[5] M. Sheiner, T. J. Dickens, O. Okoli, "Progress towards self-healing polymers for composite structural applications", *Polymer* (2016), Vol. 83, 260-282;

[6] S. Revankar, N. R. Banapurmath, A. M. Sajjan, V. Nimbagal, A. Y. R. Venkatesh, M. A. Umarfarooq, C. Vadlamudi, S. Krishnappa, "Epoxy-poly lactic acid blended composites reinforced with carbon fibres for engeneering applications", *Materials Express*, 2022, 12, 1502-1511;

[7] K. Chaudhay, B. Kandasubramanian, "Self-Healing Nanofibers for Engineering Applications", Industrial & Engineering Chemistry Research, 2022, 61 (11), 3789-3816;

[8] M. Peñas-Caballero, E. Chemello, A. M. Grande, M. H. Santana, R. Verdejo, M. A. Lopez Machado, "Poly(methyl methacrylate) as a Healing Agent for Carbon Fibre Reinforced Epoxy Composites", *Polymers*, 2023, 15, 1114.

ID 47
ANALYTICAL DESIGN OF AUXETIC COMPOSITE LAMINATES

Cristiano Veloso[1(*)], Carlos Mota[2], Luís Nobre[3], João Bessa[4], Fernando Cunha[5], Raúl Fangueiro[6]

[1, 2, 3, 4, 5, 6] Fibrenamics, University of Minho, Guimarães, Portugal

[6] Department of Textile Engineering, University of Minho, Guimarães, Portugal

[(*)] Email: cristianoveloso@fibrenamics.com

ABSTRACT

Auxetic composite laminates, i.e. laminates with NPR (Negative Poisson's Ratio), are regarded as a promising solution to combat LVI (Low-velocity impact) delamination within the realm of metamaterials. In order to maximize the auxetic effect, with the minimization of the Poisson's ratio, an analytical study is required, with respect to material properties and stacking sequences. This work focuses on the analysis of C/E (Carbon/epoxy) auxetic laminates and their respective auxetic domains for IP (In-plane) and TTT (Through-thethickness) configurations via an in-house developed MATLAB algorithm.

INTRODUCTION

Auxetic metamaterials exhibit a unique material behaviour due to their NPR, causing a synchronous orthogonal compression or dilation. This behaviour is at the source of various property enhancements, especially in the area of impact: a local material densification occurs under the impact zone, increasing resistance. For composite laminates, auxeticity can be designed with unidirectional laminae, under a two-dimensional framework: IP (In-plane) auxeticity refers to NPR on the face plane (*x-y*) of the laminate, while TTT (Through-thethickness) auxeticity implies NPR along the thickness plane (*x-z* or *y-z*) of the laminate. The advantages of the application of such laminates include a reduction in delamination propagation, and improved energy absorption in low-velocity events (Veloso et al., 2023).

The design of IP and TTT auxetic laminates hereby presented is based on the CLT (Classical Lamination Theory). A MATLAB algorithm was developed to analyse the micro and micromechanics domains of a laminate. The micromechanics section refers to the definition of nine independent elastic lamina constants (E_1, E_2, E_3, G_{12}, G_{13}, G_{23}, v_{12}, v_{13} and v_{23}, with *1-2-3* referring to the local lamina axis for longitudinal, transverse and thickness direction) using a formulation for effective properties estimated using Maxwell's methodology (Mccartney, 2017). Macromechanics – at the laminate level – make use of CLT, calculating E_x, E_y, G_{xy}, v_{xy} and v_{xz}, with material invariants and geometric factors relevant to the calculation of the extensional stiffness matrix of each laminate. Important to note that the *xz* and *yz* plane behaviours are similar regarding Poisson's ratio calculation, although they are phased out by the 45° direction. Hence, a larger focus, concerning the TTT planes, is given the to *xz* direction in this study.

For this work, the possible domain was restricted to C/E T300/8500 bidirectional symmetrical ($[(\theta_1 / \theta_2)_n]_S$) laminates, with a θ in the range of *[-90°/90°]* in 0.1° intervals, accounting for 3243601 iterations. A fiber volume fraction of 0.65 was employed. Important to note that the algorithm was validated against literature cases for similar codes (Donoghue et al., 2009; Harkati et al., 2009), showing good correlation.

RESULTS AND CONCLUSIONS

Figure 1 displays the IP and TTT NPR domains for C/E T300/8500 ($[(\theta_1 / \theta_2)_n]_S$) laminates. The IP NPR domain repeats in the first and third quadrants, i.e. a similar v_{xy} was estimated for ($[(\theta_1 / \theta_2)_n]_S$) and ($[(-\theta_1 / -\theta_2)_n]_S$) sequences. The two IP NPR areas in the first quadrant are symmetric by the θ ($\theta_1 = \theta_2$) direction, as ($[(\theta_1 / \theta_2)_n]_S$) and ($[(\theta_2 / \theta_1)_n]_S$) configurations yielded similar v_{xy}. The TTT *xz* NPR domain repeats in the second and fourth quadrants, with symmetry by the −θ direction.
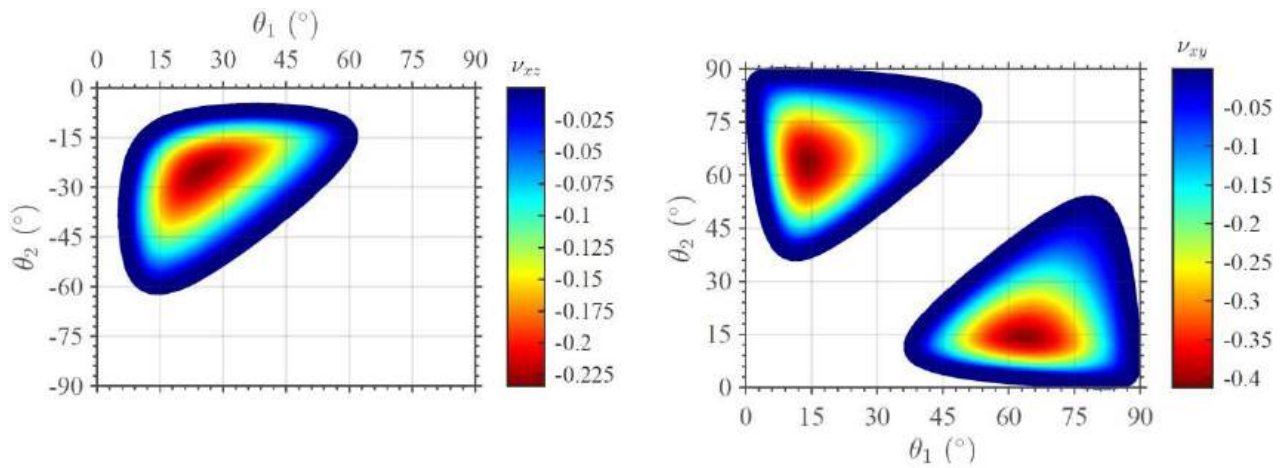
Fig. 1 NPR domain of C/E T300/8500 ($[(\theta_1/\theta_2)_n]_S$) laminates in the a) xy plane b) xz plane.

Table 1 shows the maximum NPR values obtained. Larger IP NPR values ($v_{xy, min}$ = - 0.412) were achieved when compared to TTT NPR Poisson's ratios ($v_{xy, min}$ = $v_{xy, min}$ = - 0.234). As previously alluded to, the TTT *xz* and *yz* behaviours are similar, albeit phased out regarding the stacking sequence orientations. Moreover, minimum v_{xy} configurations yielded maximum v_{xz} values, and an enhancement in the shear resistance of TTT NPR laminates was verified.

Table 1 Largest NPR yielding configurations for C/E T300/8500 laminates.

	v_{min}	($[(\theta_1/\theta_2)_n]_S$)	E_x (GPa)	E_y (GPa)	G_{xy} (GPa)
v_{xy}	-0.412	($[(14.0°/63.6°)_n]_S$)	46.1	22.7	5.69
v_{xz}	-0.234	($[(-24.8°/24.7°)_n]_S$)	68.7	8.45	24.2
v_{xz}	-0.234	($[(-65.3°/65.2°)_n]_S$)	8.45	68.7	24.2

This study revealed, thus, the preponderance of the analytical design of auxetic laminates, as it affects not only the Poisson's ratio value, but also the shear and elastic moduli, which will in turn deeply affect the laminate's behaviour during an impact event.

REFERENCES

[1] Veloso, C., Mota, C., Cunha, F., Sousa, J., & Fangueiro, R. (2023). A comprehensive review on in-plane and through-the-thickness auxeticity in composite laminates for structural applications. *Journal of Composite Materials.*

[2] Mccartney, L. (2017). Predicting Properties of Undamaged and Damaged Carbon Fibre Reinforced Composites. In *The Structural Integrity of Carbon Fiber Composites: Fifty Years of Progress and Achievement of the Science, Development, and Applications* (pp. 425–467).

[3] Donoghue, J., Alderson, K., & Evans, K. (2009). The fracture toughness of composite laminates with a negative Poisson's ratio. *Physica Status Solidi (b)*, *246*, 2011–2017.

[4] Harkati, H., Bezazi, A., Wahid, B., & Scarpa, F. (2009). Influence of carbon fibre on the through-the-thickness NPR behaviour of composite laminates. *Physica Status Solidi (b)*, 2111–2117.

ID 48

EXPERIMENTAL AND NUMERICAL ANALYSIS OF STAINLESS-STEEL AND UHMWPE FML PLATES UNDER BALLISTIC IMPACT

Valverde Marcos, Borja[1][(*)], **Rubio Díaz, Ignacio**[1], **Wang, Liu-Jiao**[2], **Santiuste Romero, Carlos**[2] , **Miguélez Garrido, M.Henar**[2], **Loya Lorenzo, José Antonio**[2,3]

[1] Department of Mechanical Engineering, Universidad Carlos III de Madrid, Madrid, Spain Madrid, Spain.

[2] Department of Continuous Mechanics and Structural Analysis, Universidad Carlos III de Madrid, Leganés, Madrid, Spain.

[3] University Center of Guardia Civil, Aranjuez, Madrid, España

[(*)] Email: jloya@ing.uc3m.es

ABSTRACT

This study introduces an experimental and numerical approach to assess the mechanical response of Fiber Metal Laminates (FML) comprised of layers of stainless steel and Ultra High Molecular Weight Polyethylene (UHMWPE) subjected to ballistic impact. Constitutive models for the constituent materials were formulated and integrated into a commercial Finite Element Method (FEM) code. The resulting model accurately anticipates the ballistic limit, trauma, and damage propagation in FML plates with varying layer configurations.

INTRODUCTION

he utilization of advanced materials, such as metals and composites in the formation of Fiber Metal Laminates (FML), has the potential to yield more efficient and lighter solutions compared to monolithic armors. The synergy of their properties not only provides high energy absorption capacity but also ensures appropriate structural resistance (Sadighi et al., 2012).

The integrated methodology employed, encompassing manufacturing, empirical data, and numerical analysis, facilitates the development of calibrated numerical models. These models prove capable of predicting the ballistic behavior of FML plates with varying numbers of layers.

By combining stainless-steel (X5CrNi18-10) layers with a thickness of 0.3 mm and HMPE layers (Dyneema HB80), Fiber Metal Laminate (FML) sequences were manufactured with a nominal thickness of 2 mm. This process involved a combination of pressure and temperature, utilizing a servohydraulic universal testing machine (SERVOSIS 100Tm). To ensure proper interaction between the steel and Dyneema, as well as effective interface strength, the surfaces were chemically treated.

An experimental ballistic impact campaign employing 7.5 mm tempered steel spheres is conducted using a Sabre ballistic gas-gun. Projectile velocity during impact is measured using a Photron Ultima SZ1 fastcam, allowing the derivation of the ballistic curve for each considered thickness (Rodríguez-Millan et al., 2016). The ballistic limit and energy absorption are determined for Fiber Metal Laminate (FML) coupons. Furthermore, the analysis extends to back-face deformation, petalling, and damage propagation in terms of delamination at the metal-composite interfaces, matrix, and fiber cracks.Numerical modeling is executed in the ABAQUS/Explicit commercial Finite Element Method (FEM) code. Constitutive models have been individually developed for both materials, utilizing a VUMAT Fortran subroutine for the composite. The foundational mechanical properties are extracted from own tests and scientific literature. Models for both stacking sequences are formulated, incorporating cohesive interfaces be-

tween distinct materials. The numerical predictions of Fiber Metal Laminate (FML) plates under impact conditions are then juxtaposed with the corresponding experimental results.
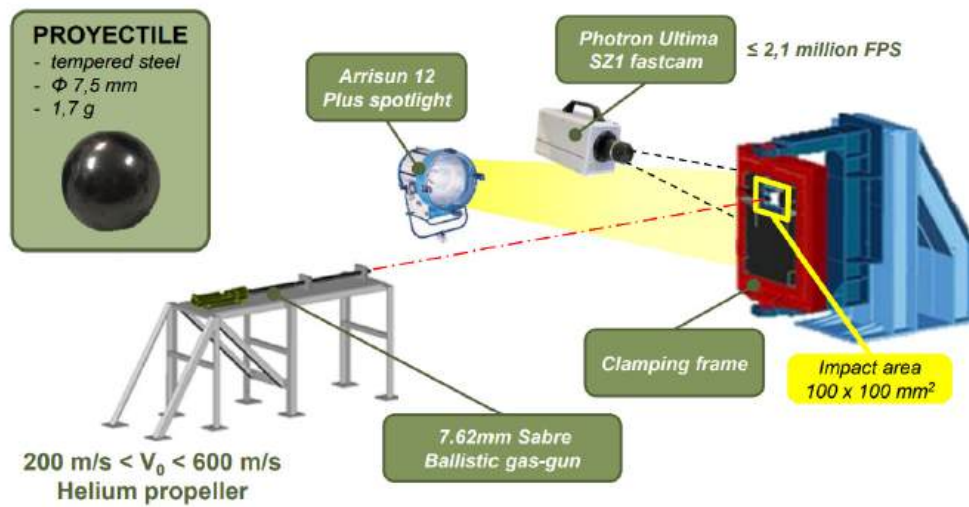
Fig. 1a) Shooting and recording set. b) Penetration-time evolution(.22 LR bullets).

RESULTS AND CONCLUSIONS

Both experimental and numerical ballistic curves exhibit a high degree of agreement within the tested velocity range, with the ballistic limit reaching approximately 300 m/s. Regarding back-face deformation (see Fig. 2, for example), the model shows a qualitatively accurate prediction.
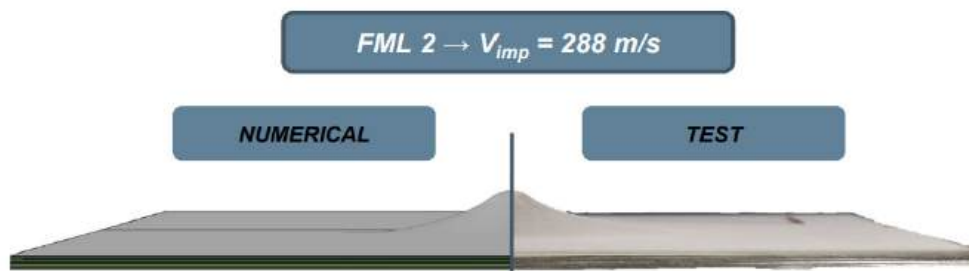
Fig.2 Back-face deformation for FML1 at 280 m/s. Left: Numerical. Right: Experimental.

Relative to other interesting parameters, as perforation with the staking sequence, petalling, or damage extension, the FML numerical model achieved leads to prediction that agree with experimental tests performed on the manufactured plates.

ACKNOWLEDGMENTS

REFERENCES

[1] Sadighi, M., Alderliesten, R.C., Benedictus, R. (2012). Impact resistance of fiber-metal laminates: a review. International Journal of Impact Engineering, , 49, 77-90

[2] Rodríguez-Millan, M., Ito, T., Loya, J.A., Olmedo, A., Miguelez, M.H. (2016). Development of numerical model for ballistic resistance evaluation of combat helmet and experimental validation, Materials & Design, 110, 391-403.

ID 51
HIGH TEMPERATURE REGULATION OF IMPROVED FLEXIBLE COMPOSITES FOR SATALLITE IMPACT SHIELDS

Daniel Barros[1](*), Carlos Mota[2], Luís Nobre[3] João Bessa[4], Fernando Cunha[5] and Raul Fangueiro[6]

[1, 2, 3, 4, 5, 6] Fibrenamics, University of Minho, Guimarães, Portugal

[6] Department of Textile Engineering, University of Minho, Guimarães, Portugal

(*) Email: danielbarros@fibrenamics.com

ABSTRACT

In order to protect the satellite against hypervelocity impacts (HVI), extant impact shields have been constructed from metal plates featuring a rear back bumper composed of aramid/Nextel® fibers, chosen for their commendable impact resistance and elevated thermal endurance. However, emerging materials such as Ultra-High Molecular Weight Polyethylene (UHMWPE), exhibiting superior impact resistance, stance an excellent alternative to improve the HVI impacts, but due to its low working temperatures, it begins to lose properties when subjected to temperatures above 125ºC. Consequently, this study aims to investigate the possibility of developing systems capable to control and reduce the high temperatures to which satellites are exposed in spatial environment, that can reach 150ºC. The investigation contemplates the prospect of fabricating solutions using UHMWPE fibers with addition of Phase Change Materials (PCMs) to absorb the excess heating and maintain an equilibrium with the uppermost temperature range.

It was developed an array of configurations by incorporating of 20, 40, 60wt% of PCMs into the flexible matrix by mechanical mixing. The objective was to verify the efficiency of PCNs in reducing the average temperature on the surfaces and interior of the composite using thermocouples and verify if its phase transition they absorb enough heat so that the panel does not reach temperatures exceeding 125ºC during working time.

INTRODUCTION

As human endeavors in space exploration intensify, the proliferation of satellites and spacecraft deployed into orbits has concurrently risen. Over decades, the accumulation of space garbage in Earth's orbit is increasing, compounding the risk of collisions with satellites and spacecraft due to the concurrent presence of pre-existing meteoric fragments. The space debris, capable of achieving hyper-velocities exceeding 10 km/s, corresponding to high amount of kinetic energy which features a significant threat to the structural integrity and functionality of space assets (Wen, Chen, & Lu, 2021). The frequency of such collisions necessitates intensive research and development efforts towards the creation of shielding systems and mechanism capable of mitigation the associated hypervelocity impact challenges. One innovative approach is the exploration and refinement of new/novel Stuffed Whipple shield systems (Olivieri & Giacomuzzo, 2022).

Comprising two aluminum alloy plates separated by a back bumper typically crafted from fibrous materials, these shield systems have traditional incorporated thermal-resistance solutions using aramid and ceramic fibers (Nextel® and basalt) to address both impact resistance and the dynamic thermal environment of space (raging maximum temperatures of 150ºC). Recent investigations highlight the efficacy of UHMWPE as a promising material for configurations aimed at countering HVIs (Xu, Yu, & Cui, 2023). Nevertheless, UHMWPE's operational limitations, characterized by a maximum working temperature of 125ºC, impede its use under conditions exposing it to 150ºC. This way, to use UHMWPE for satellite protection, the imperative lies in controlling and narrowing the thermal variation experienced by this shielding solution.

In satellite orbits, temperature control is vital. Insulation materials counter extreme fluctuations. Satellites when exposed to sunlight can reaches 150ºC, and the heart shadow can drop to -150ºC. Phase Change Materials (PCMs) excel in absorbing/releasing thermal energy, enhancing management (Khan, Asfand, & Al-Ghamdi, 2023). To mitigate high temperatures to which satellites are subject, insulating materials such as polymers and ceramics are used, and in the most extreme cases, active cooling systems are used such as cryogenic coolers (Espacial, 2023). Finally, recent studies, shows that having flexible bumpers solutions present better absorption capacity comparing to the convention harder laminates used in ballistic application (Kumar & Kim, 2023).

RESULTS AND CONCLUSIONS

This study focuses on flexible composite developement using UHMWPE (from dyneema®) and aramid fibers (from Dyneema® and CastroComposites) with PCMs (from PCM Products or Rubitherm), incorporated into the flexible matrix such silicone rubber or polyurethane (from Elit, Easycomposite or Vsure). The selected PCMs presents melting temperature around 110 to 120ºC, temperatures that temperatures that were initially evaluated by the Differential Scanning Calorimetry (DSC) technique. These PCMs were added to the flexible matrix by mechanical mixing in 20, 40 and 60wt%.

Produced the sample, they were thermal characterized by subjecting to 150ºC using a heating stove and a hot compression molding. According to (Moulahi, Trigui, & Boudaya, 2016), it was also tested the PCM performance considering The Transient Guarded Hot Plate Technique (TGHPT), were the temperatures of the solution were measured inside of a hot compression molding. These tests show the capacity of PCMs thermal energy absorption as a good opportunity to mitigate the high temperatures a satellite can be subjected to.

It is expected that with the addition of PCMs, when the panel is subjected to sunlight, it will not reach the possible temperature of 150ºC, as it has PCMs in its structure that will absorb part of this heat, ending up not being transferred to the UHMWPE fibers.

REFERENCES

[1] Espacial, N. E. (2023, 10 23). *Sistemas de Controle Térmico em Satélites: Componentes e Suas Funções*. Retrieved from Nova Economia Espacial: https://newspaceeconomy.ca/2023/10/23/thermal-control-systems-in-satellites-components-and-their-functions/

[2] Khan, M., Asfand, F., & Al-Ghamdi, S. (2023). Progress in research and develpment of phase change materials for thermal energy storage in concentrated solpar power . *Applied Thermal Engineering, 219*.

[3] Kumar , S., & Kim, Y. (2023). Hybrid interspaced and free-boundary aramid fabric back bumper for hypervelocity impact shielding system. *Internation Journal of Impact Engineering, 171*.

[4] Moulahi, C., Trigui, A., & Boudaya, C. (2016). Smart macroencapsulated resin/wax composite for energy conservation in the built environment: Thermophysical and numerical investigations . *Journal of thermplastic composite materials* , 1-28.

[5] Olivieri, L., & Giacomuzzo, C. (2022). Experimental fragments distributions for thin aluminium plates subjected to hypervelocity impacts. *Internation Journal of Impact Engineering*.

[6] Tian, M., Hao, Y., & Qu, L. (2019). Enhanced electrothermal efficiency of flexible graphene fabric Joule heaters with the aid of graphene oxide. *Materials Letters, 234*, 101-104.

[7] Wen, K., Chen, X.-W., & Lu, Y.-g. (2021). Research and development on hypervelocity impact protection using Whipple shield: An overview. *Defence Technology*, 1864-1886.

[8] Xu, H., Yu, D., & Cui, J. (2023). The Hypervelocity Impact Behavior and Energy Absorption Evaluation of Fabric. *polymers, 15*.

ID 52

COMPARISON OF MECHANICAL BEHAVIOR AGAINST LOW AND HIGH VELOCITY IMPACT ON ARAMID AND UHMWPE PLATES

Valverde Marcos, Borja[1](*), Rubio Díaz, Ignacio[1], Wang, Liu-Jiao[2], Santiuste Romero, Carlos[2] , Miguélez Garrido, M.Henar[2], Loya Lorenzo, José Antonio[2]

[1] Dept of Mechanical Engineering,Universidad Carlos III de Madrid, Madrid, Spain Madrid, Spain.

[2] Dept. of Continuous Mechanics and Structural Analysis, Universidad Carlos III de Madrid, Leganés, Madrid, Spain.

ABSTRACT

This work compares the response of aramid and UHMWPE fibers to low and high velocity impact events, using Kevlar® as aramid fiber (K-129) and two types of Dyneema® as UHMWPE samples (HB-31 and HB-210). Drop-weight tower and gas gun tests are performed in fiber plates manufactured using the high strength fibers. Dyneema samples shown better impact response in terms of maximun force and ballistic limit, and Kevlar plates shown higher values of maximun force in drop-weight tests and less permanent trauma in front and back face of the plate in low and high velocity tests.

INTRODUCTION

High-performance lightweight personal protection systems is a work field constantly evolving whose main target is the combination of low weight and comfort in the protection with a high resistance to different load solicitations which may be exposed during its life in service, such as ballistic impacts [1]. Ultra-high molecular-weight polyethylene (UHMWPE) and aramid fibers are characterized by their high tensile strength, low density and degradation resistance, making them one of the most suitable fiber-reinforced composites for use in personal ballistic protection [2].

Different test methods have been used to characterize aramid and UHMWPE fibers at different strain rates and impact energies: drop tower and ballistics tests [3]. These two methodologies provide information on the impact strength and damage suffered by the fiber plates (strain trauma, perforation mechanism and delaminated area).

RESULTS AND CONCLUSIONS

The low velocity impact tests were conducted using a INSTRON-CEAST Fractovis 9350 DropWeight Tower. Samples were prepared in 150x100 mm^2 format with 7,5 mm thickness and compared to impact tests up to 100 J. The results shown that, at the same impact energy, aramid plates supported higher peak-force than the UHMWPE ones. Furthermore, comparing the two Dyneema types, HB-210 samples supported also higher peak-force than HB-31. Similar behavior were observed in terms of absorved energy and saturation energy. In all samples tested, only impactor indentation and delamination damage were observed, with no fiber cracks or penetration detected, as is shown in Fig. 1., where HB-31 plates were the most damaged.
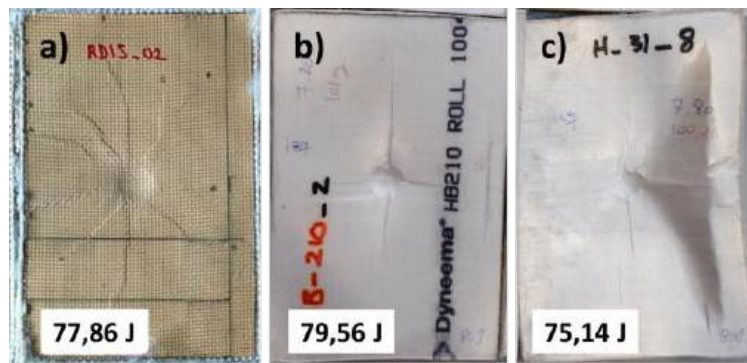
Fig. 1 Impactor indentation damage at 80J nominal impact energy in drop-weight testsf a) K-129 b) HB210 c) HB-31.

For high velocity impact tests, 150x150 mm^2 plates with two different thickness were manufactured (3.5 mm and 7.5 mm). The samples were impacted in a gas cannon with 7.5 mm caliber hardened steel spherical projectiles [4]. The results obtained showed that, for the same impact velocity, Dyneema had better ballistic properties than the Kevlar plates for both different thicknesses. However, the back face trauma obtained was almost 30% lower in the aramid samples in all cases. And also, the HB-31 deformation was higher than the obtained in HB-210 plates. The plates were completed damaged, penetrated and delaminated.
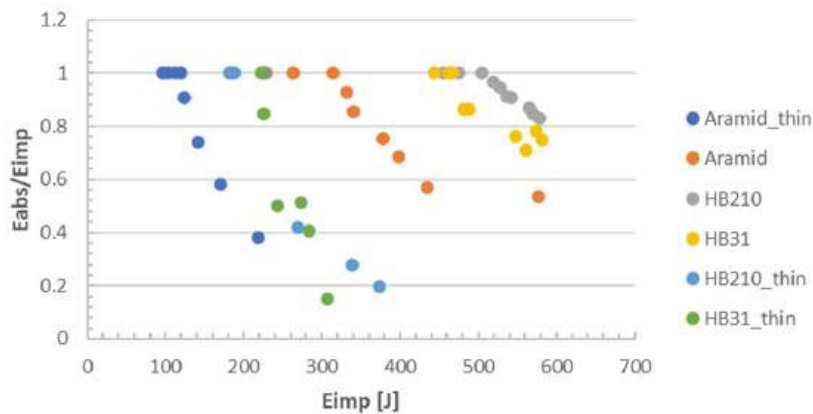
Fig. 2 Absorber energy versus impact energy in ballistic tests.

ACKNOWLEDGMENTS

REFERENCES

[1] M. K. Hazzard, R. S. Trask, U. Heisserer, M. Van Der Kamp, S. R. Hallett, "Finite element modelling of Dyneema® composites: from quasi-static rates to ballistic impact," *Composites Part A: Applied Science and Manufacturing*, vol. 115, pp 31–45, 2018.

[2] I. Rubio, M. Rodríguez-Millán, A. Rusinek, M. H. Miguélez, J. A. Loya, "Energy absorption analysis of aramid composite during blunt projectile impact," *Mechanics of Advanced Materials and Structures*, vol. 29:27, pp 5726–5737, 2022.

[3] M.M. Moure, I. Rubio, J. Aranda-Ruiz, J.A. Loya, M. Rodríguez-Millán, "Analysis of impact energy absorption by lightweight aramid structures," *Composite Structures*, vol. 203, pp 917– 926, 2018.

[4] I. Rubio, M. Rodríguez-Millan, M. Marco, A. Olmedo, J.A. Loya, "Ballistic performance of aramid composite combat helmet for protection against small projectiles," *Composite Structures*,vol. 226, pp 111-153, 2019

ID 54
RECENT DEVELOPMENTS OF AUXETIC KNITTED FABRICS AND THEIR POTENTIAL APPLICATIONS

Hoa Nguyễn[1], Raul Fangueiro[2], Fernando Ferreira[3], and Quyền Nguyễn[4(*)]

[1,2,3,4] 2C2T-Centro de Ciência e Tecnologia Têxtil, Universidade do Minho, Guimarães, Portugal

[(*)] Email: quyen@2c2t.uminho.pt

ABSTRACT

Knitting technology has become increasingly versatile and is now utilized in many areas due to its various advantages, such as high structural variability, materials adaptability, and productivity. Knitted fabrics with a negative Poisson ratio have immense potential in both the apparel and industrial sectors. This article provides an overview of the auxetic principles and their recent developments in knitted structures, which have auxetic effects created from conventional fibres and yarns. It also highlights their potential applications.

INTRODUCTION

Poisson's ratio is one of the essential mechanical properties of materials. It measures the deformation in the material in a direction perpendicular to the direction of the applied force (Lim, 2015). Most materials exhibit a positive Poisson's ratio; they laterally shrink when stretched or expand when compressed. Unlike conventional, auxetic materials exhibit a negative Poisson's ratio (NPR), which laterally expands when stretched and laterally contracts when compressed (Boakye et al., 2019; Wang & Hu, 2014). The auxetic textile has been produced based on two approaches: utilize auxetic fibres to produce an auxetic textile structure or make use of conventional fibres to produce an auxetic textile structure (Darja et al., 2014). Research works on textile materials with NPR, including auxetic fibres, auxetic yarns, and auxetic fabrics (Darja et al., 2014; Hu et al., 2019). Auxetic fabrics have been produced based on woven structures (Zulifqar, 2019), knitted structures (Alderson et al., 2012; Glazzard & Breedon, 2014; Knittel et al., 2015; Luan, West, Denhartog, & McCord, 2019; Osman & Mohmmed, 2020; Sun, Miao, Raji, & Ma, 2018; Wang & Hu, 2017; Yuping, Liu, Shuaiquan, & Hong, 2021), nonwoven structures (Rawal et al., 2019; Verma et al., 2020), and braided structures (Magalhaes et al., 2016; Subramani et al., 2014). This review emphasises auxetic knitted structures and mechanisms, including weft-knitted auxetic structures and warp-knitted auxetic structures, and the potential applications of auxetic knitted structures.

RESULTS AND CONCLUSIONS

The auxetic knitted fabric has been researched and manufactured with various materials (including conventional and high-performance fibres) and various auxetic structures (including foldable, rotating, re-entrant structures, and so on). Auxetic materials can be used as medical textiles. Auxetic fabrics can be used in protective clothing and equipment because of their excellent energy absorption properties and shape fitting. Although many application potentials were proposed in this paper, their practical applications are very few due to limited NPR.

REFERENCES

[1] Alderson, K., Alderson, A., Anand, S., Simkins, V., Nazare, S., & Ravirala, N. J. p. s. s. (2012). Auxetic warp knit textile structures. *249*(7), 1322-1329.

[2] Boakye, A., Ma, P., Raji, K., & Yuping, C. (2019). A Review on Auxetic Textile Structures, Their Mechanism and Properties. *Journal of Textile Science & Fashion Technology, 2*. doi:10.33552/JTSFT.2019.02.000526

[3] Darja, R., Tatjana, R., & Alenka, P.-Č. J. A. C. S. (2014). Auxetic textiles. *60*(4), 715-723.

[4] Glazzard, M., & Breedon, P. (2014). Weft-knitted auxetic textile design. *physica status solidi (b), 2.* doi:10.1002/pssb.201384240

[5] Hu, H., Zhang, M., & Liu, Y. (2019). *Auxetic textiles* (1 ed.). Elsevier Ltd.: Woodhead Publishing.

[6] Knittel, C. E., Nicholas, D. S., Street, R. M., Schauer, C. L., & Dion, G. J. F. (2015). Self-folding textiles through manipulation of knit stitch architecture. *3*(4), 575-587.

[7] Lim, T. C. (2015). *Auxetic materials and structures* (Vol. 2779). Singapore: Springer.

[8] Luan, K., West, A., Denhartog, E., & McCord, M. (2019). Auxetic deformation of the weft-knitted Miura-ori fold. *Textile Research Journal, 90*, 004051751987746. doi:10.1177/0040517519877468

[9] Magalhaes, R., Pichandi, S., Lisner, T., Rana, S., Ghiassi, B., Fangueiro, R., . . . Lourenco, P. (2016). Development, Characterization and Analysis of Auxetic Structures from Braided Composites and Study the Influence of Material and Structural Parameters. *Composites Part A Applied Science and Manufacturing, 87*, 86-97. doi:10.1016/j.compositesa.2016.04.020

[10] Osman, N., & Mohmmed, R. (2020). Negative Poisson's Ratio Based on Weft knitted Fabric with Different Loop Length. *International Journal of Engineering and Information Systems (IJEAIS), 4*(4), 21-26.

[11] Rawal, A., Sharma, S., Kumar, V., Rao, P. K., Saraswat, H., Jangir, N. K., . . . Dauner, M. J. M. o. M. (2019). Micro-mechanical analysis of nonwoven materials with tunable out-of-plane auxetic behavior. *129*, 236-245.

[12] Subramani, P., Rana, S., Oliveira, D. V., Fangueiro, R., Xavier, J. J. M., & Design. (2014). Development of novel auxetic structures based on braided composites. *61*, 286-295.

[13] Sun, W., Miao, X., Raji, K., & Ma, P. (2018). Three-Dimensional Deformation of Warp-Knitted Spacer Fabrics Under Tensile Loading. Autex Research Journal, 19. doi:10.1515/aut-2018-0050

[14] Verma, P., Smith, C. L., Griffin, A. C., & Shofner, M. L. J. E. R. E. (2020). Wool nonwovens as candidates for commodity auxetic materials. *2*(4), 045034.

[15] Wang, Z., & Hu, H. (2014). Auxetic Materials and Their Potential Applications in Textiles. *Textile Research Journal, 84*(15). doi:10.1177/0040517512449051

[16] Wang, Z., & Hu, H. (2017). Tensile and forming properties of auxetic warp-knitted spacer fabrics. Textile Research Journal, 87(16), 1925-1937. doi:https://doi.org/10.1177/0040517516660889

[17] Yuping, C., Liu, Y., Shuaiquan, Z., & Hong, H. J. T. R. J. (2021). Design and manufacture of three-dimensional auxetic warp-knitted spacer fabrics based on re-entrant and rotating geometries. 00405175211037204.

[18] Zulifqar, A. (2019). Study of auxetic woven fabrics.

ID 55
NUMERICAL STUDY OF VERTICAL BARRIERS AGAINST ACCIDENTAL BLASTS CAUSED BY FAILURE OF SAFETY MEASURES

Abraham Fernández del Rey[1](*), Josué Aranda Ruiz[1], José A. Loya Lorenzo [1,2]

[1]Department of Continuous Mechanics and Structural Analysis, Universidad Carlos III de Madrid, Leganés, Madrid, Spain.

[2]University Center of Guardia Civil, Aranjuez, Madrid, Spain

(*)Email: abfernan@ing.uc3m.es;

ABSTRACT

The increased use of renewable energy has highlighted the importance of hydrogen as an energy carrier, supported by initiatives such as the European Horizon 2020 programmes. However, there are risks associated with large-scale hydrogen storage, which are being minimised through investment in safety. Given the possibility of accidental leakage or even explosions, the need for protective measures in hydrogen storage areas is emphasised. In this context, vertical barriers are essential to mitigate the shock wave. The study proposes a numerical analysis of different arrangements of these barriers and provides design recommendations. It advocates the inclusion of these measures in the currently undeveloped hydrogen use regulations.

INTRODUCTION

The increasing use of renewable energies has driven the development of energy vectors supported by national and international administrations. Among the technological solutions, hydrogen has emerged as one of the most favoured, as evidenced by initiatives such as the European Horizon 2020 programmes and the Hydrogen Roadmap. The use of hydrogen brings with it the need to address the issue of its storage, which, in large quantities, can pose a significant risk. Therefore, one of the main objectives is to minimise this risk by investing heavily in safety, with a particular focus on the prevention of undesirable events. In this context, a model known as the Cumulative Effect Model [1] has been developed to assess the causality of accidents. According to this approach, most accidents can be attributed to organizational and supervisory factors, preconditions and specific actions.

Since accidents can leak through containment measures [2], it is essential to understand and implement measures to protect the environment around hydrogen storage sites in order to protect people and property.

In this context, vertical barriers play a crucial role as the last element of defense against the shock wave generated by deflagration or detonation in hydrogen storage.

In this study, the authors perform a numerical analysis of the characteristics of various vertical barrier arrangements. From this analysis, they derive design recommendations and propose the inclusion of barriers with these characteristics as part of hydrogen use regulations, which have not yet been developed.

RESULTS AND CONCLUSIONS

For the purpose of this study, the authors have adopted a parametric approach by solving different configurations of materials and geometric dimensions of vertical barriers. On one hand, different explosive charges have been taking into account by varying critical parameters such as equivalent charge and distance, among others. On the other hand, in order to study the behaviour of the vertical barrier during detonations and hydrogen deflagrations,

the models representing this barrier were parameterized. Overall, after combining the variations in charge and barrier geometry with own and published material properties, the residual resistance and protective capacity of the developed models were analysed.

In conclusion, and by comparing the results obtained with experimental results published in the literature, it is possible to make a series of recommendations for the design of vertical barriers to ensure their effectiveness in protecting both people and equipment in the environment of hydrogen storage tanks.
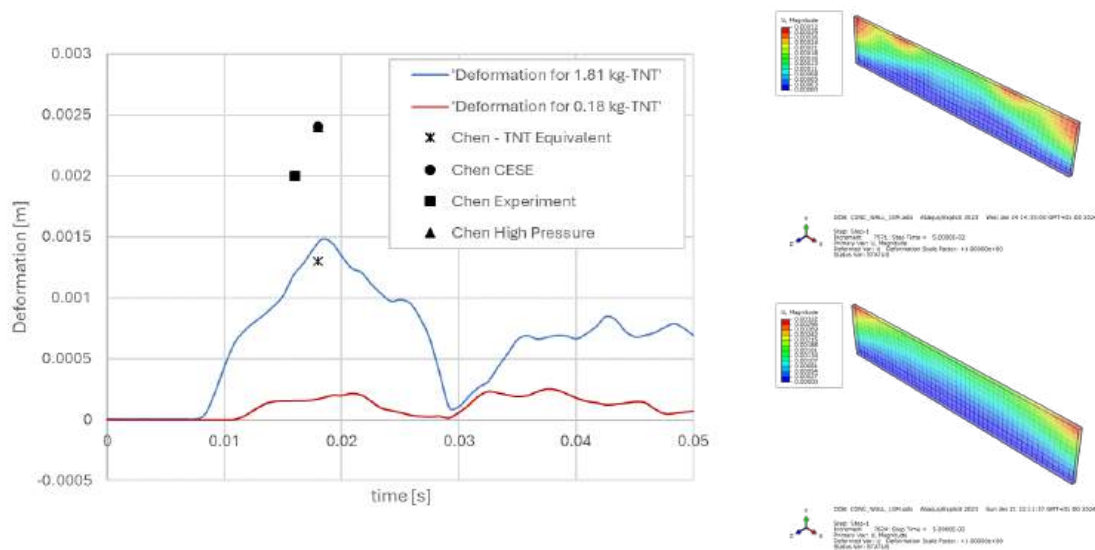
Fig. 2 Vertical barrier deformation history chart (left) and deformation (right) for a TNT equivalent mass of 0.18 kg-TNT (Up) and 1.81 kg-TNT (Down).

ACKNOWLEDGMENTS

REFERENCES

[1] Reason, James (18 de marzo de 2000). «Human error: models and management». British Medical Journal 320 (7237): 768-770. PMC 1117770. PMID 10720363. doi:10.1136/bmj.320.7237.768

[2] Chen, Di / Wu, Chengqing / Li, Jun. Assessment of modeling methods for predicting load resulting from hydrogen-air detonation 2023-12 Process Safety and Environmental Protection , Vol. 180 Elsevier BV p. 752-765

ID 56

STUDY OF THE MECHANICAL PERFORMANCE OF ALUMINUM 5083-H111 FOR A WIDE RANGE OF TEMPERATURES AND LOADING RATES

Afonso Gregório[1(*)], **Leigh Sutherland**[2], **Tiago Silva**[3], **Abílio de Jesus**[3], **Pedro Rosa**[1]

[1]IDMEC, Instituto Superior Técnico, Universidade de Lisboa, Lisboa, Portugal

[2]CENTEC, Instituto Superior Técnico, Universidade de Lisboa, Lisboa, Portugal

[3]INEGI, Faculdade de Engenharia, Universidade do Porto, Porto, Portugal

[(*)] Email: afonsogregorio@tecnico.ulisboa.pt

ABSTRACT

In this paper, the mechanical response of the aluminum alloy AA5083-H111 was assessed in conditions analogous to those found in military applications. Thermal sensitivity was evaluated from -70ºC to 100ºC and loading rate sensitivity was evaluated in order to account for the material energy absorption capabilities. These conditions ranged from quasi-static deformation to severe impact (strain-rates up to $2000s^{-1}$). Experiments were carried out to very high strains (over 1) by means of uniaxial compression tests conducted on a custom split-Hopkinson pressure bar (SHPB). Results show that AA5083-H111 maintains its mechanical strength almost entirely over the tested range of temperatures for quasi-static deformation. They also show that its performance under impact is not compromised at lower temperatures, from -70ºC to 25ºC, but is hindered when operating temperatures exceed 50ºC.

INTRODUCTION

Since production of aluminium has become commercially viable, one of the sectors that have registered bigger growth on aluminium alloys utilization was the military industry. This sector comprises not only the nowadays on-demand applications such as in automotive, aerospace and shipbuilding industries, but also applications in body armour and artillery. Aluminium alloys are desirable for their low density and higher ratio between mechanical strength and weight when compared to steel. They also present good machinability and formability thus allowing scalable production at low manufacturing costs [1]. In concern to military applications, studies have also shown that aluminium alloys can be effectively used in defensive structures, allowing for over 25% reduction in weight when compared to steel [2]. Finite element (FE) modelling is probably the best option to estimate energy absorption of complex structures (e.g. armoured vehicles, ship hulls, artillery launchers) [3]. In literature, although most of the authors advocate the need for proper calibration of the input data for FE simulation, the published research often considers material as homogeneous and isotropic with elasto-rigid plastic deformation since information on the materials thermo-viscoplasticity is scarce, particularly for high strains. These considerations are not representative of most real-life scenarios and may represent a major drawback for the reliability of numerical estimates. To evaluate how these alloys perform under impact, in harsh environments, a study was conducted on AA5083-H111, under conditions similar to those found in military applications. The selection of this alloy owing to its resistance to corrosion by seawater and adverse atmospheres, its ability to retain exceptional strength after welding, and for having the highest mechanical strength of the non-heat treatable alloys.

Experiments were designed in order to evaluate the mechanical response of AA5083-H111 under a wide range of temperatures (-70 to 100ºC) and loading rates (up to $2000s^{-1}$). The corresponding stress–strain curves were obtai-

ned by means of uniaxial compression tests carried out in a customized SHPB shown in Figure 1.
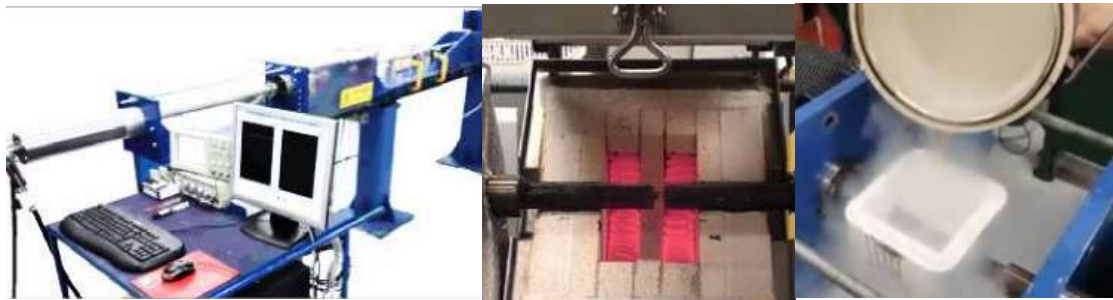
Fig. 1 (a) Custom SHPB apparatus a...etail on (b) the heating furnace and (c) cryogenic chamber.

(a) (b) (c)

RESULTS AND CONCLUSIONS
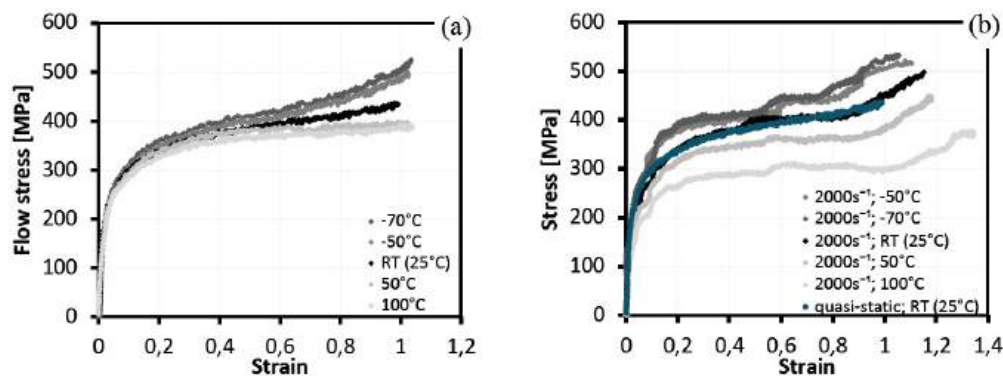
Fig. 2 Flow stress curves of AA 5083-H111 for temperatures ranging from -70°C to 100°C for (a) quasi-static conditions and (b) dynamic conditions (25°C quasi-static curve is plotted for comparison).

Figure 2(a) shows that AA5083-H111 exhibits low sensitivity to temperature exposure in the range of 25°C to 100°C, being able to maintain its resistance almost entirely at 50°C and a slight reduction of 6% was observed for 100°C at a strain level of 0,6. On the other hand, it seems to respond well to cold working conditions, with its mechanical resistance increasing roughly 7% at -70°C for the same strain level. It is only as deformation increases that greater deviations arise as strain hardening was observed to increase when testing temperature decreased. Figure 2(b) shows that for dynamic conditions the flow stress is distributed over a wider range of values, for specimens at the same initial temperature, from early stages of deformation. For the lower temperatures however, from -70°C to 25°C, the material is rather insensitive to loading rate. In the case of 25°C, for a strain-rate of 2000s^{-1}, the flow curve overlaps almost entirely that of the quasi-static condition. For the cooler temperatures, -50°C and -70°C, a slight increase of flow stress was observed. In contrast, for the greater temperatures, 50°C and 100°C the material displays negative strain-rate sensibility. This effect is more pronounced for the initial temperature of 100°C, as for the same 0,6 strain, the flow stress had reduced 20% when compared to quasi-static conditions.

REFERENCES

[1] B. Davoodi, G. H. Payganeh, M. R. Eslami, "Cutting forces in dry machining of aluminum alloy 5083 with carbide tools", in. Advanced Materials Research, 2012, 445, pp. 259-262.

[2] T. Børvik, A. H. Clausen, O. S. Hopperstad, M. Langseth, "Perforation of AA5083-H116 aluminium plates with conical-nose steel projectiles—experimental study", in International Journal of Impact Engineering, 2004, 30, pp. 367-384.

[3] P. K. Singh, A. Das, S. Sivaprasad, P. Biswas, R. K. Verma, D. Chakrabarti, "Energy absorption behaviour of different grades of steel sheets using a strain rate dependent constitutive model", in Thin-Walled Structures, 2017, 111, pp. 9-18.

ID 58
LOAD CARRYING SYSTEM DESIGN OPTIMIZING

Nataliya Sadretdinova[1,2], Chi Tiet Nung[2], Yordan Kyosev[2]

[1] Kyiv National University of Technologies and Design

[2] Dresden Technical University

(*) natalija.sadretdinova@mailbox.tu-dresden.de

ABSTRACT

The research refers to the development of a virtual model for an ergonomic load carrying system using 3D CAD software. As a rule, carrying systems are a multi-technological product, as they combine several features in terms of ergonomics, functionality, durability, and load-bearing capacity. The engineering and manufacturing of personal load carrying equipment is a complex task that requires a lot of time and effort. The development of modern virtual techniques, recently have been widely implemented in the design of functional clothing, can simplify significantly this process, especially in the stages of preliminary research, model design, and manufacturing of a prototype. With this background and based on the existing prototypes, a military load carrying system concept was designed and visualised using a 3D CAD solution. Factors such as ergonomics and interface pressure distribution were taken into account. In addition, the problems occurring in the virtual simulation of multi-layer carriage systems were considered and appropriate solutions were offered.

INTRODUCTION

During military operations or campaigns, soldiers often have to carry heavy loads that create extreme physiological loading (soft tissue deformation) often resulting in discomfort, pain and musculoskeletal injuries. A qualitative synthesis of the studies shows that carrying loads can lead to low back pain; and it can also trigger neck, thoracic, and shoulder pain [1]. The main factor causing these disadvantages is an unequal pressure distribution of the ammunition on the surface of the human body. Study [2] shows that the pressure value when using carrying systems can be significantly reduced with the correct choice of the item design parameters and optimisation of its placement on the body. The most cost-effective and sustainable way to assess the fit quality of products nowadays is their virtual simulation in 3D software [3]. Despite the widespread utilization of virtual methods in research for modelling casual and sportswear, applying these methods to specialized equipment poses several challenges, including a lack of information regarding the materials utilized, the absence of digital tools for simulating them accurately, and ensuring the correct interaction of multi-layer systems within the selected functional environment. Therefore, this study aimed to develop a virtual model of a load carrying system that can simulate real-life scenarios (different loads, materials, and belt designs), which helps optimise pressure during garment-body interaction.

RESULTS AND CONCLUSIONS

The load carriage system applied in this study as a prototype is a commercially available system, commonly used in reinforced. The comfort of the prototype was studied in two areas: ergonomic adjustments and pressure level distribution on the body surface. To evaluate the ergonomics of the selected prototype, including dynamics, a subject wore a belt under two conditions: without a load and with a 5 kg load, while being scanned utilizing the Move4D scanning system. For all measurements, the subjects had to assume a static, kneeling position and walk for 15 seconds. The obtained frames were used to compare the fit of the belt in different body positions within the motion and to create an animated avatar for further application in 3D simulation programs.

Analysis of the cross-sectional image at the high-hip level, generated using Geomagic Qualify software showed that the belt rests unequaly around the human body. The higher average distance of 8 mm was found in the lateral

hip area. When performing the specified movements, the belt moves relative to the body in both vertical and horizontal directions by an average of 4%. When using additional loads, the adhesion around the circumference of the abdomen decreases and increases in the area of force application due to the torque effect.

To evaluate the interface pressure distribution exerted by the load bearing belt on the hip area the texsens® pressure mapping system was adjusted under the belt. The pressure measurements were conducted at 9 different hip regions, both without and with a weight of 5kg on the belt. The results show that the highest pressure level is located in the abdomen and is transferred to the lumbar region while loading and moving (Fig.1a.). Consequently, enhancing the design of the belt is imperative to guarantee the optimal functionality of the load-carrying system.

In order to address this concern, a new equipment belt solution was developed. Pattern pieces for shell fabrics, lining, and padding were generated using the Grafis CAD system. The belt design accommodates the waist-to-hip ratio of males, featuring a robust 50 mm outer belt for standard pouch or gear attachment, and a wider, padded inner belt for support and comfort. The harness incorporates padded front and back shoulder straps with a specific configuration.
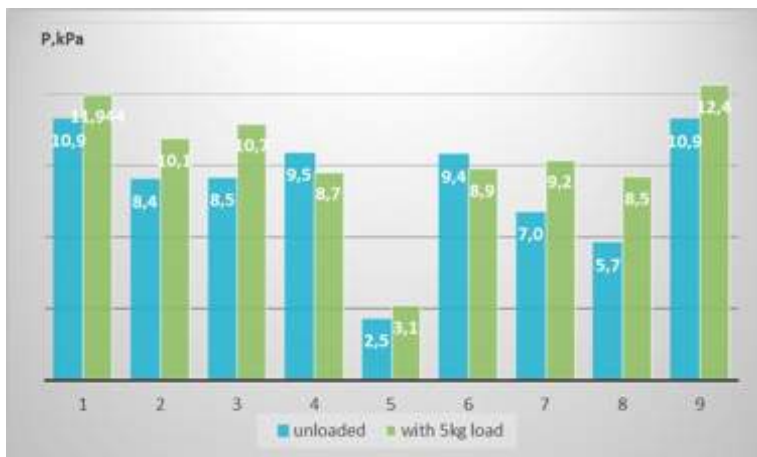
Fig. 1 Pressure distribution study a) pressure test results
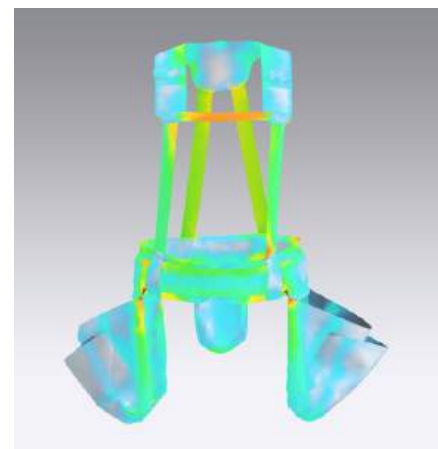
b) load carrying system simulation with pressure map

The initial step toward digitalization encompassed fabric parameter assessment using the Vizoo measurement system and the creation of a digital fabric twin. Through simulations in Clo3D, the effects of weight on garment pressure and elasticity were analysed, both in static and dynamic scenarios (Fig.1b). The results obtained from the simulation were confirmed by testing the physical prototype.

Results demonstrate the efficacy of Clo3D in evaluating garment comfort by simulating diverse solutions and analysing pressure distribution on the garment. The results provide a theoretical basis and practical guidance for engineers involved in tactical wearing systems design and assist in developing and evaluating the garment design for different operating conditions while using a virtual simulation system.

REFERENCES

[1] Hadid, Amir et al. "Novel model for load carriage ergonomics optimisation." Extreme Physiology & Medicine, vol. 4,Suppl 1 A12. 14 Sep. 2015, doi:10.1186/2046-7648-4-S1-A12

[2] X. Dai, X. Zeng, S. Liu and Y. Hong, "Is skin pressure in load carriage over-evaluated?", J. Biomech., vol. 130, Jan. 2022.

[3] X. Wu , Z. Cheng , VE. Kuzmichev, Dynamic Fit Optimization and Effect Evaluation of a Female Wetsuit Based on Virtual Technology. Sustainability, vol. 15(3), 2023.

ID 59
CORRELATION BETWEEN EXPERIMENTAL THERMAL RESISTANCES AND VARIOUS MODELS

Solène Champigny[1](*), Cyprien Bourrilhon[2], Fabien Salaün[1], Cédric Cochrane[1]

[1] Univ. Lille, ENSAIT, ULR 2461 – GEMTEX – GEnie des Matériaux TEXtiles, F-59000 Lille, France

[2] Institut de Recherche Biomédicale des Armées (IRBA), Brétigny-sur-Orge, France

(*) Email: solene.champigny@ensait.fr

ABSTRACT

Comfort is an essential element of clothing. Thermal comfort is one of the most important features. Especially for military personnel who have to operate in different parts of the world and in different weather conditions. Thermal comfort plays a crucial role in risking or saving a soldier's life. This study is based on the comparison between thermal resistance measurements using a thermal manikin heated at 34°C on a climatic chamber at 20°C and 50% RH; and several existing models. Ten garments and six outfits composed of these garments were analyzed.

INTRODUCTION

In order to maintain comfort in a given environment, it is important to maintain the human body's thermal balance at zero [1]. This balance is affected by the clothing worn, which can be described in terms of its thermal insulation and resistance to evaporation. Thermal resistance can be measured by means of a thermal manikin, which has a heated skin and temperature sensors. The heat flow required to maintain a given skin temperature is measured [2]. In the military context, the thermal comfort provided by clothing is crucial. We examined cold weather outfits from the French military. It was discovered that the thermal resistance of an outfit differs from the sum of the thermal resistances of the individual garments it comprises. The study sought to develop a model for both single- and multi-layered garments. Various models already exist for calculating the thermal conductivity of media. The aim of this study is to determine whether there is a correlation between the results of these models and experimental results.

RESULTS AND CONCLUSIONS

The thermal resistance of ten items of military clothing and six outfits made up of these ten garments was measured using a thermal manikin. Theoretical values were calculated using four models: series, parallel, Maxwell-Eucken and Levy's (Equ 1-4) [3]. The aim was to compare the experimental values with the theoretical values.

The conductivity of each model was compared to the experimental results using a 1:1 line (Fig 1 a). The Levy's model has the regression curve closest to the 1:1 line, while the series model has the best R². The correlation between the models and the experimental results is very good.

A graph was also plotted for multilayer models, and appropriate coefficients were determined using a solver (Fig1 b). This resulted in excellent outcomes and strong correlations. The coefficients identified by the solver correspond to the air layers between each garment.
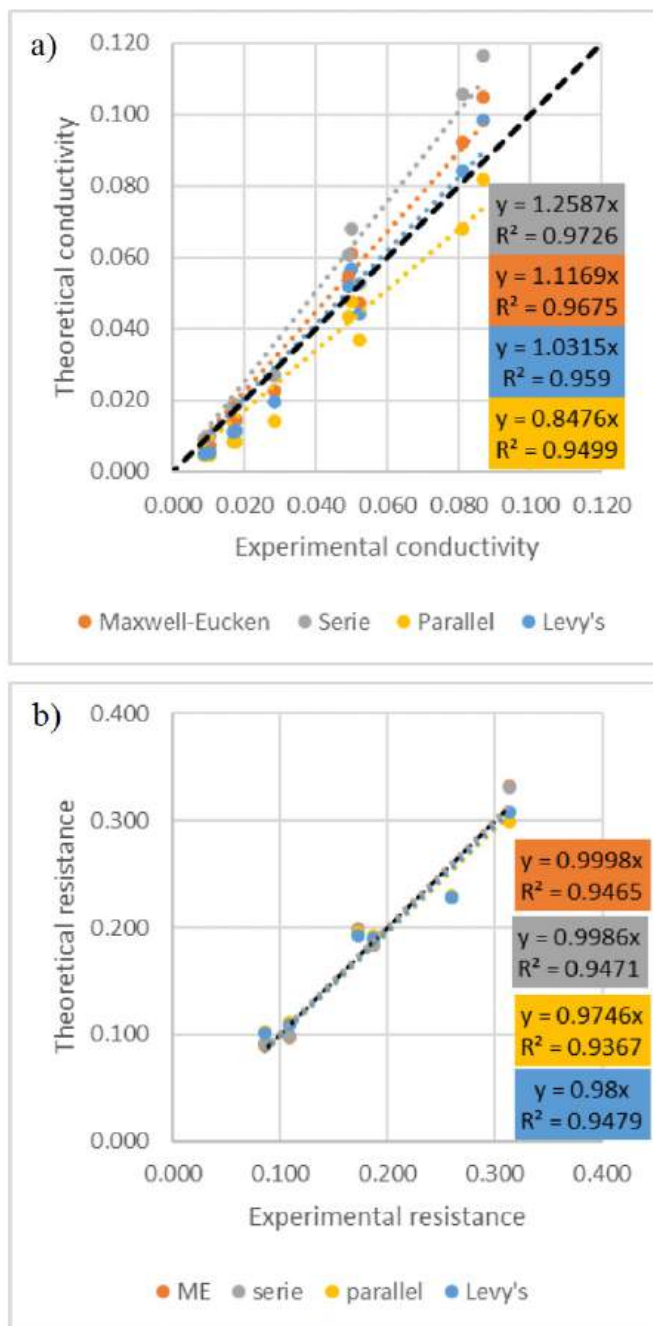
Equ 1. Maxwell-Eucken's model
$$\lambda_{eff} = \lambda_{air} \frac{2 \times \lambda_{air} + \lambda_f - 2 \times (\lambda_{air} - \lambda_f)\epsilon_f}{2 \times \lambda_{air} + \lambda_f + (\lambda_{air} - \lambda_f)\epsilon_f}$$

Equ 2. Series model
$$\lambda_{eff} = \frac{1}{\frac{\epsilon_f}{\lambda_f} + \frac{\epsilon_{air}}{\lambda_{air}}}$$

Equ 3. Parallel model
$$\lambda_{eff} = \epsilon_f \times \lambda_f + \epsilon_{air} \times \lambda_{air}$$

Equ 4. Levy's model
$$\lambda_{eff} = \lambda_{air} \frac{2 \times \lambda_{air} + \lambda_f - 2 \times (\lambda_{air} - \lambda_f)F}{2 \times \lambda_{air} + \lambda_f + (\lambda_{air} - \lambda_f)F}$$

$$F = \frac{\frac{2}{G} - 1 + V_2 - \sqrt{\left(\frac{2}{G} - 1 + V_2\right)^2 - \frac{8V_2}{G}}}{2}$$

$$G = \frac{(\lambda_{air} - \lambda_f)^2}{(\lambda_{air} - \lambda_f)^2 + \frac{\lambda_{air} \times \lambda_f}{2}}$$

Fig 1. Models' results curves of a) thermal conductivity in a single-layered clothing b) thermal resistance of multi-layered clothing

This study shows that these models provide a reliable method for obtaining a theoretical value for the thermal resistance of both single- and multi-layer garments.

REFERENCES

[1] M. N. Cramer, D. Gagnon, O. Laitano and C. G. Crandall, "Human temperature regulation under heat stress in health, disease, and injury", *Physiological Reviews*, vol. 102, pp. 19071989, 2022.

[2] J. Wang, J. K. Carson, M.F. North and D. J. Cleland, "A new structural model of effective thermal conductivity for heterogeneous materials with co-continuous phases", *International Journal of Heat and Mass Transfer*, vol. 51, pp. 2389-2397, 2008.

[3] J. Wang, J. K. Carson, M.F. North and D. J. Cleland, "A new structural model of effective thermal conductivity for heterogeneous materials with co-continuous phases", International Journal of Heat and Mass Transfer, vol. 51, pp. 2389-2397, 2008.

ID 61

ASSESSMENT OF THE INFLUENCE OF GRAPHENE SHEET SIZE ON THE DEVELOPMENT OF ADVANCED TEXTILE SUBSTRATES WITH CONDUCTIVE PROPERTIES FOR DEFENSE FIELD

Maria J. Martins[1], Leonor Cunha[2], Adriana Pereira[3], Ana Barros[4], André Barbosa[5], Nuno Araujo[6], Maria António[7], Gilda Santos[8](*)

[1-8] Department of Technology and Engineering, Citeve - Technological Center for the Textile and Clothing Industries of Portugal, Vila Nova de Famalicão, Portugal

(*) Email: gsantos@citeve.pt

ABSTRACT

This work aims to compare the conductive properties of textiles treated with various graphene-based materials, aiming to evaluate the influence of graphene sheet size on the development of advanced textile substrates with conductive properties for defense applications. Two synthetic fabrics, polyester (PES) and polyamide (PA), were chosen for these studies due to their versatility and extensive use across various sectors, including defense. The assessments of graphene flake size impact were conducted on both fabrics through functionalization with various graphene-based materials. After evaluating the graphene-based materials for optimal conductivity, it was observed that graphene-based materials with larger flake sizes exhibited enhanced conductivity properties.

INTRODUCTION

Graphene-based materials have attracted interest in multiple fields including the defense due to their electronic, mechanical, and thermal properties [1]. Different methodologies have been explored to find new ways to synthesize, process, and deposit graphene for diverse applications [2]. In this study, a chemical approach to produce conductive fabric coated with graphene was employed. This process included the adsorption of graphene oxide (GO) onto the fabric surface, followed by chemical reduction of GO to produce reduced GO (rGO) deposited onto the fabric surface. The textile substrates selected for this assessment were PES and PA because they are synthetic fibres widely used for various purposes due to its versatility and cost-effectiveness. Furthermore, from an environmental perspective, these types of materials are highly promising in terms of recycling, as they are 100% recyclable.

In this study, the influence of graphene sheet size on the conductive properties of graphene-coated fabric were investigated using PES and PA substrates functionalized with three types of GO materials followed by chemical reduction, each characterized by varying flake sizes. In this particular case, PES fabric was chosen as the preferable substrate to assess the chemical reduction of GO due to the polar groups (C-O and C=O) of its structure that can improve the adhesion of GO in fibres. Subsequently, the conductive properties of rGO-coated fabrics were compared with those of synthetic fabrics coated with commercially obtained functionalized graphene (FG).

RESULTS AND CONCLUSIONS

The results demonstrated the successful preparation of advanced textile substrates through the adsorption of graphene sheets onto the fabric surface, as evidenced by the presence of D and G bands characteristic of graphe-

ne-based materials in the Raman spectra of the textile materials (Fig.1). Moreover, the results showed a significant influence of graphene sheet size on the conductive properties of the PES fabric substrates, as illustrated in Table 1. When comparing the commercially acquired FG material (Sample 1) with the rGO-coated fabric possessing a comparable flake size (Sample 2), it becomes evident that the FG textile exhibits superior conductive properties. However, as we increase the rGO flake size (Sample 3 and Sample 4), a discernible trend towards enhanced conductive properties emerges, culminating in the optimal performance observed with the rGO material featuring a flake size of 1-10 μm (Sample 4). Consequently, the results obtained with PES were compared with those from PA fabric. Despite PA containing C=O and N-H groups in its structure, the material functionalized with FG exhibits lower electrical performance than PES (Sample 5). However, when the PA fabric was functionalized with rGO material with a higher flake size, the conductive properties improved compared to the results obtained for FG material, likely due to the presence of functional groups that can enhance the adhesion of GO to the fibres (Sample 6-8). Furthermore, the results obtained for PA functionalized with rGO proved to be more promising than those obtained for the PES substrate.

a)   b)
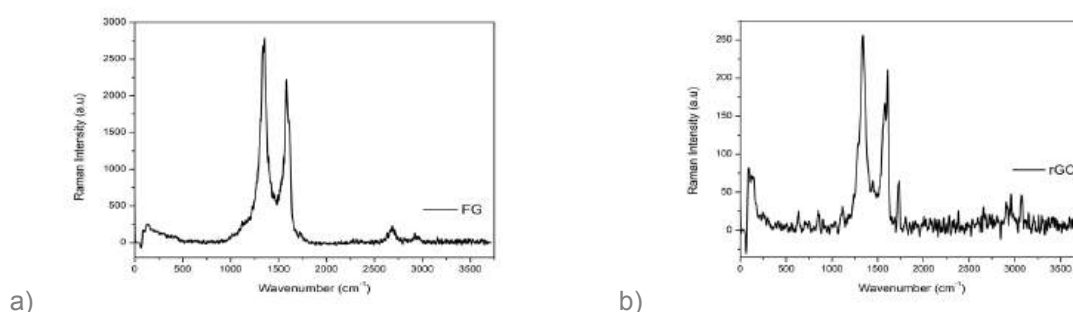
Fig. 1 Raman spectra of PES substrate functionalized with a) FG and b) rGO.

Table 1 Conductive properties of developed graphene-coated fabrics.

Sample	Textile substrate	Graphene-based material	Flake size (μm)	Resistance (kΩ/cm)	Conductivity (S/m)
1	PES	FG	0.1-1	15.7	6.36×10^{-3}
2	PES	rGO	0.1-1	175.2	5.71×10^{-4}
3	PES	rGO	1-4	144.4	6.93×10^{-3}
4	PES	rGO	1-10	3.8	2.60×10^{-2}
5	PA	FG	0.1-1	64.6	1.55×10^{-3}
6	PA	rGO	0.1-1	96.6	1.04×10^{-3}
7	PA	rGO	1-4	32.7	3.06×10^{-3}
8	PA	rGO	1-10	2.3	4.31×10^{-2}

In conclusion, this study demonstrates the inherent correlation between graphene flake sizes and graphene properties. Observing that by increasing the size of GO flakes and subsequently performing chemical reduction of the material, it is possible to achieve promising conductivity results when compared to commercially obtained graphene material.

As a prospective direction for future research, it would be valuable to explore the behaviour of GO material using different textile substrates. This could provide further insights into how different substrate compositions interact with graphene coatings and influence the overall conductive properties of the resulting fabric composites.

REFERENCES

[1] Yu, X., Cheng, H., Zhang, M. et al, "Graphene-based smart materials", *Nature Reviews Materials 2*, 17046 (2017). https://doi.org/10.1038/natrevmats.2017.46

[2] Worku, A., Ayele,D., "Recent advances of graphene-based materials for emerging technologies", *Results in Chemistry 5* (2023). https://doi.org/10.1016/j.rechem.2023.100971

ID 62

FERRITE-GRAFT-CNT AND PBSA COMPOSITES FOR EM SHIELDING AND HEAT DISSIPATION IN DEFENCE APPLICATIONS

Miks Bleija[(*)], **Artis Krikovs, Sergejs Gaidukovs**

Institute of Chemistry and Chemical Technology, Faculty of Natural Sciences and Technology, Riga Technical University, P. Valdena 3, LV-1048 Riga, Latvia

[(*)] Email: miks.bleija@rtu.lv

ABSTRACT

Hybridizing electrical (carbon nanotube (CNT)) and magnetic (Fe_3O_4) fillers enables electromagnetic interference (EMI) shielding and electrostatic discharge (ESD) compliance. In this work, we synthesized CNT-graft-Fe_3O_4 nanoparticles via co-precipitation and incorporated them in a biodegradable PBSA (poly(butylene succinate-co-adipate)) matrix at 0.1-2 vol.%. We investigated the properties of the composites using hydrostatic densimetry, light flash analysis, broadband dielectric spectroscopy, and four-point surface resistivity testing. The composites containing the synthesized nanoparticles showed a higher volume percolation threshold and a lower surface percolation threshold, while displaying additional ferrimagnetism. Thus, the investigated composites can be used in ESD compliant packaging at low filler loadings and show potential for EMI shielding applications in the defence sector.

INTRODUCTION

The high aspect ratios of multiwalled carbon nanotubes (MWCNTs) enable them to form percolated networks at very low concentrations, resulting in highly conductive composites (Potschke, Arnaldo, and Radusch 2012). Iron (II,III) oxide, known as a spinel ferrite (Fe_3O_4), is a commonly used ferrimagnetic filler. The combination of CNTs and ferrites enables a hybrid strategy for enhanced electric/magnetic loss in composite materials, which can then be exploited for electromagnetic interference (EMI) shielding properties. Co-precipitation is one of the most common and easiest ways to synthesize nanosized (5-20 nm) ferrites (Colombo et al. 2012)

In this paper, we created novel composite materials from a biodegradable PBSA matrix filled with hybrid fillers (MWCNT-g-Fe_3O_4). The aim is to combine electrical and magnetic properties for use in dielectric and electromagnetic applications. The nanoparticles were synthesized via co precipitation. Composites were prepared using solvent casting. Their density, thermal conductivity, broadband AC electrical conductivity, and surface electrical resistivity were investigated to determine their EMI and ESD potential.

RESULTS AND CONCLUSIONS

This work examined how Fe_3O_4 co-precipitation grafting on multiwalled carbon nanotubes affects composite thermal conductivity, volume conductivity and surface resistivity. We showed that the grafting of Fe_3O_4 reduced the percolation threshold of surface resistivity, but increased the percolation threshold of volume conductivity. This helps adjust composite properties to achieve better ESD performance. The difference in volume and surface behaviors shows possible inductive losses in higher frequency modes, which lends promise to further investigation of EMI shielding properties, as well as possible anti-radar applications. The lower conductivity of MWCNT-g-Fe_3O_4 could be attributed to higher electric losses, due to the generation of eddy currents in Fe_3O_4 domains (Biswas et al. 2020).
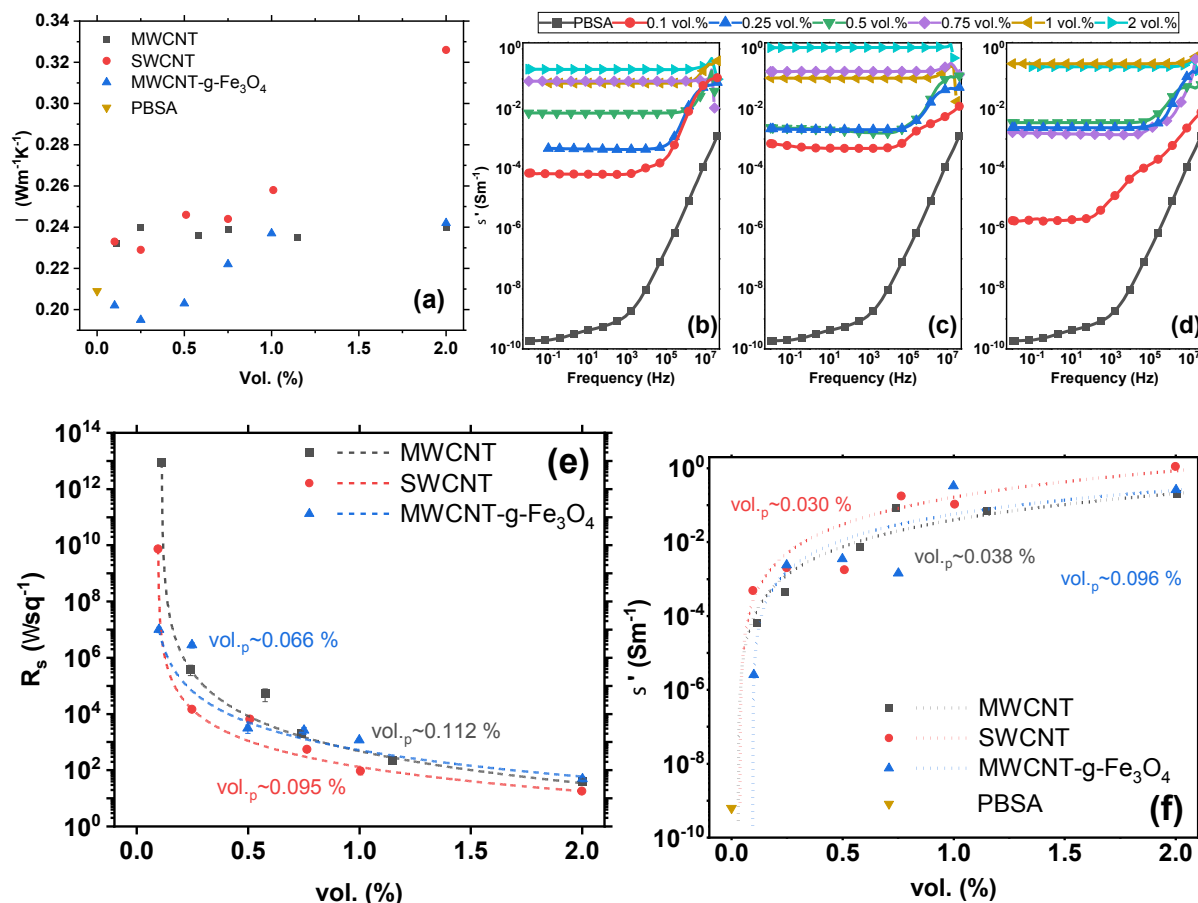
Fig. 1 Thermal conductivity (a), AC conductivity of MWCNT (b), AC conductivity of SWCNT (c), AC conductivity of MWCNT-g-Fe3O4 (d), percolation of surface resistivity (e), percolation of volume conductivity at 112 Hz (f), with percolation thresholds given in the figure

The introduction of Fe_3O_4 lowered the percolation threshold of the surface resistivity, while increasing the resistivity at higher filler loadings. This effect could be caused by a change in particle morphology – Fe_3O_4 grafting increases the thickness of the nanotubes, while changing their flow behavior. Thus, the grafting with Fe_3O_4 allows the modification of electrical properties to allow use in ESD applications.

REFERENCES

[1] P. Biswas, G. W. Mulholland, M. C. Rehwoldt, D. J. Kline, and M. R. Zachariah, "Microwave absorption by small dielectric and semi-conductor coated metal particles," *Journal of Quantitative Spectroscopy and Radiative Transfer*, vol. 247, no. May, pp. 106938, 2020.

[2] M. Colombo, S. Carregal-Romero, M. F. Casula, L. Gutierrez, M. P. Morales, I. B. Bohm, J. T. Heverhagen, D. Prosperi, and W. J. Parak, "Biological applications of magnetic nanoparticles," *Chemical Society Reviews*, vol. 41, no. 11, pp. 4306–4334, 2012.

[3] P. Potschke, M. H. Arnaldo, and H-J. Radusch, "Percolation behavior and mehanical properties of polycarbonate composites filled with carbon black/carbon nanotube systems," *Polimery*, vol. 57, no. 3, pp. 204–211, 2012.

ID 66
UNIFYING COMFORT AND PROTECTION IN A CBRN SUIT

Tânia Ferreira,[1(*)] **A. Catarina Vale,**[2] **Alexandra Pinto,**[3] **Diana Sousa** [4]**, Inês P. Moreira,**[5] **Carlos Silva,**[6] **Fernanda Gomes,**[7] **Paula Lopes,**[8] **Inês Cruz,**[9] **Amin Taoufiq,**[10] **Raquel Pinheiro,**[11] **Pedro Magalhães,**[12] **Joana C. Antunes,**[13] **Mariana Henriques**[14] **Pedro Neto,**[15] **Wilson Antunes,**[16] **Fernando Cunha,**[17] **and Raul Fangueiro**[18]

[1, 2, 5, 13, 17,18] Fibrenamics Association, Institute for Innovation in Fibrous and Composite Materials, University of Minho, 4800058 Guimarães, Portugal;

[1, 2, 5, 13, 17, 18] Centre for Textile Science and Technology (2C2T), University of Minho, 4800-058 Guimarães, Portugal;

[3, 4, 7, 14] CEB, Centre of Biological Engineering, LIBRO–Laboratório de Investigação em Biofilmes Rosário Oliveira, University of Minho, 4710-057 Braga, Portugal;

[6, 12] TINTEX Textiles SA, Zona Industrial, Polo 1, Campos, 4924-909 Vila Nova de Cerveira, Portugal.

[3, 4, 7, 14] LABBELS – Associate Laboratory, Braga, Guimarães, Portugal

[8, 9, 10, 11, 15, 16] Academia Militar (CINAMIL), Unidade Militar Laboratorial de Defesa Biológica e Química (UMLDBQ), Instituto Universitário Militar), Av. Dr. Alfredo Bensaúde, 1849-012 Lisboa, Portugal.

(*) Email: taniaferreira@fibrenamics.com

ABSTRACT

With increasing global security threats impacting military, emergency responders, and civilians, there is a pressing need for advanced technology to safeguard individuals in high-risk situations. Existing protective gear offers limited protection in terms of lifetime usage, prompting a call for innovative solutions. Our approach involves cutting-edge materials and layered fabrics designed to actively shield users against multiple external threats, while staying committed to comfort and usability. Our multilayered textiles range from the macro to the nanoscale, incorporating a hydrophobic outer layer and a functionalized chemical, biological, radiation, and nuclear (CBRN) protective coating on the inner side. The layer is made of polyurethane, zinc oxide nanoparticles (ZnO), and graphene nanoplatelets (Gf), through a specialized coating technique. ZnO are known for their shielding properties, corrosionresistance, antibacterial and antifungal properties, its viability as an effective UV filter, and above all it is very easy to use. [1] On another hand, Gf is capable of strong adsorption capabilities that enable the removal and immobilization of pathogens and pollutants from air, soil and water and exhibit antimicrobial properties to combat harmful pathogens. [2] For enhanced comfort and moisture management, an additional layer of lining fabric has been positioned between the functionalized inner layer and the users' undergarment. This approach holds promise in enhancing safety for first responders and soldiers, especially considering the heightened concerns of bioterrorism. [3]

INTRODUCTION

If CBRN weapons exist, the world will never be safe enough. Yet, mankind must be prepared through every available means to face the alarming challenges that may arise if one of these weapons is deployed. Accordingly, first responders and soldiers must be adequately protected, so that their exposure to CBRN hazards is minimized, by inactivating/degrading toxic chemicals or preventing the dissemination of infectious microorganisms to society at large. [4] Nowadays, the protective clothing used mainly by the military involves multiple fabric layers that use activated carbon to absorb harmful substances. Additionally, there is a separate layer for filtration, ensuring passive protection. Unfortunately, a significant issue arises due to the buildup of secondary contaminants within the carbon filter. This leads to heavy, warm, and non-breathable clothing, which led us to look deeply in the question of comfort. [5]

To overcome this issue, one approach involves enhancing textiles with nanomaterials endowed with active protection abilities to counteract contaminants buildup within the textile substrates. Zinc oxide nanoparticles (ZnO NPs) are noteworthy for their affordability, biocompatibility, and unique hexagonal prism shape, which boosts surface roughness, enhancing cell attachment [6]. Also the inclusion of UV protection, photocatalytic activity, antimicrobial properties, self-cleaning attributes, energy harvesting capabilities, and biosafety features in these materials allows for the incorporation of multiple functionalities into their substrates. These functionalities encompass water resistance, antimicrobial effects, UV blocking, flame retardancy and corrosion inhibition. Notably, the introduction of zinc-doped nanoparticles has demonstrated the ability to impart superhydrophobic properties to fabrics, such as those derived from cotton. This not only facilitates ease of cleaning but also provides additional functionalities, including microbicidal capacity. On its turn, Gf shows excellent mechanical characteristics, high electrical conductivity properties, high UV shielding, rapid heat dissipation, high hydrophobicity, high thermal stability, high antimicrobial activity, and high biocompatibility. [5]

RESULTS AND CONCLUSIONS

In the process of developing CBRN protective clothing, an outer coating was carefully spread onto a military-grade camouflage woven fabric to provide water- and oil-repellence and protect against generic threats, and an inner coating contained a paste composed of ZnO, Gf and a polyurethane-based ligand spread by knife coating (thickness of 0.15 mm) while being aimed at CBRN protection.

In what concerns the inner layer, challenges of liquid and gas were performed to test the performance of chemical protection with a retention rate of 99.9±0.1% (DMMP; neurotoxic agents' simulant) and 49.8±1.6% (CEES; sulphur mustard simulant) for the formulation with Paste A + ZnO (*$p < 0.05$). In parallel, qualitative, and quantitative tests (JIS L 1902 standard) using *S. aureus* and *E. coli* were performed for the antimicrobial assessment at the front and back sides of the coated textiles following 24 h of incubation, as typically done to screen technical textiles' efficacy against biological threats. The tests revealed that fabrics functionalized with ZnO NPs successfully eradicated all *S. aureus* and *E. coli* colonies in WF1, as well as MS2 bacteriophages (*$p < 0.05$). To finish, radiological protection was also achieved, following validation through a qualitative test based on the scanning electron microscopy observation before and after the EDX maximum irradiation (30 kV).

a)

Sample	Retention rate of DMMP (%)/ CEES (%)	Min Dose (g/human) DMMP/ CEES	Max Dose (g/human) DMMP/ CEES
Paste A	89.9±1.8	13.4	53.7
Paste A+ZnO	99.8±0.1/ 49.8±1.6*	0.2/ 71.7	0.9/ 287.4
Paste A+ZnO+Gf	99.9±0.1/ 56.4±1.9	0.2/ 62.4	0.8/ 249.7

b)

c)
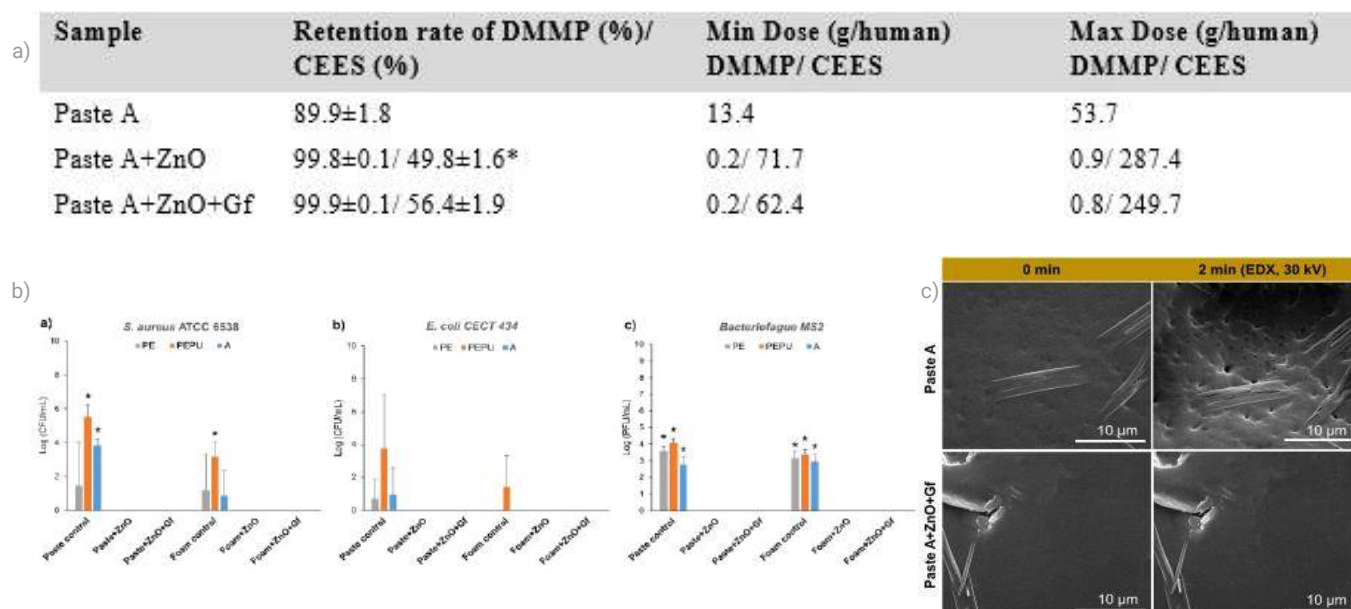
Fig.1 – a) Agent Liquid (DMMP and CEES) challenge for reference and functionalized samples; b) Antibacterial activity of textile functionalized with ZnO alone and in combination with Gf (paste versus foam, and different binders), against Staphylococcus aureus ATCC 6538, Escherichia coli CECT 434 and antiviral activity against MS2 bacteriophage compared with the respective positive control (without functionalization); c) Surface morphology micrographs obtained from paste A+ZnO+Gf and its control (Paste A), before and after EDX irradiation (30 kV, 2 min).

As for the inner layer, two different lining woven fabrics were considered for comfort purposes, one composed of polyamide and elastane (lining 1, L1) and the other one composed of MAC and cotton (lining 2, L2), with both being highly breathable textile substrates. The results lead us to conclude that both linings are superhydrophilic and have a very good overall moisture management capacity (between 0.6-0.8), yet with only L2 enabling high outwards water vapor permeability. L2 lining is also more permeable to air (**$p < 0.005$) than the L1 knit, thus L2 was the obvious choice to ensure comfort as the inner layer of the protective suit.

In short, the produced coated fabrics are combined with specific linings following a rationale that enables the development of active, yet comfortable, protective garments for both military and civilian applications.

REFERENCES

[1] Hinging Zhan, *et al*. "In situ growth of flower-like ZnO onto graphene oxide for the synergistically enhanced anti-corrosion ability of epoxy coating.", Ceramics International, 2024, 50, p. 5914-5926.

[2] Hasan Eskalen, *et al*. "Preparation and study of radiation shielding features of ZnO nanoparticle reinforced borate glasses". Applied Radiation and Isotopes, 2023, 198.

[3] Kulathi Nishshankage, et al. "Current trends in antimicrobial activities of carbon nanostructures: potentiality and status of nanobiochar in comparison to carbon dots". Biochar, 2024

[4] Joana C.A., "Recent Trends in Protective Textiles against Biological Threats: A Focus on Biological Warfare Agents.," Polymers 2022

[5] Schreuder-Gibson HL, *et al*.. "Chemical and biological protection and detection in fabrics for protective clothing". MRS Bulletin, 2003, 28, p. 574-578.

[6] Boticas I, *et al*. "Superhydrophobic cotton fabrics based on ZnO nanoparticles functionalization. SN Applied Sciences, 2019, 1, p- 1376.

ID 67

EXPERIMENTAL INVESTIGATION OF THE DYNAMIC RESPONSE OF LOW-DENSITY FOAM-WRAPPED ALUMINUM TUBES UNDER LOCALIZED BLAST LOADING

Ben Rhouma Mohamed[1,2(*)], Aminou Aldjabar[1,2], Maazoun Azer[3], Belkassem Bachir[1], Tysmans Tine [2], and Lecompte David[1]

[1]Royal Military Academy, Structural and Blast Engineering Department

Avenue de la Renaissance 30, 1000 Brussels, Belgium

[2]Vrije Universiteit Brussels, Mechanics of Materials and Constructions Department

Pleinlaan 2, 1050 Brussels, Belgium

[3] Military Academy of Fondouk Jedid, Civil Engineering Department, 8021 Nabeul, Tunisia

[(*)] Email: Mohamed.BenRhouma@mil.be

ABSTRACT

This study aims to assess the effectiveness of a sacrificial cladding system, consisting of a low-density foam and an outer lightweight skin, enveloping a specifically studied structure. The structure in question is a simply supported aluminum column exposed to a blast wave generated by an explosive-driven shock tube. The chosen sacrificial cladding includes closed-cell polyurethane foam (PU) with a density of 30 kg/m³ and a 1mm aluminum sheet. The raw specimens, with dimensions of 1200 mm x 100 mm x 2 mm (height x diameter x wall thickness), are obtained by cutting from 6m-long aluminum columns. The study involves a series of experiments using the Explosive shock-driven shock tube (EDST) as a laboratory loading tool. The local deformation, indicated by mid-span indentation, is quantified through 3D laser scanner measurements. Furthermore, the impact of the proposed cladding on local deformations of the retrofitted aluminum columns is examined. The results reveal that the maximum localized indentation is reduced by 5%, 28% and 46% when using 30 mm, 50 mm and 100 mm of PU foam, respectively.

INTRODUCTION

In 2022, the Explosive Violence Monitoring Project documented 22,772 deaths and injuries resulting from the use of explosive weapons globally [1]. Over the past two decades, the frequency of incidents involving explosives has increased fivefold, impacting civilian populations, military personnel and infrastructure [2]. Consequently, there is a critical need to study the behavior of structures, structural components and materials under blast loading.

Sacrificial cladding emerges as a passive protective solution designed to absorb blast-induced energy, thereby reducing damage to the target [3]. The crushable core typically involves cellular structures or materials, such as metallic foam [4]–[6], polymeric foam [3][7], thin-walled tubular cores [8][9] and mineral foam [10][11]. Polyurethane (PU) foam, widely adopted for its lightweight nature, cost-effectiveness and low plateau stress characteristics, serves as a common choice for energy absorption [12]. It is often affixed to the façade of the protected structure to mitigate transmitted pressure to an acceptable threshold. While research on sacrificial cladding's anti-blast performance is extensive, studies focusing on circular structures are relatively limited. This paper aims to assess the blast absorption capacity of a sacrificial cladding composed of polymeric foam and a thin outer skin. The evaluation is conducted around a thin-walled circular member serving as a witness structure, represented by a pinned-pinned aluminum column. The investigation focuses on the reduction of damage to the aluminum column, providing insights into the protective capabilities of the proposed sacrificial cladding.

RESULTS AND CONCLUSIONS

To measure the deformation on the loaded side of different test configurations, indentation assessments are carried out using a handheld scanner combined with the Krypton K610 camera system. This methodology is distinguished by its non-invasive and non-destructive characteristics, ensuring the maintenance of the structural integrity of the scanned object.

In the analysis, the deformation parameters are identified and illustrated in Fig. 1, with detailed values provided in Table 1. Specifically, d1 and d2 denote the axial and radial width of the local deformation zone, corresponding to the loaded side of the area of interest, as depicted in Fig. 1.a. The parameter b represents the distance from the highest point of the concave deformation zone to the back surface of the column's cross-section, while a is the distance from the lowest point of the center of the concave deformation zone to the back surface of the column's cross-section. The variable l signifies the width of the radial center section of the concave deformation zone, and r denotes the diameter of the non-deformed column, as illustrated in Fig. 1.b. Global and local deflections are respectively represented by δg and δl, while ∅ denotes the central flexural angle of the aluminum column, as depicted in Fig. 1.c. These identified parameters offer a comprehensive understanding of the deformation characteristics on the loaded side of the tested configurations.

Fig. 1 Schematic representation of deformation parameters of the aluminum column showing: (a) blast-loaded area of interest, (b) cross-section deformation parameters (c) global and local deflection investigated parameters.

Table 1 Deformation parameters of the aluminum column

configuration	d_1(mm)	d_2(mm)	b(mm)	a(mm)	l(mm)	δ_g(mm)	δ_l(mm)	$\varnothing$(°)
Bare aluminum column	85.1	204.2	73.8	56.2	110.8	112.3	48.1	171
30mm- PU foam-1mm thin outer skin	96.3	161.7	74.2	61.0	116.7	107.6	44.9	173.0
50mm- PU foam-1mm thin outer skin	80.3	150.3	77.0	72.2	107.5	106.4	33.7	177.0
100mm- PU foam-1mm thin outer skin	59.4	121.9	94.7	83.9	101.1	104.1	18.8	178.5

It is shown based on the experimental results that the deformation parameters are greatly influenced by the application of the different layers of PU foam wrapped around the aluminum column. Notably, a reduction of 21%, 26% and 40% in radial width d_2 is observed for the aluminum columns enveloped with PU foam of thicknesses 30 mm, 50 mm, and 100 mm, respectively.

The levels of flattening and radial deformation experience a significant reduction in the wrapped columns compared to their bare counterparts. The inclusion of a 30mm PU foam layer yields a significant reduction in deflection at the central point δ_l, amounting to a reduction ratio of 6.7%. Furthermore, when the layer thickness is increased to

100 mm, the deflection value further diminishes to 18.8 mm, showcasing a substantial 58.1% reduction compared to the case with a 30mm PU layer thickness.

Based on the experimental findings, it is shown that the application of different layers of PU foam around the aluminum column has an impact on deformation parameters. Specifically, there is a reduction in radial width (d_2) for the aluminum columns enveloped with PU foam of varying thicknesses. The reductions are 21%, 26%, and 40% for PU foam thicknesses of 30 mm, 50 mm and 100 mm, respectively.

The levels of flattening and radial deformation exhibit a significant decrease in the wrapped columns compared to their bare counterparts. Introducing a 30mm PU foam layer results in a 6.7% reduction in deflection at the central point (δ_l). Moreover, increasing the layer thickness to 100 mm leads to a further reduction in the deflection value to 18.8 mm, indicating a 58.1% reduction compared to the case with a 30mm PU layer thickness. These results underscore the efficacy of the PU foam layers in minimizing deformation and enhancing the structural performance of the aluminum columns under the applied loading conditions.

REFERENCES

[1] "Report on Improvised Explosive Device (IED) Incidents. Available online." https://reliefweb.int/report/world/report-improvised-explosive-device-ied-incidents-january-june-2023 (accessed Jul. 17, 2023).

[2] "START. National Consortium for the Study of Terrorism and Responses to Terrorism," *Global Terrorism Database.*, 2017. https://www.start.umd.edu/gtd/ (accessed Jul. 20, 2023).

[3] H. Ousji, B. Belkassem, M. A. Louar, B. Reymen, L. Pyl, and J. Vantomme, "Experimental Study of the Effectiveness of Sacrificial Cladding Using Polymeric Foams as Crushable Core with a Simply Supported Steel Beam," *Adv. Civ. Eng.*, vol. 2016, 2016, doi: 10.1155/2016/8301517.

[4] J. Lu, Y. Wang, X. Zhai, X. Zhi, and H. Zhou, "Impact behavior of a cladding sandwich panel with aluminum foam-filled tubular cores," *Thin-Walled Struct.*, vol. 169, p. 108459, 2021, doi: https://doi.org/10.1016/j.tws.2021.108459.

[5] L. Jing, Z. Wang, V. P. W. Shim, and L. Zhao, "An experimental study of the dynamic response of cylindrical sandwich shells with metallic foam cores subjected to blast loading," *Int. J. Impact Eng.*, vol. 71, pp. 60–72, 2014, doi: https://doi.org/10.1016/j.ijimpeng.2014.03.009.

[6] L. Jing, Z. Wang, and L. Zhao, "Dynamic response of cylindrical sandwich shells with metallic foam cores under blast loading — Numerical simulations," *Compos. Struct.*, vol. 99, pp. 213–223, 2013, doi: 10.1016/j.compstruct.2012.12.013.

[7] S. Vavilala, P. Shirbhate, J. Mandal, and M. D. Goel, "Blast mitigation of RC column using polymeric foam," *Mater. Today Proc.*, vol. 26, no. xxxx, pp. 1347–1351, 2019, doi: 10.1016/j.matpr.2020.02.273.

[8] X. Li, P. Zhang, Z. Wang, G. Wu, and L. Zhao, "Dynamic behavior of aluminum honeycomb sandwich panels under air blast : Experiment and numerical analysis," *Compos. Struct.*, vol. 108, pp. 1001–1008, 2014, doi: 10.1016/j.compstruct.2013.10.034.

[9] S. Palanivelu *et al.*, "Performance of a sacrificial cladding structure made of empty recyclable metal beverage cans under large-scale air blast load," *Appl. Mech. Mater.*, vol. 82, pp. 416–421, 2011, doi: 10.4028/www.scientific.net/AMM.82.416.

[10] A. Aminou, B. Belkassem, O. Atoui, L. Pyl, and D. Lecompte, "Numerical modeling of brittle mineral foam in a sacrificial cladding under blast loading," *Mech. Ind.*, vol. 24, p. 27, 2023.

[11] A. Jonet, B. Belkassem, O. Atoui, L. Pyl, and D. Lecompt, "Blast Mitigation Using Brittle Foam Based Sacrificial Cladding: A Feasibility Study," 2019.

[12] H. Ousji *et al.*, "Air-blast response of sacrificial cladding using low density foams: Experimental and analytical approach," *Int. J. Mech. Sci.*, vol. 128–129, pp. 459–474, 2017, doi: 10.1016/j.ijmecsci.2017.05.024.

ID 68
EVALUATION OF TENSILE PROPERTIES OF INPLANE AUXETIC COMPOSITE LAMINATES

Cristiano Veloso[1](*), Carlos Mota[2], Luís Nobre[3], João Bessa[4], Fernando Cunha[5], Raúl Fangueiro[6]

[1, 2, 3, 4, 5, 6] Fibrenamics, University of Minho, Guimarães, Portugal

[6] Center for Textile Science and Technology, University of Minho, Guimarães, Portugal

(*) Email: cristianoveloso@fibrenamics.com

ABSTRACT

The concept of a metamaterial – a material with properties not commonly found in Nature – has recently gained importance within the realm of material science. Auxetic metamaterials, i.e. materials with NPR (Negative Poisson's ratio), are at the root of various enhancements in shear, fatigue, fracture, and energy absorption response. The auxetic effect can be achieved in a composite laminate via the manipulation of its plies' angular structure, and amplified with high material anisotropy. This work focuses on the experimental evaluation of the tensile properties of IP (In-plane) auxetic composite laminates, and their comparison to the properties of conventional, i.e. PPR (Positive Poisson's ratio), lay-up sequences.

INTRODUCTION

Auxetic metamaterials exhibit a unique material behavior due to their NPR (Negative Poisson's ratio), causing a synchronous orthogonal compression or dilation. This response, in the event of an impact, forces the material to flow towards the indented area, increasing local resistance. Auxeticity can be generated in composite laminates with unidirectional laminae, in a two-dimensional framework: IP (In-plane), referring to NPR on the face plane (*x-y*) of the laminate, and TTT (Through-the-thickness) auxeticity, implying NPR along the laminate's thickness plane (*x-z* or *y-z*). Auxetic laminates present desirable properties for impact, especially in the low-velocity range where they can limit the propagation of internal delamination when compared to conventional lay-up sequences (Veloso et al., 2023).

For both cases, higher material anisotropy, i.e. E_x/E_y and E_x/G_{xy} ratios, augments the auxetic effect, hence why carbon and aramid fibers are preferred to glass for the construction of such laminates (Harkati et al., 2007). Regarding the design of IP auxetic laminates, bidirectional ($[(\theta_1/\theta_2)_n]_S$) lay-ups with balanced (similar number of plies oriented at both angles) symmetric architecture are of common practice, with the minimization of v_{xy} for C/E (Carbon/epoxy) laminates occurring typically with laminae oriented in the range around θ_1 = 15°, θ_2 = 62°, depending on the type of carbon and epoxy used (Miki & Murotsu, 1989; Zhang et al., 1999). The minimization of the IP Poisson's ratio leads to the maximization of the TTT Poisson's ratio, and vice-versa.

In the present work, tensile tests were performed, in a MTS Exceed E45 tensile testing machine using videoextensometry techniques, to 16-ply T300/8500 C/E $[(26°/76°)_4]_S$ auxetic laminates, and results where compared against the control sequences $[(0°/90°)_4]_S$ and $[0°]_{16}$. Composite plates were prepared with a target fibre volume fraction of 0.65, yielding, approximately, a 4 mm thickness. Specimens were prepared in accordance with the ISO 527-4 standard and coated with matte spray. Two points were marked in the *x* and *y* directions within the gauge length, each at an 8 mm distance to the centerline, totaling a 16 mm gauge length. G/E (Glass/epoxy) end tabs were applied to prevent gripping issues.

RESULTS AND CONCLUSIONS

Figure 1 exhibits the obtained elastic modulus in the longitudinal direction, E_x, and the IP Poisson's ratio, v_{xy}, for T300/8500 C/E *[(0°/ 90°)_4]_S*, *[(26°/ 76°)_4]_S* and *[0°]_16* specimens.

a)   b)
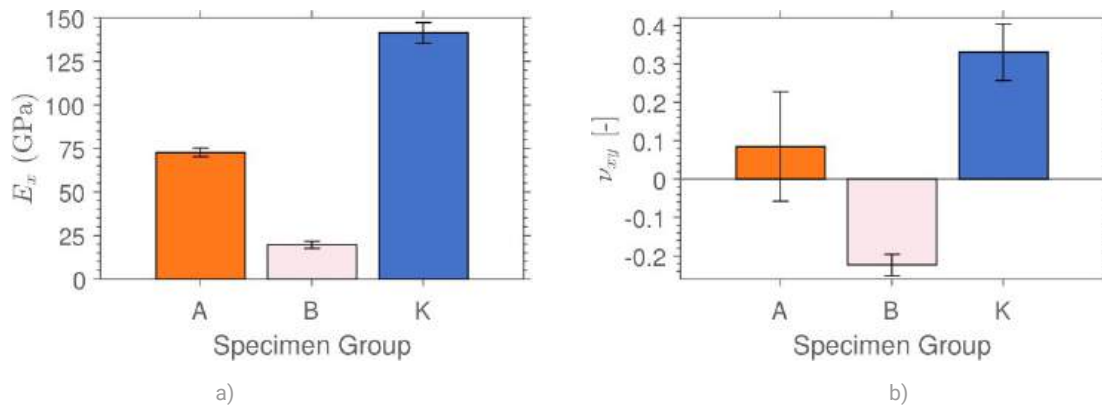
Fig. 1 Tensile properties of T300/8500 C/E [(0°/ 90°)_4]_S, [(26°/ 76°)_4]_S and [0°]_16 laminates (Specimen groups A, B and K, respectively): a) Longitudinal elastic modulus, E_x b) IP Poisson's ratio, v_xy.

Table 1 summarizes the elastic (E_x and v_{xy}) and failure (X^f, UTS (Ultimate tensile strength)) tensile properties of tested laminates, along with elastic property predictions calculated via an in-house developed MATLAB algorithm. The *[(26°/ 76°)_4]_S* lay-up sequence achieved IP NPR, as expected, with an inherent comparative reduction in E_x. In addition, a substantial reduction of the UTS in the auxetic lay-up was verified, corroborating with previous findings on the topic (Lin & Wang, 2022), due to the combined effect of a large IP NPR with a large TTT PPR, inducing larger strain mismatches and leading to premature failure.

Table 1 Predicted (P) and experimental (E) tensile properties of the tested C/E T300/8500 laminates.

Specimen group	E_x (GPa)		v_{xy}		X^f (GPa)
	P	E	P	E	
A (*[(0°/ 90°)_4]_S*)	79.51	72.73	0.02500	0.08476	755.7
B (*[(26°/ 76°)_4]_S*)	23.15	19.57	-0.2069	-0.2233	124.0
K (*[0°]_16*)	150.6	141.3	0.2482	0.3301	1494

Thus, it was possible to experimentally validate the IP auxetic *[(26°/ 76°)_4]_S* configuration, along with its predicted inherent loss of elastic properties. Further studies on the topic are necessary, particularly to analyse the issue of lower UTS in auxetic laminates.

REFERENCES

[1] Veloso, C., Mota, C., Cunha, F., Sousa, J., & Fangueiro, R. (2023). A comprehensive review on in-plane and through-the-thickness auxeticity in composite laminates for structural applications. *Journal of Composite Materials*.

[2] Harkati, H., Bezazi, A., Scarpa, F., Alderson, K., & Alderson, A. (2007). Modelling the influence of the orientation and fibre reinforcement on the Negative Poisson's ratio in composite laminates. *IMRI: Journal Articles (Peer-Reviewed), 244*.

[3] Miki, M., & Murotsu, Y. (1989). The Peculiar Behavior of the Poisson's Ratio of Laminated Fibrous Composites. *JSME International Journal. Ser. 1, Solid Mechanics, Strength of Materials, 32*(1), 67–72.

[4] Zhang, R., Yeh, H.-L., & Yeh, H.-Y. (1999). A Discussion of Negative Poisson's Ratio
Design for Composites. *Journal of Reinforced Plastics and Composites, 18(17)*, 1546–1556.

[5] Lin, W., & Wang, Y. (2022). *Effect of Negative Poisson's Ratio on the Tensile Properties of Auxetic CFRP Composites*.

ID 69

DAMAGE MONITORIZATION CAPACITY OF BALLISTIC COMPOSITES AFTER A HIGH-VELOCITY IMPACT: SMART SHIELDS

Daniel Barros[1](*), Luís Nobre[2], Carlos Mota[3], João Bessa[4], Fernando Cunha[5] and Raul Fangueiro[6]

[1, 2, 3, 4, 5, 6] Fibrenamics – Institute for Innovation in Fiber-based Materials and Composites, Campus de Azurém, University of Minho, 4800-058 Guimarães, Portugal.

[6] Center for Textile Science and Technology, University of Minho, Guimarães, Portugal

(*) Email: danielbarros@fibrenamics.com

ABSTRACT

This study aims to assess the ability of monitoring post-high-speed impact damage in multilayer composites by leveraging the piezoresistive effect. The multilayer composite panels were fabricated using aramid woven fabrics impregnated with thermosetting epoxy resin, incorporating two additional layers of carbon (CF) and glass (GF) fibers woven fabrics at the surface and bottom of the panel. To quantify the resistivity of each panel, a digital multimeter was employed, connected to the CF and GF layers, were pre-functionalized with 1, 2 and 3% graphene nanoplates (GNPs) based on prior research findings. Resistivity evaluation for each panel involved measuring the electrical signal in the CF and GF functionalized layers for panels both before and after impact with varying penetration depths. Subsequently, the obtained resistivity data were analysed and correlated with the extent of damage caused by each panel.

INTRODUCTION

The escalating frequency of international conflicts and acts of terrorism has heightened tensions between nations, often culminating in warfare that predominantly unfolds on the battlefield. Consequently, substantial investments are directed towards the advancement of novel offensive and defensive systems, continuously enhancing their efficacy. The imperative development of sophisticated protective systems has become essentially for soldiers and military vehicles from high-velocity impacts capable of compromising structural integrity and functioning of vehicles as well as the life of the soldier. For this purpose, multilayer composites have been devised utilizing a diverse array of materials, including ceramics, metals, and high-performance fibers for protection against ballistic and explosion impacts [1]. While these protective shields effectively mitigate the impact of threats, assessing post-impact damage and verifying sustained performance pose significant challenges. Therefore, it is thus advantageous to integrate ballistic shields capable of indicating whether the panel maintains its intended specifications following one or multiple impacts. Carbon-based materials (CBMs), owing to their electrical conductivity, finding application in high-performance technologies, such as aerospace applications. They are instrumental in development of smart materials and solutions, particular in sensor technologies. CBMs, including particles such as carbon nanotubes (CNTs) or GNPs, can be applied in the form of filaments/fabrics, such as carbon fibers. Taking advantage of electrical conductivity of CBMs facilitates the creation of sensors for detecting damage or strain through resistivity and piezoelectricity measurement [2].

Various research groups have explored methods for damage detection based on electrical resistance measurement and piezoelectric effects. These approaches may involve embedded sensors within the solution or the using of CBMs that, through piezoelectric properties, enable the measurement of strain or changes in electrical resistivity to localize impact-induced damages [3]. Self-sensing mechanisms via resistivity and piezoresistive effect can be achieved using electric conductive fibers or, in non-conductive materials, through functionalized with con-

ductive particles. The resultant electrical signals can be transmitted via conductive fibers or, post-functionalization, through contact between the various conductive particles, creating a semi-conductor where higher resistivity values are observed [4].

RESULTS AND CONCLUSIONS

The main objective of this work was to fabricate multilayer aramid composite panels incorporating conductive layers comprised of carbon and glass fibers (sourced from CastroComposites) functionalized with GNPs (from Graphnest) in 1, 2 and 3wt%, and added into a flexible matrix by mechanical mixing. The aramid (also from CastroComposites) was impregnated using an epoxy resin (from Resinex) and the composite were prepared by hot pressing molding at 80ºC for 15 minutes. The various combinations resulting from these preparations are illustrated in figure 1.
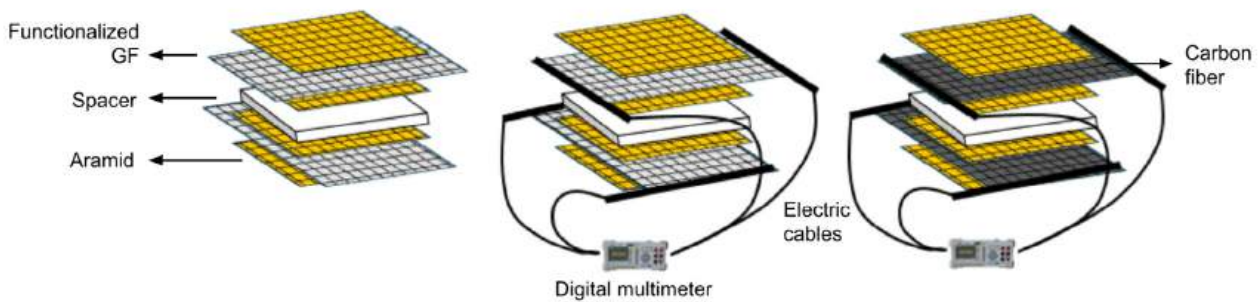
Fig.1 – Scheme of the different compositions developed.

After production, all samples were subjected to penetrating impacts at different heights, according to adaptation of the ASTM D7136 standard "Standard Test Method for Measuring the Damage Resistance of a Fiber-Reinforced Polymer Matrix Composite to a Drop-Weight Impact Event". Then, through the piezoresistive effect, it was evaluated the resistivity measured to each panel after different penetration depths, to verify the possibility of damage evaluation, using a digital multimeter. Finally, the implementation of a monitoring and calculation system was planned to enable the percentage-based assessment of the panels' capacity to resist further impacts.

REFERENCES

[1] Y. Jiang, K. Qian and Y. Zhang, "Experimental characterization and numerical simulation of ballistic penetration of columnar ceramic/fiber laminate composite armor," Materials & Design, vol. 224, 2022.

[2] H. Rocha, C. Fernandes, N. Ferreira, U. Lafont and J. P. Nunes, "Damage localization on CFRP composites by electrical impedance tomography," Materials Today Communications , vol. 32, 2022

[3] S. Nonn, M. Schagerl, Y. Zhao and S. Gschossmann, "Application of electrical impedance tomography to an anisotropic carbon fiber-reinforced polymer composite laminate for damage localization," Composites Science and Technology, vol. 160, pp. 231-236, 2018.

[4] M. Sannamani, J. Gao, W. Chen and T. Tallman, "Damage detection in non-planar carbon fiber-reinforced polymer laminates via electrical impedance tomography with surface-mounted electrodes and directional sensitivity matrices," Composites Science and Technology, vol. 224, 2022.

ID 70

ELECTROSPUN MEMBRANES BASED ON PAN/AC FOR AIR FILTRATION AND ACTIVE DEGRADATION OF MICROORGANISMS

Joana M. Rocha[1], Rui P. C. L. Sousa[1], Joana C. Araújo[1], Sofia M. Costa[1], Vasco Pontes[1], Wilson Antunes[2], Raul Fangueiro[1], Diana P. Ferreira[1,*]

[1]Centre for Textile Science and Technology (2C2T), University of Minho, Guimarães, Portugal

[2]Centro de Investigação da Academia Militar (CINAMIL), Unidade Militar Laboratorial de Defesa Biológica e Química (UMLDBQ, Instituto Universitário Militar), Av. Dr. Alfredo Bensaúde, 1849-012 Lisboa, Portugal

(*) Email: diana.ferreira@det.uminho.pt

ABSTRACT

COVID-19 pandemic has increased the demand for new materials with high filtration efficiency and active degradation of microorganisms. In this work, electrospun membranes based on polyacrylonitrile (PAN) and cellulose acetate (CA) were developed and optimized. The functionalization of these membranes with metal oxide nanoparticles (NPs) was carried out. The produced membranes were characterized by Attenuated Total Reflection Fourier Transform Infrared (ATR-FTIR), Field Emission Scanning Electron Microscopy (FESEM), Energy Dispersive Spectroscopy (EDS), Ground State Diffuse Reflectance (GSDR), Thermogravimetric analysis (TGA), Water Contact Angle (WCA), mechanical assays, water vapor**,** and air permeability**.** The filtration efficiency and the antimicrobial activity were also studied. These fibrous materials show potential to be applied as active filtration layers on a multi-layer facemask prototype.

INTRODUCTION

The development of facemasks with high filtration efficiency and microorganisms' degradation has become a widely studied field in the past few years, mostly due to the high demand for these materials caused by the COVID-19 pandemic (Naragund, 2022). New materials with enhanced filtration ability, along with multifunctionality and biodegradability, are pursued. Besides, the active degradation of microorganisms is an important feature to avoid their penetration through the mask (Ji, 2021).

Electrospinning is one of the most used techniques to manufacture active layers of nanofiber for facemask applications. Its versatility, wide range of spinnable materials and a good cost-effectiveness ratio, makes it a promising technique for a large array of applications (Costa, 2022). Electrospun membranes are characterized by their small diameters, from nanometers to micrometers, their high surface-to-volume ratio, high porosity, easy surface functionalization, and high flexibility to tune the shape and size, making these structures very attractive for the development of high-performance filters (Haider, 2018). The functionalization of electrospun membranes with metal oxide nanoparticles (NPs) is a growing field. NPs can provide new features to these materials, such as the degradation of chemical/biological harmful agents (Araújo, 2021).

Polyacrylonitrile (PAN) is a synthetic polymer commonly used on the production of electrospun membranes, due to its mechanical, thermal, and chemical stability. Cellulose acetate (CA) is a natural polymer with high interest due to its biocompatibility. The combination of these two polymers can join promising properties for the development of filtration layers. Herein, the development and optimization of PAN/CA electrospun membranes are reported. The functionalization of the membranes with metal oxide NPs was also approached, in order to achieve active filtration. Characterization of all the membranes was carried out by ATR-FTIR, FESEM, TGA, WCA, EDS, GSDR, mechanical assays, water vapor**,** and air permeability**.** Filtration efficiency and antibacterial activity were also evaluated.

RESULTS AND CONCLUSIONS

The membranes were produced by electrospinning using a 150 mm needle-collector distance, a needle diameter of 0.61 mm, a 30 kV applied voltage, a feed rate of 1 mL/h, and a static collector. The polymeric formulation contained PAN and CA in a ratio of 10:1. All membranes were functionalized with different metal oxide NPs with several concentrations (0.5, 1 and 3 % (w/v)). Fig. 1 shows FESEM images of the electrospun membranes.
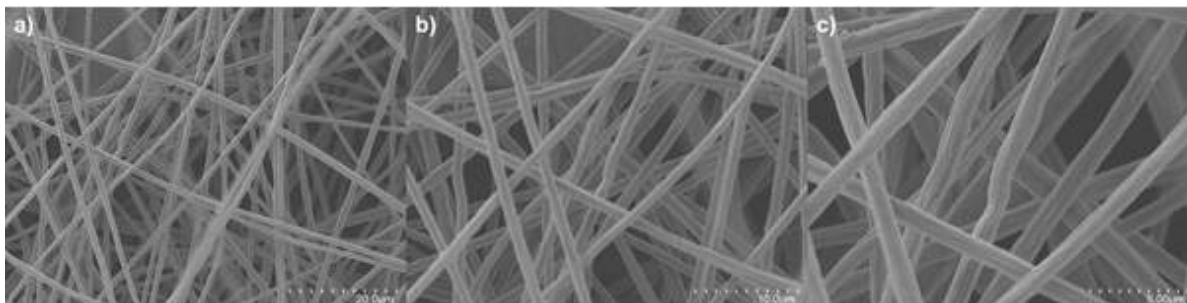
Fig. 1 FESEM images of PAN/CA electrospun membranes in different magnifications (a) 20 µM (b), 10 µM, and (c) 5 µM.

The formation of defect-free electrospun fibers was successfully accomplished. ATR-FTIR show the typical C≡N peak from PAN at 2243 cm^{-1}, but also confirms the presence of CA with peaks at 1055, 1238, and 1367 cm^{-1}. TGA shows the main degradation processes occur between 280 and 450 ºC. Further studies will be conducted to assess the influence of the introduction of NPs in filtration and antibacterial activities. Additionally, the application of the developed membrane as an active filtration layer on facemask prototypes will be studied.

ACKNOWLEDGMENTS

REFERENCES

[1] V. S. Naragund and P. K. Panda, "Electrospun nanofiber-based respiratory face masks—a review", *Emergent Mater.*, vol. 5, no 2, pp. 261–278, 2022.

[2] S. Ji, *et al.*, "ZnO/Ag nanoparticles incorporated multifunctional parallel side by side nanofibers for air filtration with enhanced removing organic contaminants and antibacterial properties", *Colloids Surf. A: Physicochem. Eng.*, vol. 621, pp. 126564, 2021.

[3] S. M. Costa, *et al.*, "Antibacterial and biodegradable electrospun filtering membranes for facemasks: an attempt to reduce disposable masks use", *Appl. Sci.*, vol. 12, pp. 67, 2022.

[4] A. Haider, S. Haider, I. K. Kang, "A comprehensive review summarizing the effect of electrospinning parameters and potential applications of nanofibers in biomedical and biotechnology", *Arab. J. Chem.*, vol. 11, pp. 1165–1188, 2018.

[5] J. C. Araújo, R. Fangueiro, D. P. Ferreira, "Protective multifunctional fibrous systems based on natural fibers and metal oxide nanoparticles", *Polymers*, vol.13, pp. 2654, 2021.

ID 71
THE IMPACT OF ZINC OXIDE AND GRAPHENE-BASED NANOPARTICLES ON THE CHEMICAL AND BIOLOGICAL PROTECTION OF 3D KNITTED STRUCTURES

Liliana Leite [1(*)], **Vânia Pais**[1], **João Bessa**[1], **Fernando Cunha**[1], **Cátia Relvas**[2], **Noel Ferreira**[2], **Raul Fangueiro**[1,3]

[1] Fibrenamics – Institute for Innovation in Fiber-based Materials and Composites, Campus de Azurém, University of Minho, 4800-058 Guimarães, Portugal

[2] A. Ferreira & Filhos, Rua Amaro de Sousa 408, 4815-901 Caldas de Vizela, Portugal

[3] Center for Textile Science and Technology, University of Minho, Campus de Azurém, 4800-058 Guimarães, Portugal

[(*)] Email: lilianaleite@fibrenamics.com

ABSTRACT

Chemical Protective Clothing (CPC) is essential to prevent severe consequences when there is a risk of exposure to harmful substances. This study investigates the use of zinc oxide and graphene-based nanoparticles to enhance the protection of 3D knitted structures against chemical and biological threats, employing antibacterial assays and chemical resistance tests for evaluation. The results show that both nanoparticles have a positive impact on the protective properties, with zinc oxide standing out the most, especially for biological protection.

INTRODUCTION

The accessibility to the development and diffusion of warfare agents has experienced a notable upswing, primarily driven by technological innovation and the widespread dissemination of knowledge on a global scale (Singh, 2020). Chemical Protective Clothing (CPC) stands out as a crucial component in this panorama. CPC is important in scenarios with a large spectrum of exposure, covering areas such as military and law enforcement operations, laboratory personnel, and the day-to-day operations within the chemical industry (Mao, 2014). Three-dimensional (3D) fibrous structures have emerged as a promising textile approach for the development of CPC, making it possible to achieve multilayer systems with one-step manufacturing and the purposeful placement of different fibers and yarns to specific locations on the structure, consequently increasing its protection capacity. Additionally, nanotechnology has emerged as a promising way to develop protective fabrics with unique capabilities such as UV protection, antibacterial characteristics, and chemical resistance (Antunes, 2022). This work aims to study the impact of zinc oxide and graphene-based nanoparticles on the chemical and biological protection of functionalized 3D knitted structures. The structure itself was developed to promote physiological comfort and protection. Polymeric formulations of 2 % (w/v) of zinc oxide (ZnO) and graphene nanoplatelets (GNPs) were prepared and applied by knife-coating on the 3D knit. The samples were then characterized to evaluate their protection performance and comfort properties. For biological protection, antibacterial assays were conducted with Gram-negative (*Escherichia coli*) and Gram-positive bacteria (*Staphylococcus aureus*), measuring the bacterial growth after 1h and 24h. For chemical protection, tests were performed to evaluate the ability of the materials to repel and resist the penetration of acidic and basic chemical solutions.

RESULTS AND CONCLUSIONS

The results showed that the ZnO functionalization had a significant impact on the protection performance of the fabrics. For S. aureus (Figure 1a), bacterial growth was significantly lower for the condition where ZnO was used.

However, GNPs showed values similar to the controls, indicating a lack of antibacterial activity. The results for E. coli (Figure 1b) showed that the fibrous structures functionalized with ZnO or GNPs inhibited the growth of these bacteria. Following the conclusions made for S. areus, ZnO exhibited a higher antibacterial performance for gram-negative microorganisms. Regarding chemical protection, the results (Table 1) showed a high resistance to penetration and a high repellence efficiency for H2SO4, with both samples displaying the maximum level of performance (level 3) for both measurements. Concerning textile behavior in contact with NaOH, the results presented also showed a level 3 penetration and repellence performance for the functionalized knits under evaluation. When compared to the control sample, the outcomes obtained showed an important increase in performance, which is central to ensuring the protection of end users.

This study demonstrates significant differences in the protective qualities of knits when employing ZnO nanoparticles. Compared to GNPs, the antibacterial mechanism of action of ZnO may be more effective for the bacteria under study. On the other hand, graphene has a natural tendency to aggregate, which could compromise functionalization and subsequent activity.
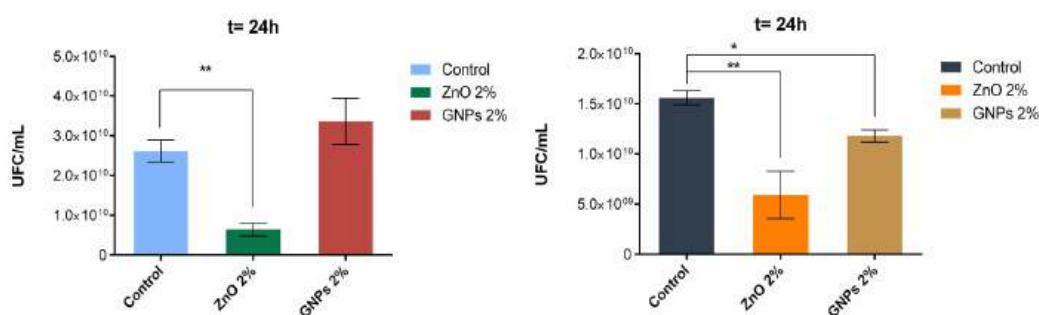
Fig. 1 Evaluation of the antibacterial activity for a) Staphylococcus aureus ATCC 6538 and b) Escherichia coli ATCC 25922 of knitted samples functionalized with zinc oxide nanoparticles (ZnO) and graphene nanoplatelets (GNPs) at a concentration of 2 % (w/v), after 24 hours of incubation at 37 ºC and 200 rpm. The controls refer to an untreated knitted structure.

Table 1 Values of penetration and repellency performance levels attributed according to ISO 14325 for polyester knits functionalized knitted samples functionalized with zinc oxide nanoparticles (ZnO) and graphene nanoplatelets (GNPs) at a concentration of 2 % (w/v).

	H_2SO_4 30% (v/v)		NaOH 10% (w/v)	
	Penetration Performance Level	Repellence Performance Level	Penetration Performance Level	Repellence Performance Level
Control	2	1	1	1
ZnO 2 %	3	3	3	3
GNPs 2 %	3	3	3	3

REFERENCES

[1] J. C. Antunes, I. P. Moreira, F. Gomes, F. Cunha, M. Henriques, and R. Fangueiro, "Recent Trends in Protective Textiles against Biological Threats: A Focus on Biological Warfare Agents" *Polymers*, vol. 14, no. 8, pp. 1–32, 2022.
[2] N. Mao, "High performance textiles for protective clothing" in *High Performance Textiles and Their Applications*. Woodhead Publishing, 2014, pp. 91–143.
[3] V. V. Singh, M. Boopathi, V. B. Thakare, D. Thavaselvam, B. Singh, "Protective equipment for protection against biological warfare agents" In *Handbook on Biological Warfare Preparedness*. Academic Press, 2020, pp. 173–194.

ID 72

EVALUATING THE CHARACTERISTICS OF SANDWICH COMPOSITE STRUCTURES UNDER QUASI-STATIC LOADING

Opukuro David-West[1](*), **Anish Girish Advani**[1]

[1, 4, 5] Materials & Structures Research Group, School of Physics, Engineering and Computer Science, University of Hertfordshire, Hatfield, United Kingdom, AL10 9AB.

(*) Email: o.david-west@herts.ac.uk

ABSTRACT

The integrity of composite structures used in aircraft is crucial and is regularly a subject of discussion. Sandwich composite panels with carbon fibre reinforced laminate skin and flax fibre reinforced laminate skin; both with hemp as the core material were subjected static loading test of 10 mm/min indenter speed. The carbon fibre skin panels were more tolerant to the loading, but the flax fibre skin panels although with lower peak load did not show interlaminar failure like delamination in the response.

INTRODUCTION

Engineered structures made of composite materials designed for specific requirements have gained applications in various industries, including the aviation sector. The present awareness to protect the environment has now triggered the consideration of materials that are environmentally friendly, sustainable, and renewable without a compromise on the integrity. Hence, the development of novel hybrid and sandwich structures will help to achieve the balance between a specific strength application and percentage of renewable resources in the content.

The process of hybridisation enables one component to complete what is lacking in the other within the structure. Chitturi et al [1] manufactured layered composite structures using glass fabric and polycarbonate sheet and achieved the reduction in weight compared to glass fibre reinforced composite. Also, the inclusion of the polycarbonate improved the impact strength. Sarwar et al [2] conducted tests on Kevlar/Flax/epoxy hybrid and Flax/epoxy composites and observed that hybridisation improved the strength and stiffness. While Zhua et al [3] presented results about the crushing characteristics of composite tubes made aluminium and carbon fibre reinforced polymer under static and dynamic tests.

The development of solutions leading to better damage management, lighter and with minimal impact on the environment is still a topic of discussion. This study is based on the experimental analysis of sandwich composites made of synthetic and natural fibre as reinforcements. The findings are intended to serve as pointers in practical design applications.

RESULTS AND CONCLUSIONS

Sandwich composite plates made of cured carbon fibre reinforced ([0/30/60/90/30/60/0] and [0/30/60/90]s) and flax fibre reinforced ([0/30/60/90]s and [0/±45/90]s) composite skin and hemp fibre core manufactured by hand lay-up were tested under the quasi-static loading rate of 10 mm/minute using the instrumented Tinus Olsen universal testing machine. The boundaries of the test samples were firmly clamped during the test.

In Fig. 1 is a representative image of the tested sandwich composite with carbon fibre reinforced epoxy composite skin; part of the rear ply can be seen broken. The behaviour of all the four plates tested under the static loading of a 12 mm indentor are presented in Fig. 2; as can be seen the peak loads are from the carbon fibre reinforced plates. The data plotted in Fig. 2 were normalised with the sample thickness. This prImarily is due to the strength

of this type of fibre compared to flax. The drops in load is primarily because of failure such as matrix crack, fibre breakage and delamination, but significant here is the very long sharp drop in load from 2160 N/mm to 775 N/mm for [0/30/60/90/30/60/0] skin plate and 2302 N/mm to 1115 N/mm for [0/30/60/90]s skin panel, which happens within the hemp core material. This is very significant and can serve to absorb shock and prevent catastrophic failure; hence the effectiveness of this action can be improve by increasing the core thickness.

Fig. 1 Tested carbon fibre reinfoced skin sandwich plate.
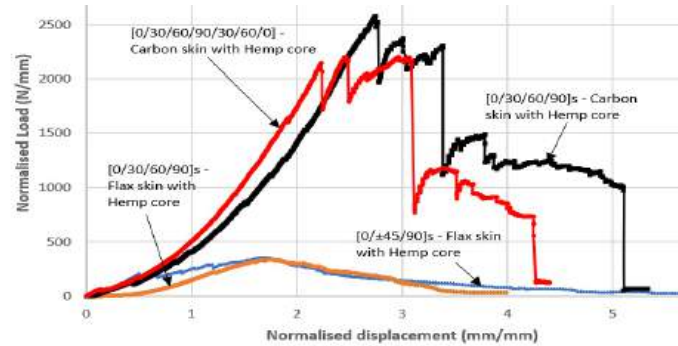
Fig. 2 Normalised load – displacement plots of the tested sandwich composites.

Fig. 3 Tested flax fibre reinfoced skin sandwich plate.
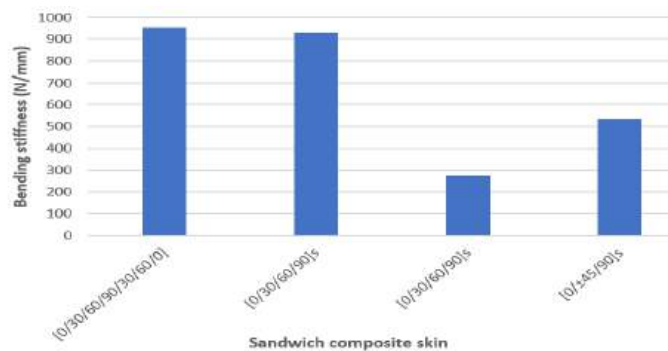
Fig. 4 Comparison of the composite panels bending stiffnesses

In Fig. 3 is a rear end image of tested flax fibre reinforced composite panel, showing the breakage of fibre within the loading zone; but the peak loads are much lower as shown in Fig. 2. Hence, this is recommended for secondary components subjected to low level loads. The bending stiffnesses of the panels are compare in Fig. 4 and as expected the highest values are from the ones with carbon fibre skin reinforcements. The ±45 plies presence in the [0/±45/90]s flax laminate skin induced better bending resistance compared to the spiral arrangement of the [0/30/60/90]s flax laminate skin panel.

REFERENCES

[1] S. K. Chitturi, A. A. Shaikh, Al. H. Makwana, Static analysis of thermoset-thermoplastic-based hybrid composite. International *Journal of Structural Integrity, Vol. 11 No. 1, 2020*, pp. 107-120.

[2] A. Sarwar, Z. Mahboob, R. Zdero, H. Bougherara, Mechanical characterization of a new Kevlar/Flax/epoxy hybrid composite in a sandwich structure. Polymer Testing 90 (2020) 106680.

[3] G. Zhua, J. Liao, G. Sunb,, Q. Li, Comparative study on metal/CFRP hybrid structures under static and dynamic loading, *International Journal of Impact Engineering 141 (2020)* 103509.

ID 73
BALLISTIC RESISTANCE OF MODULAR PROTECTIVE SANDWICH PANELS

Petr Hála[1][(*)], Jiří Mašek[2], Alexandre Perrot[3], Přemysl Kheml[4], Radoslav Sovják[5]

[1, 4, 5] Faculty of Civil Engineering, Czech Technical University in Prague, Czech Republic

[2] SPOLCHEMIE, a.s., Ústí nad Labem, Czech Republic

[3] SYNPO , a.s., Pardubice, Czech Republic

[(*)] Email: petr.hala@fsv.cvut.cz

ABSTRACT

A novel ballistic system has been devised for specialized applications, including designated checkpoints, fortified posts, and mobile city barriers. This system comprises lightweight, easily manipulable panels endowed with interlocking mechanisms for seamless assembly, forming a ballistic structure. The adaptability of the system allows for the creation of diverse configurations, such as free-standing walls or enclosed structures with tetragonal or hexagonal bases. The construction process, executed by a mere two individuals, is expeditious and devoid of the necessity for technological interruptions or heavy machinery. The initial panel iteration, fabricated entirely from high-performance fiber-reinforced concrete (HPFRC), exhibited a drawback wherein projectile impacts resulted in potentially hazardous debris dispersion. This study introduces an innovative sandwich panel featuring glass/epoxy (G/E) or aramid/epoxy (A/E) layers and a polyurethane (PU) coating to reduce weight and mitigate fragmentation.

INTRODUCTION

Fig. 1 depicts panels constructed from HPFRC and the resultant structures. Mára et al. (2020) subjected these panels, or the entire system, to various tests, including bending, shearing, punching, blasting, and ballistic assessments. Their findings concluded that the panels demonstrated adequate resistance against blasts and ballistic threats. Subsequent research by Hála et al. (2023a) revealed that coating HPFRC panels with PU effectively prevented scabbing and narrowed the fragment beam on the front. This contribution proposes a novel panel design featuring a sandwich structure comprising an HPFRC core, additional G/E or A/E layers, and PU coatings.

Fig. 1 Mobile Ballistic Barrier Comprising Bulletproof Panels (Hála et al., 2023b)

The proposed sandwich structure comprises an HPFRC core with 1.5% volume of fibers, additional glass (INTER-GLAS™ twill 2/2) or aramid (Twaron®, twill 2/2) / epoxy (CHS-EPODUR® 582-0542) composite layers, and polyurethane coatings with a 30% weight of filler. The polymeric layer is glued to the HPFRC core with a high performance structural epoxy adhesive. HPFRC and epoxy composites contribute to penetration resistance, with HPFRC being cost-effective. Epoxy composites and PU serve to reduce fragmentation, with PU offering economic advantages. Through meticulous design of these three materials, considering their thickness and positioning in the sandwich structure, lightweight and cost-effective bulletproof panels can be manufactured.

Ballistic testing, following the European standard (EN 1522:1998), was conducted on the designed sandwich

RESULTS AND CONCLUSIONS

Table 1 presents the thicknesses of individual layers in sandwich panels meeting European ballistic class requirements. The areal density of the final panels ranged from 94 kg/m^2 to 189 kg/m^2. Values in italics, untested, are derived from the design for higher classes. Fig. 2 illustrates results obtained by numerical methods using the LS-DYNA solver. The color in the figure indicates damage to the HPFRC, with the red areas being completely damaged.

Table 1 The thicknesses of individual layers in sandwich panels meeting European ballistic class requirements

	FB1	FB2	FB3	FB4	FB5	FB6	FB7
Polyurethane	2×5	2×5	2×5	2×5	2×5	2×5	2×5
Glass/Epoxy	2×3	2×3	2×3	2×3	2×3	2×3	2×3
HPFRC	30	30	30	30	40	60	70
Total	46	46	46	46	56	76	86
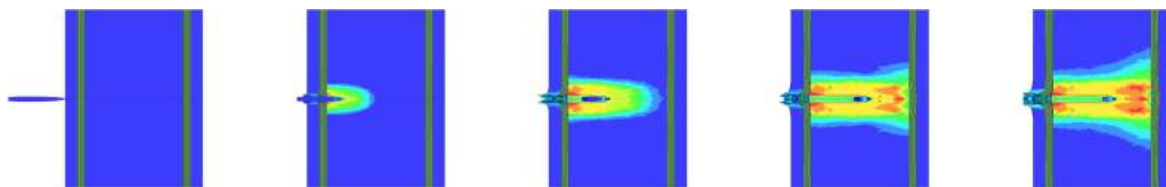
Fig. 2 Simulation of a 5.56×45 projectile penetrating the sandwich panel

Our results show that the panels designed in this way are mobile, bulletproof, with scabbing being completely eliminated. In the prospective future work these panels will be applied exposed to explosion and their design will be optimized to resist blast and increase their cost effectivity.

ACKNOWLEDGEMENTS

REFERENCES

[1] Mára, M., Talone C., Sovják, R., Fornůsek, J., Zatloukal, J., Kheml, P. & Konvalinka, P. (2020). Experimental Investigation of Thin-Walled UHPFRCC Modular Barrier for Blast and Ballistic Protection. Applied Sciences, vol. 10, no. 23, p. 8716.

[2] Hála, P., Perrot, A., Vacková, B., Kheml, P., & Sovják, R. (2023a). Experimental and numerical study on ballistic resistance of polyurethane-coated thin HPFRC plate. Materials Today: Proceedings, vol. 93, no. 4, pa. 607-613

[3] Hála, P., Kheml, P., Perrot, A., Mašek, J. & Sovják, R. (2023b). Lightweight Protective Sandwich Structure with UHPC Core. International Interactive Symposium on Ultra-High Performance Concrete 3(1): 16.

[4] Windows, doors, shutters and blinds - Bullet resistance - Requirements and classification, EN 1522, European Committee for Standardization, Brussels, Belgium, 1999.

[5] Livermore Software Technology Corporation. (2020). LS-DYNA Version 11.2. Livermore, CA: Livermore Software Technology Corporation.

ID 74
MECHANICAL BEHAVIOR SIMULATION OF POLYMER BONDED EXPLOSIVE AT MESO SCALE BY NUMERICAL MANIFOLD METHOD

Ge Kang[1(*)], Peng-wan Chen[1]*

[1]Stake Key Laboratory of Explosion Science and Technology, Beijing Institute of Technology, Beijing 100081, China;
[(*)] Email: 6120220277@bit.edu.cn

ABSTRACT

In the present work, based on the PBX meso-structures with highly-filled grains, the numerical manifold method is utilized to simulate the meso-scale mechanical response of PBX at different loading levels. The effects of strain rates and temperatures on the meso damage morphology of PBX are studied. The damage evolution laws caused by interfacial debonding and micro-cracks in the meso structure are analyzed. Based on their isotropic assumption, the macroscopic equivalent damage evolution equations caused by these mesoscale damages are derived respectively.

INTRODUCTION

Polymer bonded explosives (PBX) is a kind of multi-phase composite material consisting of the polymer binder and highly-filled grains along with interfaces among the binder and grains. The filled ratio (volume fraction) of the grains is around 92.7% [1], while the binder's content is very low. The modulus among the binder and grains exist significant difference [2]. The soft binder make PBX absorb most of the deformation energy when it is under service, while the hard grains make failures easier to develop along the weaker grain/binder interfaces. Therefore, the polymer binder, filled-grains and their interfaces all have significant effects on the mechanical properties of PBX. In the present work, a continuous-discontinuous coupled numerical method, (numerical manifold method, abbreviate NMM [3]), is developed and applied. Due to its superiority, NMM theory has been developed rapidly [4]. To further simulate the meso-mechanical response of PBX under complicated loading levels, by adding the relative constitutive model of PBX single-phase material (grains and polymer binder), interfacial cohesive model and the fracture criterion into the NMM program framework, a series of mesoscopic simulations of PBX meso-structures, with the highly-filled grains (>90%), are carried out under different strain rates and temperatures. The deformation and failure mechanisms of PBX, and the mechanical response law of PBX under complicated loading levels are investigated.

RESULTS AND CONCLUSIONS

Tensile failure morphology of meso-structure under five typical different strain rates are displayed in Fig.1. The changes of strain rates can result in the change of the final failure position (failure bank). Under uniaxial tensile condition, the failure mode of the meso structure mainly is the interfacial debondings, which is similar to the results of relevant experimental observations. The crack propagation path mainly develops along the grain interface at the meso-scale. Through the analysis of the microscopic morphology of the tensile fracture surface, it can also be seen that the complete grains are pulled out from the binder and convex particles and concave are formed. At the same time, transgranular fracture can occur in some special grains during the tensile loadings, and the reason for the phenomenon is related to the forming conditions and load environment of the PBXs.

Generally, the grains with initial internal defects (such as microcracks, voids, etc.) are more prone to be fractured. The changes of elastic modulus E, ultimate strength σ_m and strain ε_m corresponding to σ_m at different strain rates and different temperatures are statistically analyzed, as shown in Table 1.

Table 1. Three mechanical property parameters at different strain rates with T = 25 °C.

Strain rates (/s-1)	E (/GPa)	σm (/MPa)	εm
0.001	1.038989	1.294245	0.013939
0.01	1.161857	1.374873	0.011617
0.1	1.420531	1.450694	0.010941
1	1.638285	1.498770	0.009860
10	1.790512	1.576239	0.009054
100	1.986679	1.673671	0.004769
300	3.175062	1.770388	0.004497
500	4.052736	1.825838	0.004168
700	4.965221	1.866457	0.003792
1000	8.329041	1.918683	0.003632

(a)   (b)   (c)   (d)   (e)
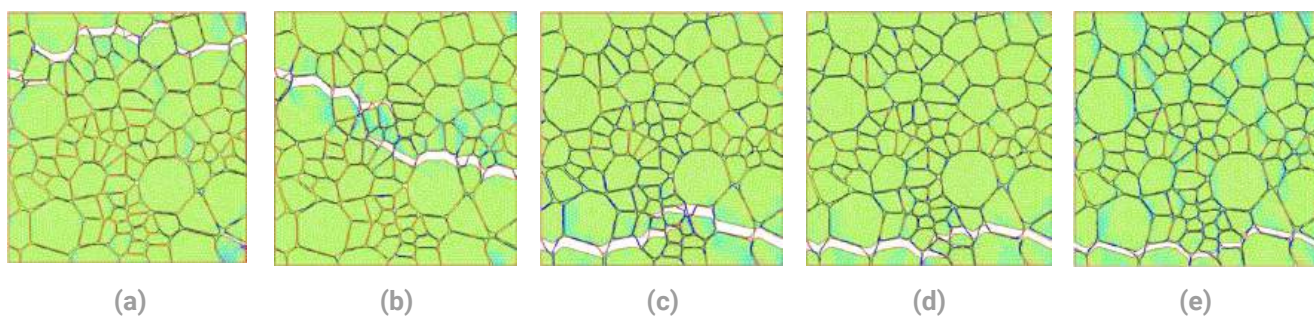
Fig.1 Tensile failure morphology at different strain rates at T = 25 °C, (a) 0.001 s-1, (b) 1 s-1, (c) 100 s-1, (d) 700 s-1, (e) 1000 s-1

Overall, in this study, the NMM program framework was improved, and the mechanical properties of PBX explosives at different strain rates and temperatures were analyzed. The effects of different loading conditions on the mesoscopic fracture mechanism of explosives were discussed. Based on the mesoscopic damage form of explosives, the macroscopic damage evolution equation of explosives was established.

REFERENCES

[1] D.J. Benson, P. Conley, "*Eulerian finite element simulations of experimentally acquired HMX microstructures*", Model. Simul. Mater. 7(3), 1999, 333-354.

[2] C. Yu, L. Yang, H.Y. Chen, Y.H. Qin, T.L. Wang, W. Sun, C.W. Wang, "*Microscale investigations of mechanical responses of TKX-50 based polymer bonded explosives using MD simulations*", Comput. Mater. Sci. 172, 2020, 109287.

[3] G.H. Shi, "*Discontinuous deformation analysis: a new numerical model for the statics and dynamics of block systems*", Eng. Computation, 9(2), 1992, 157-168.

[4] X.M. An, G.W. Ma, Y.C. Cai, H.H. Zhu, "*A new way to treat material discontinuities in the numerical manifold method*", Comput. Method. Appl. M. 200(47-48), 2011, 3296-3308.

ID 75
SIMPLE MECHANOCHEMICAL SYNTHESIS OF TRANSITION METAL HYDRIDES FOR ENERGY STORAGE APPLICATIONS

Marek Polański[(1*)]**, Iwona Wyrębska**[1],

[1,] Military University of Technology, Warsaw, Poland

[(*)] Email: marek.polanski@wat.edu.pl

ABSTRACT

Here we demonstrate surface wear-activated spontaneous reactions of transition metals (titanium, vanadium, niobium, hafnium, zirconium, tantalum) alloys with hydrogen at room temperature. Those metals, in the form of powders, are converted into hydrides just by intensive mixing under hydrogen pressure in a planetary mill without grinding media. The reaction starts when oxide impurities are removed from metallic particles. Thermal gravimetric measurements and XRD phase analysis show that metals convert to stoichiometric hydrides or their mixtures. The most intensive research was performed for titanium and its alloys [1] which were found to react with hydrogen as well. The Ti-5553 (β) alloy can react more readily than grade 5 Ti (Ti-Gd5) (α') and grade 2 Ti (Ti-Gd2). After hydrogenation, titanium alloy particles remain coherent. The method seems cost-effective for synthesizing titanium hydride and other hydrides and producing spherical hydrogenated alloyed powders for additive manufacturing titanium foams.

INTRODUCTION

Popular alternatives to pressurized gas vessels and cryogenic liquid are solid-state hydrogen storage materials (SSHSM). Their hydrogen packing volumetric capacity doubles that of hydrogen cryogenic liquid phase. Recent research by Patel et al. [2] found that reactive milling without grinding balls can activate and hydrogenate difficult-to-activate materials like FeTi. Intensive mixing of the alloy under hydrogen pressure cleaned particle surfaces and allowed full hydrogenation.

This work showed that titanium and its alloys and other transition metals can be hydrogenated in a planetary mill by mixing titanium powder under hydrogen pressure without grinding media. Once begun, the reaction proceeds spontaneously and appears to be blocked only by the particle surface oxide layer. It takes longer for titanium powder kept in air before the experiment to react because the reaction seems to be dependent on particle surface cleanliness. The reaction was observed in both α' and β titanium alloys.

RESULTS AND CONCLUSIONS

The results showed a significant ability of using the method for synthesis of transition metal hydrides. Figure 1 shows both hydrogen absorption curves as well as thermogravimetric curves of desorption of hydrogen from syntehsized samples. All investigated elements were able to absorb (at room temperature) and desorb (at elevated temperature) a significant amount of hydrogen. Figure 2 shows the XRD patetrns of synthesized materials proving the existence of stoichiometric hydrides.
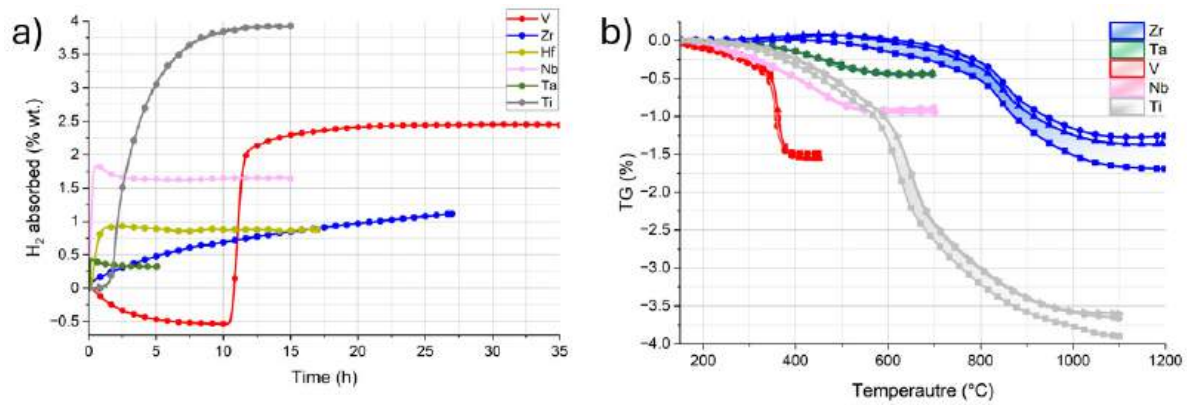
Fig. 1 a) Hydrogen absorption curves during mixing under hydrogen in planetary ball mill (500 rpm, 50-100 bar); b) Thermogravimetric curves of decomposition of synthesized hydrides.
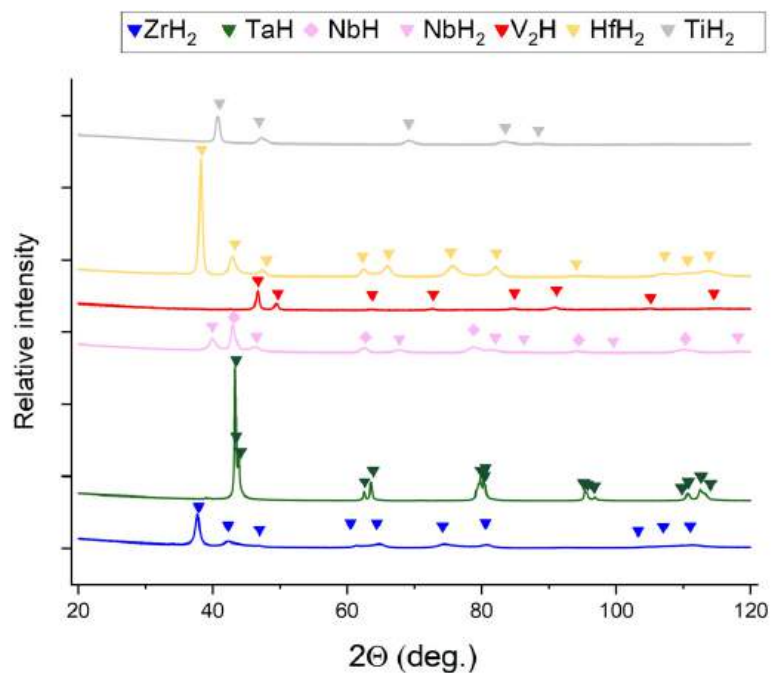
Fig. 2 X-Ray diffraction patterns of synthesized hydrides.

By using this simple synthesis method, great potential of conversion of transition metals and alloys into energy storage materials may be utilized.

REFERENCES

[1] I. Wyrębska, K. Tomczyk, D. Siemiaszko, D. Zasada, J. Dworecka-Wójcik, M. Pęska, R. Chulist, S. Koter, M. Polański, Spontaneous room temperature reaction of titanium and its alloys with hydrogen during self-shearing reactive milling, Chemical Engineering Journal, 485 (2024).

ID 76

TUNING THE MECHANICAL PROPERTIES OF CRCOFEMNNI HIGH ENTROPY ALLOY VIA COLD SPRAY ADDITIVE MANUFACTURING ASSOCIATED WITH HEAT TREATMENT

Bemechal Tsegaye Mengiste[a], Ali Arab[b]*, Yansong Guo[a], Yinze Lei[a], Xiaoshuai Li[a], Pengwan Chen[a], Jing Xie[a]*

[a] State Key Laboratory of Explosion Science and Technology, Beijing Institute of Technology, Beijing, 100081, China
[b] Multidisciplinary Center for Infrastructure Engineering, Shenyang University of Technology, Shenyang 110870, China

[(*)] Email : aarab1362@gmail.com (Ali Arab), jxie@bit.edu.cn (Jing Xie).

ABSTRACT

The CoCrFeMnNi high entropy alloy (HEA) is the most studied HEA because of its excellent combination of strength and ductility. However, despite the advantage of CoCrFeMnNi HEA, its application is limited owing to its low yield strength. In this study, an emerging cold spray additive manufacturing technique was applied to fabricate a bulk CrCoFeMnNi high entropy alloy to improve the yield strength of CrCoFeMnNi. The paper presented an experimental investigation of the microstructure and mechanical properties of the as-sprayed and heat-treated CrCoFeMnNi high entropy alloy samples under compressive loading conditions at different strain rates. Post-heat treatment was applied to tune inter-particle bonding and ductility. Quasi-static compression tests ($0.001\ s^{-1}s^{-1}$) and dynamic impact tests (up to $3900\ s^{-1}s^{-1}$) were carried out on the as-sprayed and heat-treated samples. The as-sprayed samples showed mechanical anisotropic and brittle behavior. However, after heat treatment, the as-sprayed samples exhibited high ductility. This work showed excellent yield and ultimate compressive strength compared to other CrCoFeMnNi high entropy alloy manufacturing methods.

INTRODUCTION

High entropy alloys (HEAs) are emerging novel alloys, mainly constructed from five or more principal elements in an equiatomic or near equiatomic mixture. Unlike conventional alloys, HEAs have excellent physical and mechanical properties, including high hardness, super-conductivity, wear resistance, corrosion resistance, and thermal stability. Among the different HEAs, the extensively studied alloy is CrCoFeMnNi HEA, exhibiting a single-phase FCC solid solution with excellent damage tolerance, relatively low yield stress, superior ductility, and good fracture toughness at ambient and cryogenic temperatures (Cantor, 2021). Owing to the extraordinary behavior of CrCoFeMnNi HEA, different fabrication techniques have been used, such as casting, laser powder-bed fusion (Jin et al., 2022), arc cladding (Wang et al., 2020), etc., to explore its industrial application.

Cold spray additive manufacturing (CSAM) is a new emerging solid-state powder deposition technology for coating, repairing, and near-net shape manufacturing (Yin, Aldwell and Lupoi, 2017). CSAM is a promising method to fabricate high-strength CrCoFeMnNi HEA. CSAM uses high-pressure carrier gases (usually N2 and He) to accelerate the microscopic powder particles on the substrate, which consolidate powders and form highly dense bulk deposits.

RESULTS AND CONCLUSIONS

The as-sprayed vertical and horizontal samples exhibit extraordinary mechanical properties, especially the YS and UCS, compared to any manufacturing methods for this alloy. (Fig.1). The optimum post-heat treatment process

improves the unfavorable mechanical properties of the CSAM deposits. The basic mechanical properties of the as-sprayed and sintered vertical and horizontal samples are listed in Table 1.

Table 1. Basic properties of the as-sprayed and sintered samples

Sample property	As-sprayed	600°C/1h	900°C/1h	1100°C/1h	1200°C/1h	1250°C/1h
Density (g/cm^3)	7.57±0.003	7.58±0.001	7.67±0.002	7.68±0.003	7.73±0.002	7.77±0.01
Rel. Density (%)	95	95	96	96.4	97	97.5
Fraction porosity (%)	11 ± 0.4	10.8 ± 0.1	10.01± 0.2	8.05± 0.03	5 ± 0.3	4 ± 0.2
Hardness (HV)	376.49	370.6	362.7	350.3	190.90	140.92
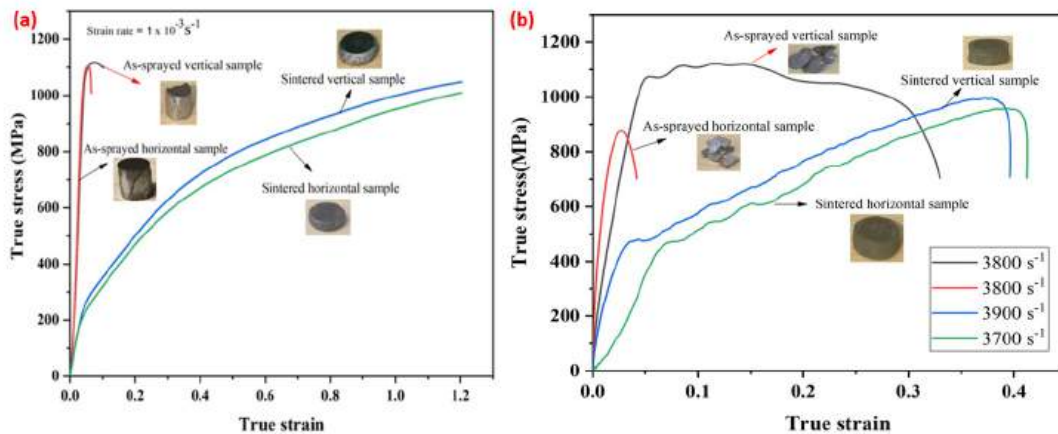
Fig. 1 Compression true stress-strain curve for as-sprayed and sintered HEA samples (a) Quasi-static (b) dynamic at room temperature and different strain rates

The sintered vertical and horizontal samples showed significantly higher than the cast CrCoFeMnNi HEA. Thus, the mechanical performance of as-sprayed deposits is expected to be suitable for structural application.

REFERENCES

[1] Cantor, B. (2021) 'Multicomponent high-entropy Cantor alloys', *Progress in Materials Science*, 120(September 2020), p. 100754. Available at: https://doi.org/10.1016/j.pmatsci.2020.100754.

[2] Jin, M. *et al.* (2022) 'Thermally activated dependence of fatigue behaviour of CrMnFeCoNi high entropy alloy fabricated by laser powder-bed fusion', *Additive Manufacturing*, 51(October 2021), p. 102600. Available at: https://doi.org/10.1016/j.addma.2022.102600.

[3] Kim, Y. and Lee, K. (2022) 'Journal of Materials Science & Technology ultra-strong CrMnFeCoNi high-entropy alloy additively manufactured by laser powder b e d fusion', *Journal of Materials Science & Technology*, 117, pp. 8–22. Available at: https://doi.org/10.1016/j.jmst.2021.12.010.

[4] Wang, C. *et al.* (2020) 'Effect of the macro-segregation on corrosion behavior of CrMnFeCoNi coating prepared by arc cladding', *Journal of Alloys and Compounds*, 846, p. 156263. Available at: https://doi.org/10.1016/j.jallcom.2020.156263.

[5] Yin, S., Aldwell, B. and Lupoi, R. (2017) 'Cold spray additive manufacture and component restoration', *Cold-Spray Coatings: Recent Trends and Future perspectives*, pp. 195–224. Available at: https://doi.org/10.1007/978-3-319-67183-3_6.

ID 77

POLYMER COMPOSITE AND STRUCTURES FOR ENHANCED ELECTROMAGNETIC PROTECTION AND CYBERSECURITY

Sergejs Gaidukovs[1](*), Miks Bleija[1], Oskars Platnieks[1]

[1] Riga Technical University, Faculty of Natural Sciences and Technology, Institute of Chemistry and Chemical Technology, Riga, Latvia

(*) Email: sergejs.gaidukovs@rtu.lv

ABSTRACT

The reported research results address challenges in the electromagnetic defence of critical infrastructure and mission-critical equipment, including potential vulnerability to electromagnetic interference (EMI) and possible loss of mission-critical data, especially in mobile, field-deployable systems that are less protected than static, permanent sites. To achieve this, we develop an innovative toolset of technologies that are lightweight, easy to move, and fast to deploy while still being highly efficient at protecting our data and systems both passively and actively. This includes the development of novel advanced materials shields, electronics and AI cybersecurity technologies. Thus, the goal of the research is to develop a prototype set of tools that provide enhanced electromagnetic protection and cybersecurity in the field by researching and developing innovative lightweight and field-deployable shielding solutions in tandem with AI-based monitoring solutions for electromagnetic and cyber domains that can allow identification of potentially dangerous situations where shielding is not sufficient to prevent data theft or other types of electronic warfare and data or equipment loss is imminent, thus as a last resort can initiate the destruction of secure data drives before the data falls into the wrong hands closing the complete data protection loop strategy: shielding, monitoring, and prevention/data destruction.

INTRODUCTION

The current growing worldwide challenges to defend society from military, cyber and hybrid threats and attacks at National and International levels, demand Government and NATO, to react and develop new strategies to resist and counteract. One of such challenges is cybersecurity and electromagnetic defense of critical infrastructure, as well as mission-critical equipment. The present world relies on safe and secure data transmission to properly function critical infrastructure and beyond. Energy distribution, information and communication systems, transportation, safety, and economic security infrastructures are all vulnerable to electromagnetic interference (EMI). Low-frequency EMI has been well-studied and accounted for in standard policies and procedures, such as those arising from lightning and other sources. However, the high-frequency EMI elimination remains a significant challenge to be solved even nowadays. For example, the growing threat from very small and inexpensive but high-power, high-frequency devices in the hands of terrorist organizations are posing new challenges. Even though static infrastructure has a relatively good set of solutions for these problems, more and more, due to decentralization and the need to respond and operate more rapidly on a global level, a similar grade of protection is required to be deployable in the field, both to passively and actively protect the data of our operations, mislead the enemy and mask our forces and devices. Such use cases require an innovative tool-set of technologies that are lightweight, easy to move and fast to deploy while still being highly efficient at protecting our interests. These current needs provide a significant opportunity to cultivate the development of novel advanced materials and cybersecurity technologies. New advanced materials to assess and alleviate the rising threat of intentional high-power signal interference will significantly contribute. Therefore, improving resilience to electromagnetic effects (e.g., EM attacks) and cyber-attacks in critical infrastructure and mission-critical hardware is required to fill the gap.

Thus, the goal of the current research project is to develop a prototype set of tools that provide enhanced electromagnetic protection and cybersecurity in the field by researching and developing innovative lightweight and field-deployable shielding solutions in tandem with AI-based monitoring solutions for electromagnetic and cyber domains, that together with other sensors can allow identification of potentially dangerous situations where shielding is not sufficient to prevent data theft or other types of electronic warfare, and data or equipment loss is imminent, thus as a last resort can initiate the destruction of secure data drives, before the data falls into the wrong hands, closing the complete data protection loop strategy: shielding, monitoring and prevention/data destruction. The concept of the project is shown in Figure 1 below.
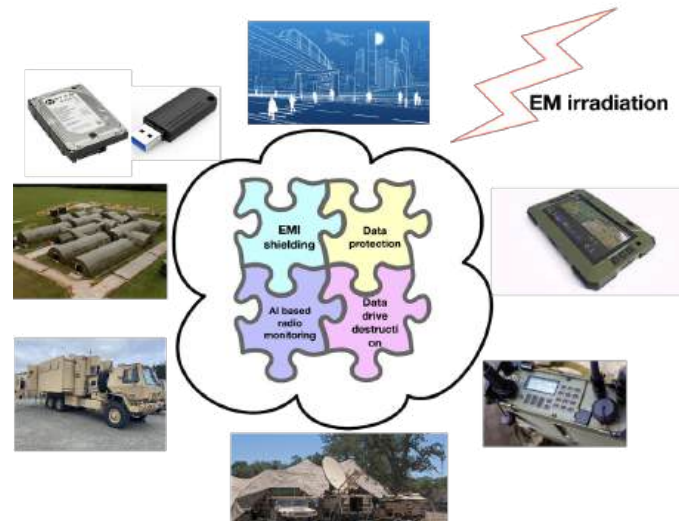

Fig. 1 Concept of the research project

Acknowledgement

ID 79

HEAT TREATMENT OF ADDITIVELY MANUFACTURED 18NI-300 MARAGING STEEL AS A POTENTIAL MATERIAL FOR BLAST AND BALLISTIC PROTECTION ARMOURS

Natalia Rońda[(1*)] **Paweł Płatek**[1] **Marek Polański**

[1] Military University of Technology, Warsaw, Poland

[(*)] Email: natalia.ronda@wat.edu.pl

ABSTRACT

The aim of this research work was to study the effect of ageing temperature on the phase composition and properties of 18Ni-300 maraging steel additively manufactured by LENS® technology. For this purpose, samples were additively produced and heat-treated later on. Microstructure observation and elemental distribution maps were made. In addition, mechanical properties (hardness, yield and ultimate tensile strength and toughness) were measured. Samples after different treatments have shown great differences in properties such as hardness, elongation at break, and yield strength, proving that a 3D printed element can be tuned (heat treated) locally to increase its wear resistance or energy absorption abilities.

INTRODUCTION

Although additive manufacturing seems like a new technology, it has actually turned out that it has been around for several decades. Additive Manufacturing (AM) of metallic materials is the process of creating an object by applying layers of material based on computer-aided design until a desired geometry is achieved [1]. Additive manufacturing has several benefits over subtractive manufacturing techniques such as casting, machining, etc. First, the amount of material required is less than for a traditional subtractive method, where material is removed from a piece until the desired geometry is obtained. Secondly, additive manufacturing allows for production of parts or objects that traditional methods cannot easily do [2-4].

The 18% nickel maraging steels belong to the group of high-alloy steels that exhibit superior strength and toughness compared to most other steels yet have a similar ductility. Due to this unique combination of mechanical properties, maraging steel has become a pivotal material in ballistic applications [5,6]. Heat treatment of maraging steel consists of solution and ageing treatment. This involves heating the steel to an austenitizing temperature followed by cooling to form a fully martensitic microstructure. The final stage following the quenching is the strengthening by ageing. Aging leads to precipitation hardening [7-9].

RESULTS AND CONCLUSIONS

The results showed that the aging temperature significantly affects the phase composition and mechanical properties, as shown in Fig. 1. Increasing aging temperature resulted in an increase of revered austenite. Too high aging temperatures (over-aging) cause deterioration of yield strength and hardness of additively manufactured and hot forged 18Ni-300 maraging steel, which is caused by decomposition of intermetallic precipitation and more reverted austenite. On the other hand, too-low temperatures are not sufficient for the formation of intermetallic precipitation that improves the strength of additively manufactured 18Ni-300 maraging steel.
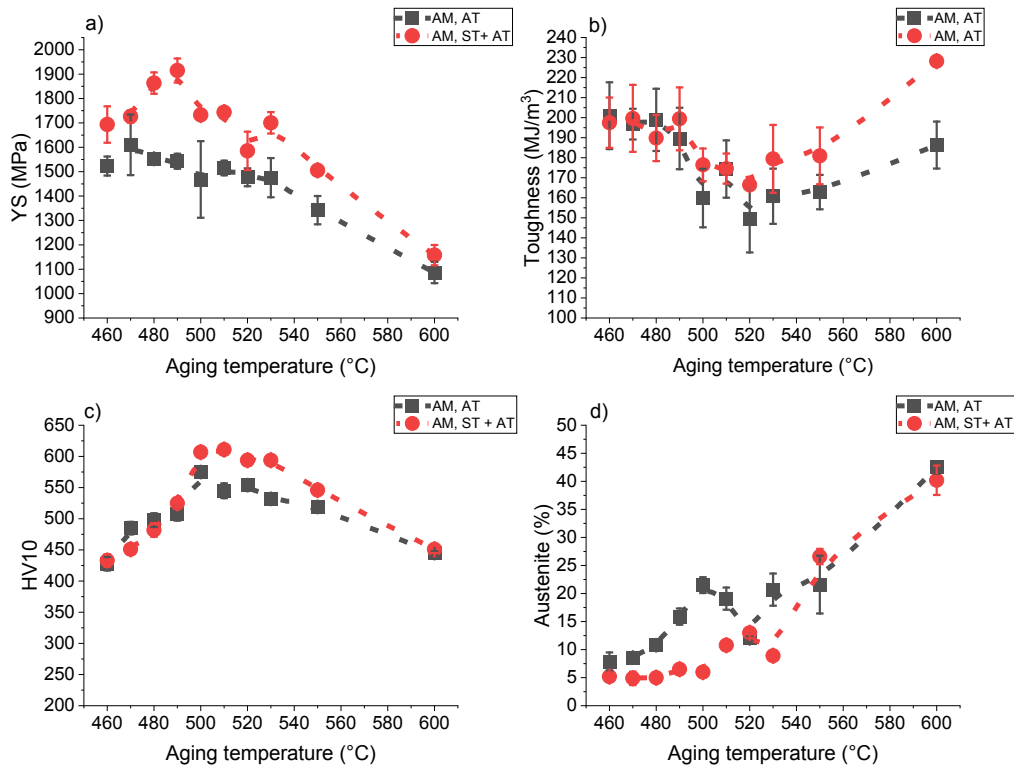
Fig. 1 a) yield strength, b) toughness, c) microhardness, d) austenite content as a function of aging temperature.

REFERENCES

[1] Gardan, J., Additive manufacturing technologies: state of the art and trends. International Journal of Production Research, 2015

[2] Siemiński, P. and G. Budzik, *Techniki Przyrostowe. Druk 3D. Drukarki 3D*. 2015.

[3] Yang, L., et al., *Additive Manufacturing of Metals: The Technology, Materials, Design and Production*. 2017.

[4] Gibson, I., D. Rosen, and B. Stucker, *Additive manufacturing technologies*. Vol. 17. 2015: Springer.

[5] Sha, W. and Z. Guo, *Maraging steels: Modelling of microstructure, properties and applications*. 2009. 1-203.

[6] Mouritz, A.P., *Introduction to aerospace materials*. 2012: Woodhead Publishing.

[7] Sha, W., A. Cerezo, and G.D.W. Smith, Phase Chemistry and Precipitation Reactions in Maraging Steels" Part I. Introduction and Study of Co-Containing C -300 Steel. Metallurgical Transactions A, 1993.

[8] Sha, W., et al., Phase transformations in maraging steels. 2012: Woodhead Publishing Limited.

[9] Shin, J.-H., J. Jeong, and J.-W. Lee, Microstructural evolution and the variation of tensile behavior after aging heat treatment of precipitation hardened martensitic steel. Materials Characterization, 2015: p. 230-237.

ID 82
INNOVATIONS AND TRENDS IN FIELD ARTILLERY WEAPON SYSTEMS

Ricardo Freitas[1](*), **Humberto Gouveia**[1](*)

[1]CINAMIL, Academia Militar, Instituto Universitário Militar, Lisbon, Portugal

(*) Email: freitas.rm@exercito.pt; gouveia.hmr@exercito.pt

ABSTRACT

The aim of this article is to analyse innovations and trends in the evolution of Field Artillery weapon systems. Based on a sample of 118 weapon systems used or under development between 1941 and 2026 by various countries around the world. In terms of the gun barrel, the analysis highlights the evolution of the calibre over time, revealing a clear preference for medium calibre systems, especially the 155mm calibre, which is widely standardised among NATO countries, which implications for interoperability and operational effectiveness. Tube length, which has a direct influence on increasing range and accuracy, shows the demand for longer tubes (50-60 calibres) to meet the contemporary needs of Field Artillery to achieve ever greater ranges. Rate of fire is addressed, considering the relationship between range, precision and destructive power. Mobility becomes a crucial point, with a noticeable shift towards self-propelled wheeled systems, offering greater speed and manoeuvrability. The analysis also covers traction systems, autonomy and organic ammunition supply, emphasising the lack of a clear trend in these aspects. Regarding protection and armour, there is concern for the safety of servicemen, driving the transition from towed to self-propelled systems, with an emphasis on protecting the garrison with armored cabins.

The conclusions highlight technological evolution, the standardisation of the 155mm calibre, the continuous search for the greater range in Field Artillery and the paradigmatic shift towards mobility and garrison protection. The study identifies essential requirements for the development and acquisition of weapon systems, considering contemporary operational needs.

INTRODUCTION

This article aims to analyse the systems developed or under development by the defence industry in terms of Field Artillery weapon systems, in order to identify the main trends that will provide the Field Artillery system with significant improvements in fulfilling its mission, both in terms of its ability to respond in support of the forces it supports and in guaranteeing its own survival. With a brief survey and analysis of developments in the field of Field Artillery, we can easily see that there is a great deal of emphasis on the 155 mm calibre (already used by most NATO countries), a great demand for automated systems that can be operated by small crews. The spectre of today's warfare, where the war is fought by highly mobile units and on very large battlefields, raises concerns that were not felt before. There is a growing need to have highly mobile Field Artillery units capable of accompanying manoeuvre units and thus being able to exercise effective Fire Support. It is of the utmost importance to ensure the protection and safety of the crew while they operate, and more and more priority is being given to the crew operating from the inside. In addition to the need to accompany manoeuvre, there is also the need to cover an increasingly large area of the battlefield, which leads to a preference for systems with tube lengths in the 45 to 52 calibre range.

RESULTS AND CONCLUSIONS

Technological progress in the defence market, especially in the arms and ammunition sector, has seen remarkable advances in recent years. As far as specific Field Artillery weapons and ammunition are concerned, the focus has been on achieving ever greater ranges and precision. As far as the weapon systems themselves are concerned, there is a tendency to focus on mobility, range, crew protection and the standardisation of components with a view to greater interoperability between systems and forces.

The standardisation of the 155 mm calibre among NATO countries shows a concern for the compatibility of resources between different systems and platforms, promotes greater interoperability and directs the defence industries towards the development of weapons and ammunition in this calibre, making it the dominant calibre among the ammunition and weapon systems offered by Field Artillery (Fig. 1 and 2).

The quest to reach ever greater distances in Field Artillery requires constant evolution in weapon systems. One of the crucial elements in this progress is the length of the tube, which has undergone a remarkable transformation over time. The current trend is for longer tubes, generally in the 50 to 60 calibre range (Fig. 3). This increase in barrel length is not only a response to the challenge of reaching greater distances, but also a strategy to improve shooting accuracy.

At the same time, there has been a significant change in the mobility paradigm. Towed weapon systems, once predominant among Field Artillery units, are progressively being replaced by self-propelled guns with a trend towards wheel-mounted guns (Fig. 4). This transition not only allows for greater mobility on the battlefield, but also results in a reduction in the number of servicemen needed to operate a weapon system.

As far as garrison protection is concerned, the most important features are the armour that provides protection against direct fire, grenades or shrapnel from artillery ammunition and the isolation of the cabins with the capacity to defend against nuclear, biological and chemical attacks. The possibility of garrisons being able to operate under the protection of armoured vehicle cabins contributes to their greater safety and consequently results in an increase in the survivability of Field Artillery units.

Fig. 1. Evolution of the Calibre
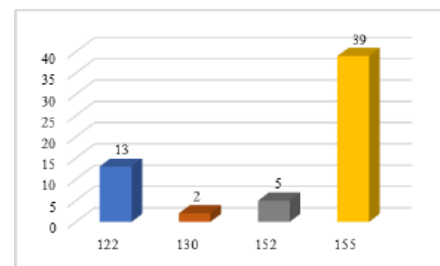
Fig. 2. Average calibre distribution
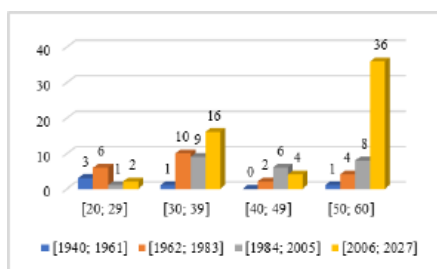
Fig. 3. Tube length evolution
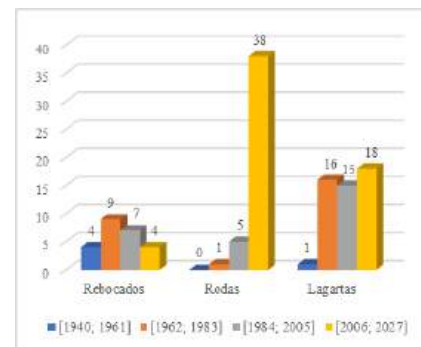
Fig. 4. Traction systems evolution

REFERENCES

[1] USDA (1994). TM 9-2350-311-10 - Operator's Manual for Howitzer, Medium, Self-Propelled, 155mm. Washington DC: U.S. Department of the Army.

[2] Military Today. (s/d). Artillery [online]. [accessed 2024-01-08]. Available from: http://www.military-today.com/artillery.htm.

[3] USDA (2020). FM 3-09 - Fire Support and Field Artillery Operations. Washington DC: U.S. Department of the Army.

[4] Segura, C. (2023). 155mm howitzers: The NATO weapon proving crucial to Ukraine's defense [online]. El País. [accessed 2024-01-08]. Available from: https://english.elpais.com/international/2023-02-20/155mm-howitzers--the-nato-weapon-proving-crucial-to-ukraines-defense.html

[5] Gould, J. (2022). South Korea's status as rising defense player on display at AUSA [online]. Defense News. [accessed 2024-01-08]. Available from: https://www.defensenews.com/digital-show-dailies/ausa/2022/10/11/

ID 88

ECOBALLIFE - RESEARCH IN ECO-DESIGNED BALLISTIC SYSTEMS FOR DURABLE LIGHTWEIGHT PROTECTIONS AGAINST CURRENT AND NEW THREATS IN PLATFORM AND PERSONAL APPLICATIONS

Gilda Santos[1(*)], André Barbosa[1], Iñigo Agote[2], Cristina Guraya Diez[2], José Gisbert Gomis[3], Adriana Juan Polo[3]

[1]CITEVE - Centro Tecnológico das Indústrias Têxtil e do Vestuário de Portugal, V. N. Famalicão, Portugal

TECNALIA - FUNDACION TECNALIA RESEARCH & INNOVATION, Spain

AITEX - Asociación de investigación de la Industria Textil, Alicante, Spain

[(*)] Email: gsantos@citeve.pt

ABSTRACT

ECOBALLIFE is a project funded by the European Defence Fund (EDF) under the 2021 EDF call on Materials and structures for enhanced protection in hostile environments. The project aims to enhance the interoperability and integration of defence systems and capabilities across the EU, strengthening competitiveness and innovation of the European defence industry, and contributing to the strategic sovereignty of the EU. During the 42month run, the project involves 16 partners from EU countries to deliver several outputs and outcomes, such as reports, publications, guidelines and recommendations, tests, prototypes, and demonstrators. ECOBALLIFE showcases the potential and benefits of the EDF for the advancement of European defence and security. The project is coordinated by TECNALIA (Spain) and is managed by the European Defence Agency (EDA) under a Contribution Agreement with the European Commission.

INTRODUCTION

The ECOBALLIFE project will endeavour to achieve the following objectives: i) Strengthen the European defence capabilities and the competitiveness of the European defence industry by identifying, creating, and improving knowledge, new materials and technologies; ii) Research and identify new material concepts and technologies to create proof-of-concept of new personal and military platform protection solutions that can protect against current and emerging threats; iii) Optimise existing solutions to assure reliability throughout their entire life and defining new solutions that increase the level of protection against current and emerging threats; iv) Contribute to advancing European defence and security by providing cutting-edge knowledge and solutions for personal and military platform protection; v) Optimise existing solutions to assure reliability throughout their entire life.

RESULTS AND CONCLUSIONS

To date, all the technical requirements and specifications available of both personal and platform protection systems were obtained and analysed, taking into account 5 aspects: 1) Required ballistic performances (including definition of threats, multi-hit capabilities, applicable standards, etc.); 2) Weights and dimensions limitations; 3) Environmental conditions; 4) Eco-design and life cycle of materials; 5) Protections acceptance criteria (in terms of resistance to ageing, maximum acceptable pre damages in operational field and acceptable production defects).

Table 1 Ballistic levels correspondence between NIJ Standards 0101.07 and 0101.06 (superseded).

Level	Protection System	Test Threat* *According to NIJ Standard 0123.00	Reference Velocity (m/s)* *According to NIJ Standard 0123.00
NIJ HG1 Corresponding to NIJ0101.06 Level II	Soft Armour	9mm Luger FMJ RN 124 grain	398
		.357 Magnum JSP 158 grain	436
NIJ HG2 Corresponding to NIJ0101.06 level IIIA		9mm Luger FMJ RN 124 grain	448
		.44 Magnum JHP 240 grain	436
NIJ RF1 Corresponding to NIJ0101.06 Level III	Hard Armour	7.62x51mm M80 Ball NATO FMJ Steel Jacket 147 +0/-3 grain	847
		7.62x39mm MSC Ball Ammunition Type 56 from Factory 31	732
		5.56mm M193 56 +0/-2 grain	990
NIJ RF2 New intermediate		7.62x51mm M80 Ball NATO FMJ Steel Jacket 147 +0/-3 grain	847
		7.62x39mm MSC Ball Ammunition Type 56 from Factory 31	732
		5.56mm M193 56 +0/-2 grain	990
		5.56mm M855 61.8 ± 1.5 grain	950
NIJ RF3 Corresponding to NIJ0101.06 level IV		30.06 M2 AP 165.7 +0/-7 grain	878

Requirements have been defined for Ballistic performances, including the definition of the main threats to overcome and protection levels, multi-hit capabilities, applicable standards; and Ergonomic constraints, dimensions, comfort and compatibility with other equipment requirements. Table 1 indicates the correspondence between NIJ standards 0101.07 and 0101.06, since the first one introduces new changes and improvements in the way body armour is manufactured and rated.

A Military Protection Research Ecosystem (MPRE) living lab (LL) is envisioned as an arena to collect information from European stakeholders of the military protection systems supply chain and, in turn, to develop new, more advanced protection solutions in military platforms and personal protective equipment. Accordingly, it will hold different group activities, such as workshops, networking sessions, etc; allowing a full definition of new protection systems, their production processes throughout the value chain and the assessment of their durability. The identification of new materials and technologies will allow the creation of specific proof of concepts to define new protection systems for military platforms and military personal protective equipment. The MPRE will comprise stakeholders from several areas, such as public institutions and advisors, defence technologists, military industries, and civil industries, among many others.

To comply with the eco-design objectives (i) high-performance solutions able to protect against current and novel threats, (ii) environmentally friendly processes and products and iii) contribute to the circular economy) for novel personal/platform protection materials to reach, a checklist was elaborated. This first approach is in line with the European Green Deal and, directed at each of the consortium partners/solutions. So far, from the main 5 addressed stages (System design; Production; Logistics & Distribution; Use and End-of-life), results show more challenges to overcome regarding the Logistics & Distribution and End-of-life stages. The consortium will focus on surpassing these difficulties, putting the EU at the forefront of sustainable military technology.

ACKNOWLEDMENTS

ID 89

EMERGING MATERIALS AND CAPABILITIES FOR BIOSENSORS: A ROADMAP FOR DEFENCE

Cláudio Santos[1(*)], Corrado Di Natale[2], Jose Manuel Ramos[3], Jordi Ferre[3], Ferran Sabaté[3], Nuno Correia[1]

[1] INEGI - Institute of Science and Innovation in Mechanical and Industrial Engineering, Porto, Portugal

[2] Department of Electronic Engineering, University of Rome Tor Vergata, Rome, Italy

[3] AITEX - Textile Industry Research Association, Alicante, Spain

(*) Email: cmsantos@inegi.up.pt

ABSTRACT

Biosensor's technologies for defence applications have been the object of interest for a long time, by supporting the development of critical capabilities that range from threat detection to medical diagnostics for military personnel. This paper presents the preliminary findings for a technology roadmap performed with field experts in 2023. Cross-cutting capabilities such as reduced detection time or latency and higher sensitivity of synthetic biosensors have been identified as critical developments in the realm of materials science for biosensors.

INTRODUCTION

Biosensors are widely regarded as chemical sensor where the sensitive material is a biomolecule, such as a protein, an antibody, or a strain of nucleic acids. Biomolecules are used in technological devices to improve their sensitivity and selectivity found in biological processes.

The applications of defense are many, such as the early detection of biological threats (pathogens, chemical agents or toxins), monitoring of troops health, environmental situational awareness (such as in air and water quality in military installations or combat zones), food and water safety of military supplies and rapid diagnostics of infectious diseases or exposure to chemical agents. Biosensors can play a critical role in remote areas with limited resources, where access to laboratory facilities are made difficult.

Given their strategic importance to defense, a technology roadmapping exercise supported by the European Defense Agency and a consortium composed of two European RTOs (AITEX and INEGI) and the University of Rome Tor Vergata. Through a thorough bibliographical survey and a dedicated workshop performed in mid-2023, experts from academia and industry were able to identify critical technologies and capabilities to foster the development of novel applications of biosensors for the military. In addition to this, other externalities comprising ethics, legacy parts and supply chain dependencies from critical raw materials were assessed to evaluate the risk exposure of biosensors development and implementation.

RESULTS AND CONCLUSIONS

The findings of the technology roadmap include several potential technological streams for development from the materials science. Notably, the combination of electrochemical sensors with nanomaterials can improve the accuracy of physiological monitoring and, consequently, the quality of emergency responses [1]. Additionally, the replacement of natural bioreceptors with synthetic receptors made of inorganic materials [2] to improve the durability and resistance of materials, and the enhancement the physical-chemical interaction of the target molecule with the sensor's material aimed at the reduction of detection time or latency were identified as critical developments to be made in biosensors materials.

Still in the field of synthetic bioreceptors, it is well known that their capability to replicate biological process is still limited. Efforts have been made in the design of receptors by making the template matching as in molecular im-

printing or in the Selex procedure used for apatamers design, and in improving the in-silico design of receptors to expand the configuration of receptors for a greater variety of target molecules and microorganisms. The genetic manipulation of organisms is another field of interest, in the sense that these developments can produce biomolecules with altered binding properties.

In terms of supply chain, even if the materials for biosensors are largely available, the integration of biosensors in deployable systems depends, like any other electronic system, from critical raw materials [3] such as antimony, cobalt, manganese, titanium, light and heavy rare earth, tungsten, vanadium, which poses significant dependencies risks due to geopolitical reasons.

Finally, the resulting biosensors technology roadmap indicates the need for the consideration of several emerging technologies, namely from nanotechnology, artificial intelligence and materials science. Interdisciplinarity for the development of biosensors applications in defence is key to further enhance their sensitivity, selectivity, and scalability while ensuring regulatory compliance, ethics and data privacy.

REFERENCES

[1] Finabel. European Army Interoperability Center. The future of biosensors in Europe Defence. 2020

[2] A. Raziq, A. Kidakova, R. Boroznjak, J. Reut, A. Öpik, V. Syritski, Development of a portable MIP-based electrochemical sensor for detection of SARS-CoV-2 antigen, Biosens Bioelectron. 178 (2021). https://doi.org/10.1016/j.bios.2021.113029.

[3] European Comission. Internal market, industry, entrepreneurship, and SMEs: critical raw materials. 2023. Webpage: https://single-market-economy.ec.europa.eu/sectors/rawmaterials/areas-specific-interest/critical-raw--materials_en

ID 92
UNDERWATER TERITORIAL SEA - DEFENSE SURVEYER, UNTES-DES

Vlado Valkovic[1]
[1] CROATIA

ABSTRACT

TBA

ID 93

ENVIRONMENTALLY-FRIENDLY 155-MM INERT ARTILLERY PROJECTILES: ADVANCING ARTILLERY PRACTICE FOR SUSTAINABLE MILITARY TRAINING

Cláudia Macedo[1](*), Humberto Gouveia[2], Ricardo Simoes[3], António Brito[4], José Borges[5]

[1, 2, 5] Centro de Investigação, Desenvolvimento e Inovação da Academia Militar, Academia Militar, Instituto Universitário Militar, Rua Gomes Freire, 1169-203, Lisboa, Portugal

[3] Instituto Politécnico do Cavado e do Ave (IPCA), Campus de Barcelos, Vila Frescainha, 4750810 Barcelos, Portugal

[4] Departamento de Engenharia de Polímeros (DEP)/Instituto de Polímeros e Compósitos (IPC), Campus de Azurém, Universidade do Minho, 4800-058 Guimarães, Portugal

(*) Email: macedo.cdo@exercito.pt

ABSTRACT

The training exercises provide valuable opportunities for the participating units to develop their capability (NATO, 2023). Day-to-day activities include updating and maintaining the military's practices to ensure military proficiency is addressed and provided by appropriate training (USDA, 2012).. The training enhances units' operational readiness by leveraging military capabilities to support training for operations. The exercises provide training in realistic environments, threats, and scenarios, enhancing preparedness from the smallest to the largest unit. Defence industries offer a range of high-performance ammunition in different areas to fulfill the requirements and serve the needs of militaries – all dedicated to helping artillery personnel achieve their critical national and global missions for specific applications (USDA, 2020). Defence industries supply an extensive array of 155 mm ammunition for various missions in an operational training environment (General Dynamics, 2023; USDA, 2003). The 155-mm caliber artillery round, the NATO-standard artillery shell, is one of the most requested artillery munitions for artillery training exercises; hundreds of high-explosive 155-mm artillery shells are consumed for artillery practice applications for soldiers' training and combat, being used in current 155-mm artillery weapon systems (European Defense Agency, 2022).

Ukrainian forces are suffering from a shortage of artillery shells on the front line, prompting some units to cancel planned assaults. There is an urgent need for artillery ammunition. Consequently, European defence companies face a surge in demand in the ammunition area, requiring them to produce more (European Parliament, 2023). The current manufacturing capacity in the European Union sits at approximately 230,000 rounds per annum, an amount that Ukraine uses almost every month - European states have decided to ramp up production capacity in the European defence industry (Rheinmetall, 2023). European countries have been invited to transfer ammunition urgently from their stocks to Ukraine to refill supplies; countries have agreed to procure ammunition rounds jointly (European Defense Agency, 2023).

Demand for 155-mm high-explosive artillery ammunition is very high due to Ukraine's requirements and the need to replenish EU countries' largely empty ammunition depots. Europe's insufficient supply of shells has been a persistent problem due to the cost of combat 155-mm artillery shells. The militaries jointly purchase new ammunition at scale to reduce the cost of 155-mm caliber artillery rounds. The military's joint acquisition of ammunition is time-consuming. The timely availability of 155-mm caliber ammunition is critical to consistently promoting the military's

training exercises. Meanwhile, the militaries and society, in general, are increasingly concerned about the environmental challenges of 155-mm caliber ammunition, i.e., the hundreds of kilograms of high-explosive chemical components in 155-mm artillery shells per training exercise and the heavy metals in the shells' forged steel fragments, contaminating the soil and atmosphere.

An artillery training projectile intending to provide an environmentally friendly round of 155-mm inert artillery projectiles for artillery practice applications for soldiers' training is discussed in this paper — a new cost-saving bimaterial plastic-metal shell for artillery practice applications for military personnel' training exercise. The environmentally friendly round of 155-mm inert artillery projectiles helps to alleviate a shortage of combat highexplosive ammunition, addressing the current shortage of combat 155 mm high-explosive ammunition stocks and attaining NATO's objectives of the combat high-explosive ammunition war reserve.

The 155 mm caliber artillery training projectiles comprise an assembly consisting of a metallic cylindrical body and several parts in plastic materials, e.g., a boattail base, a single rotating band, a bourrelet, and an ogive. The projectile is inert and is fitted with a (dummy) fuze. The ogive has a threaded fuze cavity at the nose. Facilitating the handling, the eyebolt lifting plug is installed in the nose fuze well. The eyebolt lifting plug is removed in firing, and the (dummy) fuze is threaded into the fuze cavity. The deep fuze cavity contains a smoke canister, which visually demonstrates functioning. The projectile's ogive has a plastic band to simulate a bourrelet. The bourrelet on the rear of the ogive encircles the cylindrical body to maintain projectile in-bore centring. The cylindrical body of the projectile consists of a solid projectile body weighted with lead to equal the weight of the service 155mm artillery projectile. The rotating band fitted to the projectile on the body's bottom engages the barrel riffling to spin the projectile for stability in flight. The boattailed base of the projectile is screwed into the projectile body. The plastic boattailed base, a single rotating band, a bourrelet, and an ogive provide the projectile's external geometry, contributing to the aerodynamic forces and moments acting on the symmetric projectile. The solid cylindrical body provides the projectile's weight (90 % of the projectile's weight), contributing to conserving the angular momentum to the trajectory's stability of the artillery projectile (Carlucci & Jacobson, 2017).

The large-caliber artillery training projectile must be a 155-mm artillery round, which large-caliber artillery training projectile must fit larger current conventional weapons to be fired from a 155-mm howitzer. Conducting live firing exercises, the 155-mm artillery training projectile must ensure the operator's firing procedures (handling, loading, and ramming ammunition procedures), e.g., the projectile must be loaded into the weapon chamber using normal loading and ramming procedures, must ballistically match the high-explosive projectile using conventional propelling charges and preserving the use of the procedures and tactics of the exercise control settings (e.g., maintaining the use of the firing table of the 155-mm high-explosive projectiles) to simulate the realistic training at the battery and for forward observer units. The 155-mm training projectile may be considered an equivalent blast accompanying a high-explosive projectile's functioning; it may have an identical bang signature and a similar smoke signature to the 155-mm high-explosive projectile for forward observer training.

The 155-mm artillery training projectile must have an equivalent physical property to conventional 155-mm highexplosive projectiles—the training projectile must have a similar weight and an equal size to conventional highexplosive artillery projectiles to ballistically match the conventional high-explosive artillery projectiles having equivalent precision in its flight environment to an average 155mm conventional high-explosive projectile, preserving the use of the procedures and tactics of the training firing exercise. While many aspects of 155-mm highexplosive ammunition are still under consideration, training projectiles may reflect several benefits to artillery practices.

The artillery round is a 155-mm training projectile without a main high explosive charge; the 155-mm training projectile is less toxic munition than the conventional high-explosive ammunition that poses less risk to the environment to support continued military training; the artillery training projectile contains no high-explosive charge, which makes the projectile safer for the militaries. The 155-mm training round has less practice for storage than conventional 155-mm high-explosive projectiles, and the training projectile has fewer requirements for transport than traditional 155-mm high-explosive rounds. The training projectile without high explosive charge has less risk to the live firing exercises in the warmest months of the year than conventional explosive projectiles, providing less fire risk; the inert 155-mm training round is all-weather availability.

The new cost-saving 155-mm artillery training projectile takes advantage of having an environmentally friendly training projectile at a lower cost than conventional high-explosive rounds.

REFERENCES

[1] Carlucci, D.E., & Jacobson, S.S. (2017). Ballistics: Theory and Design of Guns and Ammunition, Third Edition (3rd ed.). CRC Press.

[2] European Defence Agency. Defence Data 2020-2021: Key findings and analysis. Belgium: Elisabeth Schoeffmann (EDA); 2022

[3] European Defence Agency. Collaborative Procurement. [Internet]. [cited 2024 Feb 02]. Available from: https://eda.europa.eu/webzine/issue25/focus/eda-steps-in-for-a-two-year-fast-track-project-for-155mmartillery--shells

[4] European Parliament: EU legislation in Progress – Act in support of ammunition production. [Internet]. [cited 2024 Feb 02]. Available from: https://eur-lex.europa.eu/eli/reg/2023/1525

[5] General Dynamics: Artillery 155mm M107 HE [Internet]. [cited 2023 Oct 19]. Available from: https://www.gdots.com/munitions/artillery/155m-m107/

[6] NATO Exercises [Internet]. [cited 2023 Oct 19]. Available from: https://www.nato.int/cps/en/natohq/topics_49285Reheinmetall: Rheinmetall wins major artillery ammunition order for Ukraine [Internet]. [cited 2024 Feb 02]. Available from: https://www.rheinmetall.com/en/media/newswatch/news/2023/12/2023-12-04-rheinmetall--wins-artillery-ammunition-order-for-ukraine

[7] USDA. (2003). Army ammunition data sheets artillery ammunition guns, howitzers, mortars, recoilless rifles, grenade launchers, and artillery fuzes. Washington, DC: Department of the Army.

[8] USDA. (2012). Fires. Washington, DC: Department of the Army.

[9] USDA. (2020). Fire Support and field artillery operations. Washington, DC: Department of the Army.

ID 94
IONIC LIQUIDS: A PROMISING DECONTAMINATION METHOD FOR CHEMICAL WARFARE AGENTS

Andreia A. Rosatella[1,2*],Rafaela A. L. Silva[2], Inês Cruz[3], Pedro Neto[3], Paula Lopes[3], Carlos A. M. Afonso[2]

[1] CBIOS - Research Center for Biosciences & Health Technologies, Universidade Lusófona de Humanidades e Tecnologias, Campo Grande 376, 1749-024 Lisboa, Portugal.

[2] Research Institute for Medicines (iMed.ULisboa), Faculdade de Farmácia da Universidade de Lisboa, Av. Professor Gama Pinto, 1649-003 Lisboa, Portugal.

[3] UMLDBQ - Military Laboratorial Unit of Biological and Chemical Defense, Av. Dr. Alfredo Bensaúde, Edifício Lab. Militar, 1º andar , 1849-012 Lisboa, Portugal.

[*] Email: andreia.rosatella@ulusofona.pt

ABSTRACT

Abstract: Chemical warfare agents (CWAs) are still being used as destruction weapons, posing danger not only to military personnel but also to civilian populations, as witnessed in numerous terrorist attacks across different nations. Although, the World's first multilateral disarmament agreement, Chemical Weapons Convention (CWC), prohibited the development, production, and storage of CWAs, there are still occasional reports of their use in certain countries.

INTRODUCTION

In the event of a CWA attack, swift response actions are imperative to mitigate casualties. In such scenarios, the ability to promptly detect and identify CWAs is crucial, but equally pivotal is the thorough decontamination of materials, personnel, equipment, and the entire affected area. Numerous decontamination methods have been reported, however the use of bleach-based decontaminants in the field is still prevalent due to their cost-effectiveness and broad-spectrum efficacy against different CWAs. However, the drawback of these systems include their potential corrosiveness to surfaces, toxicity to human health, and harm to the environment.[1,2]

RESULTS AND CONCLUSIONS

This work reports an innovative approach to CWAs decontamination, centered on novel materials based on Ionic Liquids (ILs). These materials display the capacity to adsorb and absorb CWAs from contaminated surfaces. As proof of concept several ILs were synthesized and rigorously tested as sorbents for CWAs simulants, yielding remarkably high sorption rates.

REFERENCES

[1] 1 C. R. Jabbour, L. A. Parker, E. M. Hutter and B. M. Weckhuysen, Nat. Rev. Chem., 2021, 5, 370−387.

[2] K. Kim, O. G. Tsay, D. A. Atwood and D. G. Churchill, 2011, 5345−5403.

ACKNOWLEDGEMENTS

ID 95

BLAST IMPACT AND STRUCTURAL RESPONSE COMPUTATIONAL MODEL VERIFICATION AND VALIDATION USING SCALED TESTING WITH DIGITAL IMAGE CORRELATION

M. Edward Miyambo[1](*), J. David Reinecke[1], M. Excellent Mokalane[1], T. Pandelani[2], D.V. Von Kallon[3]

[1] Council for Scientific and Industrial Research, Defence and Security Cluster, Pretoria, 0001, South Africa

[2] University of Johannesburg, Department of Mechanical and Industrial Engineering, Johannesburg, 2028

(*) Email: mmiyambo@csir.co.za

ABSTRACT

This paper discusses the importance of understanding material behavior under high-strain rate loading, especially in the field of blast protection where explosive loads are applied at extremely high-strain rates. The goal was to characterize the material response due to explosive loading, determine the elastic/plastic deformation in hulls, evaluate attenuation methods to minimize shock loading, and derive material parameters to enhance computational modeling accuracy. To achieve this, the researchers employ instruments and techniques such as the Split Hopkinson Pressure Bar (SHPB), Universal Tensile Machine(UTM), and Digital Image Correlation (DIC). The DIC rig was designed by the Council for Scientific and Industrial Research (CSIR) to investigate material behavior due to blast loading.

For this research, the mechanical behavior of Aluminium 6082-T6 material was investigated. The quasi-static and high strain rate experiments are conducted on the Aluminium 6082-T6 material to extract the mechanical properties of the material using the universal tensile testing machine and a tensile SHPB apparatus respectively for the development of the constitutive material models.

The simulation results are compared to the 3D DIC experimental results where the structural response of the Aluminium 6082-T6 circular plate was subjected to a blast load of plastic explosive No 4 (PE4). The 3D DIC structural response and the maximum center node displacement results of the Aluminium 6082-T6 are compared to the simulation results. The Aluminium 6082-T6 circular plate material model was developed and simulated using the LS-DYNA Finite Element Analysis (FEA) program.

INTRODUCTION

With the growing dependence of engineers on finite element analysis in design processes, precise material models are essential. Precise material property data are necessary to calibrate finite element material models to ensure the reliability of numerical simulation results. This research aimed to develop a constitutive material model in LS DYNA to simulate the behavior of Aluminium 6082-T6 when subjected to explosive loading.

This material was selected due to the available experimental tensile split Hopkinson pressure bar (TSHPB) data and experimental quasi-static data, which were used as inputs for the development of the constitutive material models in the LS-DYNA software. Three computational models, MAT_003 plastic kinematic, MAT_024 piecewise linear plasticity, and MAT_015 Johnson-Cook constitutive material models ((LSTC), 2011), were used to define the materials used for the circular target plate. The load blast enhance method was used to apply the blast load on the circular target plate and the run time of the simulation was 1 minute and 4 seconds. The three material model simulations were compared to the 3D DIC results. The 3D digital image correlation (DIC) results were obtained

utilizing a technique that involved the use of two high-speed cameras placed in stereo positions, oriented towards the circular plate mounted on the DIC frame. The high-speed cameras were configured to capture the structural deformation of Aluminium 6082-T6 at a sampling rate of 40,000 frames per second, with an exposure time of 100 microseconds.

RESULTS AND CONCLUSIONS

Fig.1, shows the the displacement-time results of the circular target plate and Table 1 shows a comparison of the maximum displacement-time simulation and experimental results. The Finite Element Model (FEM) developed using the MAT_003 and MAT_015 constitutive material model, underestimates the center node displacement-time results when compared to the DIC experimental results by a percentage error of 62% and 46.72%, respectively. The center node's maximum displacement time of the LBE_MAT024 material model exhibited a percentage error of 35.2 % in comparison to the DIC experimental data.
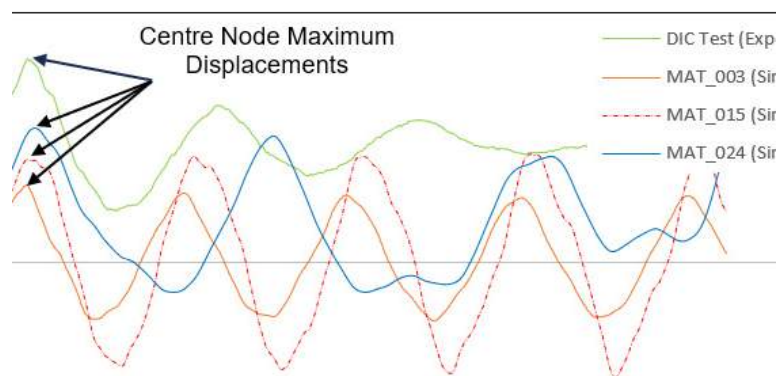
Fig. 1 Circular target plate experimental versus simulation center node displacement-time results

Table 1 Comparison of circular target plate center node displacement-time results

LS-DYNA Constitutive material model	Centre node displacement-time (mm)	Percentage difference (%)
DIC experimental results	24.4	N/A
MAT_003	9.23	62
MAT_015	13	46.72
MAT_024	15.3	35.2

The maximum displacement-time results of the center node, obtained from the MAT_024 constitutive material model, show a better correlation with the experimental results, in comparison to the maximum displacement-time results of the center node obtained from the MAT_003 and MAT_015 constitutive material models.

 Although the load blast enhances method does not require hours to run the circular target plate FEM, the accuracy of the center node maximum displacement-time results extracted from the circular target plate could be improved by implementing the Particle Blast Method (PBM) (Teng & Wang, 2014).

REFERENCES

[1] L. S. T. C. (LSTC), "LS-DYNA Keyword User's Manual," vol. II, pp. -Key Words-R10.0, 2011.

[2] A. Berndt, "A Correlation Study of a Plate Subjected to a Blast Load," Pretoria, 21 August 2018.

[3] L. Shoke, T. Sono and A. Olubambi, "Utilization of ISO 6892:2009 testing standard for determining tensile pro-peties of TM380 mild steel," The Journal of the South African Institute of Mining and Metallurgy, vol. 113, pp. 1-6, April 2013.

[4] T. H and W. J, "Particle blast method (PBM) for the simulation of blast loading," Detroit, 2014.

ID 96
THE PEEL RESISTANCE OF UHMWPE COMPOSITES

O. Banabila[1], N. Alhamed[2], R. Alameri[1], R. Santiago[1], W.J. Cantwell[2].
[1]Advanced Materials Research Center, Technology Innovation Institute, Abu Dhabi, United Arab Emirates.
[2]Aerospace Engineering, Khalifa University of Science and Technology, Abu Dhabi, United Arab Emirates.

ABSTRACT

This paper investigates the peel resistance of ultra-high molecular weight polyethylene (UHMWPE) composites similar to that used in a range of ballistic resistance applications. Thin laminates based on woven UHMWPE composites were manufactured at different pressures and temperatures in order to identify the influence of varying processing conditions on the delamination resistance of these tough composites. This is considered to be an important consideration, given that these parameters may vary within a given structure during the manufacturing cycle. Following this, the influence of crosshead displacement rate and temperature on the peel resistance of these composites is investigated in order to generate data for determining the constants in the Johnson-Cook equation. Finally, the failure processes and mechanisms in these composites are investigated using scanning electron microscopy techniques.

Peel tests on thin laminates manufactured at temperatures between 120 and 135 °C indicated that the delamination resistance of these laminates is insensitive to processing temperature within this manufacturing window. Similarly, tests on laminates prepared using pressures between 20 and 35 MPa did not highlight any processing sensitivity. The influence of varying test conditions was then investigated by conducting tests at temperatures between 23 and 100 °C and crosshead displacement rates between 0.2 and 200 mm/minute. Here, it was observed that the peel strength dropped rapidly as the test temperature was increased due to similar reductions in the yield properties of the PE matrix. In contrast, the peel strength increased steadily as the crosshead displacement rate was increased, again due to rate effects in the polymer matrix. An examination of the fracture surfaces of the failed samples highlighted the presence of significant matrix ductility and fiber fracture in all samples.

KEYWORDS

UHMWPE, Peel testing, Delamination, Composite

ID 98
MECHANICAL RESPONSE OF 3D PRINTED POLYMERIC ORIGAMI HONEYCOMB STRUCTURES

Marcin Sarzynski[1], Pawel Platek[1(*)], Igor Czernichowski[(1)], Pawel Baranowski[(1)]
[1] Military University of Technology Warsaw, Poland
[(*)] Email: pawel.platek@wat.edu.pl

ABSTRACT

This study presents the results of experimental and numerical investigations of the mechanical response of cellular structures manufactured using 3D printing technology. Several variants of honeycomb-based topologies and additional deformation initiators with various geometrical parameters of deformation initiators defined on the lateral surface were produced from PLA thermoplastic material using the FFF 3D printing technique, and then subjected to compression in the in-plane and out-of-plane directions. It was demonstrated that the use of additional initiators significantly reduced the peak of force occurring in the initial period of deformation of the structure in the out-of-plane direction. Moreover, thanks to them, it is possible to homogenize the mechanical response of the structure regardless of the direction of its deformation.

INTRODUCTION

The increasing popularity and accessibility of additive manufacturing techniques have led to a growing interest in regular cellular structures as mechanical energy absorbers. The ability to manufacture structures with complex topologies, along with the simplicity and speed of 3D printing processes and the wide range of available materials (including plastics and metallic alloys), has resulted in numerous noteworthy publications on this subject [1]. Despite the considerable number of published works, there remains an issue with the anisotropic mechanical properties of honeycomb-based structures [2-3]. Depending on the direction of compression loading, these structures exhibit varying mechanical responses: in-plane loading results in a wide range of energy absorption, while out-of-plane loading leads to high stiffness. Therefore, the authors endeavoured to address the anisotropic mechanical properties of the structure by introducing additional deformation initiators on the lateral surface.

RESULTS AND CONCLUSIONS

An assessment of the impact of additional initiators on the deformation process of cellular structure was conducted based on experimental and numerical studies. The initial stage of the investigations involved developing the geometries of the structures presented in Figure 1. Contrary to the typical honeycomb structure, additional initiators with different geometric parameters were defined on their side surfaces. Particular variants of structures were produced using 3D printing technology with PLA thermoplastic material. After production, they were evaluated for geometric accuracy and then subjected to compression tests under quasi-static loading conditions. Based on these tests, the mechanical response was obtained in the form of force-deformation curves, allowing for the definition of the effectiveness of various structure variants in terms of energy absorption. The next stage of the research involved computer simulations conducted using the LS-Dyna solver. The proposed numerical model replicated the conditions of the experimental test. Data and parameters for constitutive model for describing the PLA material were determined based on additional tests for characterizing its mechanical properties.
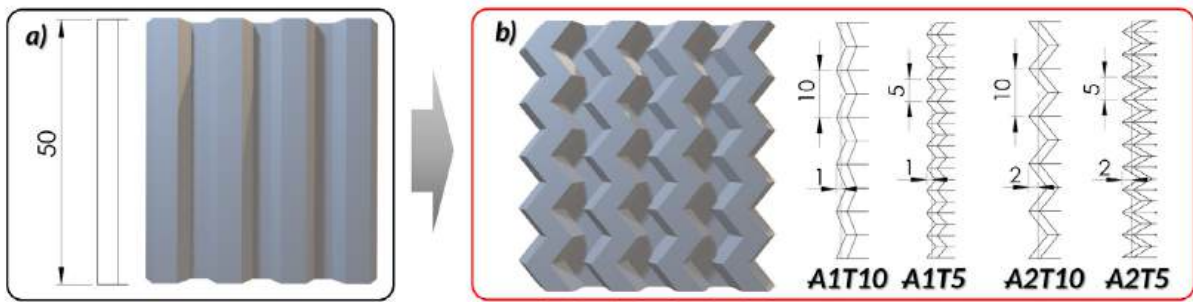
Fig. 1 Variants of honeycomb structures subjected to mechanical tests a) standard honeycomb,

b) – origami type honeycomb structures
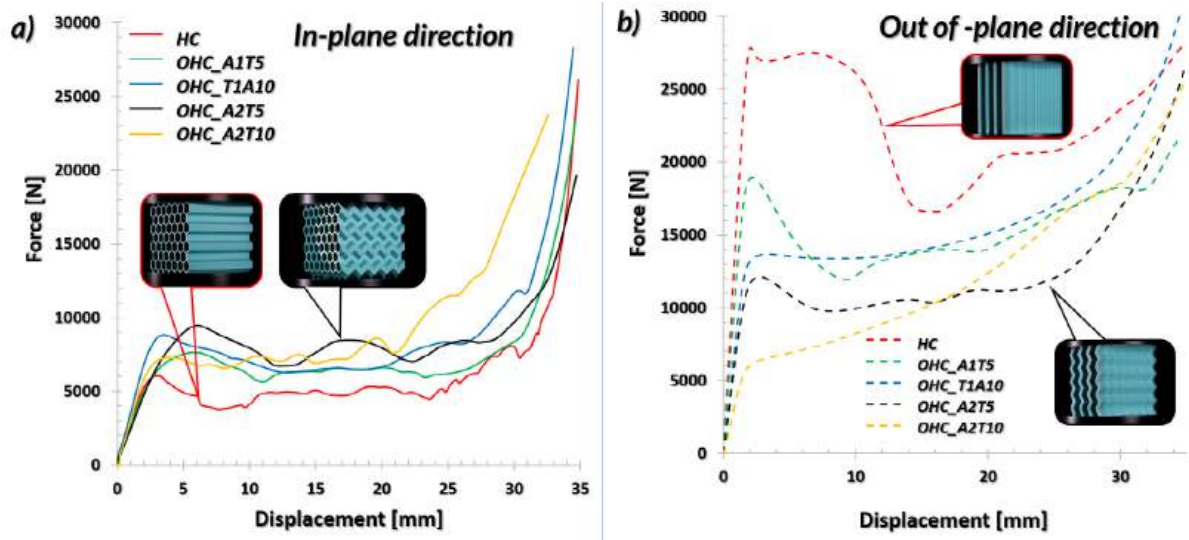
Fig. 2 Mechanical response of structures subjected to compression tests a) in-plane direction,

b) – out of plane direction

It was demonstrated that the use of initiators of the deformation process in cellular structures significantly affects the anisotropy of the structure (Fig. 2). Furthermore, in the case of loading samples in the out-of-plane direction, it is possible to significantly minimize the force peak at the initial stage of deformation.

REFERENCES

[1] A. du Plessis et al., "Beautiful and Functional: A Review of Biomimetic Design in Additive Manufacturing," Addit. Manuf., vol. 27, no. March, pp. 408–427, 2019.

[2] N. S. Ha and G. Lu, "Thin-walled corrugated structures: A review of crashworthiness designs and energy absorption characteristics," Thin-Walled Struct., vol. 157, no. July, p. 106995, 2020.

[3] J. Zhang, G. Lu, and Z. You, "Large deformation and energy absorption of additively manufactured auxetic materials and structures: A review," Compos. Part B Eng., vol. 201, no. August, p. 108340, 2020.

ID 100
LOW-VELOCITY IMPACT RESISTANCE OF AUXETIC COMPOSITE LAMINATES

Cristiano Veloso[1(*)]**, Carlos Mota**[2]**, Luís Nobre**[3]**, João Bessa**[4]**, Fernando Cunha**[5]**, Raúl Fangueiro**[6]

[1, 2, 3, 4, 5, 6] Fibrenamics, University of Minho, Guimarães, Portugal

[6] Department of Textile Engineering, University of Minho, Guimarães, Portugal

[(*)] Email: cristianoveloso@fibrenamics.com

ABSTRACT

Composite laminates display unique stiffness and strength-to-weight ratio properties, which makes them superior in many engineering applications to commonly used high end metallic alloys. However, their structural arrangement – under the form of fabric plies bonded by a matrix – inevitably comes with poor TTT (Through-the-thickness) properties. This factor is linked with an increased propensity to BVID (Barely visible impact damage), mostly under the form of ply delamination, especially in the context of OOP (Out-of-plane) LVI (Low-velocity impact) events. This work focuses on a possible solution to this property deficiency, by means of auxetic laminates, which are tested against LVI, and compared with a control layup sequence, to ascertain the magnitude of auxetic-inherent enhancements.

INTRODUCTION

The architecture of a composite laminate, i.e. a sequence of plies bonded together by a matrix, carries a considerable drawback. Properties in the IP (In-plane) plane – or face plane, *x-y* – are majorly controlled by the constituent ply fabric's properties, but in the TTT (Through-the-thickness) plane – *x-z* - the matrix properties take a preponderant role (Zhang et al., 1999). Given the relatively lower properties of the matrix – especially in FRP (Fibrereinforced polymer) composites – the TTT properties provide a diminished resistance. This risk of damage, that emerges mostly under the form of delamination, is increased, which pertains an issue regarding LVI (Low-velocity impact) events. These events are common during the manufacturing, installation and transportation stages, in events such as a tool drop, and dangerous given that this type of BVID (Barely visible impact damage) can go unnoticed, and can amount up to 50% reductions in strength (Richardson & Wisheart, 1996).

Auxetic laminates can limit this internal delamination propagation, due to their NPR (Negative Poisson's ratio) behaviour, which originates a synchronous orthogonal compression or dilation (Veloso et al., 2023). Distinct lay-up sequences offer the largest auxeticity in *xy* or *xz*, which implies unequal deformation mechanisms. Thus, the present study intends to verify whether a given auxetic mechanism enables a superior OOP (Out-of-plane) LVI resistance. For that, 16-ply T300/8500 C/E (Carbon/epoxy) $[(14°/\ 64°)_4]_S$ (IP NPR – Group A, with a predicted v_{xy} of -0.41) are compared to $[(\pm 25°)_4]_S$ (TTT NPR – Group B, with a predicted v_{xz} of -0.23) laminates against OOP LVI tests performed according to the ASTM D7136 standard. Six specimens of each lay-up configuration were tested in a Rosand IFW5 falling weight machine, with an average thickness of 4.6 mm. The impact energy was set at 30 J, achieved with a 16 mm diameter hemispheric steel striker weighting 4.23 kg.

RESULTS AND CONCLUSIONS

Figure 1 exhibits the averaged force-time and force-displacement curves obtained from the performed LVI tests. Subsequently, Table 1 refers to the peak values of applied force, the corresponding specimen displacement, and the absorbed energy at the end of the test.
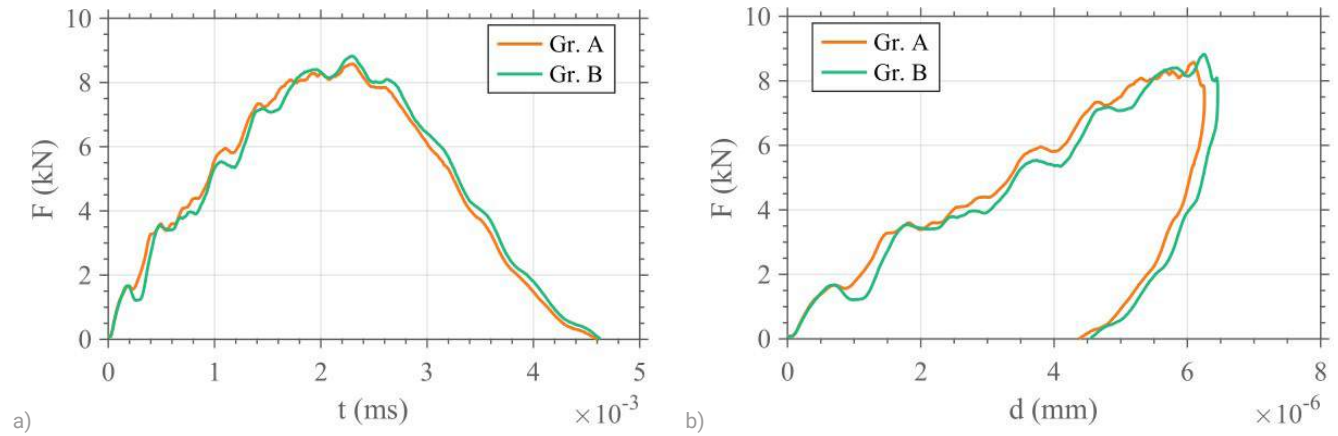
Fig. 1 Averaged force-time a), and force-displacement b), graphs for the for the tested C/E T300/8500 laminates.

The loading profile is similar amongst both groups. Peak load and displacement values are slightly superior in TTT NPR groups. In TTT NPR specimens, more elastic energy is released during the unloading stage, making for a slightly larger value of E_a in the IP NPR group.

Table 1 Maximum force (F_{peak}) and displacement (d_{peak}), and absorbed energy (E_a) values for the tested C/E T300/8500 laminates.

Specimen group	F_{peak} (kN)	d_{peak} (mm)	E_a (J)
A (IP NPR)	8.58	6.10	25.9
B (TTT NPR)	8.82	6.25	25.7

Further analysis to the delamination area and damage extent are required to validate the benefit of each auxetic mechanism. Results show that there is not a relevant difference between the impact resistance of both groups, and that other elastic variables may become the differentiator for the selection of a given auxetic configuration for an application, which can include areas where LVI resistance is important, such as the aerospace, aeronautical and automotive industries. Moreover, important to note that the level of impact energy influences the capacity of LVI resistance in auxetic laminates (Alderson & Coenen, 2008). Hence, more testing with further energy levels is recommended.

REFERENCES

[1] Zhang, R., Yeh, H.-L., & Yeh, H.-Y. (1999). A Discussion of Negative Poisson's Ratio Design for Composites. Journal of Reinforced Plastics and Composites, 18(17), 1546–1556. https://doi.org/10.1177/073168449901801701.

[2] Richardson, M. O. W., & Wisheart, M. J. (1996). Review of low-velocity impact properties of composite materials. Composites Part A: Applied Science and Manufacturing, 27(12), 1123–1131. https://doi.org/10.1016/1359-835X(96)00074-7.

[3] Veloso, C., Mota, C., Cunha, F., Sousa, J., & Fangueiro, R. (2023). A comprehensive review on in-plane and through-the-thickness auxeticity in composite laminates for structural applications. Journal of Composite Materials, 00219983231205345. https://doi.org/10.1177/00219983231205345.

[4] Alderson, K., & Coenen, V. (2008). The low velocity impact response of auxetic carbon fibre laminates. Physica Status Solidi (b), 245, 489–496.

ID 101

ENHANCEMENT OF AUXETIC COMPOSITES MECHANICAL PROPERTIES BY MATRIX FUNCTIONALIZATION WITH GRAPHENE NANOPLATELETS AND SHEAR THICKENING FLUIDS

José Sousa[1](*), Carlos Mota[2], Luís Nobre[3], João Bessa[4], Fernando Cunha[5], Nelson Oliveira[6] and Raul Fangueiro[7,8]

[1,2,3,4,5,7] Fibrenamics, University of Minho, Guimarães, Portugal

[6] SpaceEngineer, Coimbra, Portugal

[8] Center for Textile Science and Technology, University of Minho, Guimarães, Portugal

(*) Email: joseduarte@fibrenamics.com

ABSTRACT

The main purpose of this project was adding graphene nanoplatelets (GNPs) and a nonnewtonian fluid, such as shear thickening fluids (STFs) to a matrix of auxetic composite laminates and analyse its influence when the samples are under shear strength and low velocity impacts (LVI) efforts. Carbon fibre laminates were tested, displayed in auxetic orientations. To study the mechanical properties enhancements in the produced samples, several tests were performed, however, the most relevant for this paper are Interlaminar Shear Strength (ILSS), Drop-Weight Impact and Compression After Impact (CAI). The intention with this testing was to study the impact strength increase of the laminates by adding between 20wt% of STF in the matrix and the improvements achieved in interlaminar adhesion by the addition of 0.5, 1 and 2wt% of GNPs also in the matrix.

INTRODUCTION

Carbon fiber reinforced polymer (CFRP) matrix composites are increasingly used in a variety of industries, such as aerospace, marine, automotive, energy, civil infrastructure, and high-end sports. This is due to their significant weight-saving capability and extraordinary properties, including the high specific stiffness and specific strength, excellent fatigue and corrosion resistance, and low coefficient of thermal expansion. However, despite having extraordinary properties, these composites are susceptible to the low velocity impact of foreign objects in service life (e.g., tool drop impact, and the impact of debris from the runway). The impact will cause delamination, matrix cracking, and fiber breakage, which results in significant degradations in mechanical properties. Several studies point to a mitigation of these issues from the introduction of auxeticity in these CFRP. Auxetic materials are defined by their ability to display negative Poisson's ratios. This distinctive characteristic has been proven to enhance the resistance of materials to impact events. The creation of a negative Poisson's ratio at the laminate level can be achieved through the design of angle-ply composite laminates. This is made possible by capitalizing on the substantial anisotropic nature of each individual layer and exploiting the strain mismatch between neighboring layers. Results show consistently reduced fiber and matrix tensile damage in the auxetic laminate in all plies, in comparison to the nonauxetic counterpart laminates (up to 40% on average). However, the auxetic laminate does not present a clear advantage on mitigating the delamination damage or the matrix compressive damage (Wang, 2022).

Due to the main propose of CFRP auxetic laminates, impact resistance and energy absorption, and presented results by Wang, whose approach to auxetics has not been able to mitigate the delamination damage, it was

intended to develop techniques that would be able to increase the resistance of auxetic laminates to impact and improve their interlaminar adhesion to reduce their delamination.

In another study, Sun et al. (2021) evaluated the resistive force and energy dissipation of STFimpregnated FRP (FRP-STF) and corresponding neat FRP specimens when subjected to a drop hammer test. The three types of fabrics (CFRP,GFRP,BFRP) were soaked in a diluted SiO_2-PEG solution and then heated to evaporate the solvent. Several layers were then bonded using a thermoplastic adhesive and compacted using a flat vulcanizer. From the samples, impacted with 30J of energy with a corresponding velocity of 5 m/s, it was concluded that the STF CFRP impregnated samples were able to increase the absorbed energy in 15.4% in relation to their neat specimens being able to absorb up to 45% of the impact energy with lower velocity impacts. In terms of maximum enhancement resistive force, the STF has a significant effect on the CFRP, with a 78.0% increase compared to neat CFRP.

Finally, Liu et al. (2020) studied the rheological properties of STFs in the impact performance of Kevlar fabrics. The fabrics were impregnated with STFs composed out of silica particles with different sizes and weight fractions. After impregnation the samples were hit with a blade-like projectile weighing 137g at several different velocities up to 85 m/s. In the best performing STF configuration the samples were able to absorb 56.6% more energy than the neat Kevlar fabrics.

The interlaminar shear strength (ILSS) is one of the most influential parameters that governs the delamination resistance and bond-strength. The effects of nanoparticles on ILSS have been studied extensively, as evident by the available relevant literature. The NPs that have been investigated include CNTs, GNPs, multi-walled CNTs (MWCNTs), CNFs, silica and alumina, as well as a few other types of NPs. All the reviewed articles have reported an increase of ILSS with no degradation of the other mechanical properties. Graphene nanoparticles have also been shown to be very effective in improving the interlaminar shear strength of FRPs. Shen et al., incorporated graphene oxide (GO) nanoparticles in GF/EP composites and obtained a 32.7% increase in the ILSS at room temperature (De Cicco et al., 2017).

Considering the good results collected in the bibliography, regarding the energy absorption by the incorporation of STF and the improvement in interlaminar adhesion in CFRP laminates, it is intended at the end of this study to achieve an auxetic composite material reinforced by carbon fibers that presents improvements in these fields.

RESULTS AND CONCLUSIONS

This study focuses on developmet of auxetic CFRP laminates with STFs and GNPs aditivation. For this purpose, T300 unidirectional carbon fibers (from CastroComposites), SR1600/SD2630 epoxy matrix with slow reactivity and high degradation temperature (from Sicomin), STFs (from Spacegineer) and GNPs (from Graphnest) were used.

To evaluate the efficacy of the developed solution, a diverse array of configurations was generated, incorporating 0.5, 1, 2wt% GNPs and 15 and 20wt% STFs by adding them to the composite matrix. The matrix was functionalized with GNPs by dispersing them in both parts of the epoxy resin for 30 minutes using sonication, followed by one hour of mechanical mixing. Subsequently, the STFs were added to the matrix by heating them to 120°C, as well as the part A of the epoxy resin that had already been added with the GNPs, in order to decrease its viscosity and then facilitate mechanical mixing for 25 minutes at 150 rpm. Finally, the curing agent (part B of the resin) was added, also with GNPs, and both parts were mechanically mixed for 25 minutes at 150 rpm.

Once the impregnation solution had been prepared, the composite samples were produced by stacking the carbon fibres in the $[0/15/75/15]_s$ sequence and impregnating them using the hand-lay-up process. The composites were then obtained by subjecting the impregnated fibre stacks to a hot compression moulding process, being cured after a temperature cycle of 90 minutes at 50 °C and 240 minutes at 130 °C and a constant pressure of 50bar.

To evaluate the intended improvements in the development of these additive auxetic laminates, impact resistance tests were performed in accordance with ASTM D7136/D7136M followed by compression after impact tests in accordance with ASTM D7137/D7137M and interlaminar shear strength (ILSS) tests in accordance with ASTM D2344/D2344M.

REFERENCES

[1] De Cicco, D., Asaee, Z., & Taheri, F. (2017). Use of Nanoparticles for Enhancing the Interlaminar Properties of Fiber-Reinforced Composites and Adhesively Bonded Joints— A Review. *Nanomaterials 2017, Vol. 7, Page 360*, *7*(11), 360.

[2] Shen, X. J., Meng, L. X., Yan, Z. Y., Sun, C. J., Ji, Y. H., Xiao, H. M., & Fu, S. Y. (2015). Improved cryogenic interlaminar shear strength of glass fabric/epoxy composites by graphene oxide. *Composites Part B: Engineering*, *73*, 126–131.

[3] Sun, L., Wei, M., & Zhu, J. (2021). Low velocity impact performance of fiber-reinforced polymer impregnated with shear thickening fluid. *Polymer Testing*, *96*, 107095.

[4] Wang, Y. (2022). Auxetic Composite Laminates with Through-Thickness Negative Poisson's Ratio for Mitigating Low Velocity Impact Damage: A Numerical Study. *Materials 2022, Vol. 15, Page 6963*, *15*(19), 6963.

[5] Lulu Liu, Z. Y. (2020). The influences of rheological property on the impact performance of kevlar fabrics impregnated with SiO2/PEG shear thickening fluid. *Thin-Walled Structures*.

ID 102
HIERARCHICAL SANDWICH HONEYCOMB CORES

Jochen Pflug[1](*)

[1] EconCore N.V., Belgium, jochen.pflug@econcore.com
(*) Email: jochen.Pflug@econcore.com

ABSTRACT

Hierarchical structuring prevents microstructural buckling enabling significantly higher compression strength of sandwich structures. Sandwich constructions provide a maximal buckling resistance at minimal weight. Ultra lightweight structures are possible if the work sharing and the synergy effects of core and skins in sandwich constructions are also applied on lower hierarchical levels, leading not to a hierarchical honeycomb but to a hierarchical sandwich honeycomb.

INTRODUCTION

Expanded honeycomb cores from aluminum and phenol resin impregnated aramid paper (Nomex®) can be considered the state-of-the-art in the field of lightweight cellular cores for sandwich construction. Their exceptional weight specific out-of-plane compression and shear strength are the key performance characteristics which contribute to the success of honeycombs as sandwich core material. Structural hierarchy has been introduced to the sandwich concept to further improve the weight specific mechanical properties (Lakes, 1993), (Kooistra, 2005), (Kazemahvazi, 2009), (Gibson, 2012). Hierarchical structuring prevents microstructural buckling enabling significantly higher compression strength than the first order structures from which they are derived.

Fig. 1: Hierarchical honeycomb structure with honeycomb cores within the sandwich cell walls and within the sandwich skins.

Structural hierarchy can be considered at different levels, either for the face sheets with a thin sandwich panel replacing the single face sheet or in the honeycomb core replacing monolithic cell walls with thin sandwich cell walls, Fig. 1. A layered combination of sandwich constructions with sandwich face sheets on a hierarchical core with large cell size prevents wrinkling and dimpling failure modes. Sandwich cell walls are especially efficient for honeycomb cores with a large cell size enabling a highly buckling resistant microstructure at very low densities. Such hierarchical sandwich honeycomb cores are proposed as a new class of honeycomb core materials (Pflug, 2026, 2018) and are protected by granted patents (Pflug 2016, 2019).

RESULTS AND CONCLUSIONS

The hierarchical sandwich honeycombs show significantly higher compressive strength than the conventional Nomex® and aluminum honeycomb cores at equal densities. The higher bending stiffness of the cell walls prevents cell wall buckling up to the yield strength of the material. Aluminum based hierarchical sandwich honeycombs with a core density of 46 kg/m³ reach a compressive strength of 3.9 MPa. The stainless steel based hierarchical sandwich honeycombs enable very lower densities for applications with very high temperatures during operation. The additional complexity of the hierarchical concept adds extra geometrical parameters and material parameters. To achieve optimum performance in terms of strength over density the global buckling of the sandwich cell walls and the buckling of the skins need to be avoided to reach the theoretical compression strength of the skin material with a minimum additional weight of core material in the sandwich cell walls.

Structural hierarchy in the form of hierarchical sandwich construction is effectively enhancing the weight specific mechanical performance of the honeycomb core as compared to its classical design especially the very low core densities. Fig. 2 shows potential applications of hierarchical sandwich honeycomb cores.

Fig. 2 Potential applications of hierarchical sandwich honeycombs with sandwich skins (left: aircraft interior wall, right: nose fairing structure in a space launcher).

For future hierarchical sandwich honeycombs based on carbon fibre and glass fibre reinforced composite pultruded and extruded profiles provide attractive opportunities for ensuring very high specific mechanical performances at very low core density and represent good candidates for future investigations and structural optimizations.

REFERENCES

[1] R.Lakes, "Materials with structural hierarchy", *Nature* 361 (1993), p. 511-515

[2] G.W.Kooistra, H.N.G.Wadley, "Hierarchical Corrugated Core Sandwich Panel Concepts", *J. Appl. Mech.*, 2005; 74(2)

[3] S.Kazemahvazi, D.Zenkert, "Corrugated all-composite sandwich structures", *Composites Sci. and Tech.*, 2009; 69(7-8)

[4] L.J.Gibson, "The hierarchical structure and mechanics of plant materials", *Journal of the Royal Society Interface*, 2012; 9(76)

[5] J.Pflug, I.Verpoest, D.Vandepitte, "Hierarchical sandwich honeycomb cores", ICSS11, Fort Lauderdale, Florida, 2016

[6] J.Pflug, "Continuously produced honeycomb core materials", PhD Thesis, Leuven, 2018

[7] J.Pflug, "Honeycomb core with hierarchical cellular structure", EconCore N.V., Patent Publication, WO2016184528 (2016)

[8] J.Pflug, "Hierarchical honeycomb core with sandwich cell walls", EconCore N.V., Patent Publication, WO2019158743 (2019)

ID 104

HIGH PERFORMANCE POLYMER/CARBON NANOCOMPOSITES: COMBINING MECHANICAL PERFORMANCE, TEMPERATURE RESISTANCE AND ELECTRICAL CONDUCTIVITY

Maria C. Paiva[(1,*)], **Sofia Silva**[2], **Nelson Durães**[2], **José A. Covas**[1], **Paulo F. Teixeira**[2]

[1] Institute for Polymers and Composites, Dep. Polymer Engineering, University of Minho, 4800-058 Guimarães, Portugal

[2] CeNTI—Centre for Nanotechnology and Smart Materials, R. Fernando Mesquita 2785, 4760-034 Vila Nova de Famalicão, Portugal

[(*)] Email: mcpaiva@dep.uminho.pt

ABSTRACT

High performance polymers combine lightweight and mechanical performance in a wide temperature range, which make them interesting for aeronautic and aerospace applications. The combination with carbon nanoparticles such as nanotubes and graphene is expected to enhance the mechanical performance and bring new functionalities such as electrical conductivity. The limiting factor is the ability to prepare homogeneous composites with well dispersed nanoparticles at the minimal concentration that will endow the desired properties, and to keep these properties when the composite is further processed to form the final part. The work presented here focuses the problems associated to the preparation of poly(etherether-ketone) (PEEK) nanocomposites with carbon nanotubes and graphene. The nanoparticle dispersion in PEEK was studied and optimized, and the composites obtained were then set into filament form, either as a monofilament for 3D printing and as a textile multifilament yarn.

INTRODUCTION

Aromatic polymers typically present excellent mechanical properties, high thermal resistance and favor the interactions with graphene-like surfaces such as carbon nanotubes (CNT) and graphite nanoplates (GnP) via π-π stacking [1]. The present work reports the production of an electrically conductive PEEK composite and the processing of conductive filament using PEEK, GnP and CNT [2,3].

The compositions and processing conditions that yielded higher composite electrical conductivity were selected. The filament processing was optimized, the nanocomposites produced were characterized for morphology, electrical, mechanical and thermal properties. Then, i) monofilaments were produced and tested for 3D printing and ii) the melt spinning of multifilaments was tested.

RESULTS AND CONCLUSIONS

The work was carried out using i) PEEK Victrex 450 G®, from Victrex (Lancashire, UK), carbon nanoparticles were MWCNT NC 7000/Nanocyl, Belgium and xGnP-M/XG Science Inc, USA; ii) commercial PEEK masterbatch, PLASTICYLTM PEEK1001, with 10 wt.% of multiwalled CNT, was supplied by Nanocyl. The use of masterbatch dilution was selected for composite preparation with safe handling of the CNT.

The electrical percolation threshold obtained for composites produced by direct mixing of PEEK/CNT or by masterbatch dilution was quite similar, observed in the concentration range 1-3 wt% CNT, as observed in Figure 1 a).

The effect of CNT concentration on the linear viscoelastic response of the nanocomposites at 400°C is shown in Figure 1 b), presenting the frequency-dependent response of the dynamic complex viscosity (η^*). PEEK/CNT composites present plastic response of the complex viscosity versus frequency in the concentration range studied.

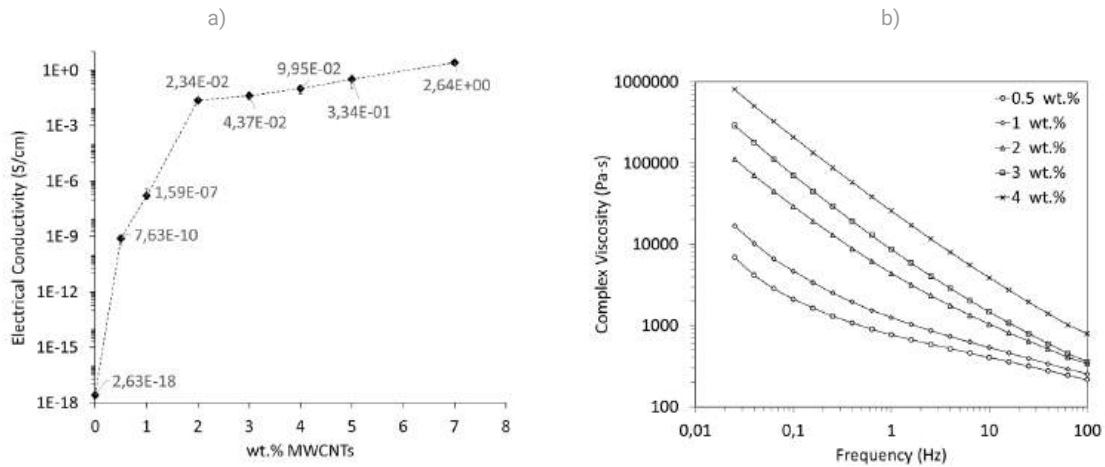a)   b)

Fig. 1 a) electrical percolation threshold evaluation for nanocomposites prepared by masterbatch dilution; b) complex viscosity of PEEK/CNT nanocomposites as a function of frequency at 400 °C

The thermal stability of PEEK was not affected by the addition of CNT or GnP. The compounding conditions for optimal dispersion of the nanoparticles were studied, and the conditions for monofilament production and multifilament spinning were selected. The electrical conductivity of the monofilament obtained was lower than that of the equivalent nanocomposites, however at 4 wt.% CNT/3 wt.% GnP, values ~10 S/m were obtained (Figure 2). Electrical conductivity was lost on the multifilament yarn produced.
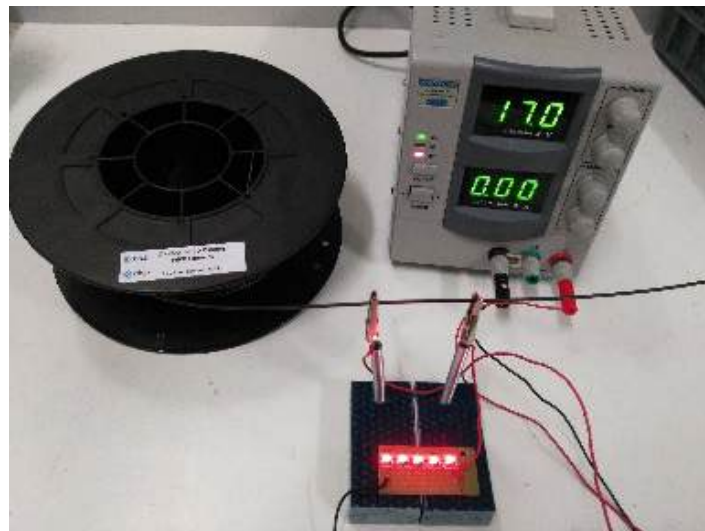
Fig. 2 Spool with electrically conductive PEEK nanocomposite monofilament

REFERENCES

[1] Yang, J. et al. "Preparation and properties of poly (p-phenylene sulfide)/multiwall carbon nanotube composites obtained by melt compounding". Compos. Sci. Technol. 69, 147–153, 2009.

[2] Sofia Silva, José M. Barbosa, João D. Sousa, Maria C. Paiva, Paulo F. Teixeira, "High-Performance PEEK/MWCNT Nanocomposites: Combining Enhanced Electrical Conductivity and Nanotube Dispersion". Polymers, 16, 583, 2024.

[3] J. Gonçalves, P. Lima, B. Krause, P. Pötschke, U. Lafont, J.R. Gomes, C.S. Abreu, M.C. Paiva, J.A. Covas, "Electrically Conductive Polyetheretherketone Nanocomposite Filaments: From Production to Fused Deposition Modeling", Polymers, 10, 925, 2018.

ID 105
RECYCLED CARBON COMPOSITES IN AEROSPACE APPLICATIONS

I. ten Bruggencate[1], F.W.J. van Hattum[1*], Johan Meuzelaar[2], Thomas de Bruijn[2]

[1] ThermoPlastic composites Application Centre, Saxion University of Applied Sciences, Enschede, The Netherlands
[2] GKN/Fokker Aerostructures B.V., Hoogeveen, The Netherlands
[*] Email: f.w.j.vanhattum@saxion.nl

ABSTRACT

Thermoplastic composites are increasingly used in industries such as aerospace, and have thus far been claimed as well-recyclable. However, in practice the material is hardly recycled. At the ThermoPlastic composite Application Centre in the Netherlands, a low shear recycling process has been developed that can process thermoplastic composite waste, while retaining the highest possible material properties. Its use has been demonstrated on the design, manufacturing and flight-testing of aerospace parts made of 100% recycled composite material. The research thus proved the successful use of recycled thermoplastic composites with functional integration in the development and production of complex-shaped aerospace part.

INTRODUCTION

Continuous fiber reinforced thermoplastic composites (TPC) are gaining interest in aerospace and more recently also sporting goods, automotive and industrial sectors. The growing demand results in increasing post industrial waste. During the production process up to 1/3 of the material is waste resulting in circa 1000 ton of high-end TPC till 2024 in the Netherlands only. Lately, also more low-cost high-volume materials are used and resulting in more production waste. Since there is no adequate recycling solution for TPC materials, the waste is often disposed. The result is a considerable economical loss. For high-end TPC roughly 100M euro is estimated. Beside the economic motivation, legislation and more environmental awareness is making recycling more interesting. In contrary to their thermosetting counterparts TPC can be reprocessed by reheating and is therefore considered to be recyclable.

RESULTS AND CONCLUSIONS

The current research project developed a recycling route for TPC materials and parts made thereof. The research focused on the optimum process and process settings to cost-effectively reprocess TPC waste to obtain the highest performance possible. For this, post-industrial carbon fibre reinforced polyphenylene sulphide (C-PPS) material was shredded, and processed with a low shear mixer with varying batch compositions to obtain plate material. Material data such as tensile strength and impact sensitivity were collected by means of mechanical and impact testing. The results were used in the design of two prototype parts for the aerospace industry from recycled thermoplastic composites (rTPC). Integration of lightning strike protection during processing was studied, characterized and validated through impact and tensile testing in critical usage conditions. Finally, based on above results, na aerospace fairing cover was developed, produced and flight-tested. To stretch process boundaries, in addition, two complex-shaped fairing covers were developed and produced, that will be tested on an experimental rotocraft. The project covers the total value chain, from design and size reduction to the forming of parts. Costs both economic and environmental including the cost of the recycling, are included in the value of the solution and the feasibility and risks involved are validated on the demonstrator parts.
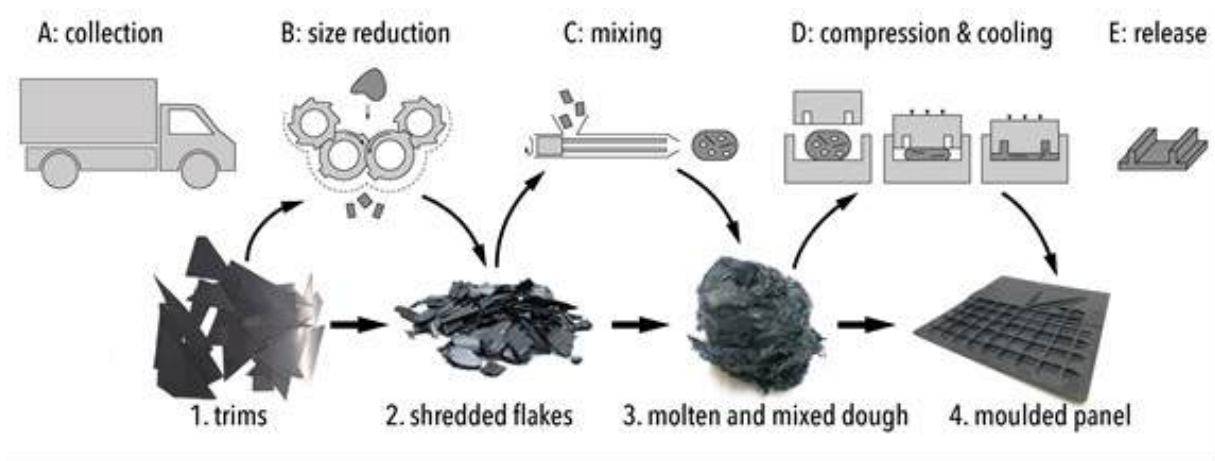
Fig. 1 Developed thermoplastic composite recycling process

Fig. 2 Manufactured demonstrator access panel

The research thus proved the successful use of recycled thermoplastic composites with functional integration in the development and production of complex-shaped aerospace part, showing both economic and environmental benefits, while maintaining performance.

REFERENCES

[1] T.A. de Bruijn, G.A. Vincent and F.W.J. van Hattum, "Recycling of long fibre thermoplastic composites by low shear mixing", SAMPE Europe Conference, pp.540-546, Liège, Belgium, 2016.

[2] T.A. de Bruijn, G.A. Vincent, J. Meuzelaar, J.P. Nunes and F.W.J. van Hattum, "Design, Manufacturing & Testing of a Rotorcraft Access Panel Door from Recycled Carbon Fiber Reinforced Polyphenylenesulfide", SAMPE Journal, vol. 56, no. 2, pp.26-33, 2020.

[3] T.A. de Bruijn and F.W.J. van Hattum, "Rotorcraft access panel from recycled carbon PPS–The world's first flying fully recycled thermoplastic composite application in aerospace", Reinforced Plastics, vol. 65, no. 3, pp.148-150, 2021.

ID 106

MONITORING COMPOSITE PARTS IN THE CONTEXT OF MAIT-MANUFACTURING, ASSEMBLY, INTEGRATION AND TEST

Helena Rocha [(1*)], **Hugo Gomes**[1], **Paulo Antunes**[1]

[1,] PIEP-Innovation in Polymer Engineering, Universidade do Minho, Guimarães, Portugal

[(*)] Email: helena.rocha@piep.pt

ABSTRACT

The aim of this work is to demonstrate the potential of the integration of optical sensorization for monitoring of composite parts in the context of MAIT-Manufacturing, Assembly, Integration and Test. The monitoring system is based on the structural data obtained through an embedded optical sensing network in the composite laminate of a transversally reinforced curved plate. The embedded optical sensorization system considered within the scope of this work is capable of multi-point and multivariable sensing (temperature and strain), enabling data monitoring throughout the entire production cycle and structural testing phases.

INTRODUCTION

Composite materials are widely used in critical components or structures with high thermomechanical performance. Thus, it is of high importance to thoroughly monitor the operational service life of these structures while in service, as well as to maintain strict control over their processing conditions. This detailed monitoring is essential to assess structural integrity and ensure optimized performance over time. By carefully recording and analyzing the critical variables associated with ongoing operations, it is possible to identify patterns, anticipate structural or material malfunctions and implement proactive corrective measures. The versatility of composite materials and associated production techniques increases the potential for the application of different sensorization methodologies, allowing application contexts that cannot be replicated to other materials and/or production processes.

The incorporation of sensing systems during the production process represents an innovative approach that enables the production of smart components with integrated sensors into their structure with the ability to monitor a wide range of physical variables relevant to evaluate the performance and quality of the product [1]. In this way, it is possible to obtain critical information and monitor, continuously and in real time, the component during the Manufacture, Assembly, Integration and Testing (MAIT) phases. This new approach to continuously monitor components and processes is highly disruptive, and composite materials are a broad field of application of this integral monitoring concept.

In this study, it was considered the insertion of an optical FBG (Fibre Bragg Grating) sensor network, as shown in Figure 1, on a CFRP (Carbon Fibre Reinforced Polymer) composite curved panel, which allowed to monitor relevant data from the manufacturing phase until the test stage. In fact, with the same optical network it was possible to retrieve thermomechanical data essential to monitor the resin infusion process, cure kinetics and, finally, to assess the kinematics of impact events.

RESULTS AND CONCLUSIONS

Figure 1 shows the configuration of optical fiber embedded (and respective sensors) in the composite laminate that allowed the monitoring of the resin flow front (see Figure 2), resulting from the vacuum-assisted resin infusion process (VARI). Subsequently, after curing the part, and using the same network of optical sensors, the impact energy is evaluated by monitoring the strain transients, as shown in Figure 3.

a)

b)
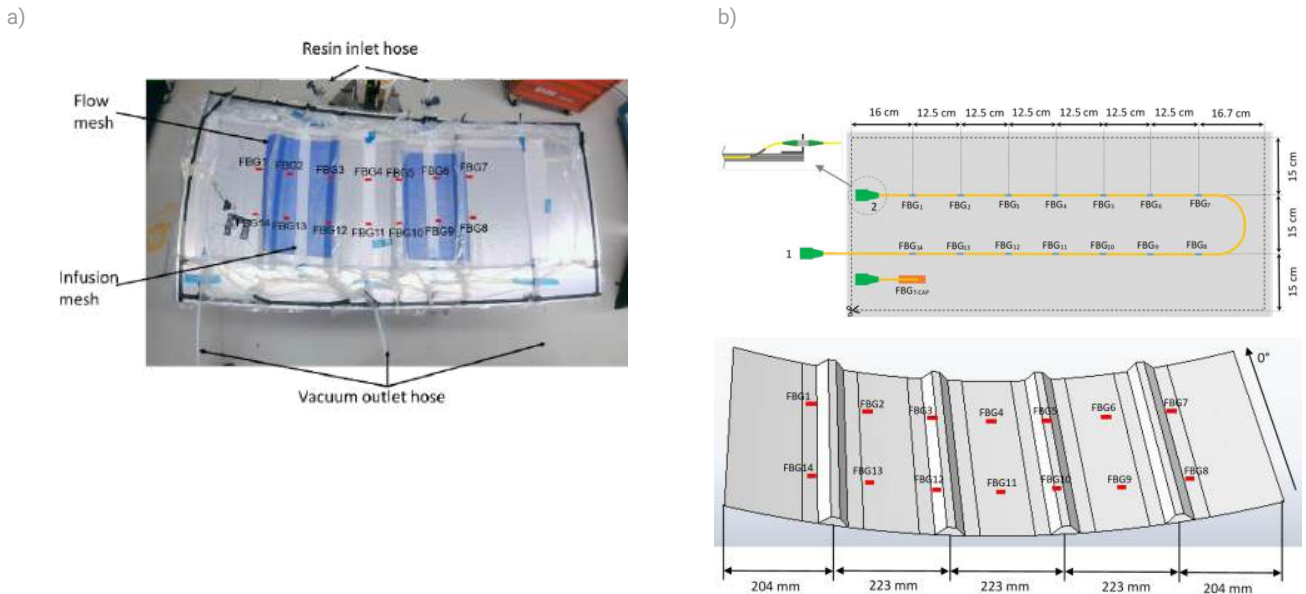
Fig 1 In a) vacuum-assisted resin infusion process and indication of the positioning of FBG sensors (14), b) diagrams of the arrangement of the FBG sensor network considered.
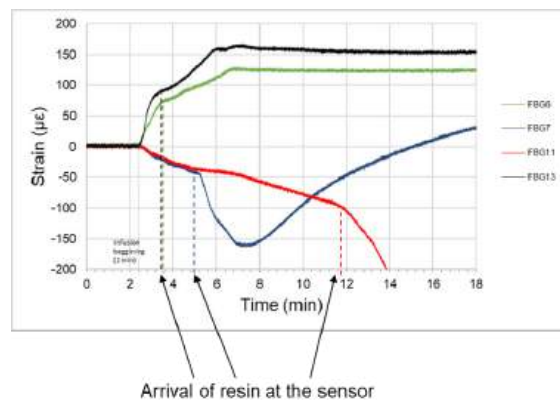
Fig 2 Monitoring of the resin front, through deformation monitoring by embedded optical sensors (time-of-arrival of resin on sensors)
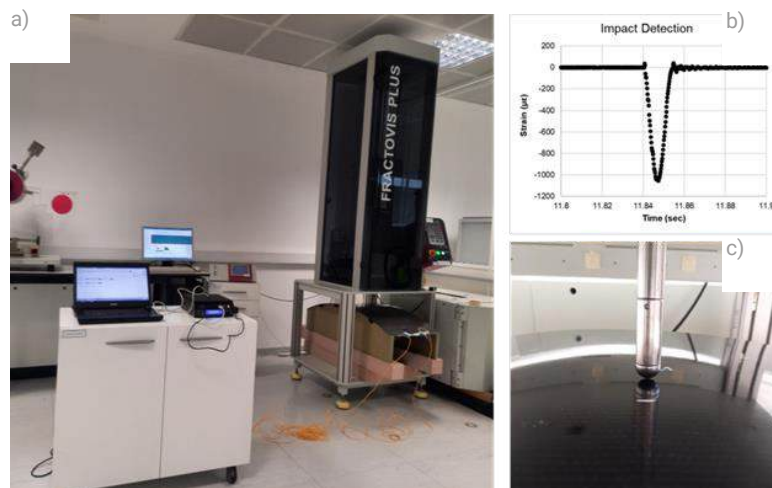
Fig 3 Impact monitoring, by strain transient monitoring, through embedded optical sensors. In a:) impact testing machine (weight drop) and optical signal acquisition system; b) strain transient generated by impact loading; c) impactor and sensorized composite plate.

REFERENCES

[1] Rocha Helena, Antunes Paulo, Lafont Ugo, and Nunes João P., "Processing and Structural Health Monitoring of a Composite Overwrapped Pressure Vessel for Hydrogen Storage," *Struct Health Monit*, vol. in press, 2023.

ID 107
CONSIDERATIONS ON THE NUMERICAL SIMULATIONS FOR THE DEVELOPMENT OF A LIGHT ELECTRONIC ENCLOSURES

Filipa Carneiro[1](*), **Susana Costa**[1], **Lourenço Bastos**[1], **Luciano Rietter**[1], **Rui Oliveira**[1], **Ricardo Freitas**[1], **Agnieszka Rocha**[1], **Bruno Vale**[1], **Carlos Ribeiro**[1], **David Serrão**[1], **Joana Silva**[1], **Nuno Gonçalves**[1], **Carlos Ribeiro**[1], **Susana Silva**[2], **Aníbal Portinha**[2], **Pedro Bernardo**[2], **Gustavo Dias**[3]

[1,] PIEP - Innovation in Polymer Engineering, Universidade do Minho, Guimarães, Portugal

[2,] Bosch Car Multimedia, Braga, Portugal

[3,] IPC – University of Minho Campus de Azurém, Guimarães, Portugal [(*)] Email: fiipa.carneiro@piep.pt

ABSTRACT

This work outlines the methodology, materials selection and performance evaluation criteria employed in the development of a lightweight yet robust electronic enclosure with enhanced thermal management and electromagnetic compatibility. The study also explores and proposes strategies that align with the industry's evolving priorities, facilitating the swift adaptation to stringent standards while concurrently enhancing performance and sustainability across the applications. This study validates the efficacy of an innovative simulation-based methodology, showcasing its capability to, systematically, reduce both the weight and cost of components. The findings underscore the potential for widespread application of this methodology in advancing cost-efficient and lightweight design practices across several industrial sectors, beyond the automotive sector.

INTRODUCTION

The automotive sector is facing a paradigm shift characterized by heightened demands in sustainability, emissions reduction, efficiency and safety. Analogue to the automotive sector, aerospace and defense demands for materials and solutions with improved performance for its specific – and usually harsh – conditions. This work underscores the critical need for developing innovative lightweight solutions for the automotive industry taking into consideration aspects useful for aerospace and defense. More specifically, the work focuses on the development of a Lightweight Electronic Enclosure (LEE) achieved by the replacement of traditional metallic materials by functional polymeric and composite alternatives.

The development of products for these sectors with more restrictive requirements leads to the necessity of full support of the numerical simulations, which come to aid product developers in ensuring a proper operation. Using modelling and simulation resources, the approach aims to predict and evaluate the fulfilment of specifications.

Numerical simulations involve replicating relevant physics to emulate real-world conditions, enabling the assessment of mechanical strength, thermal dissipation and electromagnetic protection in the LEE. Ensuring that the enclosure can withstand usage loads while providing an effective thermal path for heat dissipation and protect internal electronics from undesirable external influences. This iterative numerical method enhances the accuracy and efficiency of predicting product performance, contributing to informed decision-making throughout the development lifecycle.

ID 108

ELECTRICALLY CONDUCTIVE PEEK NANOCOMPOSITE FILAMENTS FOR ADDITIVE MANUFACTURING IN SPACE APPLICATIONS

Renato Reis[1], Ugo Lafont[2], Maria C. Paiva[3], José A. Covas[3]

[1]Pólo de Inovação em Engenharia de Polímeros, University of Minho, 4500-058 Guimarães, Portugal
[2]European Space Research and Technology Centre, Keplerlaan 1, NL-2200 AG Noordwijk, The Netherlands
[3]Institute for Polymers and Composites/i3N, University of Minho, 4800-058 Guimarães, Portugal

ABSTRACT

This study displays the development of an electrically conductive filament for Fused Deposition Modeling (FDM) 3D printing. The developed nanocomposites filament produced by melt mixing technology, based on polyetheretherketone (PEEK) with carbon nanotubes (CNT) and graphite nanoplates (GnP), were extensively characterized to evaluate significant properties and performance.

INTRODUCTION

Due to the promising properties, the conductive PEEK nanocomposite filaments allows for the creation of robust and durable structural parts for space applications due the level of electrical conductivity (1.5-13.1 S/m) that enables fabrication of 3D printed antennas, sensors, and other electronic components directly in space; the enhanced thermal conductivity enables better heat dissipation in extreme space environments; the reduced friction coefficient may minimizes wear and tear in mechanisms used onboard spacecraft; the good printability and mechanical performance that will allows for the creation of robust and durable structural parts for space use.

This research paves the way for utilizing conductive PEEK nanocomposite filaments in space additive manufacturing, a development that could revolutionize the creation of lightweight, multifunctional, and in-situ manufactured components for future space exploration. Due to their exceptional properties, these filaments enable on-demand manufacturing of lightweight, customized electronic components for satellites and spacecraft, development of electrically conductive coatings for shielding against electromagnetic radiation and electrostatic discharge, additive manufacturing of heating/cooling elements for managing thermal fluctuations in space and fabrication of lightweight, structurally sound components to reduce spacecraft weight and enhance overall efficiency.

KEYWORDS

PEEK; carbon nanotubes; graphite nanoplatelets; nanocomposites; filaments; fused deposition modeling (FDM); conductivity; space materials

ID 112

EFFECT OF GRAPHENE NANOPLATELET CONTENT AND TEXTILE SUBSTRATE ON THE THERMOELECTRIC PROPERTIES OF CONDUCTIVE TEXTILES

Luisa M. Arruda[1(*)]**, Beate Krause**[2]**, Antonio J. Paleo**[3]**, Petra Pötschke**[4]**, Raul Fangueiro**[5]

[1,5]Fibrenamics, Institute of Innovation of Fiber-based Materials and Composites, University of Minho 4710-057 Guimarães, Portugal

[2,4]Leibniz-Institut für Polymerforschung Dresden e.V. (IPF), Hohe Str. 6, 01069 Dresden, Germany

[3,5]Centre for Textile Science and Technology (2C2T), University of Minho, 4800-058 Guimaraes, Portugal

[(*)] Email: luisa.arruda@fibrenamics.com

ABSTRACT

This study investigates the thermoelectric (TE) properties of eight conductive textiles (CTs) that were functionalised with a polyurethane (PU)-based coating paste through screen-printing. Two key parameters were varied: the textile substrate (woven and knitted fabric) and the concentration of commercial graphene nanoplatelets (GNPs) at 5%, 7%, 10% and 15 wt%. Furthermore, a wash testing program was compiled to test the washability and the influence on the TE properties of the CTs with the highest electrical conductivity after the 1st, 5th, 10th, 15th, and 20th wash cycles. The stability of the coating was confirmed as the CTs maintained the same TE behaviour after 20 washing cycles. These results provide valuable insights for the development of functional thermoelectric fabrics.

INTRODUCTION

Thermoelectric (TE) materials represent a pivotal frontier in the realm of energy conversion, capable of harnessing temperature differentials to generate electric potential or vice versa— an effect known as the thermoelectric effect. These materials play a crucial role in power generation and refrigeration applications, where the quest for materials with robust TE properties is relentless. The efficacy of these materials within thermoelectric systems hinges on key factors such as electrical conductivity (s), thermal conductivity (k), and the Seebeck coefficient (S; generated thermoelectric voltage (U) divided by the applied temperature difference), which are all temperature-dependent. The power factor (PF), another TE parameter, can be calculated as $PF=S2·s$. Amidst this landscape of innovation, TE materials are spearheading transformative technologies, particularly in domains like wearable electronics and personal protection. Conductive textiles (CTs), with their inherent attributes of flexibility, wearability, comfort, and breathability, emerge as an ideal canvas for the integration of materials with enhanced TE properties (Ding et al., 2024). This symbiosis not only augments the functionality of textiles but also unlocks avenues for energy harvesting and power generation from the human body or ambient environments. In the realm of personal protection and defense, the integration of CTs with high TE properties hold promise in reshaping the design paradigms of protective gear by offering additional power sources for communication devices, lighting, and heating systems, heralding a potential revolution in protective equipment (Freer et al., 2019). Conversely, carbon-based nanomaterials, notably graphene, have emerged as frontrunners in the field of TE materials with enhanced properties, owing to their theoretically exceptional s and S (Mulla et al., 2023). Hence, this study embarks on an exploration of the thermoelectric behavior of CTs, based on the graphene functionalisation protocol from previous study (Arruda et al. 2022). This endeavor entails examining the influence of two critical parameters—the concentration of graphene

and the structure of the textile substrate—on their thermoelectric performance.

RESULTS AND CONCLUSIONS

The thermoelectric parameters of the GNP powder used in this study were characterized with a S at 28.5±0.7 µVK-1, a s at 117.0±32.0 Sm-1 and a PF at 8.9×10-2 µWm-1K-2. The CT samples produced with woven and knitted fabrics exhibited similar s values which increases with the GNP content, as shown in Fig. 1a. The S-value decreases slightly, whereby the PF increases with increasing GNP content. It is worth noting that the CT based on the knitted fabric functionalised with 5% GNPs had the highest S 17.8±6.6 µVK-1. The highest PF at 8.9×10-4 µWm-1K-2 was found for the knitted fabric with 15% GNP. The results highlight the promising applicability of the CT functionalized with 15% GNPs, which was subjected to washing resistance tests. As illustrated in Fig. 1b, the S-values for CTs with 15% GNPs remained stable after the washing tests. The slight drop in conductivity s leads to marginally lower PF values. This shows its potential for practical applications, which needs to be further consolidated.
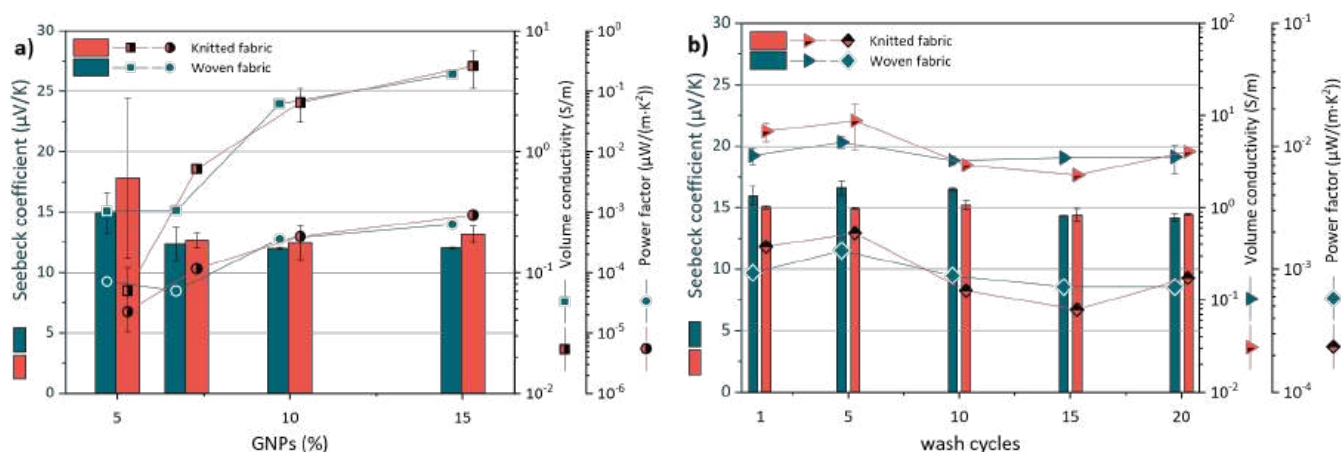
Fig. 1 Seebeck coeffcent, volume conductivity and power factor of CTs made with woven and knitted fabrics: (a) textiles with 5%, 7%, 10% and 15 wt% GNPs; (b) effect of washing on textiles with 15 wt% GNPs.

This study showed that mainly the % of active material and in minor extent the architecture of the textile structure influences the thermoelectric behavior of the final CTs. For future work, it is expected to carry out more quantitative analysis between CTs produced with other type of textile structures and carbon nanostructures.

REFERENCES

[1] Y. Ding et. al, "Porous Conductive Textiles for Wearable Electronics," *Chem. Rev*, vol. 124, no.4 February, pp. 1535-1648, 2024.

[2] R. Mulla, A. Orbaek White, C. W. Dunnillab and A. R. Barron ,"The role of graphene in new thermoelectric materials," *Energy Adv.*, vol. 2, no.5 March, pp. 606-614, 2023.

[3] R. Freer and A.V. Powell, "Realising the potential of thermoelectric technology: a Roadmap," *J. Mater. Chem. C*, vol. 8, no.2 January, pp. 441-463, 2019.

[4] L. M. Arruda, I.P. Moreira, U.K Sanivada, H. Carvalho, and R. Fangueiro, "Development of Piezoresistive Sensors Based on Graphene Nanoplatelets Screen-Printed on Woven and Knitted Fabrics: Optimisation of Active Layer Formulation and Transversal/Longitudinal Textile Direction," *Mat.*, vol. 15, no.15 July, pp. 1-25, 2022.

ID 115
ACCELERATED AGING OF DYNEEMA® SB21 UD OBTAINED FROM 20 YEARS OLD BALLISTIC RESISTANT VEST

Harm van der Werff[(*)]**, Hans Meulman, Raul Perez-Graterol**

Avient Protective Materials, Geleen, The Netherlands

[(*)] Email: harm.werffvander@avient.com

ABSTRACT

The effect of accelerated aging on the ballistic V50 performance of Dyneema® SB21, isolated from 20 years old ballistic vests (that had been in use for 10 years) is presented. The 20 years old samples were aged at 90°C for 4 weeks or at 75°C and 80% relative humidity for 8 weeks. The results show that the 20 years old Dyneema® SB21 had no decrease in V50 compared to new material, and that accelerated aging of the 20 years old material did also not decrease the V50.

INTRODUCTION

The life expectancy of fiber-based ballistic composites is a crucial topic as these materials protect people during their service life. Ballistic composites with Dyneema® fibers have been introduced about 30 years ago, and the long-term ballistic performance behaviour has been investigated [1,2]. The influence of accelerated aging on pristine Dyneema® unidirectional (UD) composites for the soft ballistic (SB) application in vests on ballistic performance (V50) has been studied [1,2], and no decline in V50 could be observed at all. In [2], the ballistic performance has been tested of approx. 15 years old ballistic vests according to the SK1 TR2000 and complete recertification could be carried out with the results obtained.

In this paper, we present the effect of accelerated aging on Dyneema® SB21 material isolated from 51 vests of approx. 20 years old (26 vests from 2002 and 25 vests from 2003) from exactly the same source as the vests used in [2].

RESULTS AND CONCLUSIONS

In order to have accurate statistical data, 20x20 cm single sheets were cut from UD sheets isolated from all vests (each vests containing 34 or 35 individual sheets). All thus obtained UD sheets from the different vests were homogeneously divided into three groups and, within each group, all the sheets from the different vests were again randomized to obtain finally 3 x 30 packs consisting of 24 plies of old Dyneema® SB21 (areal density 3.48 kg/m2). One group was the reference, and one group was subjected to accelerated aging at 75°C/80%RH/8 weeks and one group was subjected to accelerated aging at 90°C / 4 weeks. Additionally, 30 similar packs of new pristine Dyneema® SB21 produced in 2021 were tested.

The accelerated aging clearly affected the colour of the SB packs (Figure 1). The old SB21 is already discolored compared to the new pristine SB21. The aged old SB21 packs are clearly more discolored again. The old Dyneema® SB21 packs aged at 75°C/80%RH/8weeks are the most brown.
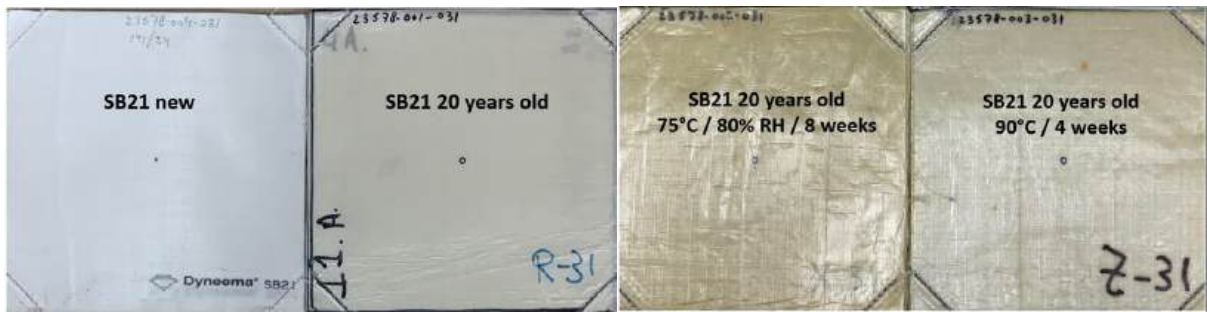
Fig. 1) Visual appearance the new, used and aged Dyneema® SB21 packs

The determination of the V50 of the Dyneema® SB21 packs, placed on clay, was carried out by placing a single shot with a 9mm DM41 FMJ bullet on the center of each pack, and velocities were adjusted +/- 20 m/s depending on whether a complete penetration or stop was observed. For each group of Dyneema® SB21 packs, 30 single shots were carried out. All the shots were then subjected to a Probit analysis (maximum likelihood) and thus an estimate of the mean V50 and a 95% confidence interval was obtained. Results are given in Figure 2. The V50 of the old Dyneema® SB21 packs is not statistically significant different from the new pristine SB21. Both accelerated aging processes carried out on the approx. 20 years old Dyneema® SB21 packs do not result into statistically significant different V50.
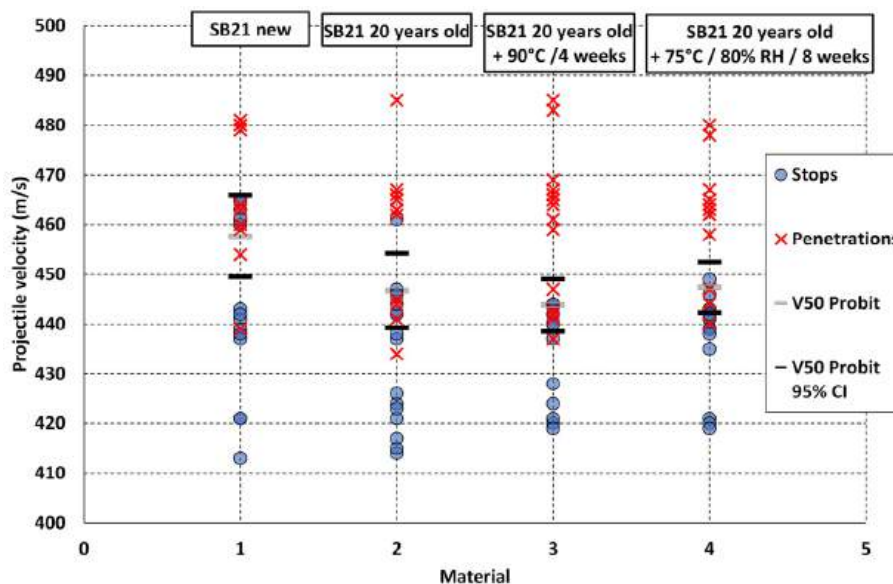
Fig. 2) Ballistic results (9mm DM41 FMJ) of the new, used and aged Dyneema® SB21 packs

These results very clearly demonstrate the extreme long-term ballistic performance stability of Dyneema® SB21 fiber-based composite sheets for ballistic protection.

REFERENCES

[1] S. Chabba, M. van Es, E.J. van Klinken, M.J. Jongedijk, D. Vanek, P. Gijsman, A. van der Waals, "Accelerated aging study of ultra high molecular weight polyethylene yarn and unidirectional composites for ballistic applications", *Journal of Material Science,* vol. 42, pp. 2891-2893 (2007).

[2] M. Hendrix, M. Herzog, "*Protective behavior of soft ballistic ultra-high-molecular-weight polyethylene*", *Scientific Articles,* Wiss. Beitr. TH Wildau, vol. 22, pp 47-51 (2018).

ID 116
IMPACT BEHAVIOUR ON COMPOSITE MATERIAL WITH EMBEDDED NON-NEWTONIAN FLUIDS

Konstantinos Myronidis[1], Abdelrahman Hegazy[1], Fulvio Pinto[1], Michele Meo[2]*

[1] Department of Mechanical Engineering, University of Bath, Bath, Ba2 7AY, UK

[2] Department Aeronautics and Astronautics, University of Southampton, UK

(*) Email: m.meo@soton.ac.uk

ABSTRACT

This research presents an innovative approach to impact protection using composite materials embedded with non-Newtonian fluids [1-3]. The study investigates the use of a non Newtonian fluid and polyborosiloxane-based shear stiffening gel (SSG), encapsulated using spherification, as a dynamic responding energy absorption medium (DrEAM). These materials are characterised by their ability to absorb energy through a phase transition, distributed in a controlled manner within smart protective layers. These layers can be designed to autonomously respond to external stimuli, such as rapid mechanical loads, by absorbing significant amounts of energy.

The findings of this research establish these novel smart protective layers as an ideal solution for a wide variety of applications where fragile and valuable goods are in transit and impact forces need to be minimised or eliminated. This includes applications such as camera lenses, electrical components, blood vials, and other medical products, overcoming the drawbacks of traditional packaging materials. Additionally, they provide a low-cost solution for the protection of CFRP laminates subjected to out-of-plane impacts, such as in aerospace or railway components.

INTRODUCTION

Over the past three decades, composite structures, which are layers of polymer matrices fortified with fibres, have emerged as the preferred material for most advanced engineering applications due to their exceptional specific mechanical properties. However, unidirectional composite materials have a drawback: they respond poorly to out-of-plane loading conditions like Low Velocity Impacts (LVI). This is mainly because of the brittle nature of the reinforcements in the laminae and their anisotropic characteristics, which can lead to hidden delamination within the structure and potentially catastrophic failure.

This study proposes the use of a multi-layered, non-Newtonian polymeric coating on the surface of composite laminates to address this inherent problem. While coatings have been widely researched for enhancing the mechanical properties of metal substrates, research on Carbon Fiber Reinforced Plastics (CFRPs) has primarily focused on in-plane properties or other non-structural properties. One of the proposed Smart Layer, a dynamic responding energy absorption medium (DrEAM), is composed of a polyborosiloxane (PBS)-based Shear Stiffening Gel (SSG) encapsulated in crosslinked vinyl-terminated polydimethylsiloxane (VPDMS). This frequency-dependent reversible network structure autonomously stiffens in response to an external stimulus, altering the way energy is distributed due to the dynamic phase transition of the embedded SSG.

RESULTS AND CONCLUSIONS

The performance of these smart layers was evaluated through static and dynamic tests, demonstrating superior performance compared to conventional protective layers. Specifically, the smart layers increased first and final compressive failure stresses by approximately 50%, and the maximum forces prior to failure in low velocity impact (LVI) tests were approximately 50% higher across the investigated impact energy levels. Furthermore, when

applied as a protective layer on the surface of Carbon Fibre Reinforced Polymer (CFRP) laminates, the smart layers modified the way energy is distributed due to the dynamic phase transition of the embedded SSG. Impacted samples were analysed using an ultrasonic Phased Array system and CT-Scan to examine the extent of internal damage. The results showed an average reduction of 65% of the extent of internal damage compared to uncoated CFRPs and outperformed conventional coatings by showing a further reduction of 33% at low energy (10 J) and more than 50% for higher energy (20 J).

Fig. 1 CFRP laminates post-impact with coatings removed, where present. a) reference laminate, b) 25%SSG and c) 75% SSG content.

The unique properties of these smart layers are largely due to the shear stiffening characteristics of the fluid/gel, which introduces an additional energy absorption mechanism through a frequency-dependent viscous-rubbery phase transition. This innovative feature allows the smart layers to respond dynamically to different impact conditions, providing optimal protection at all times. The post-impact results from LVI and Non-Destructive Testing (NDT) firmly establish these smart layers as a unique, cost-effective solution that can effectively address the inherent poor performance of CFRPs under impact loading. This represents a significant advancement in the field and opens up new possibilities for the use of CFRPs in a wide range of applications.

REFERENCES

[1] N.J. Wagner, J.F. Brady, Shear thickening in colloidal dispersions, Phys. Today, 62 (10) (2009), pp. 27-32

[2] F. Pinto, M. Meo, Design and manufacturing of a novel shear thickening fluid composite (STFC) with enhanced out-of-plane properties and damage suppression, Appl. Compos. Mater., 24 (3) (2017), pp. 643-660

[3] R.C. Neagu, P.-E. Bourban, J.-A.E. Månson, Micromechanics and damping properties of composites integrating shear thickening fluids, Compos. Sci. Technol., 69 (3–4) (2009), pp. 515-522

[4] Cuomo S, Rizzo F, Pucillo G, Pinto F and Meo M 2018 A Thermoplastic Polymer Coating for Improved Impact Resistance of Railways CFRP Laminates Proc. ECCM18-18th Conf. on Composite Materials

ID 117
SHAPE INFLUENCE ON THE CRASHWORTHINESS PERFORMANCE OF FLAX AND HYBRID/EPOXY COMPOSITES

Valentina Giammaria[1(*)], **Giulia Del Bianco**[1], **Monica Capretti**[1], **Simonetta Boria**[1]

[1] School of Science and Technology, Mathematics Division, University of Camerino, Italy

[(*)] Email: valentina.giammaria@unicam.it

ABSTRACT

This work aims to compare the effect of different geometries and hybrid combinations on the in-plane crashworthiness performances. This comparison is made from an experimental point of view considering the load-displacement trend, the specific energy absorption (SEA) and the crush efficiency (CE) properties. Since energy absorption is an essential requirement for several applications, it is very important to understand which is the best hybrid combination before designing a structural component.

INTRODUCTION

In recent decades, the interest in natural fibers has enormously grown in several sectors, like packaging, sport, construction, shipping and automotive. High availability, low cost, sustainability, and minimal health risks are some of the benefits deriving from their use. However, there are still important problems to solve, such as poor adhesion with different types of matrices, poor thermal stability, and tendency to absorb moisture, resulting in a nonuniform dispersion of the fiber in the matrix. Moreover, we are still far from the use of "green" composites, especially in those applications for which very high mechanical performances are required (H. Pulikkalparambil et al., 2023; Elmasry et al., 2024). The high energy absorption capacity of composite materials is a fundamental aspect for several industrial applications, but the research on the in-plane crashworthiness performance is still under development and no recognized standard has been developed up to now. Therefore, this work provides an overview of the in-plane crashworthiness behavior of flax and hybrid (carbon-flax) / epoxy composites considering two different geometries: flat and corrugated (S-shape). Since this type of tests is used to evaluate the crush energy absorption properties, a complete comparison is made in terms of SEA and CE. The obtained results reveal that the use of a fully flax reinforcement is of course not comparable with carbon; therefore, hybridization represents a possible solution to improve sustainability without renouncing to the high mechanical resistance that carbon is able to guarantee.

RESULTS AND CONCLUSIONS

A preliminary experimental campaign, including tensile and compression tests, was performed on flax (F) and carbon (C) / epoxy laminates to evaluate their mechanical properties. Subsequently, dynamic in-plane crashworthiness tests are carried out on the above mentioned geometries: flat and corrugated. In the first case, the specimen is easy to manufacture since it is rectangular, altough it requires a specific anti-buckling fixture that could influence the crushing behavior. Since there is no recognized standard for this type of test, the anti-buckling fixture used in this work is the one presented by Vigna (Vigna, 2021). It consists of lateral and central columns (see Fig.1b) that support the specimen for its full length, leaving un unsupported height of 7.5 mm to avoid over-constraining and leave enough space to remove debris and foils during failure. To help delamination to start, a sawtooth shape released feature in the shorter side opposite to the impactor is required, as shown in Fig.1a. The impact energy level is of 300 J. Regarding the corrugated geometry, instead, no fixture is necessary, but only a support of 13 mm

is used to fix the sample during the test (Feraboli, 2011). This type of shape allows for the analysis of composites' behavior in presence of curvatures, which is fundamental for the investigation of more complex structures. Details on this latter geometry are shown in Fig.2. The impact energy is of 500 J, since this shape allows to reach higher values of force.
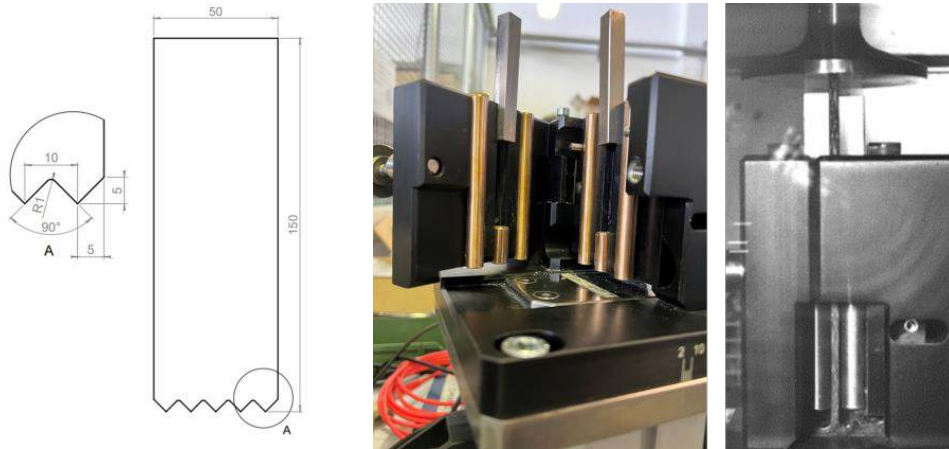
Fig. 1 Flat shape: a) geometric scheme, and b) anti-buckling testing fixture.
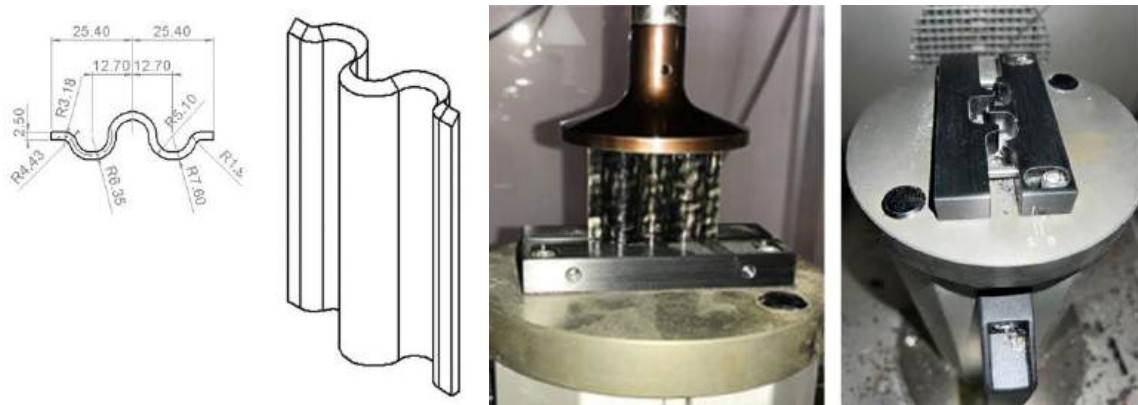
Fig. 2 Corrugated shape: a) geometric scheme, and b) testing fixture equipment.

As mentioned above, "fully" flax reinforced composites are not able to reach results comparable to carbon; therefore, two hybrid solutions are here analysed combining both these fibers: $F_2/C_4/F_2$ and $C_2/F_4/C_2$, which are called for simplicity FCF and CFC, respectively. Figs. 3 and 4 show the comparison between carbon, flax, FCF, and CFC in terms of load-displacement, SEA, and CE, revealing that in all cases the corrugated shape reaches better results. This suggests that the use of different shapes could significantly influence the mechanical response. Moreover, in terms of hybridization, it can be observed that the two hybrid solutions perform very well with respect to the "fully" flax case, but among them the best combination is FCF, whose results are very close to carbon.
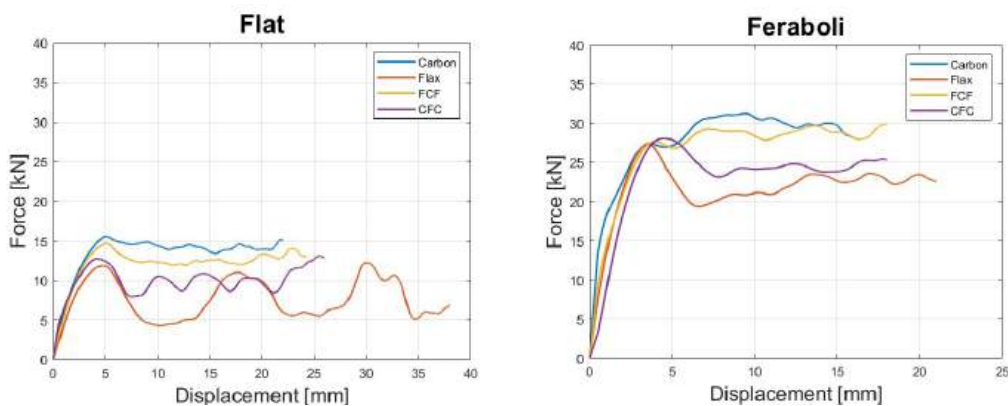
Fig. 3 Experimental load-displacement trend for a) flat, and b) corrugated shape for all materials analysed.
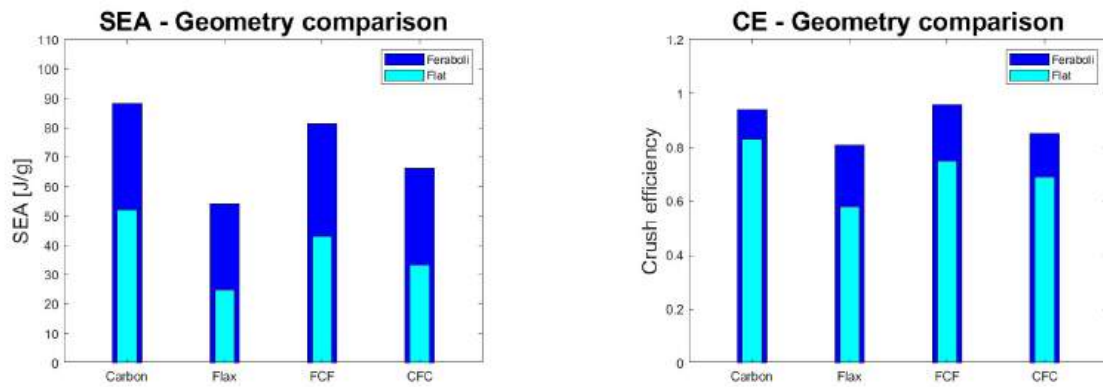
Fig. 4 Experimental comparison between flat and corrugated shape: a) SEA, and b) CE for all materials analysed.

REFERENCES

[1] H. Pulikkalparambil, S. A. Varghese, V. Chonhenchob, T. Nampitch, L. Jarupan, N. Harnkarnsujarit, "Recent Advances in Natural Fibre-Based Materials for Food Packaging Applications", *Polymers*, vol. 15, 2023.

[2] A. Elmasry, W. Azoti, E. Ghoniem, A. Elmarakbi, "Modelling of hybrid biocomposites for automotive structural applications", *Composites Science and Technology*, vol. 251, 2024.

[3] L. Vigna, A. Calzolari, G. Galizia, G. Belingardi, D.S. Paolino, "Effect of impact speed and friction on the in-plane crashworthiness of composite plates", *Procedia Structural Integrity*, vol. 33, 2021.

[4] P. Feraboli, B. Wade, F. Deleo, M. Rassaian, M. Higgins, A. Byar, "LS-DYNA MAT54 modeling of the axial crushing of a composite tape sinusoidal specimen", *Composites Part A*: *Applied Science and Manufacturing*, vol. 42, 2011.

ID 120
SURFACE FUNCTIONALIZATION STRATEGIES FOR THE CREATION OF MULTIFUNCTIONAL FABRICS

Sourabh Kulkarni [1,4]**, Shiran Yu** [2]**, Zhiyu Xia** [2]**, Alexander B. Morgan** [5]**, Jayant Kumar** [3,4]**, Ravi Mosurkal** [4,6*]**, Ramaswamy Nagarajan** [2,4*]

Departments of [1]Mechanical Engineering, [2]Plastics Engineering, [3]Physics and Applied Physics, [4]The HEROES Initiative, Center for Advanced Materials University of Massachusetts Lowell, Lowell, MA 01854, USA

[5]Center for Flame Retardant Materials Science, University of Dayton Research Institute, Dayton, Ohio 45469, USA

[6]Protection Materials Division, Soldier Protection Directorate, US Army DEVCOM - Soldier Center, Natick MA 01760, USA

*Email(s): Ramaswamy_Nagarajan@uml.edu;

ABSTRACT

A 50/50 blend of nylon and cotton (Nyco) is widely used by the US Armed forces for Army Combat Uniforms (ACU) due to its excellent combination of mechanical properties, comfort, and low cost. Despite these excellent properties Nyco is inherently flammable. The burning behavior is also unique due to the combination of a natural fiber (cotton) and a thermoplastic polymer (nylon) in the fiber blend which gives rise to the scaffolding effect. To address the flammability of Nyco fabric, several approaches have been developed for Nylon and cotton fabrics separately to impart flame retardancy. For Nylon fabric, polyphenols have been explored as char forming flame retardant. Polyphenols such as tannic acid can be coated onto the surface of the fabrics via acid dyeing techniques. The attachment of tannic acid on nylon helps improve the thermal stability and impart flame retardancy. Cellulosic fabrics on the other hand require phosphorus based flame retardant compounds for self-extinguishing characteristics. Various chemistries and processes were developed to covalently functionalize phosphorus based compounds on to cotton fabric. These compounds help in catalyzing the carbonization of cellulose, increasing the char formation, and giving rise to self-extinguishing fabrics with a char length of less than 4 inches in standard vertical flame tests. For Nyco fabrics, the combination of polyphenols along with a phosphorous containing compounds can impart FR characteristics. A systematic approach to functionalizing Nylon, Cotton and Nyco will be presented, and lessons learnt will be discussed. Detailed spectroscopic and thermal characterization of nylon, cotton and Nyco fabric as well as assessment of launder durability will also be presented.

In addition facile methods for amplifying the surface reactivity of fabrics followed by covalent attachment of antimicrobial agents such as Polyhexamethylene biguanide (PHMB) will also be presented.

POSTER PRESENTATIONS
ID 2
DEVELOPMENT OF TECHNICAL TEXTILE FABRICS FOR ELECTROMAGNETIC SHIELDING PURPOSES

Kadriye Kutlay[1](*), Nejla Degirmenci[2], Özlem Buluş[3]

[1, 2, 3] Berteks R&D Center, Bursa, Türkiye

[1] Bursa Technical University Polymer Materials Engineering, Bursa, Türkiye (*) Email: nejla.degirmenci@berteks.com

ABSTRACT

In this project; It is aimed to produce textile surfaces that provide electromagnetic shielding by using weaving and coating techniques. The material used for this purpose, knitting type, knitting density, product weight, etc. The effects of the parameters on the shielding effectiveness were examined. Electromagnetic shielding materials are frequently used in the military field for radar invisibility or interference problems. These materials are heavy and inflexible.It is aimed to develop surfaces with electromagnetic shielding efficiency as an alternative to heavier and inflexible materials that are equivalent in military fields.

INTRODUCTION

Typical metal products, which are known to be effective in EM shielding, are expensive, heavy, and are not suitable for use in all areas due to their properties such as thermal expansion and hardness. Especially in the military field, the material being heavy and hard is undesirable for use. For this reason, the use of textile products for EM protection; They are considered as an alternative because they are light, flexible and cheap. Ways to create fabric that provides EM protection:

· For example, lamination of conductive surfaces to the fabric surface; fabric coating with conductive polymers.

· Adding conductive materials such as carbon fiber and stainless steel to the surface.

Adding conductive yarn to the fabric construction or using conductive material by integrating it with fibers

In the project, textile surfaces with different properties were developed using the above 3 methods, with the information obtained after extensive literature research on these methods.

RESULTS AND CONCLUSIONS

ASTM D4935 test method was used for measurement. A shielding efficiency of 40 dB and above is aimed for the developed textile surfaces for daily use and 80 dB and above for military use.

Fig. 1 Weaving Trial

Fig. 2 Weaving Trial
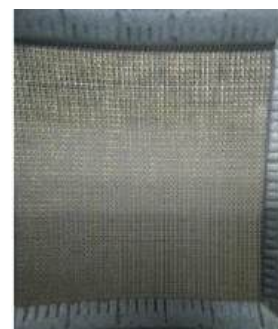
Fig. 3 Weaving Trial
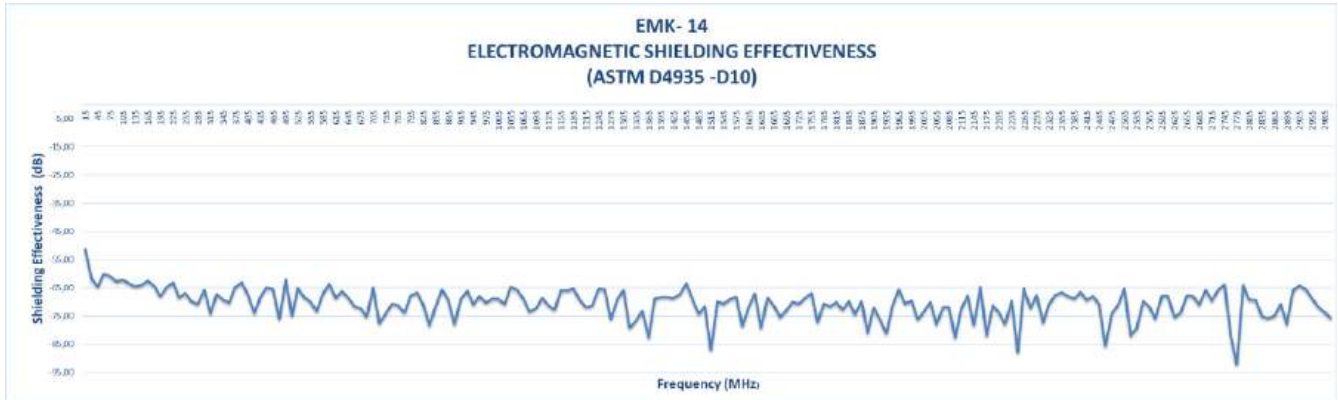
Whether the EMF property occurs in the form of absorption or reflection is an important criterion that determines the usage area of the material. While materials with high absorption properties are mostly used for military purposes, materials with high reflectivity are suitable for daily use. In the ASTM D4935 standard, how the material provides shielding can also be measured. Using these measurements, the usage areas of the collection to be created were determined before presenting it to the customer.
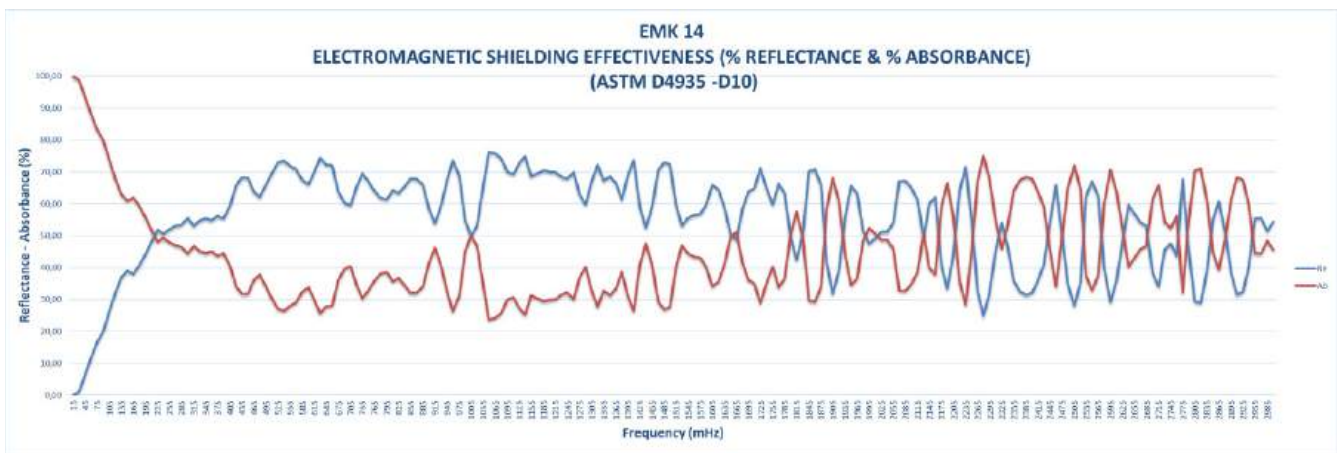
Fig. 5 Fabric EMF Test Result

REFERENCE

[1] Rana Yılmaz, "Materials with Electromagnetic Shielding Features", 2014

[2] Sonay Doğan, Ozan Kayacan, Aytaç Goren (2018): Development of Polymer Composite Structures with Electromagnetic Shielding Features, Textile and Engineer, 25: 109, 44-52.

[3] Ebru Seza Türksoy, Sümeyye Üstüntağ, Öznur Saritaş, Ömer Galip Saraçoğlu (2015): An Innovative Test Apparatus for Measurement of Electromagnetic Shielding Effectiveness of Textile Materials, Textile and Engineer, 22: 99, 15-26.

[4] Nermin Dağ, Investigation of Electromagnetic Shielding Features on Conductive Textile Surfaces, 2010

ID 3

HAND ANTHROPOMETRY OF BANGLADESHI UNIVERSITY STUDENTS

Engr. Md. Eanamul Haque Nizam [(1,1*)], Emeritus Prof. Darko Ujevic[2], Prof. Dr. Engr. Ayub Nabi Khan[3], Bristy Rani Roy[4], Badhan Chandra Roy[5]

[1*]PhD (Fellow), Faculty of Textile Science and Technology, University of Zagreb, Croatia

[1]Assistant Professor, Department of Textile Engineering, Southeast University, Tejgaon, Dhaka, Bangladesh.

[2]Emeritus Professor, Faculty of Textile Science and Technology, University of Zagreb, Croatia

Pro-Vice Chancellor, BGMEA University of Fashion and Technology-BUFT, Turag, Dhaka, Bangladesh.

[4]Textile Students, Department of Textile Engineering, Southeast University, Tejgaon, Dhaka, Bangladesh.

[5]Textile Graduate, Department of Textile Engineering, Southeast University, Tejgaon, Dhaka, Bangladesh.

[(*)] Email: eanamul.nizam@seu.edu.bd

ABSTRACT

This study represents the findings of hand anthropometry conducted on 58 males and 13 females in the 18−25-year age group of Bangladeshi university students. 25 (twenty-five) dimensions of each hand were measured together with body height, weight, and BMI. An analysis of the mean, standard deviation, and 10th, 50th, and 90th percentile values are provided in this article. This study provides information regarding gender differences, right-handed versus left-handed individuals, age groups, and so on. Due to a lack of information regarding the dimensions of openings for hand access into machines in the Bangladeshi tools. A potential comparison with anthropometry data from other world populations was performed to evaluate the effective difference.

INTRODUCTION

Hand tools have been used by humans since the beginning of time, according to research into human history. The hand axes and flints that Neanderthal Man used for his work were made of stones or bones that had been altered to fit the anthropometry of the human hand. This issue's importance has not diminished with time, on the contrary. Additionally, the physical characteristics of the workers should be compatible with the modern equipment. Measurements of the length, width, and height of the human body are the subject of the science known as anthropometry (T. Kanchan, K. Kirshan, 2011), is appropriate for this optimization. It is well recognized that mismatches between the anthropometric measurements of humans and the dimensions of equipment can lead to reduced productivity, discomfort, mishaps, injuries, and cumulative traumas. (P. Loslever, A. Ranaivosa, 1993) (S.N. Imran et.al, 1993). The use of hand anthropometric data is essential for engineers designing any hand tool; without it, the product may not be ergonomically sound. The design of handles, grip options, and operation button distances all depend on hand anthropometry data. Applications of the findings in the following paper are not limited to hand tool design. The dimensions needed for hand access openings in machinery (for automation in assembly or safety purposes, for example) can be ascertained using the data that is provided. There are a lot of factors to consider, like age group, dominant hand, gender of the operating person, and nationality. But not every task calls for a particular hand tool, and not every user benefits from having the same tool (Y.A.A Mohammad, 2005). People who will be using the tool daily should be involved in the testing process as new ergonomic designs are being tested. This study set out to measure Bangladeshis' hands precisely and compared the results with those of other studies involving different populations. The purpose of selecting hand dimensions was based on their intended use, mainly in the design of firearms (K. Sekulova et.al, 2015). The data are used more widely in hand tool design in general, though. The aging factor received special attention as well. Unlike other recently published studies on hand anthropometry, this one:

Table 1 Cluster analysis of the population

Division's	Populations	
	Male	Female
Dhaka	12	2
Chattogram	2	1
Barishal	7	4
Khulna	7	0
Mymensingh	11	1
Sylhet	6	1
Rangpur	9	3
Rajshahi	4	1
In total:	58	13

Bangladeshi uses European standards for workplaces and tool design however this standard is not sufficient.

RESULTS AND CONCLUSIONS

Few hands anthropometric survey of various nationalities such as India, Jordanian, Singaporean, and Nigerian as well as Bangladeshi female population were shown in Table 3. Here, age range and sample population size for different nationalities' population are quite similar with the present study. Mean stature and standard deviation of different population can be compared from this table.

Table 3 Sample Population Features of Various Works on Different Population.

Studies	Nationality	Range of age	Sample populations	Mean ±Standard Deviation
Present study	Bangladeshi	18-25	Male: 58	171.5±6.1
			Female: 13	161.15±3.17
Nag et.al 2003	Indian	18-60	Male: 37	157.22±8.76
			Female: 51	149.88±6.28
Mandahawi 2008	Jordanian	18-59	Male: 120	162.19±5.20
			Female: 24	132.77±7.71
Saengchaiya and Bunterngchit 2004	Singaporean	18-59	Male: 120	149.88±6.28
			Female: 150	116.19±4.64

Table 4: Comparisons of measurements for Bangladeshi male and female university students

Dimension	Age	Male					Female				
	18-25	10th	50th	90th	Mean	SD	10th	50th	90th	Mean	SD
Height		164.2	172	180.3	171.5	6.1	155.6	162	165.07	161.5	3.17
Weight		53.8	64	83.2	66.6	11.4	46.6	57	66.8	56.6	6.83
BMI		17.46	20.2	25.26	20.58	2.79	17.5	21.5	25.96	21.65	2.81
(L.H) Thumb width (Lij) [cm]		1.88	2.4	3	2.41	0.42	1.83	2.5	2.91	2.4	0.36
(R.H) Thumb width (Lij) [cm]		1.9	2.5	3	2.45	0.40	1.73	2.5	2.91	2.39	0.37
(L.H) Index finger width(Ljt) [cm]		1.5	2.3	2.8	2.25	0.44	1.8	2.2	2.67	2.18	0.29
(R.H) Index finger width(Ljt) [cm]		1.6	2.3	2.82	2.29	0.43	1.8	2.2	2.67	2.19	0.28
(L.H) Middle finger width(Ljtg) [cm]		1.8	2.2	2.92	2.26	0.43	1.63	2.25	2.7	2.27	0.33
(R.H) Middle finger width(Ljtg) [cm]		1.7	2.2	3	2.3	0.45	1.63	2.4	2.87	2.33	0.42
(L.H) Ring finger width(Ljm) [cm]		1.68	2.1	2.7	2.19	0.43	1.63	2.3	2.6	2.19	0.37
(R.H) Ring finger width(Ljm) [cm]		1.7	2.3	2.8	2.23	0.43	1.6	2.35	2.64	2.15	0.4
(L.H) Width of little finger[cm]		1.3	2	2.6	1.98	0.44	1.33	2	2.2	1.88	0.28
(R.H) Width of little finger[cm]		1.4	2.1	2.72	2.05	0.47	1.33	2.1	2.2	1.88	0.35
(L.H) Thumb length(Pjt) [cm]		5.58	6.4	7.66	6.46	0.71	5.5	6.45	7.1	6.46	0.55
(R.H) Thumb length(Pjt) [cm]		5.6	6.5	7.44	6.53	0.69	5.65	6.7	7.07	6.57	0.47

(L.H) Index finger length(Pjt) [cm]		6.5	7.3	8.16	7.4	0.72	6.49	7.35	7.5	7.18	0.33
(R.H) Index finger length(Pjt) [cm]		6.8	7.4	8.32	7.49	0.67	7.13	7.4	8.04	7.48	0.29
(L.H) Middle finger length[cm]		7.58	8.2	9.08	8.35	0.69	7.25	8	8.58	7.96	0.38
(R.H) Middle finger length[cm]		7.58	8.3	9.12	8.37	0.71	7.2	8.05	8.64	8.03	0.45
(L.H) Ring finger length[cm]		6.46	7.5	8.76	7.63	0.81	6.86	7.4	8.27	7.38	0.43
(R.H) Ring finger length[cm]		6.88	7.6	8.8	7.70	0.77	5.9	7.3	8.46	7.20	0.76
(L.H) Length of little finger(Pjk) [cm]		6	6.5	7.8	6.69	0.72	5.83	6	6.62	6.06	0.25
(R.H) Length of little finger(Pjk) [cm]		6	6.6	7.72	6.75	0.68	5.8	6	6.41	6.03	0.19
(L.H) Metacarpal hand thickness[cm]		1.5	1.9	2.22	1.90	0.30	1.3	1.9	2.07	1.83	0.25
(R.H) Metacarpal hand thickness[cm]		1.4	2	2.3	1.96	0.33	1.2	1.95	2.14	1.82	0.31
(L.H) Thumb hand thickness(Ttij) [cm]		6	6.8	7.32	6.69	0.55	5.59	6	6.07	5.93	0.15
(R.H) Thumb hand thickness(Ttij) [cm]		6	6.9	7.42	6.75	0.6	5.59	5.9	6.2	5.94	0.19
(L.H) Thumb thickness(Tij) [cm]		4.18	4.7	5.5	4.75	0.54	2.33	3.5	4.23	3.43	0.58
(R.H) Thumb thickness(Tij) [cm]		4.2	4.8	5.6	4.82	0.55	2.25	3.55	4.26	3.47	0.58
(L.H) Finger thickness[cm]		4.68	6.2	6.92	6.11	0.84	5.5	5.65	5.97	5.71	0.18
(R.H) Finger thickness[cm]		4.6	6.2	7.12	6.2	0.87	5.5	5.75	6	5.75	0.18
(L.H) Hand gripping length(Ptm) [cm]		11	11.8	12.92	11.82	0.95	11.06	12.5	12.9	12.19	0.72
(R.H) Hand gripping length(Ptm) [cm]		11	12	13.02	11.95	0.98	11.2	12.6	13	12.33	0.66
(L.H) Hand gripping width(Ltm) [cm]		9.88	10.4	12.18	10.58	0.98	8.7	10	10.41	9.74	0.61
(R.H)Hand gripping width(Ltm) [cm]		9.24	10.5	12	10.63	1.00	8.7	10	10.37	9.78	0.59
(L.H)Hand length(Pt) [cm]		17.08	18	21	18.46	1.35	17.15	17.9	18.07	17.82	0.29
(R.H)Hand length(Pt) [cm]		17.38	18.2	21.04	18.48	1.26	17.43	17.9	18.14	17.83	0.21
(L.H) Palm length(Ptt) [cm]		8.1	10.5	12	10.35	1.24	7.13	7.95	9.39	7.98	0.66
(R.H) Palm length(Ptt) [cm]		8.18	10.7	11.9	10.36	1.29	7.1	8	9.42	8	0.68
(L.H) Metacarpal hand width(Ltmk) [cm]		7.5	8.2	8.74	8.23	0.59	7.2	7.6	8.91	7.12	0.52
(R.H) Metacarpal hand width(Ltmk) [cm]		7.58	8.3	8.7	8.29	0.60	7.16	7.8	8.98	7.83	0.54
(L.H) width of hand to thumb(Ltlj) [cm]		6.56	7.8	10.06	8.19	1.27	5.9	6.45	6.64	6.31	0.27
(R.H) width of hand to thumb(Ltlj) [cm]		6.56	7.9	9.96	8.30	1.25	5.73	6.5	6.71	6.32	0.33
(L.H) Little thumbs distance(Jjk) [cm]		5.3	6.1	6.6	6.04	0.49	4.9	5.2	5.5	5.19	0.19
(R.H) Little thumbs distance(Jjk) [cm]		5.5	6.2	6.72	6.18	0.5	5.06	5.35	5.57	5.34	0.14
(L.H) Maximum grip diameter(Dgmak) [cm]		3.68	4.2	5	4.33	0.67	3.5	4.25	4.85	4.25	0.41
(R.H) Maximum grip diameter(Dgmak) [cm]		3.6	4.4	5.1	4.43	0.69	3.4	4.4	5	4.28	0.49
(L.H) Minimum grip diameter(Dgmin) [cm]		1.78	2.1	2.52	2.06	0.38	1.7	2.6	2.7	2.4	0.38
(R.H) Minimum grip diameter(Dgmin) [cm]		1.78	2.2	2.72	2.15	0.39	1.6	2.6	2.9	2.45	0.44
(L.H) Fist width(Lkt) [cm]		8.88	10.8	12.04	10.59	1.2	8.4	8.45	11.19	8.93	0.95
(R.H) Fist width(Lkt) [cm]		8.9	10.9	12.3	10.64	1.24	8.23	8.55	11.33	8.93	1.01
(L.H) Fist height(Tgkt) [cm]		5.38	6.1	6.76	6.01	0.59	5.2	5.65	6.44	5.71	0.38
(R.H) Fist height(Tgkt) [cm]		5.48	6.2	6.84	6.09	0.55	5.5	5.6	6.37	5.74	0.31

Difference between Male and female value with statically

Treatment

Treatment 1

N1: 53

df1 = N - 1 = 53 - 1 = 52

M1: 11.09

SS1: 30661.98

s21 = SS1/(N - 1) = 30661.98/(53-1) = 589.65

Treatment 2

N2: 53

df2 = N - 1 = 53 - 1 = 52

M2: 10.23

SS2: 26694.46

22 = SS2/(N - 1) = 26694.46/(53-1) = 513.35666666

T-value Calculation

s2p = ((df1/(df1 + df2)) * s21) + ((df2/(df2 + df2)) * s22) = ((52/104) * 589.65) + ((52/104) * 513.35) = 551.5

s2M1 = s2p/N1 = 551.5/53 = 10.41

s2M2 = s2p/N2 = 551.5/53 = 10.41

t = (M1 - M2)/√(s2M1 + s2M2) = 0.86/√20.81 = 0.19

The t-value is 0.18814. The p-value is .425565. The result is not significant at p < .05.

Single Sample T-Test

United fans reported higher levels of stress (M = 83, SD = 5) than found in the population, t (48) = 2.3, p = .026.

Coffee drinkers spent more time awake (M = 17.8, SD = 1.4) than the population norm, t(28) = 2.6, p < .05.

Independent T-Test

The 25 participants who received the drug intervention (M = 480, SD = 34.5) compared to the 28 participants in the control group (M = 425, SD = 31) demonstrated significantly better peak flow scores, t (51) = 2.1, p = .04.

There was no significant effect for sex, t (3--8) = 1.7, p = .097, despite women (M = 55, SD = 8) attaining higher scores than men (M = 53, SD = 7.8).

Dependent T-Test

The results from the pre-test (M = 13.5, SD = 2.4) and post-test (M = 16.2, SD = 2.7) memory task indicate that the presence of caffeine in the bloodstream resulted in an improvement in memory recall, t (19) = 3.1, p = .006.

There was a significant increase in the volume of alcohol consumed in the week after the end of semester (M = 8.7, SD = 3.1) compared to the week before the end of semester (M = 3.2, SD = 1.5), t (52) = 4.8, p < .001.

Table 5: Comparison of hand anthropometric data of selected world nationalities (M. Bures et.al, 2015)

Nationality	Values	Male (18-25 years)				Female (18-25 years)			
		Hand length	Palm length	Hand breadth	Middle finger length	Hand length	Palm length	Hand breadth	Middle finger length
Vietnamese	Mean	177	98.8	79.2	78.2	165	92.7	71	72.3
	SD	12	--	6.9	4.5	9	--	4.3	4.6
Bangladeshis [cm]	Mean	18.48	8.19	1.96	8.37	17.82	6.31	1.82	8.03
	SD	1.26	1.27	0.33	0.71	0.29	0.27	0.31	0.45
Filipinos	Mean	197.5	--	98	--	179.5	..	92.3	--
	SD	7.82	--	4.07	--	3.44	--	6.97	--
Jordanians	Mean	191.2	109.9	87.7	81.3	171.3	96.1	77.8	75.2
	SD	10.2	--	4.82	7.14	7.44	--	3.92	3.62
Turkish	Mean	190.4	108.5	87.3	81.9	172.2	97.8	76.1	74.4
	SD	9.69	--	4.67	5.15	8.14	--	4.66	3.91
Mexicans	Mean	185.5	107	85.3	78.5	--	--	--	--
	SD	7.1	--	4.9	4.4	--	--	--	--
Czechs	Mean	192	110	89	82	176	100	79	76
	SD	9.83	6.1	5.63	5.29	8.01	4.82	4.11	4.73

CONCLUSIONS:

The study described in this article aims to collect up-to-date data on manual measurements in Bangladeshis aged 18–25 years and use these data for potential design of hand tools and human-machine interaction. The statistical evaluation of the measured values was compared with six countries around the world to find differences.

Age relation – The results of this study showed that age had little effect on the relevant hand measures. Differences were found only in height and weight. The hypothesis that height decreases with age was confirmed. On the other hand, all weight-related diseases tended to increase with age. Overall, a small increase was seen for women.

Males vs. females – Our study found that women's hand sizes were about 3% to 5% smaller, depending on their size. Of course, larger differences were found in arm length and girth, and smaller differences were found in finger length.

Right vs. left hand – The differences in measurements between the two arms were not found to be significant. In the longitudinal measurements, the differences were shifted by about 1 mm, resulting in high agreement. A relatively large difference of approximately 5-6 mm was observed in the right large limb.

Comparison with other nationalities – This comparison was conducted across five nationalities (Vietnamese, Filipino, Jordanian, Turkish and Mexican men). The Czech, Turkish and Jordanian hands were very similar in size due to their relative geographic proximity. With all these statistical evaluations and comparisons, we have enough information and up-to-date data for all applications that require human (manual) intervention.

REFERENCES

[1] DIN 33402-2, "Ergonomics - Human body dimensions - Part 2: Values" (in German), Ergonomie - Körpermasse des Menchen - Teil 2: Werte, Deutsches Institut für Normung, Berlin, 2005

[2] EN ISO 15535, "General requirements for establishing anthropometric databases", 2006.

[3] EN ISO 7250, "Basic human body measurements for technological design", 1997

[4] S. N. Imrhan, M. Nguyen, N. Nguyen, "Hand anthropometry of Americans of Vietnamese origin". International Journal of Industrial Ergonomics, vol. 12, pp. 281–287, 1993

[5] K. Sekulova, M. Bures, O. Kurkin, M. Simon, "Ergonomic Analysis of a Firearm According to the Anthropometric Dimension". Procedia Engineering, vol. 100, pp. 609–616, 2015.

[6] M. Bures, T. Gorner and B. Sediva, "Hand anthropometry of Czech population," 2015 IEEE International Conference on Industrial Engineering and Engineering Management (IEEM), Singapore, 2015, pp. 1077-1082, doi: 10.1109/IEEM.2015.7385814.

[7] P. Loslever, A. Ranaivosoa, "Biomechanical and epidemiological investigation of carpal tunnel syndrome at workplaces with high risk factors". Ergonomics, vol. 36, pp. 537–555, 1993.

[8] T. Kanchan, K. Kirshan, "Anthropometry of hand in sex determination of dismembered remains - A review of literature". Journal of Forensic and Legal Medicine, vol. 18, pp. 14-17, 2011.

[9] The information has retrieved from: https://soloabadi.com/en/get-to-know-anthropometric-measurements-in--the-palm-of-the-hand/

[10] Y. A. A. Mohammad, "Anthropometric characteristics of the hand based on laterality and sex among Jordanian". International Journal of Industrial Ergonomics, vol. 35, pp. 747–754, 2005

ID 11

MG-BASED ALLOYS THIN FILMS DERIVED FROM MGAL LAYERED DOUBLE HYDROXIDES RECONSTRUCTED IN OXYGEN-RICH ENVIRONMENTS

Loredana Andreea Gavrila[1], Elena Mihaela Seftel[2], Gabriela Carja*[1]

1 Department of Chemical Engineering, Faculty of Chemical Engineering and Environmental Protection, Technical University "Gh. Asachi", Bd. Mangeron 71, Iasi 700554, Romania

2 VITO Flemish Institute for Technological Research, Boeretang 200, B-2400, Belgium

(*)Email: carja@uaic.ro

ABSTRACT

Thin films of Mg-based alloys show great promise as structural materials for applications in defense-related transportation, aircraft, and communication technologies. However, the practical implementation of magnesium alloys encounters challenges such as porosity and low oxygen content, which can negatively impact the corrosion resistance and mechanical properties of the derived thin films. Our research focuses on the fabrication of thin films of oxygen-rich Mg-based alloys derived from MgAl 2-D layered double hydroxides (LDH) that underwent structural reconstruction in an oxygen-rich environment of the aqueous solutions of hydrogen peroxide. Through comprehensive analyses using X-ray diffraction (XRD) and field emission scanning electron microscopy (FESEM), we investigated how varying concentrations of H2O2 solutions influence the oxygen content and micromorphology of the thin films.

INTRODUCTION

Magnesium alloys exhibit significant potential for applications in aerospace, aircraft, and defense technologies, being hailed as the „green engineering materials of the 21st century". Recent findings point out that the controlled incorporation of oxygen in magnesium alloys is essential for tailoring their properties to meet specific requirements, including controlled micromorphology, corosion protection and overall stability [Song et al. 2020]. The oxygen-rich magnesium alloys were obtained by the thermal treatment of MgAl 2-D layered double hydroxides (LDH) reconstructed in oxygen-rich aqueous solutions of H2O2. The concentration of H2O2 solution was used as a parameter to tailor the oxygen content in the reconstruction medium and the impact on the micromorphology features of the fabricated Mg-rich alloys films. Layered double hydroxides (LDH) are anionic clays that have received significant attention over the past decade. An intriguing characteristic of LDH is their structural „memory effect," allowing them to restore their original layered structure after calcination-induced destruction processes (Carja et al. 2013). Despite the fact that the exploitation of the memory effect has been proven to be an effective strategy to tune the properties of the LDH, it still remains a great challenge to exploit the reconstruction of the LDH in oxygen-rich environments such that to create oxygen rich mixed oxides with tuned micromorphology.

This work presents a novel procedure to fabricate Mg-rich alloys thin films (average thickness equal of 90 nm) derived by calcination of MgAlLDH structurally reconstructed in a tailored oxygen-rich environment of aqueous hydrogen peroxide solutions. The structural features of the novel Mg-based alloys thin films were studied by XRD while the micromorphology properties were analysed by FESEM analysis.

RESULTS AND CONCLUSIONS

MgAlLDH was synthesized by the co-precipitation method under a molar ratio of Mg2+/Al3+ at 2:1 (Darie et al. 2019). Subsequently, the layered structure of MgAlLDH was disrupted through thermal treatment. The structural reconstruction procedure (Carja et al. 2013) was done at room temperature under vigorous stirring with H2O2 solutions of varying concentrations, serving as an oxygen-rich reconstruction medium. Next, Mg-rich alloys were obtained from MgAlLDH calcined at 750°C. Following this, thin films were fabricated using a laboratory bench spin coater, and the structural and morphology characteristics were examined by XRD and FESEM analyses. The average size of the film thickness was 90 nm. The results indicate that the specific reconstruction procedure have a discernible impact on the textural features of the films. Such that, comparison of the surface smoothness, (see Fig.1) reveals specific textural characteristics of the thin films surface. When MgAlLDH precursor was reconstructed in H2O, the non-uniformity of the film surface became more apparent, pointing out the enhanced porosity. Reconstruction in oxygen-rich H2O2 solutions results in films with smoother surfaces and decreased meso-macroporosity features.
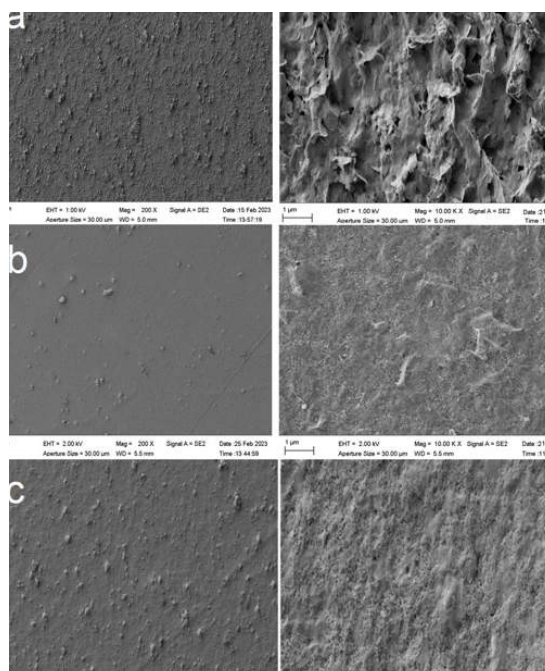

Fig. 1 SEM images of the thin films of MgAlO derived from calcined MgAlLDH (2/1)

after reconstruction in: a) H_2O b) H_2O_2 30%, c) H_2O_2 solution 10%.

In conclusion, we developed a novel procedure, employing MgAlLDH reconstructed in oxygen-rich H_2O_2 solutions as precursors, for the fabrication of thin films of oxygen-rich MgAl alloys. This innovative procedure allows for the tailoring of porosity and oxygen content according to specific requirements. The outcomes of this research hold the potential to fabricate MgAl alloy thin films with controlled porosity for addressing challenges related to corrosion resistance and mechanical performance for applications of magnesium-based alloy thin films in defense offering opportunities to improve the performance, durability, and efficiency of military equipment and infrastructure while addressing the need for lightweight and resilient materials in various defense scenarios.

REFERENCES

[1] S.Q. Pan , F. Zhang , C. Wen, R.C. Zeng, Advances in Mg−Al-layered double hydroxide steam coatings on Mg alloys: A review, Journal of Magnesium and Alloys, vol. 11, no. 5, May, pp. 1505−1518, 2023.

[2] G. Carja, L. Dartu, K. Okada, Elvira Fortunato, "Nanoparticles of copper oxide on layered double hydroxides and the derived solid solutions as wide spectrum active nano-photocatalysts", Chemical Engineering Journal, vol. 222, April, pp. 60−66, 2013.

[3] M. Darie, E.M. Seftel, M. Mertens, R.G. Ciocarlan, P. Cool, G. Carja, "Harvesting solar light on a tandem of Pt or Pt-Ag nanoparticles on layered double hydroxides photocatalysts for p-nitrophenol degradation in water", Applied Clay Science, vol. 182, December, pp. 105250, 2019.

ID 49
BEHAVIOR OF HANDGUN PROJECTILES FIRED TO BLOCKS OF BALLISTIC GELATIN

Ruano Rando, Manuel Jesús [1](*), **Jiménez Jiménez, José Ángel**[2], **Loya Lorenzo, José Antonio**[3,4]

[1] Criminal Intelligence Unit, Guardia Civil, Madrid, Spain.

[2] Ballistics and Toolmark Department, Criminalistics Service, Guardia Civil, Madrid, Spain.

[3] Department of Continuous Mechanics and Structural Analysis, Universidad Carlos III de Madrid, Leganés, Madrid, Spain.

[4] University Center of Guardia Civil, Aranjuez, Madrid, España

(*) Email: manuelruano@guardiacivil.es

ABSTRACT

The present work proposes an experimental design for the performance of ballistics tests to evaluate the behavior of projectiles fired with a handgun after impacting the human body, since, although there are several scientific publications that have analyzed the effects caused by long gun ammunition (Janzon, 1982), only a few are related to handgun ammunition. Therefore, given the interest and the need to increase the knowledge about the behavior of ammunition on the human body, the present work analyzes it by comparing different handgun ammunition fired against blocks of soft tissue ballistic simulant.

INTRODUCTION

In this work, a series of shots have been made against ballistic gelatin blocks elaborated according to a validated method for this purpose (Kerkhoff et al., 2005), controlling the weapons and ammunition, the distance at which the shots are fired, the angle of inclination and the drift, as well as the type of simulant soft tissue to be used (Haag & Jason, 2020), given their different characteristics. For this purpose, the following semi-automatic pistols have been used: Walther P22, HK USP Compact and S&W PC 1911, with which two types of projectiles of each caliber have been fired, being respectively the .22 Long Rifle (lead and electrolytic), the 9 mm P. (jacketed and semi-jacketed) and the .45 ACP (jacketed and truncated).

During the tests, the penetration of the projectiles, the volume and maximum diameter of the temporary cavities generated, as well as the behavior of the projectiles themselves, were analyzed at each instant. Additionally, as the penetration capability of a projectile is closely related to the impact kinetic energy density, DEc, (kinetic energy per cross section of the projectile, A, according to formula (1)), this value has also been determined considering the velocity, v, and the mass of each type of projectile, m. The smaller the projectile cross-section, the force of the impact is distributed over a smaller area, so the greater the pressure generated and the greater its penetration capacity (Kneubuehl et al., 2011).

$$DE_C = \frac{E_C}{A} = \frac{1}{2}\frac{mv^2}{A} \qquad (1)$$

To obtain these measurements, a combined methodology of high-speed filming and artificial vision techniques was used, as employed by the authors in previous work (Loya et al., 2017). This system consists of two synchronized Photron FastCam SZ1 cameras, capable of recording up to 2.1 million frames per second, positioned perpendicular to each other and with respect to the direction of the shot, as can be seen in Fig 1, where the red line represents the direction of the impact. Subsequently, the images were postprocessed using a proprietary code developed in Matlab to determine the variables of interest
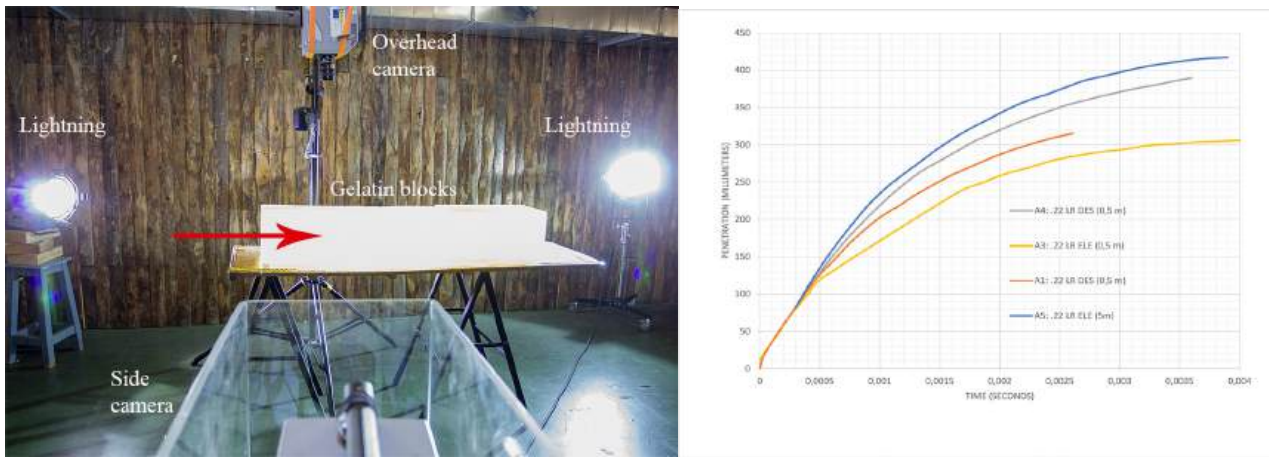
Fig. 1a) Shooting and recording set. b) Penetration-time evolution(.22 LR bullets).

RESULTS AND CONCLUSIONS

After the analysis of the results obtained from the tests in the range of projectile velocities achieved using handguns, it can be stated that there are no significant differences in terms of penetration, maximum expansion of the temporal cavity, or release of kinetic energy, between different types of projectiles within the same caliber.

Nor have any differences in behaviour been observed when varying the firing distance between 0,5 and 5 meters, which is logical since the difference is not sufficient to significantly affect the impact velocity, so its influence on the kinetic energy density does not influence the penetration produced.

Thanks to high-speed filming and artificial vision techniques, it has been possible to verify that the .22 LR caliber projectiles turn completely over, perhaps due to the relationship between diameter and length of the projectile, which can affect the cavity generated.

ACKNOWLEDGMENTS

REFERENCES

[1] Haag, L. C., & Jason, A. (2020). Synthetic gelatins as soft tissue simulants. *AFTE Journal*, *52*(2), 67−84.

[2] Janzon, B. (1982). Soft soap as a tissue simulant medium for wound ballistic studies investigated by comparative firings with assault rifles Ak 4 and M16A1 into live, anesthetized animals. *Acta Chirurgica Scandinavica*, *148*(Suppl. 508), 79−88.

[3] Kerkhoff, W., Bolck, A., Alberink, I., Mattijssen, E. J. A. T., Hermsen, R., Riva, F., Jussila, J., Leppäniemi, A., Paronen, M., Kulomäki, E., Kjellström, B. T., & Leppäniemi, A. (2005). Preparing ballistic gelatine - Review and proposal for a standard method. *Forensic Science International*, *150*(1), 91−98.

[4] Kneubuehl, B. P., Coupland, R. M., Rothschild, M. A., & Thali, M. J. (2011). *Wound Ballistics: Basics and Applications.*

[5] Loya, J. A., Rodríguez-Millán, M., Verón, E. J., Jiménez, Á., Ruano, M. J., & Rego, J. M. (2017). Aplicación práctica de técnicas de visión artificial a la balística de efectos *(in Spanish). V Congreso Nacional de I+D en Defensa y Seguridad*, 2−8.

ID 50

LOW TEMPERATURE REGULATION OF IMPROVED FLEXIBLE COMPOSITES FOR SATALLITE IMPACT SHIELDS

Daniel Barros[1](*), Carlos Mota[2], Luís Nobre[3] João Bessa[4], Fernando Cunha[5] and Raul Fangueiro[6,7]

[1, 2, 3, 4, 5, 6] Fibrenamics, University of Minho, Guimarães, Portugal

[6] Department of Textile Engineering, University of Minho, Guimarães, Portugal

(*) Email: danielbarros@fibrenamics.com

ABSTRACT

In order to protect the satellite against hypervelocity impacts (HVI), extant impact shields have been constructed from metal plates featuring a rear back bumper composed of aramid/Nextel® fibers, chosen for their commendable impact resistance and elevated thermal endurance. However, emerging materials such as Ultra-High Molecular Weight Polyethylene (UHMWPE), exhibiting superior impact resistance, stance an excellent alternative to improve the HVI. As typical a polymeric material, when exposed to negative temperatures, the impact absorption properties may reduce due to the increased hardness of the material (it becomes brittle). Consequently, this study aims to investigate the possibility of developing systems capable of controlling and increasing the low temperatures to which satellites are exposed in spatial environments, that can reach -150ºC. The investigation contemplates the prospect of fabricating solutions using UHMWPE fibers functionalized with Graphene Nanoparticles (GNPs) to increase negative temperatures through the Joule heating effect. It developed an array of configurations by incorporating 4, 8, 12 and 16wt% of Carbon-Based Materials (CBMs) into a flexible matrix by mechanical mixing. Then it was evaluated its heating capacity when applied a certain voltage (2 to 10V), to heat the composite solution when subjected to negative temperatures.

INTRODUCTION

As human endeavors in space exploration intensify, the proliferation of satellites and spacecraft deployed into orbits has concurrently risen. Over decades, the accumulation of space garbage in Earth's orbit is increasing, compounding the risk of collisions with satellites and spacecraft due to the concurrent presence of pre-existing meteoric fragments. The space debris, capable of achieving hyper-velocities exceeding 10 km/s, corresponding to high amount of kinetic energy which features a significant threat to the structural integrity and functionality of space assets (Wen, Chen, & Lu, 2021). The frequency of such collisions necessitates intensive research and development efforts towards the creation of shielding systems and mechanism capable of mitigation the associated hypervelocity impact challenges. One innovative approach is the exploration and refinement of new/novel Stuffed Whipple shield systems (Olivieri & Giacomuzzo, 2022).

Comprising two aluminum alloy plates separated by a back bumper typically crafted from fibrous materials, these shield systems have traditional incorporated thermal-resistance solutions using aramid and ceramic fibers (Nextel® and basalt) to address both impact resistance and the dynamic thermal environment of space (raging low temperatures up to -150). Recent investigations highlight the efficacy of UHMWPE as a promising material for configurations aimed at countering HVIs (Xu, Yu, & Cui, 2023). Nevertheless, UHMWPE's as well as most materials present operational limitations, losing its mechanical properties when submitted to negative temperatures becoming harder and brittle. So, when satellites are subjected to negative temperatures, the using of UHMWPE could be a problem, as it will lose its high impact absorption capacity. This way, to use UHMWPE for satellite protection, the imperative lies in controlling and narrowing the thermal variation experienced by this shielding solution.

In satellite orbits, temperature control is vital. Insulation materials counter extreme fluctuations. Satellites when exposed to sunlight can reaches 150ºC, and the heart shadow can drop to -150ºC. To mitigate low-temperature effects and ensure sustained impact performance, integrating a heating mechanism is vital. Traditional heating wires pose complexities. Our chosen approach involves Joule heating using Carbon-Based Materials (CBMs) directly within the composite. (Tian, Hao, & Qu, 2019). Finally, recent studies, shows that having flexible bumpers solutions present better absorption capacity comparing to the convention harder laminates used in ballistic application (Kumar & Kim, 2023).

RESULTS AND CONCLUSIONS

This study focuses on flexible composite development using UHMWPE and aramid fibers (from Dyneema® and CastroComposites) with CBMs (Graphenest) functionalization adding it into a flexible matrix such as silicone rubber or polyurethane (from Elit, Easycomposite or Vsure).

To evaluate the efficacy of the developed solution, a diverse array of configurations was generated, incorporating 4, 8, 12 and 16wt% Carbon-Based Materials (CBMs) by adding it to the flexible matrix by mechanical mixing. Then it was applied a certain voltage to verify the capacity to reach temperatures between 50 to 150ºC, to "fight" the negative temperatures that the solution could reach. Subsequently, it was selected the best combination and voltage to applied to reach temperatures up to 150ºC, and then the sample was subjected to negative temperatures by using liquid nitrogen (-196ºC) or dry ice (-78ºC). The idea was to measure the temperature on the surfaces and interior of the composite using built-in thermocouples, and during the cold stage, check whether with the application of electric current, the composite remains at positive temperatures, maintaining performance against the impact of the solution.

It is expected that with the addition of CBMs and by applying of a certain voltage, it will be possible to heat the composite panel, causing it to reach negative temperatures.

REFERENCES

[1] Khan, M., Asfand, F., & Al-Ghamdi, S. (2023). Progress in research and develpment of phase change materials for thermal energy storage in concentrated solpar power . *Applied Thermal Engineering, 219*.

[2] Kumar , S., & Kim, Y. (2023). Hybrid interspaced and free-boundary aramid fabric back bumper for hypervelocity impact shielding system. *Internation Journal of Impact Engineering, 171*.

[3] Olivieri, L., & Giacomuzzo, C. (2022). Experimental fragments distributions for thin aluminium plates subjected to hypervelocity impacts. *Internation Journal of Impact Engineering*.

[4] Tian, M., Hao, Y., & Qu, L. (2019). Enhanced electrothermal efficiency of flexible graphene fabric Joule heaters with the aid of graphene oxide. *Materials Letters, 234*, 101-104.

[5] Wen, K., Chen, X.-W., & Lu, Y.-g. (2021). Research and development on hypervelocity impact protection using Whipple shield: An overview. *Defence Technology*, 1864-1886.

[6] Xu, H., Yu, D., & Cui, J. (2023). The Hypervelocity Impact Behavior and Energy Absorption Evaluation of Fabric. *polymers, 15*.

ID 53

APPLICATION OF AUXETIC MATERIALS AND STRUCTURES IN THE AUTOMOBILE INDUSTRY: A REVIEW

Đạt Trương[1], Raul Fangueiro[2], Fernando Ferreira[3], and Quyền Nguyễn[4](*)

[1,2,3,4] 2C2T - Centro de Ciência e Tecnologia Têxtil, Universidade do Minho, Guimarães, Portugal

(*) Email: quyen@2c2t.uminho.pt

ABSTRACT

Auxetic materials, known for their unique ability to expand under tension and contract under compression, offer advantageous properties such as crashworthiness and shear resistance. This makes them ideal for applications in personal protection, biomedicine, aerospace, military, and, notably, the automotive industry. This article systematically presents the diverse applications of auxetic structural materials in automotive engineering, covering cellular structures and manufacturing methods, including auxetic foam, auxetic composite, auxetic fibre, and textile structures. Specific applications discussed range from engine hoods and seat belts to vehicle frames and tires. The article concludes with a comprehensive discussion of the future potential and challenges associated with integrating auxetic structural materials in the automotive sector.

INTRODUCTION

Auxetic materials, characterized by their negative Poisson's ratio, exhibit unique mechanical properties, including high indentation resistance and exceptional fracture toughness [1, 2]. Originating as natural or artificial, they encompass mineral crystals, biomaterials, synthetically created foams, polymer materials, and engineered structures [3,4]. Auxetic materials, in contrast to conventional ones, contract toward the impact site, reducing local density and enhancing impact resistance. This unique behaviour enables them to absorb energy from impacts. The exploration of auxetic structures, initiated by Gibson and colleagues in 1982, focused on a silicon rubber honeycomb structure. Studies by Mukhopadhyay, Adhikari, and Boldrin et al. predict structural influences on properties, delve into dynamic mechanical behaviour, and investigate various aspects of concave honeycomb structures. These inquiries contribute to a profound understanding of impact resistance, effective energy absorption, and diverse applications of auxetic materials, notably in the automotive industry [5-8]. This article provides a comprehensive overview of auxetic materials, emphasizing applications in the automotive industry, such as seatbelts, tires, hoods, and car frames [3, 9-11]. Despite advancements, challenges persist in technical development. Future prospects include continued application in car airbag production, a focal point in upcoming research.

RESULTS AND CONCLUSIONS

1. Cellular structure of materials, auxetic structure

1.1 Re-entrant honeycomb structure

1.2 Chiral structure

1.3 Rotating structure

1.4 Combination of multiple structures

2. Production method of the material, auxetic structure

2.1 Auxetic foam

2.2 Auxetic composite

2.3 Auxetic fibre and textile structure

3. Applications of auxetic materials and structures in the automotive industry

3.1 Seatbelts

3.2 Tires

3.3 Hoods

3.4 Car frames

4. Potential and application challenges of auxetic materials and structures in the automotive industry

CONCLUSIONS

This article provides a comprehensive overview of auxetic materials, covering concepts, classification, mechanical properties, and advanced cell structures. It explores the benefits of modern manufacturing methods and goes beyond presenting characteristics by discussing practical applications in the automotive industry, including safety ropes, flexible tires, anti-collision hoods, and chassis integration. The article addresses current successes, challenges, and future prospects for innovating and developing auxetic materials.

REFERENCES

[1] Wang Z and Hu H. "Tensile and forming properties of auxetic warp-knitted spacer fabrics," Text Res J, vol. 87, pp. 1925–1937, 2017. https://doi.org/10.1177/0040517516660889

[2] H Nguyễn, R Fangueiro, F Ferreira, Q Nguyễn. "Auxetic materials and structures for potential defense applications: An overview and recent developments," Textile Research Journal, Vol. 93, no. 23–24, pp. 5268–5306, 2023. https://doi.org/10.1177/00405175231193433

[3] Christensen J, Kadic M, Kraft O, et al. "Vibrant times for mechanical metamaterials," *MRS Communications*, vol. 5, no. 3, pp. 453-462, 2015. https://doi.org/10.1557/mrc.2015.51

[4] Bhullar SK. "Three decades of auxetic polymers: A review," *E-polymers*, vol. 15, pp. 205–215, 2015. http://doi.org/10.1515/epoly-2014-0193

[5] Nguyen T. Quyen, Nguyen Trong Quoc, Nguyen Dinh Tru, Abel J.P. Gomes, Fernando B.N. Ferreira. "An Alpha Finite Element Method for Linear Static and Buckling Analysis of Textile-Like Sheet Materials," Solid State Phenomena, ISSN: 1662-9779, Vol. 333, pp. 211-217, 2022. https://doi.org/10.4028/p-1415q2

[6] Nguyễn T. Quyền, N. Dourado, A. J. P. Gomes, F. B. N. Ferreira."A Cell-Based Smoothed Finite Element Method for Modal Analysis of Non-Woven Fabrics," Computers, Materials & Continua, vol. 67, no. 3, pp. 2765-2795, 2021. https://doi.org/10.32604/cmc.2021.013164

[7] Nguyen T. Quyen, Nguyen Trong Quoc, Nguyen Dinh Tru, Abel J.P. Gomes, Fernando B.N. Ferreira. "A Node-Based Strain Smoothing Technique for Free Vibration Analysis of Textile-Like Sheet Materials," Solid State Phenomena, ISSN: 1662-9779, Vol. 333, pp. 219-225, 2022. https://doi.org/10.4028/p-76scj1

[8] Xiao DB, Kang X, Li Y, et al. "Insight into the negative Poisson's ratio effect of metallic auxetic reentrant honeycomb under dynamic compression," *Materials Science and Engineering: A*, vol. 763, pp. 138151, 2019. https://doi.org/10.1016/j.msea.2019.138151

[9] Ju J, Kim DM, Kim K. "Flexible cellular solid spokes of a nonpneumatic tire," Composite Structures, vol. 94, no. 8, pp. 2285-2295, 2012. https://doi.org/10.1016/j.compstruct.2011.12.022

[10] Wang YL, Wang LM, Ma ZD, et al. "Parametric analysis of a cylindrical negative Poisson's ratio structure," *Smart Materials and Structures*, vol. 25, no. 3, pp. 035038, 2016. http://dx.doi.org/10.1088/0964-1726/25/3/035038

[11] Zhou G, Ma ZD, Gu JC, et al. "Design optimization of a NPR structure based on HAM optimization method," *Structural & Multidiplinary Optimization*, vol. 53, no. 3, pp. 1-9, 2016. https://doi.org/10.1007/s00158-015-1341-x

ID 57

EXPERIMENTAL AND NUMERICAL ANALYSIS OF THE HYBRID III DUMMY ON THE BALLISTIC BEHAVIOUR OF COMBAT HELMETS

Loya Lorenzo, José Antonio[1(*)], **Rodríguez Millán, Marcos**[2], **Rubio Díaz, Ignacio**[1], **Olmedo Marco, Álvaro**[3], **Miguélez Garrido, M. Henar**[1],

[1] Dept. of Continuous Mechanics and Structural Analysis, Universidad Carlos III de Madrid, Leganés, Madrid, Spain.

[2] Dept of Mechanical Engineering, Universidad Carlos III de Madrid, Madrid, Spain Madrid, Spain.

[3] FECSA, calle de Acacias 3, 28703 San Sebastián de los Reyes, Madrid, Spain.

ABSTRACT

In this work, the head-neck assembly of the Hybrid III dummy has been considered to evaluate the performance of the combat helmet against ballistic impact with live ammunition. For this purpose, a numerical model of the Hybrid III helmet, head and neck assembly has been developed, whose behaviour has been validated with our own experimental data. The model, in addition to analysing the helmet's resistance parameters, includes biomechanical aspects.

INTRODUCTION

Among the main materials used in the development of combat helmets, high-performance fibre composites, such as aramid, stand out, providing the helmet with high penetration resistance due to the excellent mechanical properties of these fibres, together with a good strength-to-weight ratio that contributes to its ergonomics. In this work, the head and neck assembly of the Hybrid III dummy system (Humanetics) has been modelled, on which a virtual model of a combat helmet is mounted for subsequent analysis in the event of ballistic impact.

Impacts were made at 430±10 m/s with a 9mm calibre FMJ projectile on the front of a combat helmet mounted on the dummy system (see Figure 1). Photron FastCam SA-Z high-speed digital cameras have been used to measure the velocity of the impact projectile and the motion of the head-helmet assembly during impact, while the dummy system allows the recording of linear accelerations at the centre of gravity of the head, and the resultant forces and moments at the base of the neck.
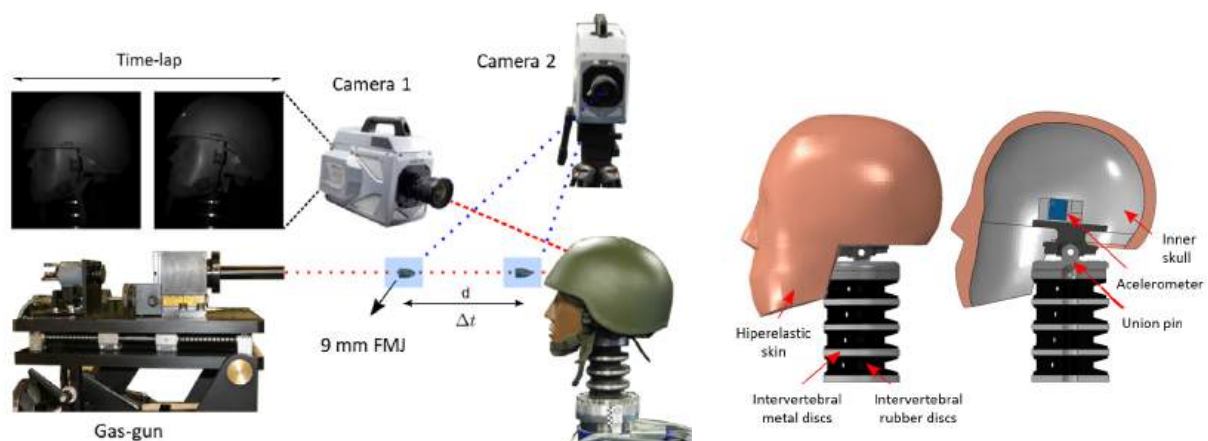

Fig. 1 left) Experimental set-up, rigth) Dummy Hybrid III numeric model

The numerical model has been developed using the commercial finite element code ABAQUS/Explicit. The combat helmet has been modelled according to previous work by the authors [1,2] meanwhile the dummy model was developed from the manufacturer's drawings and constitutive models appropriate to each participating material.

RESULTS AND CONCLUSIONS

Comparisons between the digital twin predictions and the experimental measurements of the maximum linear accelerations show good agreement (see Fig. 2a). Specifically, the numerical model provides maximum trauma values of 12.98 mm, compared to 11.46 mm for the experimental model for the helmet with size G inner foams, while for the case of the smaller size (size M), the difference is somewhat greater, obtaining 14.8 mm, experimentally compared to 19 mm numerically.
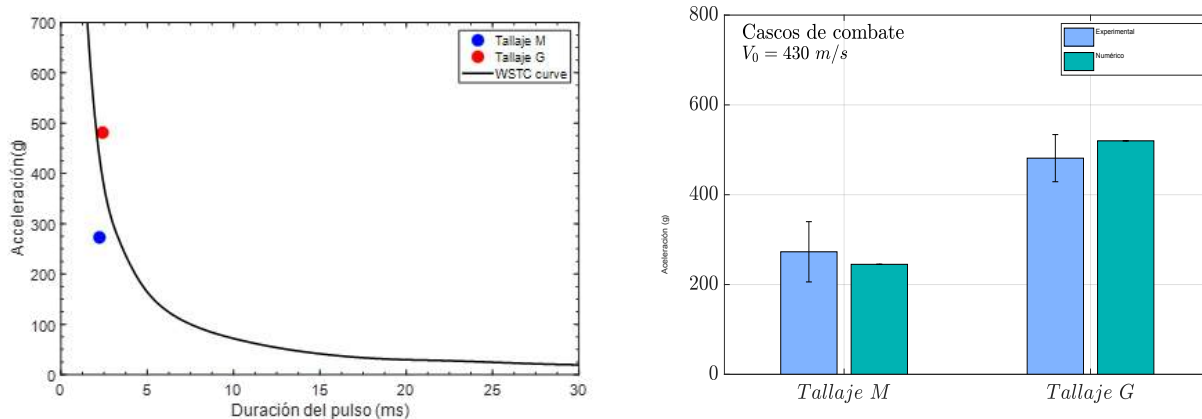
Fig. 2 a) Comparison of acceleration b) aceleración lineal with the WSTC curve

With regard to the analysis of brain damage, helmet size M, i.e. the thicker inner system, performs more safely than helmet size G, which is at the limit of safety, being on the threshold curve of the WSTC [3] (Fig2 b).

In both helmet sizes, as expected, the helmet absorbs most of the internal energy through deformation and failure of the fibre, matrix and delamination, mainly [2].

The predictive capability of the developed model has been successfully compared with experimental results of frontal impact on aramid helmet with respect to helmet strength behaviour, trauma prediction and peak head accelerations. Therefore, it is concluded that the use of the developed digital twin can be successfully used as a design tool.

ACKNOWLEDGMENTS

REFERENCES

[1] Rubio, I.; Rodríguez-Millán, M.; Marco, M.; Olmedo, A.; Loya, J.A. Ballistic performance of aramid composite combat helmet for protection against small projectiles. *Compos. Struct*. 2019, 226.

[2] Rubio Díaz, I.; Rodríguez-Millán, M.; Rusinek, A.; Miguélez, M.H.; Loya, J.A. Energy absorption analysis of aramid composite during blunt projectile impact. *Mech. Adv. Mater. Struct*. 2021, 0, 1−12.

[3] Hoshizaki, T.B.; Post, A.; Kendall, M.; Cournoyer, J.; Rousseau, P.; Gilchrist, M.D.; Brien, S.; Cusimano, M.; Marshall, S. The development of a threshold curve for the understanding of concussion in sport. Trauma (United Kingdom) 2017, 19, 196−206.

ID 60
THEORETICAL MODELING OF THE BEHAVIOR OF WOVEN FABRICS SUBJECTED TO STABBING

Cuong Ha-Minh[1]
[1] Université Paris-Saclay, France

ABSTRACT

TBA

ID 63
NUMERICAL MODELLING OF ARAMID CT 716 REINFORCED DCPD SUBJECTED TO AN IMPACT LOAD

Kayode Olaleye[1(*)], Dariusz Pyka[2], Maciej Roszak[3], Krzysztof Jamroziak[4], Mirosław Bocian[5]

[1,2,3,4,5] Department of Mechanics, Materials and Biomedical Engineering, Wroclaw University of Technology, Smoluchowskiego 25, 50-370 Wroclaw, Poland
[(*)] Email: kayode.olaleye@pwr.edu.pl

ABSTRACT

Using a FEM technique, the impact of projectile form on the ballistic characteristics and mechanism of aramid laminates is examined. Ballistic curves were obtained using ogival projectiles. Analysis was done on the targets' deformation, damage characteristics, and dynamic penetration process. We constructed a three-dimensional finite element model and discussed good simulation results.

INTRODUCTION

Since non-metallic multi-component armor systems have superior specific strength, hardness, and impact resistance capacities and can achieve better ballistic performance with less weight than traditional monolithic metal armor, they have become increasingly popular as protective structures in a variety of industries, including shipbuilding, aerospace, and the automotive industry. These systems are typically composed of ceramic plate for the frontal plate and fibre reinforced polymer (FRP) laminate for the backup plate. Therefore, conducting in-depth research on the ballistic performance of ceramic/FRP laminate composite structures is imperative [1].

Prior research has mostly concentrated on how material characteristics and projectile velocity affect the ballistic performance of aramid laminates. Nevertheless, there hasn't been much study on the impact of projectile shape, number of plies, and DCPD matrix. Using 7.62 mm ogival rigid bullets, this study performs numerical testing on 10 plies of 4 mm thick aramid laminates [2, 3]. The target plate's deformation damage process and ballistic characteristics are examined. Furthermore, the target's ballistic limit and the distribution of stress within the target plate are examined using finite element simulation, offering a thorough examination of the defense mechanism from an energy standpoint.

RESULTS AND CONCLUSIONS

One of the most important indicators of the target plate's ballistic performance is its back deformation characteristics. The rear displacement of the target plate during projectile penetrations at 100 m/s, is 0.57 mm, as shown in Fig. 1. The sample's ballistic limit will be assessed using different impact velocities with an increment of 10 m/s.

Table 1 Mechanical properties of developed composite after using the rule of mixture.

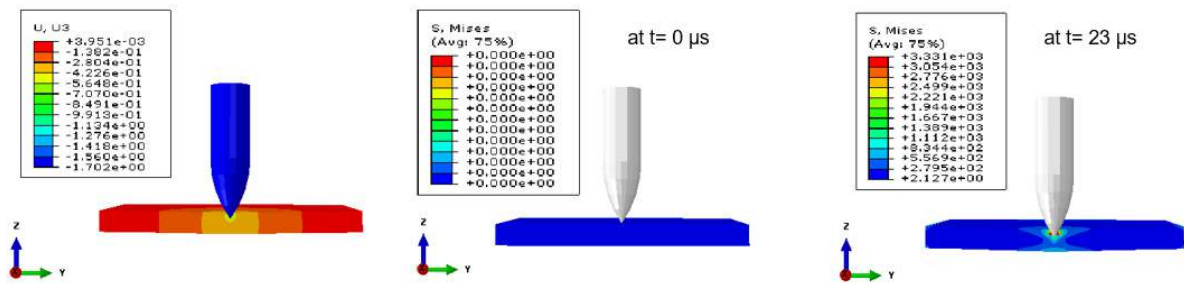| Composite	$E_1=E_2$ (MPa)	E_3 (MPa)	ρ (tonne/mm^3)	v (-)	G (MPa)	FS (-)
Aramid/DCPD	63460	9488.5	$2.0552e^{-11}$	0.32	3906.6	0.35

Fig. 1 Displacement of the target and von Misses stress at the beginning and end of the simulation.

It can be seen that the maximum stress on the backface of the composite at the end of the simulation does not exceed the yield strength of the composite mixture as shown in the table above. This accounts for the non-penetration of the bullet in the target.

REFERENCES

[1] Pyka D. , Jamroziak K and BW and BM. "Calculations with the Finite Element Method During the Design Ballistic Armour" In: Rusiński Eugeniusz and Pietrusiak D, editor. Proceedings of the 13th International Scientific Conference , Cham: Springer International Publishing; 2017, p. 451−9

[2] Jamroziak K, Bajkowski M, Bocian M, Polak S, Magier M, Kosobudzki M, et al. Ballistic Head Protection in the Light of Injury Criteria in the Case of the Wz.93 Combat Helmet. Applied Sciences 2019;9. https://doi.org/10.3390/app9132702.

[3] Bocian M., Pach J., Jamroziak K., Kosobudzki M., Polak S., Pyka D., et al. Experimental and numerical analysis of aramid fiber laminates with DCPD resin matrix subjected to impact tests. MATEC Web Conf 2017;112:4013. https://doi.org/10.1051/matecconf/201711204013.

ID 64
FOAM-COATED WOVEN SUBSTRATES AS FILTERING TOOLS TO CAPTURE DYES FROM TEXTILE WASTEWATER

Ângela Pinto[1](*,#), Tânia Ferreira[2](#), Margarida Fernandes[3], Joana C. Antunes[4], Sónia P. Miguel[5], João Bessa[6], Fernando Cunha[7], Raúl Fangueiro[8]

[1, 2, 4, 5, 6, 7, 8] Fibrenamics Association, Institute for Innovation in Fibre and Composite Materials, University of Minho, 4800-058 Guimarães, Portugal

[3, 5] CPIRN-UDI/IPG, Center for Potential and Innovation of Natural Resources, Polytechnic of Guarda, Av. Dr. Francisco Sá Carneiro, 50, 6300-559 Guarda, Portugal

[5] CICS-UBI, Health Sciences Research Center, University of Beira Interior, Avenida Infante D. Henrique, 6200-506 Covilhã, Portugal

[8] Centre for Textile Science and Technology (2C2T), University of Minho, 4800-058 Guimarães, Portugal

(#) Equal contribution

(*) Email: angelapinto@fibrenamics.com

ABSTRACT

The study evaluated the adsorption rate of methylene blue (MB) dye in different samples, including non-functionalised polyamide (PA) woven fabric and PA woven fabrics functionalised with three types of polymer-based foam coatings. Zinc oxide nanoparticles (ZnO-NPs) were then added to the latter coatings. The adsorption test was conducted by placing the fabrics in plates under orbital shaking at 50 rpm for 24 hours containing aqueous solutions de 30 mg/L of MB. The results showed that the non-functionalised PA fabric had the lowest capacity to capture MB. Moreover, the fabric coated with F3+ZnO NPs was the one with the highest MB adsorption rate, thus revealing high promise to be explored as filtering membranes of textile wastewater.

INTRODUCTION

The increase in contamination by chemical and biological compounds in soil and water has become a global concern in recent years. The textile industry, which is responsible for a significant share of water pollution, discharges large quantities of dyes and other contaminants into wastewater during finalisation processes. This contributes to the increasing difficulty of obtaining contaminant-free drinking water.

Various techniques have been explored in the treatment of contaminated water from the textile industry. Techniques such as coagulation/flocculation, oxidation, ozonation and biological treatments have several limitations, making them neither the most effective nor the most suitable for remedying the identified problem [1-4]. This highlights the ongoing need to develop suitable methods to adequately treat complex effluents.

Faced with the limitations of conventional methods for treating contaminated wastewater, there is a search for more effective alternatives. The adsorption technique stands out for its efficiency and economic viability [5,6].

In addition, the use of fibrous materials in wastewater treatment is gaining prominence due to their good flexibility, durability, and low weight, making them easy to handle. In addition, they can be modified/functionalised to enhance their capacities as filtering systems [7].

NPs such as ZnO-NPs have piezoelectric, semiconducting, and antimicrobial properties. These particles, when integrated into textile filters using the knife coating technique, provide improvements in water resistance, thermal conductivity, and corrosion resistance [8].

In summary, the search for sustainable and effective alternatives for wastewater treatment
may involve optimising the adsorption technique, incorporating fibrous materials and the

strategic use of NPs, showing promising advances in removing contaminants and improving the properties of the materials used.

RESULTS AND CONCLUSIONS

All samples were placed in 6-well plates under orbital shaking at 50 rpm for 24 hours containing aqueous solutions de 30 mg/L of MB. The appearance of the sample was recorded before it was placed in the MB solution (T=0 h) and after 24 hours of incubation (T=24 h). All the samples proven to be hydrophobic except for the non-functionalised PA fabric which showed hydrophilic character.
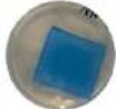
The non-functionalised PA fabric showed low capacity to capture the MB dye, since the sample showed only a slight change of its colour.

In general, within the coated fabrics it was possible to observe some differences when comparing T=0h with T=24h, especially when comparing samples functionalized with polymer formulations containing or not containing ZnO-NPs.
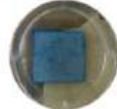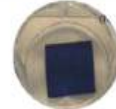
Overall, the samples coated with the polymeric formulations containing ZnO-NPs have a bluer hue than the samples functionalised with the same formulations not containing NPs, which shows that there is a greater affinity of the dye for these samples.

The best results of adsorption were obtained for the F3+ZnO-NPs coated fabric. This was also the sample with the highest resistance to abrasion when subjected to the Martindale abrasion test, thus being selected as the functionalized textile substrate with the highest capacity for MB capture.

Table 1- Photographic records of unfunctionalized PA fabric and PA fabric functionalized with the different formulations before (t=0 h) and after (t= 24 h) adsorption of MB dye.

REFERENCES

[1] Rashid, R.; Shafiq, I.; Akhter, P.; Muhammad, &; Iqbal, J.; Hussain, M. A State-of-the-Art Review on Wastewater Treatment Techniques: The Effectiveness of Adsorption Method., doi:10.1007/s11356-021-12395-x/Published.

[2] Pattnaik, P.; Dangayach, G.S.; Bhardwaj, A.K. A Review on the Sustainability of Textile Industries Wastewater with and without Treatment Methodologies. *Rev Environ Health* 2018, 33, 163−203.

[3] Mahboob, I.; Shafiq, I.; Shafique, S.; Akhter, P.; Munir, M.; Saeed, M.; Nazir, M.S.; Amjad, U. e. S.; Jamil, F.; Ahmad, N.; et al. Porous Ag3VO4/KIT-6 Composite: Synthesis, Characterization and Enhanced Photocatalytic Performance for Degradation of Congo Red. *Chemosphere* 2023, 311, doi:10.1016/j.chemosphere.2022.137180.

[4] Holkar, C.R.; Jadhav, A.J.; Pinjari, D. V.; Mahamuni, N.M.; Pandit, A.B. A Critical Review on Textile Wastewater Treatments: Possible Approaches. *J Environ Manage* 2016, 182, 351−366.

[5] Dutta, S.; Gupta, B.; Srivastava, S.K.; Gupta, A.K. Recent Advances on the Removal of Dyes from Wastewater Using Various Adsorbents: A Critical Review. *Mater Adv* 2021, 2, 4497−4531.

[6] Dimapilis, E.A.S.; Hsu, C.S.; Mendoza, R.M.O.; Lu, M.C. Zinc Oxide Nanoparticles for Water Disinfection. *Sustainable Environment Research 2018*, 28, 47−56.

[7] Lapointe, M.; Jahandideh, H.; Farner, J.M.; Tufenkji, N. Super-Bridging Fibrous Materials for Water Treatment. *NPJ Clean Water* 2022, 5, doi:10.1038/s41545-022-00155-4.

[8] Vimbela, G. V.; Ngo, S.M.; Fraze, C.; Yang, L.; Stout, D.A. Antibacterial Properties and Toxicity from Metallic Nanomaterials. *Int J Nanomedicine* 2017, 12, 3941−3965.

ID 78
EFFECT OF PHENOLIC RESIN CATALYST CONTENT ON THE THERMAL RESISTANCE AND PROPERTIES OF PHENOLIC-CARBON COMPOSITE

Lukasz Rybakiewicz[1(*)], Janusz Zmywaczyk[2]

Hassan Iftekhar[1(*)], Zulfiqar Ali[1], M. Shahid Nazir[3], S. Talha Hamdani[4], Yasir Nawab[5]

[1] Military University of Armament Technology, Rocket Technology Department, Zielonka, Poland

[2] Military University of Technology, Faculty of Mechatronics, Armament and Aerospace, Warsaw, Poland

[(*)] Email: rybakiewiczl@witu.mil.pl

ABSTRACT

The work describes the structure of phenol-formaldehyde resin and its types depending on the ratio of phenol to formaldehyde. The process of obtaining a finished product from phenol-formaldehyde resin and how cross-linking of the phenol-formaldehyde resin can be initiated are presented. The work examined how the content of the catalyst used during the production process affects the individual thermal parameters of the mentioned materials. The results include tests of thermal diffusivity, thermal conductivity, apparent specific heat, thermal expansion, coefficient of thermal expansion, thermogravimetric and derivative thermogravimetric tests, differential thermal analysis, dynamic mechanical analysis (DMA)

INTRODUCTION

Phenolic resin is a synthetic thermosetting polymer, characterized by low flammability, the formation of a char layer on the surface when exposed to a high power density heat flux, and high chemical stability. In addition, this material is a very good and stable thermal insulator. [1][2] The above mentioned properties of phenolic resin allow it to be used especially in areas exposed to high temperatures, making this material a good candidate for ablative applications. [3][4][5] Phenolic resins are most often used to make heat shields for machine or devices that are exposed to high temperatures, or to make composite parts. Combined with carbon fibers, they are a material that is used in the aerospace and defense industries and have high strength and very good thermal properties.

RESULTS AND CONCLUSIONS

The results of the dynamic tests of the elasticity (E'), loss (E") and tan d coefficients of the phenol-formaldehyde carbon composite (PFCC) with 4% wt catalyst content (KWF-4U) are shown at Fig. 1. The tests were conducted in the mechanical mode of 3 point bending in the temperature range from -120 to 160 oC for the frequency of the forcing force f = 0.5, 1.0, 3.33 and 10.0 Hz. The amplitude of deflection of the sample was assumed A = 20 mm, dynamic force Fdyn = 6N and a constant static force Fstat = 0.5N to ensure that the pusher is in contact with the surface of the sample under test. In the temperature range from -75 to -35 oC there are small temperature peaks tan d to which the activation energy corresponds Ea = 144.993 kJ/mol, most likely related to the occurrence of glass transition of phenolic resin. Additionally, you can see tan d peaks in the range (125,144) oC, to which corresponds the activation energy Ea = 368.651 kJ/mol most likely related to the softening of the material. The elastic modulus E' reaches at the temperature of the -120 oC a value of about 36 GPa for f = 1 Hz, and with increasing temperature its value systematically decreases reaching 26.5 GPa at 127 oC. The decrease in the stiffness of the sample in this temperature range is due to an increase in the free space for the movement of the phenolic resin polymer chains.

The temperature characteristics of relative elongation dL/Lo and coefficient of linear thermal expansion diff. CTE of the tested samples with different content of catalyst are shown in Fig. 2. The graph presents results for composite with fibers directed along of sample. Samples with this fibre arrangement have smaller elongation then samples with fibres in traverse direction by an order of magnitude.
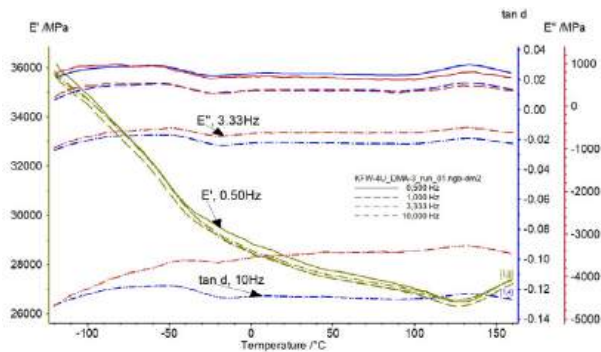

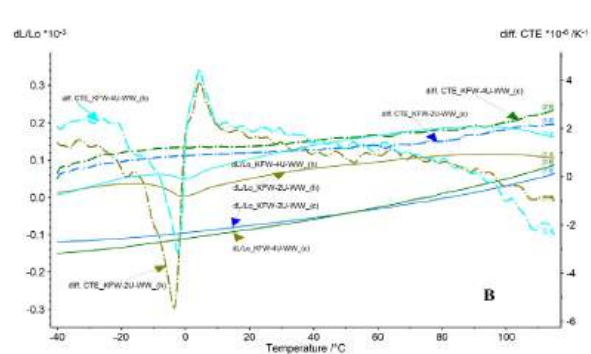Fig. 1 DMA results of KWF-4U sample

Fig. 2 Relative elongation (dL/Lo) and coefficient of linear thermal expansion (diff. CTE) of a composite

The test results confirmed the hypothesis that the influence of the content of the catalyst initiating the hardening of the phenol-formaldehyde resin (PFR) affects its thermal properties. Increasing or decreasing the catalyst content probably affects the structure of the phenol-formaldehyde resin, thereby affecting its thermal properties. The influence of the catalyst content affects the results differently in the case of PFR resin than in the case of PFCC composite. In the case of thermal diffusivity, thermal conductivity and apparent specific heat, the catalyst content inversely affects the values of the mentioned properties in the case of PFR resin and PFCC composite. Increasing the catalyst content increases the relative elongation of the PFCC composite.

REFERENCES

[1] Donghwan C, Byung IY, "Microstructural interpretation of the effect of various matrices on the ablation properties of carbon-fber-reinforced composites", Composites Science and Technology, 2001;61:271-280

[2] Cui J, Yan Y, Liu J, "Phenolic resin-MWCNT composites prepared through an in situ polymerization method", *Polymer* 2008, Vol. 40, No. 11, pp. 1067–1073

[3] Srikanth I, Daniel A, Kumar S, et al., "Nano silica modified carbon–phenolic composites for enhanced ablation resistance", *Materialia* 2010;63:200–203

[4] Wang S, Huang H, Tian Y, "Effects of zirconium carbide content on thermal stability and ablation properties of carbon/phenolic composites", Ceramics International, 2020;46:4307–4313

[5] Amirsardari Z, Mehdinavaz-Aghdam R, Salavati-Niasari M, Jahannama MR, "Influence of ZrB_2 nanoparticles on the mechanical and thermal behaviors of carbon nanotube reinforced resol composite", Journal of Materials Science & Technology 2016;32:611–616

ID 80
A SUPERVISED MACHINE-LEARNING APPROACH TO TRAJECTORY PLANNING FOR UAS

César García-Gascón[1], Pablo Castelló-Pedrero[2], and Juan A. García-Manrique[3(*)]

[1,2,3] Universitat Politècnica de València, Valencia, Spain, Design for Manufacturing Research Institute (IDF)

(*) Email: jugarcia@upv.edu.es

ABSTRACT

The use of artificial intelligence in Unmanned Aerial Systems (UAS) enables the creation of models that establish links between input parameters such as wind, temperature, air pressure and others, and the optimal trajectory. Defining the trajectory of autonomous vehicles, especially drones, is an extremely complex task due to the large number of variables that need to be considered, making it impractical to cover them all. In this context, when working with many degrees of freedom, model reduction techniques are suggested as a viable alternative. Machine learning is an approach to solving highly complex problems, particularly where systems need to make online decisions and handle multiple variables. This paper proposes to develop a simplified machine learning model to define optimal trajectories for an unmanned quadcopter. The aim is to establish a machine learning methodology that predicts the optimal trajectory between two points using model reduction techniques. This will be done using Hexagon's ODYSSEE CAE simulation platform. The algorithm will be trained with reduced order models using a database generated from experimental flights under real conditions. The UAS used is a sensor-equipped quadcopter with a black box for flight data storage. ODYSSEE CAE has several algorithms to investigate the problem, including direct interpolation methods, reduced order models and clustering. It also provides the ability to train multiple algorithms and compare the quality of the predictions on a set of validation data. Models are also trained using neural networks and Bayesian neural networks. The results show that the application of this methodology allows good accuracy predictions to be obtained, requiring only 10 training flights to optimise the trajectory by varying the parameters.

Keywords: Adrone, UAS, Machine Learning, Model Reduction
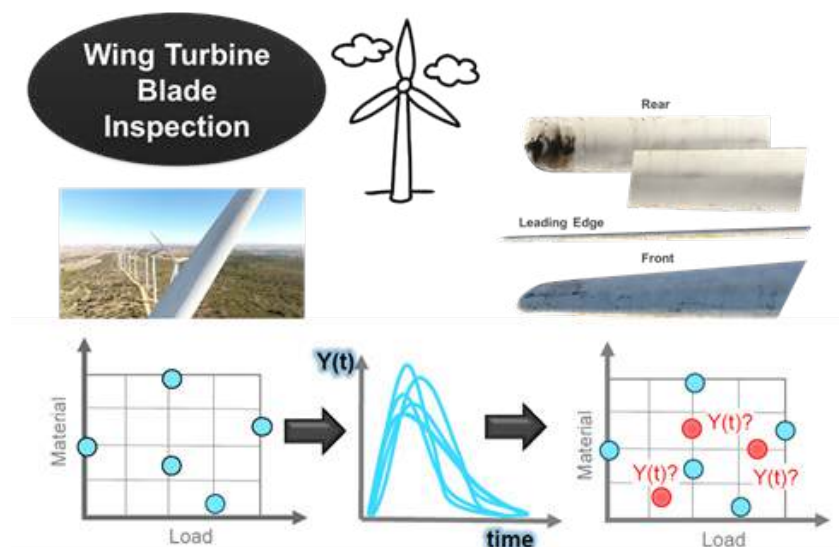
Figure 1: Machine learning drone aplication for wing blade inspection

REFERENCES

[1] Goodrich, P., Betancourt, O., Arias, A. C., & Zohdi, T. (2023). Placement and drone flight path mapping of agricultural soil sensors using machine learning. Computers and Electronics in Agriculture, 205, 107591.

[2] Agrawal, A., Bhise, A., Arasanipalai, R., Tony, L. A., Jana, S., & Ghose, D. (2023). Accurate Estimation of 3D-Repetitive-Trajectories using Kalman Filter, Machine Learning and Curve-Fitting Method for High-speed Target Interception. In Artificial Intelligence for Robotics and Autonomous Systems Applications (pp. 93-122). Cham: Springer International Publishing.

[3] Kaufmann, E., Bauersfeld, L., Loquercio, A., Müller, M., Koltun, V., & Scaramuzza, D. (2023). Champion-level drone racing using deep reinforcement learning. *Nature*, *620*(7976), 982-987.

Singh, G., Perrusquía, A., & Guo, W. (2023, July). A two-stages unsupervised/supervised statistical learning approach for drone behaviour prediction. In 2023 9th International Conference on Control, Decision and Information Technologies (CoDIT) (pp. 1-6). IEEE.

[4] Ning, Z., Yang, Y., Wang, X., Song, Q., Guo, L., & Jamalipour, A. (2023). Multi-agent deep reinforcement learning based uav trajectory optimization for differentiated services. IEEE Transactions on Mobile Computing.

south-koreas-status-as-rising-defense-player-on-display-at-ausa/

[6] Martin, T. (2022). Norway bulks up artillery with new K9 howitzer agreement, tank contract set for year end [online]. Breaking Defense. [accessed 2024-01-08]. Available from: https://breakingdefense.com/2022/11/norway-bulks-up-artillery-with-new-k9-howitzer-agreement-tank-contract-set-for-year-end/

[7] Militarnyi. (2022). Poland has signed contracts for the purchase of K2 Black Panther tanks and K9 Thunder self-propelled guns [online]. [accessed 2024-01-08]. Available from: https://mil.in.ua/en/news/poland-has-signed-contracts-for-the-purchase-of-k2-black-panther-tanks-and-k9-thunder-self-propelled-guns/

[8] Andrew Whyte, A., Tooming, M. (2023). Estonian planning new self-propelled artillery acquisition by end of decade [online]. ERR.ee. [accessed 2024-01-08]. Available from: https://news.err.ee/1609139552/estonian-planning-new-self-propelled-artillery-acquisition-by-end-of-decade

[9] Defensemirror.com. (2023). Romania Close to Procuring South Korean K9 Thunder Howitzer System [online]. [accessed 2024-01-08]. Available from: https://www.defensemirror.com/news/33952

[10] ArmyRecognition. (2023). Vietnamese army interested in South Korean-made Hanwha K9A1 Self-propelled Howitzer[online]. Army Recognition. [accessed 2024-01-08]. Available from: https://www.armyrecognition.com/defense_news_april_2023_global_security_army_industry/vietnamese_army_interested_in_south_korean-made_hanwha_k9a1_self-propelled_howitzer.html

[11] Siebold, S. (2023). Germany to buy up to 28 howitzers to help replace arms rushed to Ukraine [online]. Reuters. [accessed 2024-01-08]. Available from: https://www.reuters.com/business/aerospace-defense/germany-buy-up-28-howitzers-help-replace-arms-rushed-ukraine-2023-03-27/

[12] Frantzman, S. (2023). Elbit wins artillery weapons orders from mystery buyer in Europe [online]. DefenseNews. [accessed 2024-01-08]. Available from: https://www.defensenews.com/industry/2023/03/06/elbit-announces-howitzer-artillery-system-deals-in-europe/

[13] Higura, J. (2023). Colombia picks Elbit's Atmos howitzer over Nexter's Caesar [online]. DefenseNews. [accessed 2024-01-08]. Available from: https://www.defensenews.com/land/2023/01/06/colombia-picks-elbits-atmos-howitzer-over-nexters-caesar/?utm_source=sailthru&utm_medium=email&utm_campaign=dfn-dnr

[14] Roque, A. (2022). Lawmakers: Army should consider new alternatives to extended range howitzer [online]. Breaking Defense. [accessed 2024-01-08]. Available from: https://breakingdefense.com/2022/12/lawmakers-army-should-consider-new-alternatives-to-extended-range-howitzer/

[15] Army Technology (2023). RCH 155 Self-Propelled Howitzer, Germany [online]. [accessed 2024-01-08]. Available from: https://www.army-technology.com/projects/rch-155-self-propelled-howitzer-germany/

[16] Valpolini, P. (2022). A long-range truck-based artillery effector by Rheinmetall [online]. EDRmagazine. [accessed 2024-01-08]. Available from: https://www.edrmagazine.eu/a-long-range-truck-based-artillery-effector-by-rheinmetall

[17] Higuera, J. (2023). Colombia picks Elbit's Atmos howitzer over Nexter's Caesar [online]. DefenseNews. [accessed 2024-01-08]. Available from: https://www.defensenews.com/land/2023/01/06/colombia-picks-elbits-atmos-howitzer-over-nexters-caesar/?utm_source=sailthru&utm_medium=email&utm_campaign=dfn-dnr

[18] Eshel, T. (2022). Nexter Embarks on a New Generation Caesar MK2 Upgrade [online]. Defense Update. [accessed 2024-01-08]. Available from: https://defense-update.com/20220220_caesar-mk2.html#.ZCx6u3bMLDd

[19] Military Blog. (2023). SORA: Serbian 122mm Self-Propelled gun prototype [online]. Military-Wiki. [accessed 2024-01-08]. Available from: https://military-wiki.com/sora-serbian-122mm-self-propelled-gun-prototype/

[20] Henderson, A. (2022). Soft recoil of 105-mm Howitzer under evaluation at Yuma Proving Ground [online]. [accessed 2024-01-08]. Available from: https://www.army.mil/article/258862/soft_recoil_of_105_mm_howitzer_under_evaluation_at_yuma_proving_ground

[21] Gouveia, H., Borges, J. (2023). The Future of Field Artillery Projectiles: New Technologies, Strengths and Challenges. Developments and Advances in Defense and Security. Smart Innovation, Systems and Technologies. (328). doi.org/10.1007/978-981-19-7689-6_30

[22] Mizokami, K. (2018). The Army's New Howitzer Barrel is Ridiculously Long [online]. Popular Mechanics. [accessed 2024-01-08]. Available from: https://www.popularmechanics.com/military/weapons/a23872600/army-new-howitzer-barrel-long/

[23] Judson, J. (2021). US Army awaits acquisition strategy approval for extended-range cannon [online]. Defense-News. [accessed 2024-01-08]. Available from: https://www.defensenews.com/land/2021/10/12/us-army-awaits--acquisition-strategy-approval-for-extended-range-cannon/

[24] AM. (2020). ME 3-38-12 Fundamentos do Tiro de Artilharia de Campanha. Lisboa. Exército Português.

[25] Mavridis, G. (2022). Sigma: The newest self-propelled 155mm howitzer of Israel [online]. [accessed 2024-01-08]. Available from: https://www.pentapostagma.gr/en/national-affairs/army/7065569_sigma-newest-self-propelled-155mm-howitzer-israel

[26] Army Technology. (2019). Hawkeye Mobile Weapon System (MWS) [online]. Army Technology. [accessed 2024-01-08]. Available from: https://www.army-technology.com/projects/hawkeye-mobile-weapon-system-mws/

[27] KMW. (s/d). Performance Characteristics of the Pzh 2000 [online]. [accessed 2024-01-08]. Available from: https://www.knds.de/en/systems-products/tracked-vehicles/artillery/pzh-2000/

[28] Bierwirth, B. (2022). Arctic Artillery: Prepared for Future Competition and Conflict [online]. USFAA. [accessed 2024-01-08]. Available from: https://www.fieldartillery.org/news/arctic-artillery

[29] Peck, M. (2023). For 250 years, US troops could tow their cannons around the battlefield. The war in Ukraine shows they won't have that luxury in the future.
[online]. Business Insider. [accessed 2024-01-08]. Available from: https://www.businessinsider.com/ukraine-war--shows-towed-artillery-more-vulnerable-in-future-2023-10

[30] Konstrukta Defence. (s/d). 155mm 52Cal. SpGH DIANA [online]. Konstrukta Defence. [accessed 2024-01-08]. Available from: https://kotadef.sk/projekty/diana/?lang=en

[31] Army Guide. (s/d). G6-52 [online]. [accessed 2024-01-08]. Available from: https://army-guide.com/eng/product1207.html

ID 83

NEW FUNCTIONAL COATING PROCESSES IN TEXTILES USING MARINE ALGAE-DERIVED ACTIVE AGENTS

Tânia Ferreira,[1(*)], Carlos Silva,[2] Francisca Marques,[3] Pedro Magalhães,[4] Alice Ribeiro,[5] Joana C. Antunes,[6] João Bessa,[7] Fernando Cunha,[8] and Raul Fangueiro[9]

[1, 6, 7, 8, 9] Fibrenamics – Institute for Innovation in Fiber-based Materials and Composites,

Azurém Campus, University of Minho, 4800-058 Guimarães, Portugal;

[9] Centre for Textile Science and Technology (2C2T), University of Minho, 4800-058 Guimarães, Portugal.

[2, 3, 4] TINTEX Textiles SA, Zona Industrial, Polo 1, Campos, 4924-909 Vila Nova de Cerveira, Portugal.

[5] CeNTI – Centre for Nanotechnology and Smart Materials, R. Fernando Mesquita 2785,

4760-034 Vila Nova de Famalicão

[(*)] Email: taniaferreira@fibrenamics.com

ABSTRACT

Innovation in textile finishing processes is underway, focusing on the integration of algae applications, particularly using exhaustion and coating methods. This work involves the development of novel techniques that will undergo testing at various scales, from laboratory to industrial levels. The aim is to explore the feasibility and effectiveness of incorporating biomass algae and its extracts in fabric coating processes, paving the way for sustainable and scalable solutions in the textile industry.

Our approach involves three different substrates, two knits (K1 and K2) and a woven fabric (WF), all comprising 100% cotton in their composition. The main purpose of the coatings is to shield the users against certain daily threats, while keeping the commitment of comfort. To the selected substrates, a functionalized layer was added with a polyurethane bio-based polymeric matrix and the algae biomass to confer relevant antioxidant and UV light protective characteristics, among others.

INTRODUCTION

The market for functional textile finishing agents is poised for dynamic growth from 2023 to 2032, driven by the integration of advanced technologies, including nanotechnology, into textile finishing processes by numerous companies. These technological advancements are expected to be instrumental in enhancing various fabric attributes, such as color resilience and water resistance. Furthermore, growing concerns related to ozone layer depletion have heightened the demand for functional textile finishes with UV protective properties, in addition to antioxidant characteristics that have extreme importance in textile products having direct contact with human skin, due to their capacity to deactivate reactive and harmful species like oxygen radicals, thus reducing cellular oxidative stress and promoting biological balance. These functional characteristics can be added to the textile by several methods such as coating, exhaust and padding processes, among others. [1] This dual focus on technological innovation and environmental considerations is anticipated to shape a transformative and thriving landscape for functional textile finishing agents in the coming years. [2]

Particularly the fashion industry, encompassing apparel, footwear, and household textiles, contributes to 10% of human-generated greenhouse gas emissions and is a source of almost 20% of global industrial wastewater pollution. Given the substantial environmental impact of this sector, there is a pressing need for a shift towards circular practices. The goal of this work is to advocate for a fresh approach that emphasizes the use of marine materials and byproducts in the creation of innovative textile products and processes. These new developments aim to be

more sustainable while offering improved functional properties compared to existing alternatives, thus fostering a paradigm shift in the industry.

To overcome this issue, one approach involves enhancing textiles with algae biomass encasing abilities to turn the textile resistant to damaging oxidative reactions. In another hand, its integration in the coating composition must not affect comfort-related features such as its breathability, thus encouraging its use in fashion textile products.

RESULTS AND CONCLUSIONS

The functional algae biomass under study was firstly characterized concerning its thermal properties. The knowledge regarding the thermal degradation profile of each compound, namely the temperature marking the beginning of its thermal degradation process, was key to the coating optimization process, to ensure absence of algae biomass degradation during the functionalization steps.
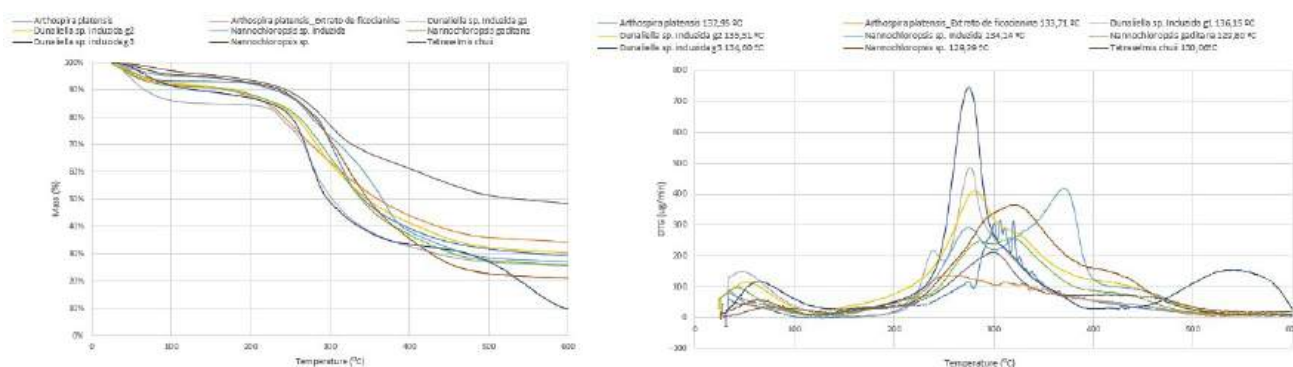

Fig. 1 Results obatined by the analysis of the algae biomass. The TGA trace was obtained in the range of 25– 600 °C under a nitrogen atmosphere, a flow rate of 200 mL/min, and a temperature rise of 10 °C/min. Results were plotted as the percentage of weight loss vs. temperature.

In the road of developing protective clothing, several coatings were carefully developed to block the detrimental action of generic threats like UV light and reactive oxidative species, though always keeping in mind the thermophysiological comfort. The coatings examined contained a paste composed by a bio-based polyurethane (PU) matrix, with or without adding algae biomass. This paste was spread by knife coating (thickness of 0.15 mm, spreading speed of 4.0 mm/s).

Then, comfort-related properties of the knits and woven fabric, functionalized plus controls, were characterized, and compared. The results show that the controls are quite similar between them, with KF1 slightly thicker, denser, and resistant to abrasion than the others, and the knits substantially more air-permeable than the fabric, particularly the KF2.

The controls were additionally examined for their moisture management properties: the WF is a fast absorbing and quick drying fabric, which means that a large spreading area can be seen, as well as a fast spreading, ergo a substrate with a poor one-way transport. The KF1 is a water repellent fabric showing no wettability, no absorption, and no spreading, leading us to conclude that it is a substrate with a poor one-way transport without external forces. For last, the KF2 is a moisture management substrate that shows a large spread area at bottom surface, fast spreading at bottom surface, unveiling excellent one-way transport capabilities.

After the coating procedure, the three substrates exhibit a high decrease in the air permeability, particularly using the formulation B, with the water vapour permeability being also considerably affected.

Table 1 Characterization of the knits and the woven fabric (control and coated), encompassing measurements of thickness, areal mass density, air and water vapor permeability, as well as abrasion after 10 000 cycles.

Thickness	(mm)	Areal Mass Density (g/cm²)	Air Permeability	Water Vapour Permeability Index (%)	Abrasion (%) mass loss 10 000 cycles
WF (control)	**0.38±0.01**	**2.26±0.07**	**184.9±6.34**	**95.80±1.39**	**0.535**
WF (A)	0.45±0.01	2.05±0.03	32.55±4.65	86.28±2.06	1.020
WF (B)	0.45±0.01	2.29±0.10	1.780±0.25	45.92±41.26	0.000
WF (C)	0.49±0.02	2.05±0.03	27.41±7.67	72.93±5.43	0.295
KF1 (control)	**0.43±0.01**	**3.14±0.10**	**312.0±8.86**	**95.37±0.00**	**1.050**
KF1 (A)	0.52±0.01	2.39±0.05	100.0±4.17	89.35±1.73	1.220
KF1 (B)	0.48±0.01	2.53±0.04	2.000±1.79	38.52±3.73	2.770
KF1 (C)	0.52±0.01	2.38±0.09	88.71±23.02	87.04±0.61	0.440
KF2 (control)	**0.40±0.01**	**2.68±0.24**	**569.50±27.98**	**96.32±0.00**	**0.860**
KF2 (A)	0.46±0.01	2.27±0.05	57.38±6.84	87.45±2.18	1.390
KF2 (B)	0.45±0.01	2.45±0.09	1.160±0.33	41.65±3.85	0.000
KF2 (C)	0.46±0.02	2.23±0.12	84.88±27.24	86.22±2.79	0.370

Subsequently, algae biomass from *Tetraselmis Chuii* was added to one of the polymeric coating matrices (A) to check its antioxidant characteristics. The results show a tremendous increase of this property after algae-included coating.
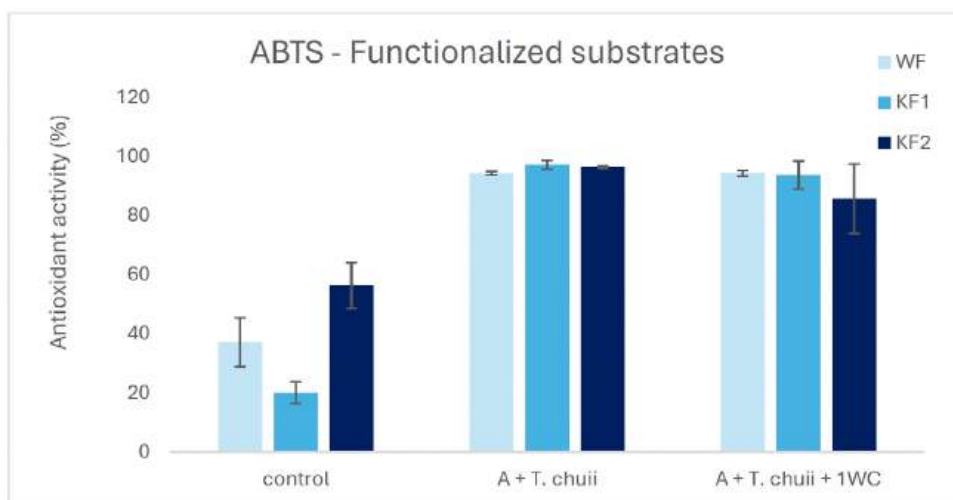

Fig. 2 Results for the antioxidant behaviour after coateing the substrates with Tetraselmis chuii and also after one washing cycle (WC).

In short, this study shows that there are substantial differences on the mechanical properties by using weaves of different architecture. In the prospective future work these fabrics will be applied as a reinforcement and mechanical characterization of the composites will be studied later.

REFERENCES

[1] Nahid Azizi, et al. "Bioinspired, metal-free modification of cotton fabric using polydopaminecoated curcumin for health-protective clothing.", Cellulose journal from Springer Science and Business Media, 2024
[2] Functional Textile Finishing Agents Market Share 2023-2032 | Industry Growth Report(gminsights.com)

ID 84
THE CERAMIC-TEXTILE STRUCTURE FOR PROTECTION AGAINST MULTIPLE BALLISTIC IMPACT

David Pacek[1]

Military Institute of Armament Technology, Poland

ABSTRACT

TBA

ID 86

A NOVEL DESIGN OF SHIP MACHINERY COMPARTMENT BILGE FOUNDATION WITH PRESSURIZED HYDRAULIC POLYMERIC COMPOSITE BED FOR ENHANCED VIBRATION ISOLATION

Anand R[1]

Defence Institute of Advanced Technology, India

ABSTRACT

TBA

ID 90

IMPACT BALLISTIC RESISTANCE OF HIGH WORKABILITY CONCRETE REINFORCED WITH CRUSHED WIND-TURBINE BLADE

Manuel Hernando-Revenga[1], Víctor Revilla-Cuesta[1], Javier Manso-Morato[1], Nerea Hurtado-Alonso[2], Abraham Fernández del Rey[3], José A. Loya[3](*)

Department of Civil Engineering, University of Burgos, Burgos, Spain

Department of Construction, University of Burgos, Burgos, Spain

Department of Continuum Mechanics and Structural Analysis, University Carlos III of Madrid, Leganés, Madrid, Spain.

(*) Email: jloya@ing.uc3m.es

ABSTRACT

The implementation of circular economy in the wind-energy sector can be promoted by recycling the dismantled wind-turbine blades through crushing to produce fibres. The use of those fibres in self-compacting concrete allows improving its ductility and energy absorption, behavior that is analysed in this research by evaluating its impact ballistic resistance. The addition of this waste fibres from a percentage of 4.5% increased the flexural strength and impact ballistic of concrete. Although concrete with those recycled fibres did not reach the performance of conventional concrete, this study meant a starting point to try to develop concrete with that waste that exhibits high resistance to such external stresses.

INTRODUCTION

The considerable increase of wind energy in the world has generated a great concern regarding the management of the waste from wind turbines that will reach the end of their useful life. It is worth noting that between 2020 and 2034, 200,000 tons of waste from wind-turbine blades, mainly composed of fibre-reinforced polymers [1], is expected to be generated, most of which is currently being disposed in landfills or incinerated [2].

One possibility with a great future perspective for blades' recycling is the obtention of fibres from them through crushing. The incorporation of fibres to concrete improves flexural strength, fracture toughness, resistance to thermal shock, fatigue, and resistance under impact loads [3]. Therefore, fibres from wind-turbine blades can improve the impact ballistic resistance of concrete. This is a serious concern in conflict areas, in which concrete is the most widely used protective engineering material in buildings, bridges, dams, nuclear power plants, and military sites and infrastructures [4].

RESULTS AND CONCLUSIONS

The composition of the concrete in this study was 320 kg/m^3 of cement CEM II/A-L 42.5 R, 155 kg/m^3 of water, 6.7 kg/m^3 of plasticizers, 680 kg/m^3 of limestone sand 0/2 mm, 660 kg/m^3 of siliceous sand 0/4 mm, and 600 kg/m^3 siliceous gravel 4/12 mm. The incorporation of fibres from wind-turbine blades was conducted by volume, thus this waste being added in four amounts: 0 kg/m^3, 49.0 kg/m^3, 73.5 kg/m^3 and 90.0 kg/m^3. The concrete mixes were named according to the volume of fibres: *R*, *W3.0*, *W4.5*, and *W6.0*. Concrete mixes that exhibited a high workability were obtained, with which specimens were produced to evaluate their flexural strength and impact ballistic resistance, test depicted in Fig.1. The results obtained in this research are illustrated in Fig. 2.

In view of the results, the flexural strength and the impact ballistic resistance of concrete with recycled fibres followed similar trends. A reduction of the flexural strength was found with the increase of the content of fibres

from wind-turbine blades up to a waste amount of 4.5%, which began to increase from that waste content. The reduction in strength could be explained by the need to increase the water/cement ratio to maintain the workability of all the mixes, which in turn caused an increase in porosity and therefore a strength reduction. This penalizing factor was compensated with percentages higher than 4.5% of fibres that effectively bridged the cementitious matrix, thus avoiding the propagation of cracks and increasing the energy absorption [5]. This performance favoured the impediment of the passage of projectiles through concrete and increased people security against this kind of attacks. In fact, the *W4.5* mix improved the impact ballistic resistance of the *W3.0* concrete mix, which had 3.0% by volume of recycled fibres from wind-turbine blades.
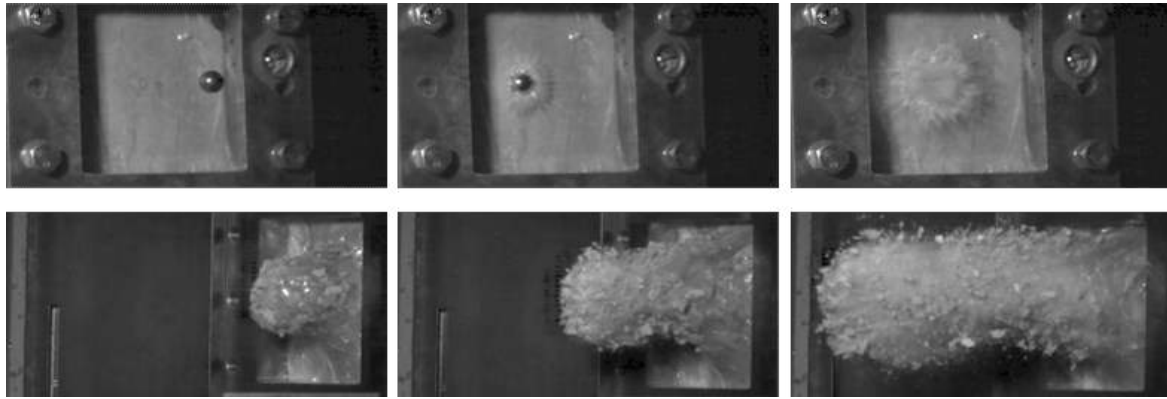

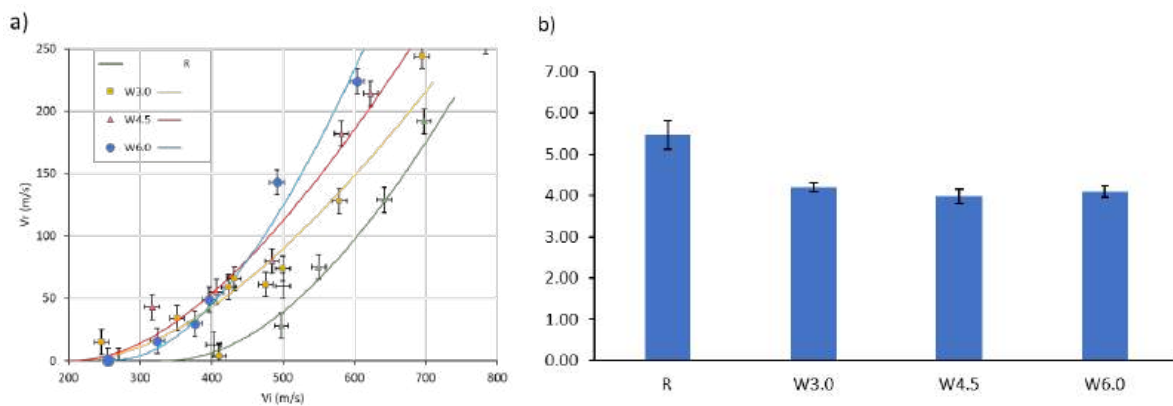Fig. 1. Ballistic impact sequence on R concrete mix.

Fig. 2. (a) Ballistic curves; (b) Cuasiestatic flexural strength.

REFERENCES

[1] H. Albers, S. Greiner, H. Seifert, U. Kühne, "Recycling of Wind Turbine Rotor Blades—Fact or Fiction? (Recycling von Rotorblättern aus Windenergieanlagen—Fakt oder Fiktion?). DEWI Mag. 2009, 34, 32–41.

[2] S.A. Hadigheh, F. Ke, and S. Kashi, "3D acid diffusion model for FRP-strengthened reinforced concrete structures: Long-term durability prediction," Constr Build Mater, 261, 120548, 2020.

[3] M.C. Nataraja, N. Dhang, and A. P. Gupta, "Statistical variations in impact resistance of steel fiber-reinforced concrete subjected to drop weight test," Cem Concr Res, 29, no. 7, 989–995, 1999.

[4] R. Yu, "Development of sustainable protective ultra-high performance fibre reinforced concrete (UHPFRC): design, assessment and modeling," 2015.

[5] S.A. Hadigheh, R. McDougall, C. Wiseman, and L. Reid, "Evaluation of composite action in cross laminated timber-concrete composite beams with CFRP reinforcing bar and plate connectors using Digital Image Correlation (DIC)," Eng Struct, 232, 111791, 2021.

ID 91
THERMOPHYSIOLOGICAL COMFORT ASSESSMENT OF DEFENSE CLOTHING SYSTEMS

Cosmin Copot[1], Magdalena Georgievska[2], Sheilla Odhiambo[1], Lieva Van Langenhove[2], Hilda Wullens[3], Alexandra De Raeve[1]

[1]Fashion and Textiles Innovation Lab (FTILab+), HOGENT University of Applied Sciences and Arts, 9051 Ghent, Belgium
[2]Department of Materials, Textiles and Chemical Engineering, Ghent University, Gent, Belgium
[3]Laboratoires de la Défense (DLD), 1800 Vilvoorde, Belgium

Comfort is a perception of well-being and is an important aspect of Personal Protective Equipment (PPE) as it affects the health, performance and work efficiency. The comfort of these garments is known to be poor. Generally, users are satisfied with their functionality (i.e. protection against rain, cold, etc.) but disappointed in the poor comfort.

Comfort is influenced by the intensity of the activity, climatic conditions, textile material properties, clothing design and fit. The comfort aspects implies three main perspectives: Thermophysiological, Sensorial and Ergonomic.

The main research question in this study was to investigate the sensorial, ergonomic and thermophysiological effects of cooling systems within military uniforms. To answer this research question, several trial tests were conducted using multiple sensing equipment and complete defense clothing systems, in specific environmental conditions, while assessing:

- Sensorial and ergonomic comfort using subjective questionnaire.
- Thermophysiological comfort using multiple sensors.
- Global effectiveness of a clothing ensemble via IR thermography.

The sensing equipment was validated in terms of accuracy and reliability and as output of this study we were able to analyze the influences on heat balance: climate, clothing, exercise level and individual factors as well as objective and subjective comfort assessment.

ID 103

EVALUATION OF IMPLANT STABILITY AND INCREASE IN BONE HEIGHT IN INDIRECT SINUS LIFT DONE WITH THE OSSEODENSIFICATION AND OSTEOTOME TECHNIQUE: A SYSTEMATIC REVIEW AND META-ANALYSIS

Dr Shruti Potdukhe[(*)1]

[1,] Lecturer, Department of Prosthodontics and Crown & Bridge, MGM Dental College and Hospital, Navi Mumbai, India

[(*)] Email: shrutipotdukhe@gmail.com

ABSTRACT

Statement of problem. Whether the use of osseodensification burs for indirect sinus lift improves primary implant stability and bone height as compared with the osteotome technique to overcome the challenges of the pneumatization of the maxillary sinus and vertical bone loss after extraction in the edentulous posterior maxilla is unclear. Purpose. The purpose of this systematic review and meta-analysis was to evaluate the difference in primary implant stability and increase in bone height in indirect sinus lift using osseodensification and the osteotome technique.Material and methods. Two independent reviewers searched the MEDLINE/PubMed, EBSCO, and Cochrane Library databases and the Google Scholar Search engine for randomized clinical trials, nonrandomized clinical trials, and cross-sectional studies published from 2000 to 2022 to identify relevant studies evaluating the primary implant stability and increase in bone height in indirect sinus lift using osseodensification and the osteotome technique. A meta-analysis was performed to evaluate the cumulative data on primary implant stability and increase in bone height.

INTRODUCTION

Following extraction, the edentulous posterior maxilla commonly exhibits physiologic changes, including pneumatization of the maxillary sinus and vertical bone loss (Alqahtani 2020). Crestal indirect sinus lift elevation is one of the safest and most straightforward ways of gaining vertical bone height. Indirect sinus lift elevation includes the Summers osteotome indirect sinus lift technique, the most common and oldest method used (Wimalarathna 2021). Osseodensification was developed by Huwais and Meyer in 2013 and is characterized by compaction of the bone along the osteotomy with densifying burs of tapered geometry and characteristic flutes, resulting in increased bone density by progressively expanding the osteotomy (Huwais 2017). Based on this principle, Huwais et al concluded that, for crestal sinus floor elevation, the osseodensification process can be used without perforating the sinus membrane (Pai 2018). The main requisites for successful implant insertion and osseointegration are sufficient bone volume and primary stability (Javed 2013). Primary implant stability depends upon the amount of bone-contacting the implant; insufficient contact may lead to implant mobility and failure (Huwais 2018). This systematic review aimed to compare the available evidence regarding the measurement of primary implant stability and the amount of increase in bone height between crestal indirect sinus lift elevation in the posterior edentulous maxilla done using osseodensification and the osteotome technique.

RESULTS AND CONCLUSIONS

Results. A total of 8521 titles were obtained by electronic database search, of which 75 were duplicates. A total of 8446 abstracts were screened, and 8411 irrelevant to the topic were excluded. Thirty-five articles were eligible for full-text assessment. After the screening of full-text articles as per the selection criteria, 26 studies were excluded. For qualitative synthesis, 9 studies were included. For quantitative synthesis, 5 studies were included. For an increase in bone height, no statistically significant difference was observed (I2 = 89%, P=.15, pooled mean difference=0.30 [-0.11, 0.70], CI=95%) [Figure 1]. For primary implant stability, the osseodensification group showed higher values than the osteotome group (I2 = 20%, P<.001, pooled mean difference=10.61 [7.14, 14.08], CI=95%). [Figure 2].
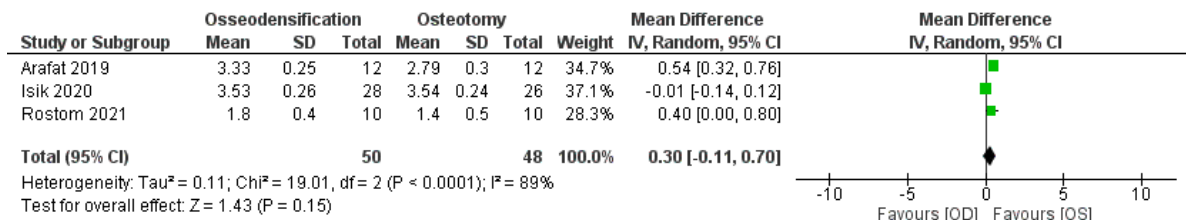
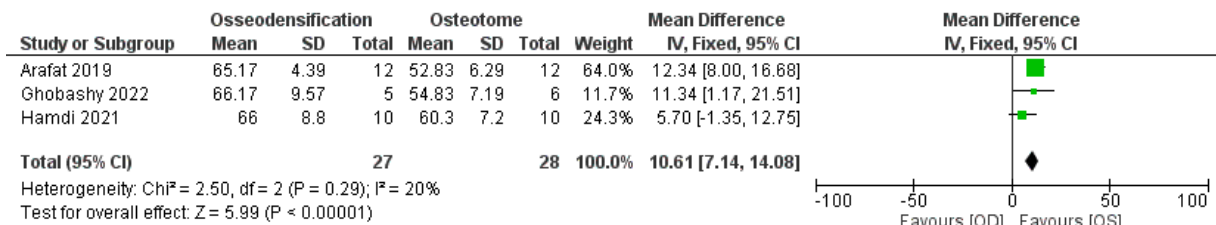Fig. 1 Forest plot for mean increase in bone height.

Fig. 2 Forest plot for implant stability.

Conclusions. The evidence obtained from quantitative analysis of the studies determined that the osseodensification group showed higher primary implant stability than the osteotome group (P<.05). However, for the mean increase in bone height, there was no statistically significant difference between the groups.

REFERENCES

[1] Alqahtani S, Alsheraimi A, Alshareef A, et al. Maxillary sinus pneumatization following extractions in Riyadh, Saudi Arabia: a cross-sectional study. Cureus. 2020;12:e6611.

[2] Wimalarathna A. Indirect sinus lift: an overview of different techniques. Biomed J Sci Tech Res. 2021;33:26101e26105

[3] Huwais S, Meyer EG. A novel osseous densification approach in implant osteotomy preparation to increase biomechanical primary stability, bone mineral density, and bone-to-implant contact. Int J Oral Maxillofac Implants. 2017;32:27e36.

[4] Pai UY, Rodrigues SJ, Talreja KS, Mundathaje M. Osseodensificationea novel approach in implant dentistry. J Indian Prosthodont Soc. 2018;18:196e200.

[5] Javed F, Ahmed HB, Crespi R, Romanos GE. Role of primary stability for successful osseointegration of dental implants: factors of influence and evaluation. Inter Med Appl Sci. 2013;5:162e167

[6] Huwais S, Mazor Z, Ioannou AL, Gluckman H, Neiva R. A multicenter retrospective clinical study with up-to-5-year follow-up utilizing a method that enhances bone density and allows for transcrestal sinus augmentation through compaction grafting. Int J Oral Maxillofac Implants. 2018;33:1305e1311

ID 111
ARMOUR'S USE OF COMPOSITE MATERIALS – A REVIEW

Aniket Jadhav[1](*), Sachin Malave[2]

[1, 2] Department of Mechanical Engineering, Smt. Kashibai Navale College of Engineering, Pune, Maharashtra, India
(*) jadhavaniketb@gmail.com

ABSTRACT

Composites with a laminated structure come from stacking ceramic and metal in a particular order. Because of their high strength and hardness, low density of ceramics, and extraordinary flexibility, metals are used as bulletproof armour. The bullet anti-penetration system includes a ceramic screen that slows down the projectile and splits it up and a metal backplate that plastically deforms to absorb the projectile's kinetic energy. Laminates have several downsides, including weak interface bonding, a tendency for tip cracks due to increased internal stress, and a jarring difference between the metal and ceramic properties. Crack migration and propagation causes abrupt changes in material characteristics at the ceramic−metal contact. A drop between the ceramic panel and metal backplate can be easily triggered when a ceramic panel is impacted, as cracks form in the interlayer. In this area, the interface bonding strength is still inadequate. In this review, we looked at the meshless smoothed-particle hydrodynamic method for high-velocity impact and massive deformation, the finite-element simulations of interface impact resistance and the first-principles predictions of interface strength. The paper concludes with numerous suggestions for future improvement: Further study is required on ceramic toughening to increase the compatibility of ceramic panels and metal backplates, the performance transition between ceramic and metal, and the reliability of ceramic−metal laminated materials. It is critical to study ways to strengthen metals. More multiscale research using methods like the phase-field method, finite element analysis, and first-principles computations, focusing on how to mix these techniques naturally and successfully, is needed to reinforce metals by introducing nano-phases into metal matrix composites while still retaining the metal's ductility. The latest study that emphasises the potential advantages of hybrid materials, specifically the combination of aramid and kenaf fibres, highlights a notable progression in the domain of armour technology.

INTRODUCTION

Body armour has shown to be quite helpful in combat situations where a high degree of ballistic performance is required. Body armour has evolved alongside technological developments to reduce casualties from bullet impact, increase energy absorption, and reduce weight [1]. Many people in the modern world wear protective body armour to ward off the effects of high-velocity hits. Many types of body armour with improved ballistic performance against such strikes have been developed. Engineers have created and applied a fibre-reinforced polymer matrix technology to absorb a lot of stress without breaking. High-tech composites like Kevlar have been lauded for their incredible durability and ability to dampen a bullet's impact. Since the elastic moduli and the inherent frequencies of these high-tech composites vary with temperature, altering the temperature is one approach to coax the desired feature out of them. Fibre type and, more crucially, ply orientation are both critical factors in determining a composite material's strength [2]. Under stress, the ply usually holds up best along the plane where the fibres are arranged. Both longitudinal and transverse waves are produced by projectile impacts, allowing for precise localization of the malfunction's origin. Impact energy can be absorbed differently, including shear plugging, delamination, and matrix cracking. Composite laminates can be damaged in various ways by impacts of different velocities. Yet, the support conditions have a much smaller effect on the vibrational response to a high-velocity impact than the response to a low-velocity impact. Panels with various fibre orientations have been created to improve efficiency [3].

The shear properties of woven fabrics were inferior to those of UD fibres, whereas the tensile qualities of UD fibres were superior. To improve ballistic performance, researchers looked into using the woven ply as the impact face of a hybrid panel made of UD and woven fabric. This article discusses the use of composite materials for ballistic protection. It examines different combinations of materials and their ability to withstand different types of threats, like projectiles and bullets. It emphasizes the importance of choosing suitable fiber reinforced matrices as well as how to optimize the design for specific purposes. It explores the ways in which the incorporation of nanomaterials, like carbon nanotubes and graphene, into traditional composite structures could result in significant improvement in mechanical properties as well as overall performance. This study is focused on the creation for hybrid materials suitable for applications in military armour. The study examines the use of different types of reinforcements such as ceramics, aramid fibers metal elements and others, to make composite armour that has enhanced multi-threat protection.

RESULTS AND CONCLUSIONS

In the end, as the dangers of weapons in combat is increasing and increase, the need for additional security measures is essential. Although traditional armour-grade materials such as ceramics and metals have been preferred due to their light weight efficiency, cost-effectiveness, as well as improved physical characteristics, they have a superior performance over other materials when it comes to ballistic impact tests. The capability of composites to slow down the speed of bullets and reduce impacts makes composites an attractive option for armour solutions that are modern. The natural fibres used as a reinforcement in composite materials provides a variety of desirable characteristics, such as a higher Specific Strength Modulus (SSM), less risk of illness, biodegradability, less weight and reduced environmental impact. Recent research has demonstrated how hybrid materials can benefit like those made from the aramid and kenaf fibres that can provide enhanced V50 performance, as well as other desirable attributes. In light of this study, it is strongly recommended that the development from hybrid materials to make armour should be explored which will result in a significant decrease in synthetic fibers as well as significant increase in usage of natural fibers. Composite materials are promising to meet the growing requirements, aided by their low production costs and their high accessibility. The ballistic impact test results that were presented earlier and the results of ballistic impact testing, incorporating hybrid composites, especially those that incorporate natural fibers such as kenaf and flax, can significantly increase the armour's protective abilities. Since the hybrid composites have the capability to increase in 85%, 95% strength to sustain the ballistic impact test. The increased ballistic protection and improved resistance to fragmentation and blast resistance to pressure provided by the hybrid Composite material prove its ability to offer superior protection.

REFERENCES

[1] A. Prakash, M. Fasil, N. Anandavalli, Ballistic performance of optimised light weight composite armour, Forces Mech. 12, 100216, 2023.

[2] L. Gilson, F. Coghe, A. Bernardi, A. Imad, L. Rabet, Ballistic limit evolution of field-aged flexible multi-ply UHMWPE-based composite armour inserts, Compos. Struct., 117414, 2023.

[3] K. Nazari, P. Tran, P. Tan, A. Ghazlan, T.D. Ngo, Y.M. Xie, Advanced manufacturing methods for ceramic and bioinspired ceramic composites: A review, Open Ceram., 100399, 2023.

ID 114
NEW CANINE UNITS TRAINING BAITS FOR THE TATP EXPLOSIVE DETECTION

Ainhoa Isla Lopez[1*]

Auziker, Spain

(*) ainhoa.isla@auziker.com

ABSTRACT

TBA

ID 118

FRACTURE BEHAVIOUR OF 4140 STEEL SUBMITTED TO ANNEALED, NORMALIZED, QUENCH AND TEMPERING HEAT TREATMENTS WITH IN-SITU HYDROGEN CHARGING

M. Umair Raza[1*], Atif Imdad[2], M. Atif Niaz[3], Kashif Imdad[1]

[1,] HITEC University, Taxila Cantt, Pakistan, [2,] University of Oviedo, Spain, [3,] University of Wah, Pakistan
Email: engr.kashif@hitecuni.edu.pk,

ABSTRACT

42CrMo4 steel underwent annealing, normalizing, quenching and tempering heat treatments to produce microstructures with varying hardness levels. Following these treatments, tensile tests on notched specimens were conducted in air and under two different hydrogenated conditions using in-situ electrochemical hydrogen charging tests. Two different electrolytes and current densities were used to create low and high hydrogenated environments. The study examined the impact of microstructure and hardness on hydrogen embrittlement, with scanning electron microscopy (SEM) employed to identify the corresponding failure micromechanisms. Introducing hydrogen during the tests led to a significant reduction in notched strength across all tested microstructures, altering the predominant failure micromechanism. The embrittlement index increased with higher hydrogen concentrations introduced through electrochemical conditions and increased steel hardness. The notched strength with in-situ hydrogen charging was lower in the normalized and annealed steels compared to quenched and tempered steels of the same hardness.
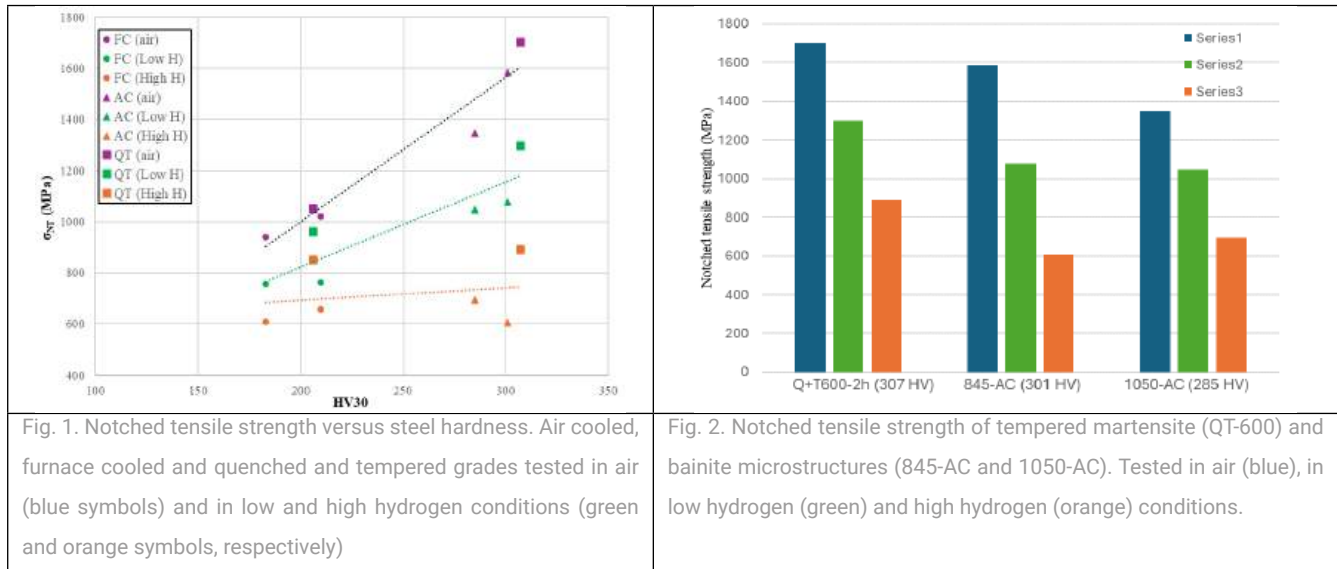
INTRODUCTION

Medium and high strength steels play vital roles in defense applications due to their exceptional mechanical properties, including high tensile strength and toughness. This study focuses on 42CrMo4 steel, that is used for the storage and transport of hydrogen and a common choice for military equipment components, to explore its behavior under hydrogen exposure, a known factor affecting mechanical properties including tensile strength, elongation, fracture toughness, and fatigue crack propagation rate [1–2]. Atomic hydrogen enters and diffuses through the steel lattice under stress and concentration gradients, becoming trapped in various lattice defects known as hydrogen traps [3,4]. These traps facilitate different damage processes, altering failure micromechanisms.

In medium and high strength steels, the most cited hydrogen-assisted micromechanisms are hydrogen-enhanced decohesion (HEDE) and hydrogen-enhanced localized plasticity (HELP) [5]. It is now widely recognized that HE is controlled by the amount of hydrogen in specific areas of the steel microstructure and by critical stress/strain levels. Depending on the steel's strength and internal hydrogen concentration, hydrogen typically induces brittle fractures with cleavage or intergranular fracture surfaces. Among the many studies on hydrogen's detrimental effects on the tensile properties of structural steels, the CHMC1-2014 document by the Canadian Standards Association (CSA) evaluates material compatibility with hydrogen [6]. While these steels offer desirable attributes, their susceptibility to hydrogen embrittlement (HE) warrants thorough investigation, particularly in the context of various heat treatments.

RESULTS AND CONCLUSIONS

Microstructural analysis revealed distinct variations in steel hardness and microstructure based on heat treatment, with quenched and tempered grades exhibiting tempered martensite microstructures and higher hardness compared to annealed and normalized counterparts. Notched tensile tests demonstrated a clear reduction in strength and elongation in the presence of hydrogen, with failure mechanisms shifting towards quasi-cleavage. Embrittlement indexes increased with hydrogen concentration and steel hardness, with quenched and tempered grades displaying better resistance to hydrogen-induced embrittlement than annealed and normalized grades.

Fig. 1. Notched tensile strength versus steel hardness. Air cooled, furnace cooled and quenched and tempered grades tested in air (blue symbols) and in low and high hydrogen conditions (green and orange symbols, respectively)	Fig. 2. Notched tensile strength of tempered martensite (QT-600) and bainite microstructures (845-AC and 1050-AC). Tested in air (blue), in low hydrogen (green) and high hydrogen (orange) conditions.

CONCLUSIONS

This study highlights the significant impact of hydrogen on the mechanical properties of 42CrMo4 steel under different heat treatments. Quenched and tempered steels showed superior resistance to hydrogen embrittlement compared to annealed and normalized grades. Understanding the interplay between microstructure, hardness, and hydrogen exposure is crucial for optimizing the performance of medium and high strength steels in defense applications.

REFERENCES

[1] S. Takagi, Y. Toji, M. Yoshino, K. Hasegawa, Hydrogen embrittlement resistance evaluation of ultra-high strength steel sheets for automobiles, ISIJ Int. 52 (2012)316–322. https://doi.org/10.2355/isijinternational.52.316.

[2] Y. Murakami, T. Kanezaki, P. Sofronis, Hydrogen embrittlement of high strength steels: Determination of the threshold stress intensity for small cracks nucleating at nonmetallic inclusions, Eng. Fract. Mech. 97 (2012) 227–243. https://doi.org/10.1016/j.engfracmech.2012.10.028.

[3] A. McNabb & P.K. Foster, A new analysis of the diffusion of hydrogen in iron and ferritic steels, Trans. Met. Soc. AIME. 227 (1963) 618–27.

[4] J.Y. Lee, J.L. Lee, A trapping theory of hydrogen in pure iron, Philos. Mag. A Phys. Condens. Matter, Struct. Defects Mech. Prop. 56 (1987) 293–309. https://doi.org/10.1080/01418618708214387.

[5] S.P. Lynch, Hydrogen embrittlement (HE) phenomena and mechanisms, Stress Corros. Crack. Theory Pract. (2011) 90–130. https://doi.org/10.1533/9780857093769.1.90.

[6] ANSI/CSA, CHMC 1-2014, Test method for evaluating material compatibility in compresses hydrogen applications –phase I-, Metals. Mississauga, ON, CSA, 2014.

ID 119
NON-INVASIVE MONITORING OF PERFORMANCE AND HEALTH THROUGH ANALYSIS DROP OF SWEAT

Maros Halama[1,2(*)], Bujar Ajdari[2], D. Halamová[3], Peter Slovenský[4]
[1]Technical University of Kosice, Institute of Materials, Kosice, Slovakia
Innosensia start-up, Division CorOne s.r.o., Branch Office Vienna, Austria
Health Care Surveillance Authority (UDZS), Toxicology Division, Kosice, Slovakia
University of Western Ontario, London, Ontario, Canada
[(*)] Email: maros.halama@gmail.com

ABSTRACT

Sweat is known to detoxify our bodies and is a valuable biofluid which serves as source of biomarkers related to next-generation personalized preventive medicine and smart healthcare. Nowadays only lab sensors can precisely detect concentration of certain biomarkers in drop of sweat. Our study and solution bring non-invasive monitoring via embedded wearable sensors in soldiers' armor. Monitoring of dehydration level, activity performance during training, stress level under military operation or state of health of soldier in real-time with high sensitivity brings interoperability advantage, preventive disease screening or collecting health data for preventive medicine approach. For detailed study we have chosen 4 biomarkers with enormous potential not only to monitor performance and stress levels but to give also overall health status. The aggregated anonymized data will be used by artificial neural network to predict future scenarios. Aim is to envision data using augmented reality mode (AR) for interactive & dynamic visualization to have finally gamification engagement. Overall, wearable smart sweat sensors have the potential to revolutionize old-fashioned approaches in military management, add value to standard health monitoring.

INTRODUCTION

Sweat, a long-overlooked biofluid is emerging as a powerful source for continuous noninvasive monitoring of an individual's athletic performance and health. Recent developments in wearable sensors technology have enabled several skin-interfaced systems capable of capturing, storing, analysing and prediction of sweat chemistry in real-time (Choi, 2018). Innovative approaches in the field incorporate soft, flexible electronics, microfluidics and multimodal biochemical sensors that can measure mainly separated biomarkers in sweat, such as sodium, chloride, glucose, and selected proteins (Hedberg, 2022). By tracking changes in sweat composition, these sensors provide valuable insights into an individual's hydration status, metabolic processes, and physiological state. As this technology continues to evolve, the potential application for example, sweat analysis can help diagnose cystic fibrosis, inform personalized hydration strategies, monitor hormones etc. Moreover, the ability of real-time and continual track of biomarkers in sweat enables early detection of potential performance & health issues and allows for preventive interventions. Project Health & Performance Predictive Guard lead by CorOne s.r.o, Innosensia Division, come out from cooperation of up-mentioned universities and institutions and has been supported by Innovation Centre of Kosice Region (ICKK). The concept was selected among TOP20 tech finalists at 44th WT Innovation World Cup 2024, held during 16th to 17th April in Munich, Germany and was presented also on Globsec Danube Tech Summit in December 2023 in Vienna House of Industry.

RESULTS AND CONCLUSIONS

Non-invasive set-up of sensors as lab-on-chip have been tested and optimised under laboratory condition exposed to drop of 50 µl of artificial sweat prepared according to the reference test method (EN 1811:2011 including 0.1 wt% urea, 0.5% wt% NaCl, 0.1 wt% lactic acid) and in real sweat collected from athletes during 30 min training. Dehydration level via measuring of concentration of Cl⁻, performance via measurements of lactate and total state of health via measurements of vitamine C have been realized on 30 different samples (including 3 patient with serious health issues). The results for CNT based sensor showed linear dependency of E vs. concentration of Na^+ as shown in Fig. 1. Similar results have been achieved using sensor for lactate and two other unspecified biomarkers (confidential part of research).
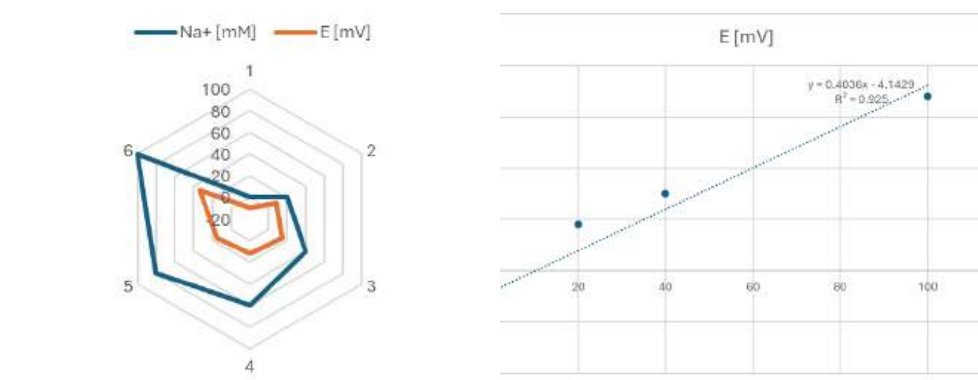

Fig. 1 a,b Monitoring of dehydration level from CNT sensor a) Linear slope for E vs. concentration of Na^+ b) Net graph E vs. concentration of Na^+

The achieved results highlight potential of sensors collecting data from human body liquid in real-time having capabilities and readiness for military forces in various domains from pilots to special units. This study shows that our solution for non-invasive monitoring of selected biomarkers from drop of sweat embedded in armour of soldier could serve also as alarm system to control, manage performance & health parameters, finally with existence of the huge database in combination with AI able to predict.

REFERENCES

[1] J. Choi, R. Ghaffari, L. B. Baker, and J. A. Rogers: "Skin-interfaced systems for sweat collection and analytics, In: Science Advances, 4(2), pp.3921, 2018

[2] E. Romanovskaia, P. Slovensky, M. Halama, M. Auinger, Y. Hedberg: "Electrochemical estimation of the gold nanoparticles size effect on cystein-gold oxidation, In: Journal of The Electrochemical Society, p. 021501, 2022

JUNE 20-22, 2024
BRAGA, PORTUGAL